Total Synthesis of jerantinine alkaloids and a biocatalytic synthesis of 2,6 - Disubstituted tetrahydropyrans using an alcohol dehydrogenase.

Ph.D. Thesis
30-09-2019

Harry Eastman

Supervisors: Dr Elaine O'Reilly

Dr John E. Moses

Abstract

This thesis is comprised of two sections; The first is a semi synthesis of the cytotoxic natural product jerantinine A. Starting from the natural product tabersonine, isolated from *Voacanga africana*, which contains the 3 stereocenters present in jerantinine alkaloids set in the correct conformation. The reaction conditions were optimised and produced jerantinine A from tabersonine in a 16% yield over 7 steps. Following this, the biological activity was evaluated using MCF-7 Cancer cell lines, a clonogenic assay, cell cycle analysis and a tubulin polymerisation assay. These results concluded that jerantinine A was a tubulin destabilising agent and were visualised using confocal microscopy.

The second section is using alcohol dehydrogenases in the formation of disubstituted tetrahydropyrans. The biocatalytic strategy of the synthesis of 2-6, disubstituted tetrahydropyrans was achieved using an alcohol dehydrogenase triggered intramolecular oxa-Michael reaction from prochiral ketoenone starting materials. These were produced in good yields with up to >99% *e.e.* and 12:1 *d.r.*. This methodology was then used in the synthesis of an analogue of the natural product brocaketone A in a 26% yield over the synthesis. 2,5-Disubstituted tetrahydrofurans were also produced using this methodology but were produced in poor *d.r.*

Acknowledgements

I would like to thank Dr. Elaine O'Reilly, Dr. James Ryan, and Dr. Anca Pordea for allowing me the opportunity to work on this collaborative project, and for their constant support and ideas.

Additionally, I would like to thank Dr. Chris Peel, Dr. Andrew Gomm, Dr. Michael Sharkey, Dr Paul Stanley, Dr. Tracey Bradshaw, Dr. Mohanned Qazzaz and Stylianos Grigoriou for all their assistance and the rest of the O'Reilly and Moses group for helping create a positive working atmosphere.

I would also like to thank my family as without their support, none of this would have been possible.

Abbreviations

δ	delta
(CH_2O)	paraformaldehyde
ADH	alcohol dehydrogenase
BC	Before Christ
DCM	dichloromethane
d.r.	diastereomeric ratio
e.e.	enantiomeric excess
GC-FID	gas chromatography - flame ionisation detector
HRMS	high resolution mass spectrometry
IR	infra-red
IMS	industrial methylated spirits
IUCN	international union of the conservation of nature
Lk-ADH	*Lactobacillus kefir* alcohol dehydrognease
M	molar
Me	methyl
MVK	methylvinyl ketone
MHz	megahertz
mmol	millimole(s)
NADH	nicotinamide adenine dinucleotide
NADPH	nicotinamide adenine dinucleotide phosphate
NMR	nuclear magnetic resonance
PI	propidium iodide
Ral-ADH	*Ralstonia sp.* alcohol dehydrogenase
r.t.	room temperature
TLC	thin layer chromatography
THF	tetrahydrofuran

Contents

Chapter 1

Section 1: Introduction

This worked resulted in the paper titled "***Sustainable Syntheses of (−)-Jerantinines A & E and Structural Characterisation of the Jerantinine-Tubulin Complex at the Colchicine Binding Site"*** published in Scientific Reports.

1.1 What are natural products?

For as long as humans have existed, we have been looking to nature for food, medicines and building materials. The earliest documented evidence of medicine coming from nature was in 2600 BC, written on hundreds of clay tablets in Mesopotamia.[1] These described approximately 1000 plant derived substances that they used to treat various conditions, from coughs and colds to parasitic infections and inflammation, many of which are still used today.[2,3] The Chinese have the *Materia Medica*, which has been extensively documented over the centuries.[1] The first record dates back to 1100 BC which includes 52 prescriptions for known illnesses. This was expanded on following the works of Shennong Herbal (~100 BC; 365 drugs) and the Tang Herbal (659AD; 850 drugs).[1,3-7]

In the past, civilizations depended greatly on local flora and fauna for their survival and they would experiment with various berries, leaves, roots, animal parts or minerals to establish what effects they had. As a result, many crude drugs were observed by the local healer or shaman to have

some medical use.[1,8] To this day, about 80% of the world's population still require traditional medicines, primarily people living in developing countries.[2,9]

There are many well-known compounds from natural products that have been used as medicinal treatments for many centuries. Shown in **Figure 1.1**, these compounds are salicylic acid **(1)**, first written by Hippocrates in the 5th century BC, describing it as a "bitter powder extracted from willow bark that could ease aches and pains and reduce fevers".[10,11] The antibiotic, penicillin **(2)** was isolated from *Penicillium sp.* fungi by Alexander Fleming in 1928. This discovery was a product of a fortuitous accident, which resulted in one of the biggest scientific discoveries of the twentieth century.[12-16] The use of morphine **(3)**, isolated from the opium poppy, has been recorded since 2600 BC in Mesopotamia primarily as a pain reliever.[2,11]

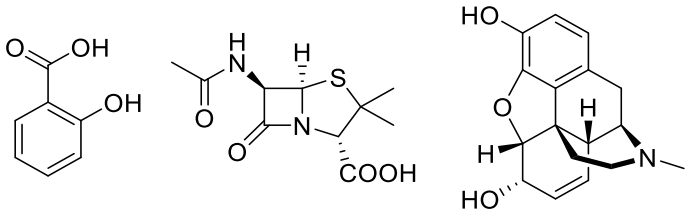

(1) **(2)** **(3)**

Figure 1.1: Compound structures of salicylic acid (1), penicillin (2) and morphine (3).

1.2 Extraction of Natural Products.

Over the years, many scientists have looked into extracting useful substances from nature. Nowadays, the approach of extraction is much more targeted. Plants of the same family generally contain the same active compounds, so an initial targeted approach to extraction can be undertaken. [17] For example, the *Eucalyptus sp.* contain the chemical

eucalyptol **(4)**, and the *Cruciferae sp.* contain cyanogenic glycosides with amygdalin shown **(5)** shown in **Figure 1.2**.[18-24]

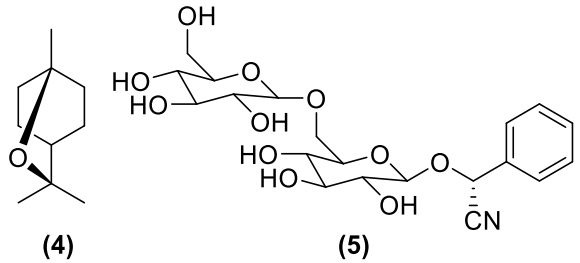

(4) (5)

Figure 1.2; Eucalyptol (4) and the cyanogenic glycoside amygdalin (5).

Extraction of natural products can be done by two methods, using water miscible solvent or water immiscible solvent. Each has distinct advantages over each other, but it depends on a few factors;

a) What is being extracted.

b) The physical state of material the extraction is from.

The natural product being isolated dictates the extraction method, if the natural product is a terpene-based compound, then extracting with water immissible solvents would work well. If the compound is an alkaloid, then going for a water-based extraction may work better.

1.2.1 Using water miscible solvents.

These include methanol, acetone and ethanol as the main solvents for extraction. These have the benefits that many alkaloid and polar natural products are soluble in these solvents coupled with having low boiling points, retrieving the crude extract is straight forward. These do come have some issues, mainly their reactivity. If the natural product has any basicity, these can form esters and undergo aldol reactions.[25]

1.2.2 Using water immiscible solvents.

These include CH_2Cl_2, $CHCl_3$ and petrol as the main solvents for extraction. These have the benefit that they will extract mainly non-polar natural products. These also have low boiling point so access to the crude extract is also straight forward, but there are many other compounds in extracts which are non-polar, such as fatty acids, steroids, hormones. These can make dilute the crude extract requiring further purification to remove these compounds.[26,27]

1.3 Semi-Synthesis of natural products.

Semi-synthesis is a method of making a natural product from a complicated starting material that can be easily accessed. This is usually done where the target molecule is very complex or large and it would be too inefficient to produce stepwise from small and cheap petrochemical building blocks. Natural products can be very complicated molecules which can have many different functional groups, fused rings and chiral centres. A semi-synthesis usually looks at starting with some of these installed in the starting material to make the rest of the synthesis easier. The semi-synthesis of paclitaxel **(7)** from 10-deaceytlbaccatine III **(6)** is shown in **Scheme 1.1**. Paclitaxel is an important drug in the treatment of cancer, but being found at 0.5 grams per forty foot of pacific yew tree bark which takes 200 years to grow. With a typical dose of this drug being 100 mgs, extraction would not be a sustainable process. Serendipitously, 10-deaceytlbaccatine III is found in the European yew tree, and in much larger quantities. These two compounds both share the baccatine core,

with the same substitutions, chirality and protection groups on almost all of the hydroxyl groups. The semi-synthesis route gave a yield of 87% over 4 steps,[28] whilst the total synthesis after 51 steps had an overall yield of 0.03%.[29,30]

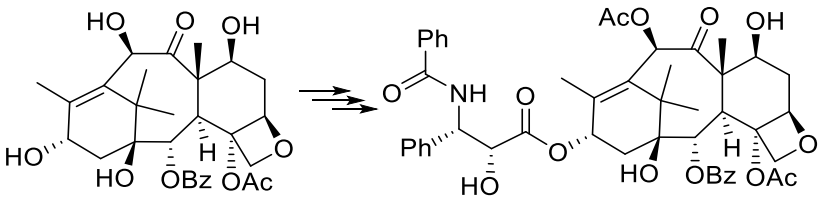

(6) (7)

Scheme 1.1; Semi-synthesis of paclitaxel (7) from 10-deaceytlbaccatine III (6).

1.4 Biosynthesis of tabersonine and jerantinine alkaloids.

Tabersonine is an aspidosperma alkaloid found in the plant *Catharanthus roseus.* The *Catharanthus roseus,* also known as the Madagascar periwinkle or rosy periwinkle is a plant that is native and endemic to Madagascar. The plant has long been used by many different South East Asian communities in herbal medicine, treating diabetes, malaria and cancer.[31] The medicinal properties of the plant are mostly due to the vinca alkaloids present. The most notable vinca alkaloids from *Catharanthus roseus* are vinblastine **(8)** and vincristine **(9)**, which are currently used to treat leukaemia and Hodgkin's lymphoma. As shown in **Figure 1.3**, tabersonine **(10)** has the same skeleton as one of the monomers in both vinblastine, vincristine and jerantinine A **(11)**. Tabersonine is a natural product present in a few plants, with its role still being debated, it is thought to be an intermediate to make other compounds.[32]

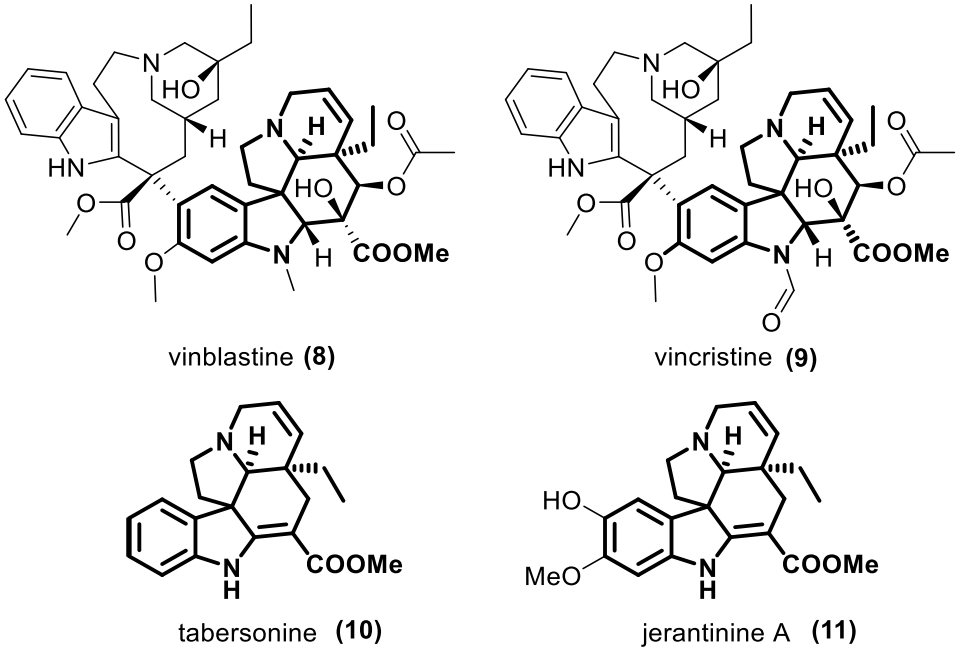

Figure 1.3; Structures of vinblastine, vincristine, jerantinine A and tabersonine.

Jerantinine A-G shown in **Figure 1.4** were first isolated from *Tabernaemontana corymbosa* by Lim *et al.*[33] The plant, which is native to the South East Asia, was found to contain the 7 new compounds after an investigation of the leaf extract. Jerantinine A and B also showed pronounced *in vitro* cytotoxicity against human KB cells.[34] *Tabernaemontana corymbosa* is on the International Union for the Conservation of Nature (IUCN) red list, meaning the plant is in danger of becoming extinct if not conserved.

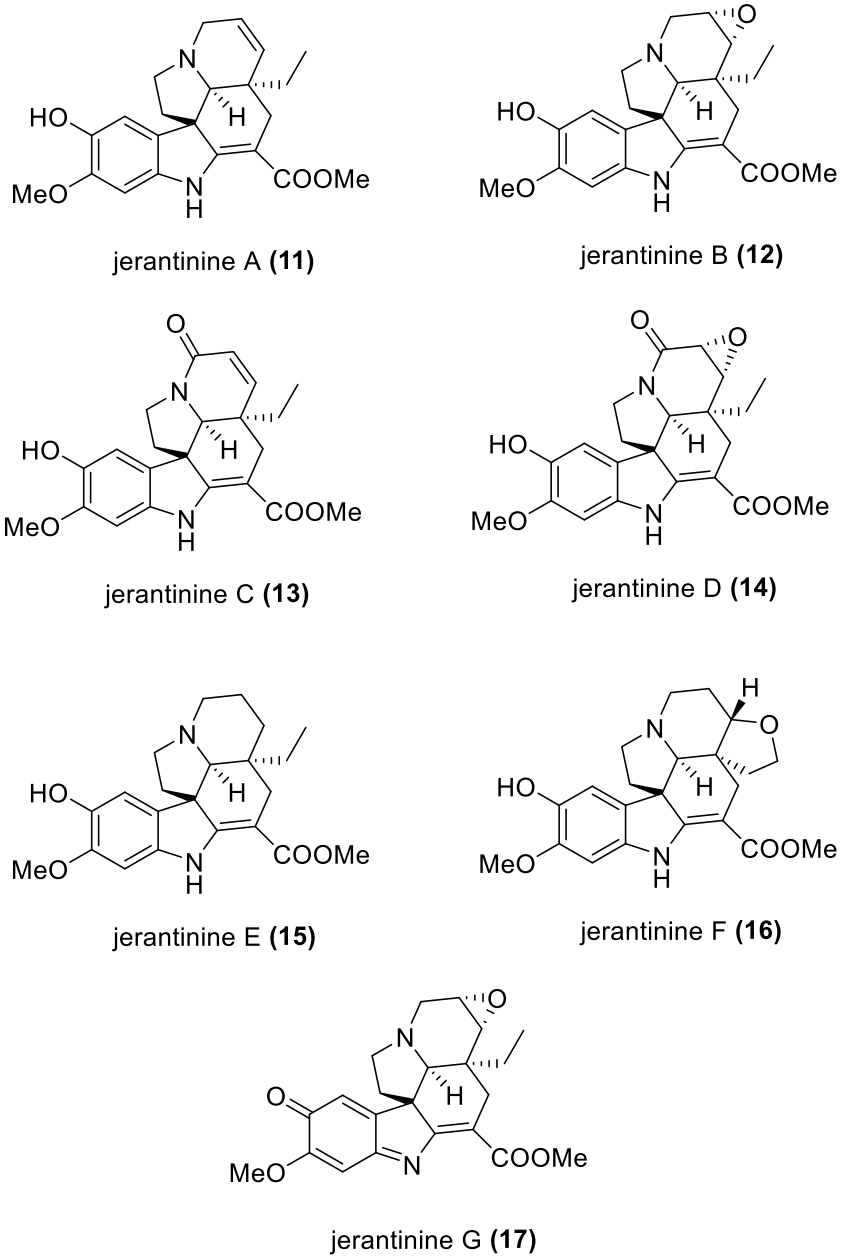

Figure 1.4. Showing jerantinine A-G.

Tabersonine is an intermediate in the biosynthesis of jerantinine alkaloids. Although little is known about the transformations to form jerantinine A-G from tabersonine, the bioretrosynthesis of tabersonine shown in **Scheme 1.2** is known, starting from strictosidine **(18)**. The natural product is formed from a Pictet-Spengler reaction from tryptamine and

secologanin **(19)**, which come from the shikimate **(20)** and terpene **(21)** pathways respectively.[35]

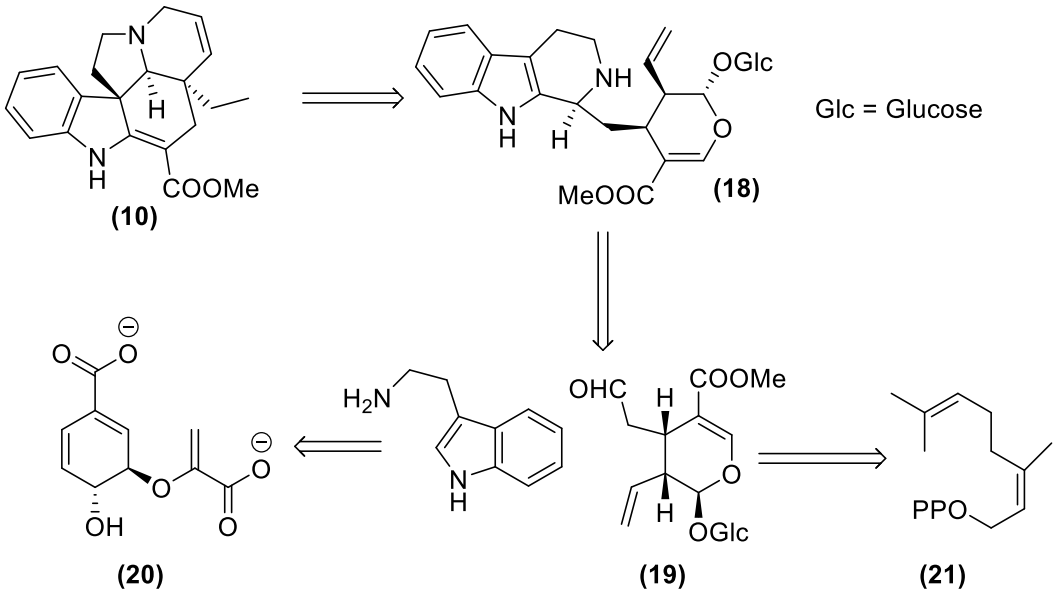

Scheme 1.2: The key intermediates in the formation of tabersonine.[36]

The formation of secologanin **(19)** comes from nerol diphosphate **(21)**. Secologanin is a common intermediate used in the synthesis of indole, cinchona and pyrroloquinoline alkaloids.[37] Geraniol diphosphate is cleaved by geraniol synthase (GES) to geraniol **(22)** before the geraniol 10-hydroxylase (G10H, CYP76B6) oxidises it to 10-hydroxygeraniol **(23)** shown on **Scheme 1.3**. This is oxidised twice by 10-hydroxygeraniol oxidoreductase (10-HGO) to yield 10-oxogeranial **(24)**. The order in which the alcohol groups are oxidised is not important,[38] as once one has been oxidised, the other is then subsequently oxidised. Iridodial forms from 10-oxogeranial, which is catalysed by iridoid synthase (IRS) and can form either **(25)** or **(26)**, depending on the environment iridodial is currently in. The stereochemistry of these molecules does matter as the

oxidation by iridoid oxidase (IO) produces just the one diastereomer of 7-deoxyloganetic acid **(27)**. Glucose is then added to form 7-deoxyloganic acid **(28)** by the 7-deoxyloganetic acid glucosyl transferase (7-DLGT).[35]

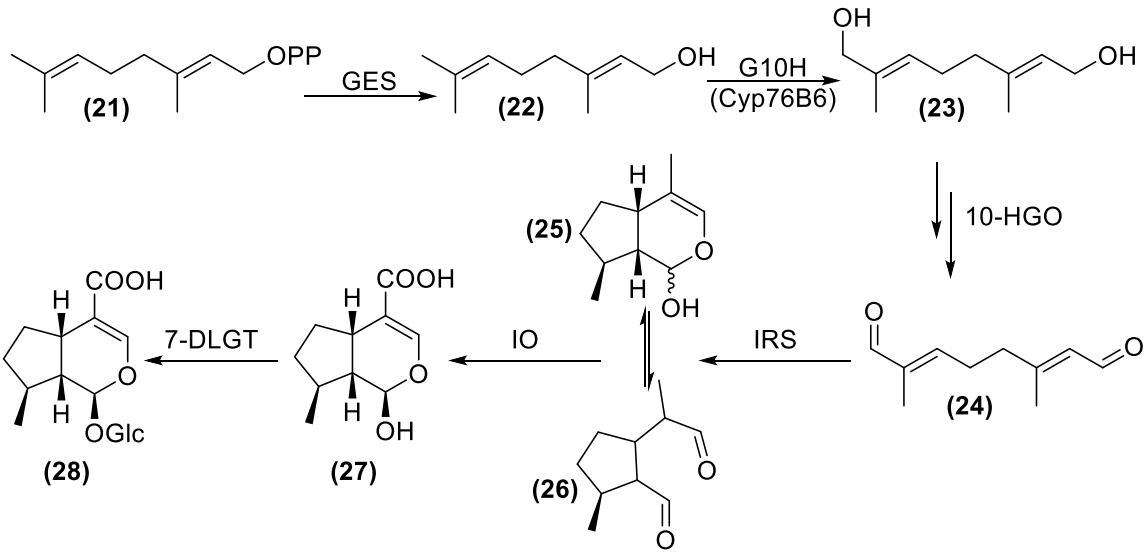

Scheme 1.3: The biosynthesis of 7-deoxyloganic acid from geraniol diphosphate.[35]

Scheme 1.4 shows loganic acid **(29)** formed from 7-deoxyloganic acid **(28)** by the 7-deoxyloganic acid hydroxylase (7-DLH). This then reacts with loganic acid *o*-methyltransferase (LAMT) to form the methyl ester and produce Loganin **(30)**. The final step to produce secologanin **(19)** is catalysed by the secologanin synthase (SLS).

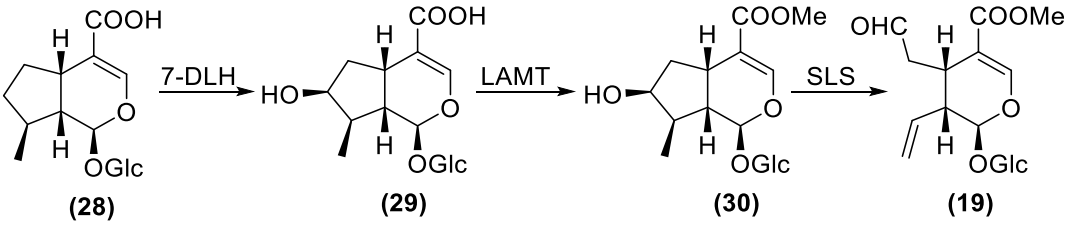

Scheme 1.4: The biosynthesis of secologanin from 7-deoxyloganic acid.[36]

At the same time that secologanin **(19)** is being produced, tryptamine is being synthesised *via* the shikimate pathway. Starting from chorismate **(31)**, anthranilate synthase (ATS) catalyses the reaction with L-glutamine to produce anthranilate **(32)**, pyruvate and L-glutamate shown in **Scheme 1.5**. Phosphoribosylpyrophosphate (PRPP) then reacts with the amine on anthranilate to produce *N*-(5' phosphoribosyl)-anthranilate and pyrophosphate as a by-product. The ribose ring then opens up to produce 1-(*O*-caboxyphenylamino)-1-desoxyribose-5-phosphate **(33)**. This then undergoes a reductive carboxylation losing carbon dioxide and a hydroxide ion to produce indole-3-glyserinphosphate **(34)**, which then produce indole **(35)**. The last step is catalysed by tryptophan synthase (TYS) and L-serine to produce the amino acid L-tryptophan **(36).**[39]

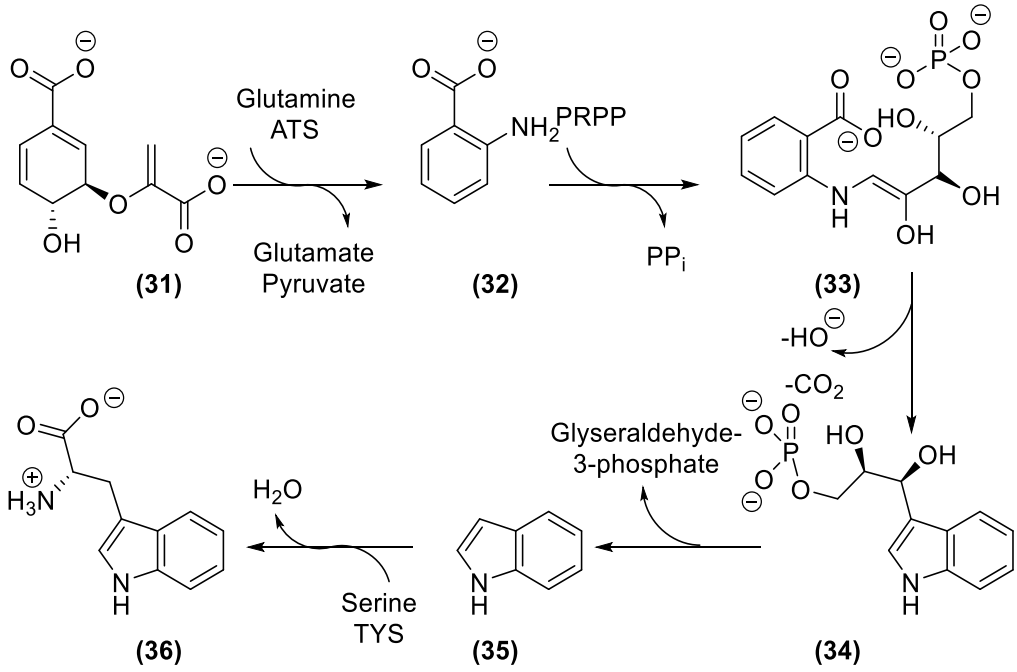

Scheme 1.5: The formation of L-tryptophan from chorismate.[36,39]

L-tryptophan **(36)** is then converted to tryptamine **(37)** by tryptophan decarboxylase (TDC) shown in **Scheme 1.6**. Secologanin and tryptamine, **(19)** and **(37)** respectively, are then catalysed by

strictosidine synthase (STR) to produce strictosidine **(18)**. Strictosidine deglucosidase (SDG) then removes the glucose group from strictosidine to produce a very reactive intermediate. The glucose served as a protecting group to mask the very reactive species **(38)** which spontaneously equibrilises to **(39)** and **(40)**. **(39)** is known as the "dialdehyde" version and **(40)** is known as the 4,21-dehydrocorynantheine aldehyde. These intermediates are responsible for the formation of a number of alkaloids such as ajmalicine, catharanthine and vindoline to name a few.[38,40]

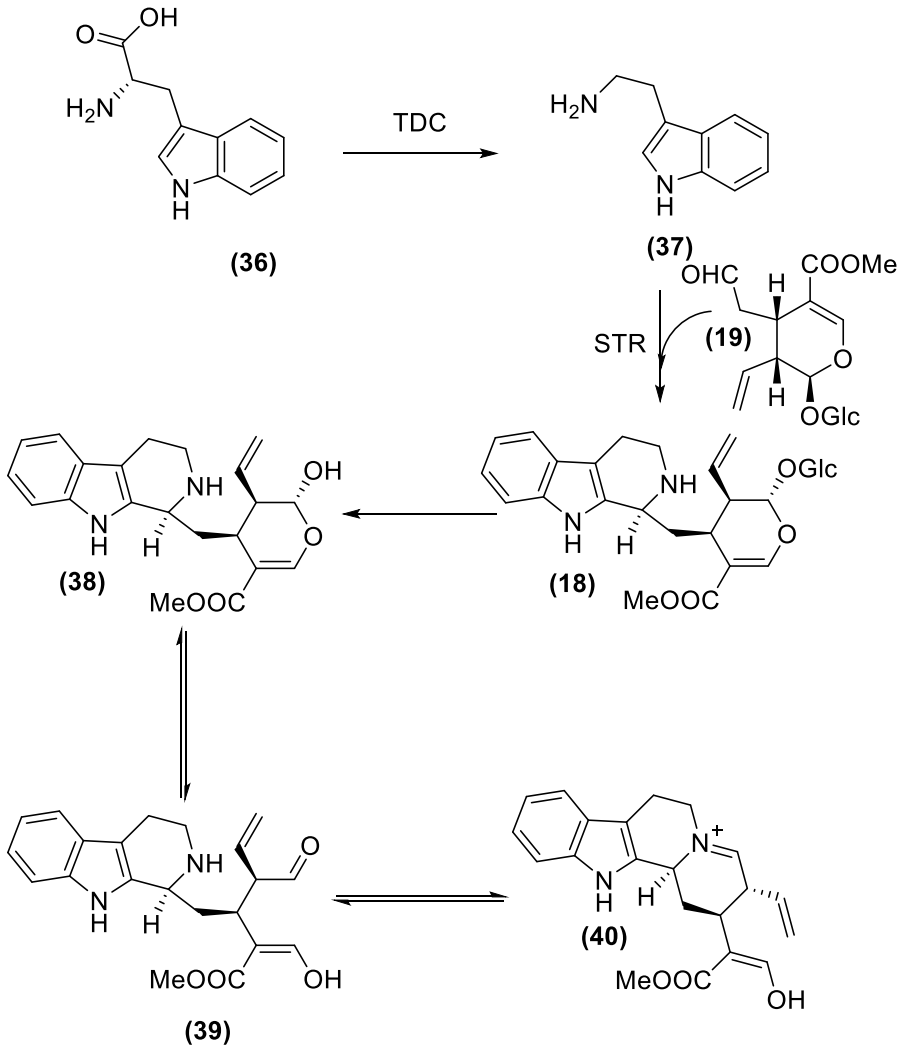

Scheme 1.6: The biosynthesis of strictosidine from the two monomers tryptamine and secologanin.

The pathways for the formation of tabersonine from strictosidine is currently unknown, as are the enzymes that catalyse their formation. Research carried out in the 1960's and 1970's, based on feeding the plant isotopically labelled substrates then extracting the intermediates, gave an insight into how tabersonine may be biosynthesised.[36] The strychnos type compound, known as preakuammicine **(41)**, is a common intermediate in the biosynthesis of aspidosperma type alkaloids, though it has never been isolated from plant material due to lability.[36]

The conclusion of the synthesis of tabersonine is shown in **Scheme 1.7**, with the reduction of preakuammicine **(41)** yielding stemmadenine **(42)**, which can rearrange to form dehydrosecodine **(43)**. This could then form tabersonine *via* a Diels-Alder reaction, though there is no evidence for this reaction in the plant.[36]

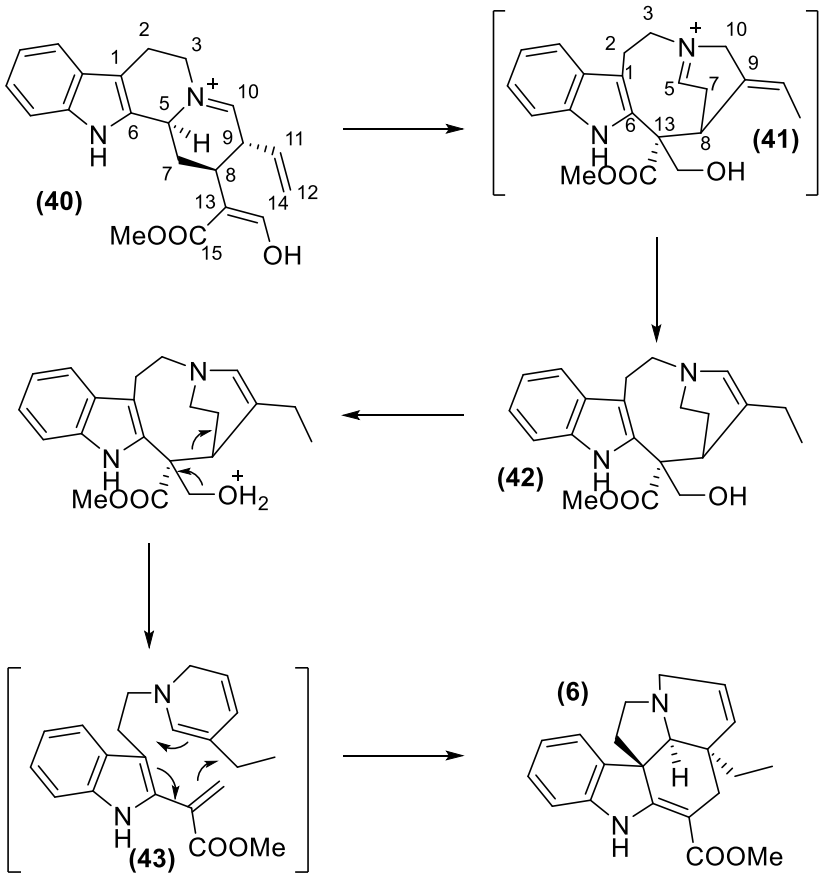

Scheme 1.7: The proposed biosynthesis of tabersonine from strictosidine.

Scheme 1.8 shows the formation of 16-methoxytabersonine **(44)** from tabersonine **(10)** in the vindoline synthesis. Firstly, tabersonine-16-hydroxylase (T16H) oxidises the *para* position on the indole ring producing the phenolic compound, which is then methylated by 16-hydroxytabersonine 16-*O*-methyltransferase (HTOM).

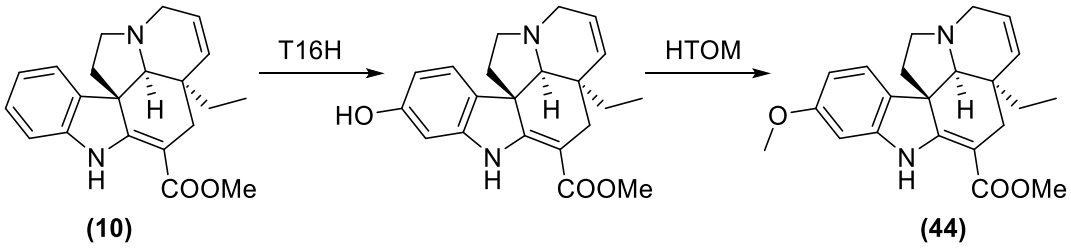

Scheme 1.8, The biosynthesis of tabersonine to 16-methoxytabersonine.

As jerantinines A-G were only discovered in 2008, the biosynthetic pathway is still unknown. However, it is likely to be reminiscent of the pathway found in *C. roseus* with initial formation of tabersonine followed by installation of the *ortho*-methoxy group through the action of similar enzymes to T16H and HTOM.[32] Another oxidation *ortho* to the methoxy group would produce jerantinine A followed by some further modifications producing the other jerantinine alkaloids shown in **Scheme 1.9**.

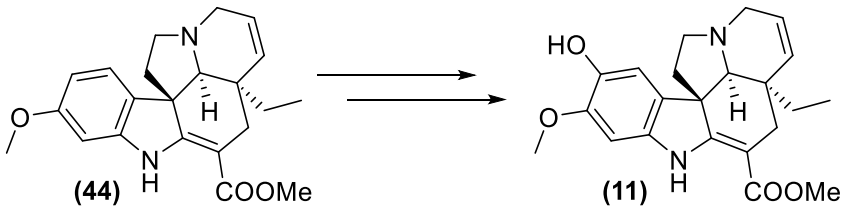

Scheme 1.9: Synthesis of jerantinine A (7), from 16-methoxytabersonine (40).

1.5 Synthesis of jerantinine E.

There has only been one formal synthesis of any jerantinine alkaloid, and that is the synthesis of jerantinine E, published by Waser *et al.* in 2013 shown in **Scheme 1.10**.[41] They studied the bio-activity of jerantinine E and elucidated the mode of action and activity. They achieve a 15.7% yield over 17 steps starting from δ-valerolactam.

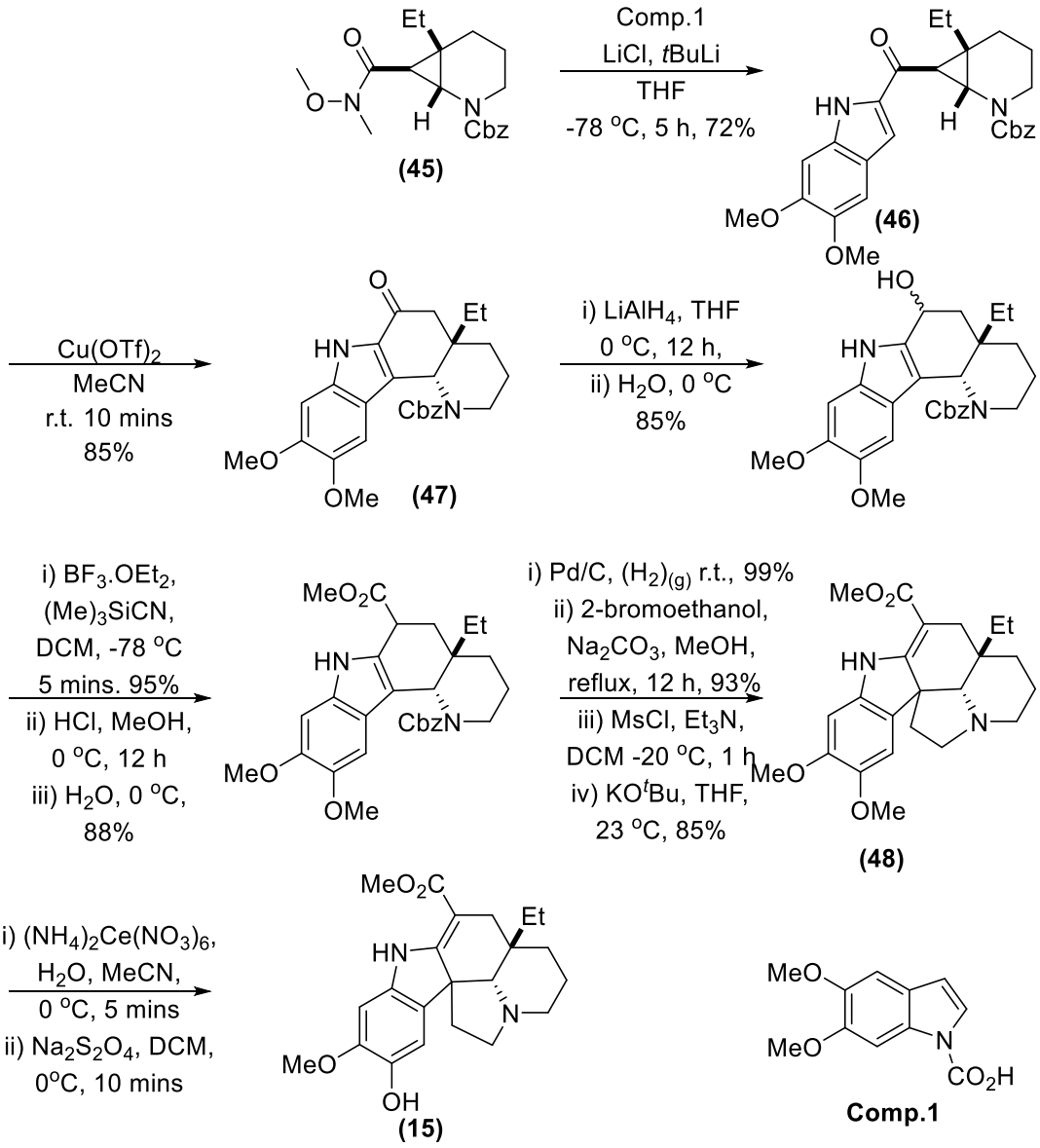

Scheme 1.10: Synthesis of jerantinine E (11) reagents and conditions.

The synthesis started from the δ-valerolactam to produce the weinreb amide **(45)** in 51% yield over 7 steps. This was reacted with 5,6-dimethoxyindole *N*-carboxylate to yield compound **(46)**. The *N*-carboxylate group was chosen for its dual function as it acted as a directing group for the lithiation as well as a protecting group that can be easily removed in aqueous work up. Compound **(46)** was then cyclised to afford the cis-diastereomer **(47)** with good regioselectivity. The resulting ketone was reduced by $LiAlH_4$ producing an alcohol. $BF_3.OEt_2$ is then added eliminating the alcohol to produce a carbocation, which then reacts with trimethylsilylcyanide. This cyanide intermediate is transformed into a carboxylic acid by a Pinner methanolysis reaction. This is followed by Cbz-deprotection and alkylation with 2-bromoethanol. The final ring is then produced *via* a ring closing procedure using mesyl chloride followed by a strong base. Finally, a selective demethylation of **(48)**, using cerium ammonium nitrate mediated oxidation followed by a reduction produced jerantinine E **(15)**.[41]

1.6 Anti-cancer properties of jerantinine alkaloids.

Since the discovery of jerantinine A-G from *Tabernaemontana corymbosa* in 2008, they have been tested as potential drug candidates. Research groups working on these compounds have found they belong to a family of anti-cancer drugs known as the microtubule targeting agents (MTAs). Vincristine, vinblastine and paclitaxol all belong to this group of compounds though the method of action of jerantinine alkaloids has been described similar to that of vincristine and vinblastine.[34,42]

Vincristine and vinblastine both disrupt the formation of microtubules and have been reported to work by stopping microtubule dynamics *via* binding to the tubulin dimers. This leads to crystallization of the microtubules and mitotic arrest, or cell death.[43],[44]

Paclitaxol on the other hand, acts in an opposite way to vincristine and vinblastine. It does not prevent the formation of the microtubule but stabilizes the microtubule polymer and stops it from disassembling. Thus, chromosomes are then unable to form the metaphase spindle configuration and hence block the progression of mitosis. Prolonged activation of the mitotic checkpoints triggers apoptosis of the cell, or for the cell to revert back to the G-phase of the cell cycle without dividing.[34,45,46]

The findings of Bradshaw *et al.* show that jerantinine A evokes potent inhibition activity against human-derived cancer cells causing high levels of G2/M blocking and the inhibition of tubulin polymerisation.[46] Jerantinine B was also studied by Bradshaw *et al.* and their study showed that jerantinine B has high levels of activity against a variety of human-derived cancer cell lines. They also studied jerantinine B acetate **(49)** and found that its activity was considerably higher than jerantinine B **(12)**. Their hypothesis for this enhanced reactivity was that the acetate group, which stabilised the jerantinine B acetate from oxidation when compared to jerantinine B, allowed it to survive longer in the cell. The acetate group also lowered its overall polarity, allowing easier diffusion across hydrophobic cell membranes increasing the intracellular concentration which also contributed to the higher potency.[34,44]

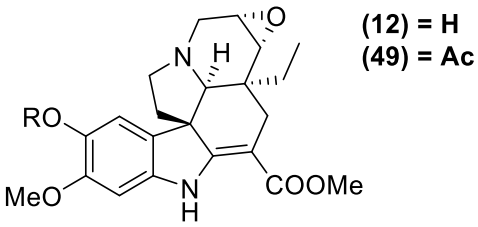

Figure 1.5; Jerantinine B and jerantinine B acetate.

1.7 Aims and Objectives.

With more research, the jerantinine alkaloids have potential to become important anti-cancer drugs. As the tree these alkaloids are isolated from is endangered, extraction of large quantities of these compounds is not a viable option, therefore a synthesis is required. Though the jerantinine alkaloids differ structurally, jerantinine A has the potential to serve as a starting point for the preparation of other derivatives and hence is the target of this investigation. There are 3 main objectives for this work;

- Find a suitable method of extracting tabersonine from *Voacanga africana* seeds.
- Semi-synthesise of jerantinine A from a commercially available source.
- Biologically evaluate jerantinine A and of synthetic intermediates.

Once a suitable method has been found for extracting tabersonine, the synthesis of jerantinine A can begin. The synthetic method that produces jerantinine A needs to produce enough for material so biological testing can happen. The initial biological tests will compare the activity of synthetic jerantinine A with the jerantinine A extracted from *Tabernaemontana corymbosa.*

Section 2: Results and Discussion.

2.1 Extraction of tabersonine.

As *Tabernaemontana corymbosa* is on the IUCN red list, jerantinine alkaloids cannot be extracted in large quantities from this plant. The initial goal was the semi-synthesis of jerantinine A starting from tabersonine, which could be isolated in yields of up to 2.5% from *Voacanga africana* seeds.[47] After grinding the seeds into a pulp, the seed matter is acidified with sulfuric acid and left to stir over night. The seed pulp was then filtered through cotton wool and sodium chloride was added to make the hydrochloride salt. This was extracted with chloroform, dried and subsequently purified *via* column chromatography with the average yield being about 1% (2 grams) of pure tabersonine per 200 grams of seeds.

As the yield of tabersonine is reported to be higher,[48] an optimisation was undertaken to increase the efficiency of extraction. Initially, the tabersonine was being ground up using a pestle and mortar and this was a time consuming process. To improve this, a food processor was employed and was capable of grinding the required 200 grams of seeds in about 15 seconds. The approach also resulted in a much finer powder being produced which had further ramifications along the extraction.

The finer the seeds resulting from the use of the food processer made the separation more problematic as the filtration took up to 5 hours. Separation of the coarser pulp following grinding with the pestle and mortar took an average of 20 minutes for the whole 2 litres of solvent

plus a washing. The problem stemmed from the pulp forming a sediment like layer on top of the cotton wool which would end up clogging the cotton wool and significantly reduce the flow. A muslin cloth was then employed to act as a "teabag" to filter the seed pulp from the extraction.

Once filtered, the sulfate salt was converted to the hydrochloride salt with the addition of sodium chloride and this was left to stir overnight. This was to form the hydrochloride salt which was found to be a lot more soluble in chloroform than the sulfate salt. 1.5 litres of chloroform was added and the biphasic mixture was stirred for 6 hours before being phase separated. This was initially done using a separating funnel, but was found to be difficult due to the large volume of solvent being used. Another way was found using suction to remove the aqueous top layer. The organic layer was filtered through Celite® to remove most of the particulates, any water that had also passed through the Celite® was then removed by phase separation. This then underwent standard drying procedures to produce an orange solid which mainly consisted of tabersonine hydrochloride.

The next step was to free base the tabersonine, allowing it to be further purified. This was initially done by dissolving the tabersonine hydrochloride in the minimal amount of chloroform and adjusting the pH using ammonium hydroxide solution, which produced a yellow cloudy emulsion that was impossible to separate. To proceed, the solvent was removed and dissolved in 1:1 chloroform to water. As this would prove time consuming, other bases were evaluated to try and reduce this problem. Saturated sodium hydrogen carbonate was tested, with no formation of an emulsion, though the volume of saturated solution required to basify was substantial. 2 M sodium hydroxide solution was

then tested, which was found to be very effective requiring a small quantity of the 2 M sodium hydroxide solution to basify the whole extraction. Once basified, it was separated under standard separating procedures yielding an orange solid.

2.2 Optimisation of extraction of tabersonine.

Using the starting extraction as a benchmark, conditions were changed to see how they affected the yield. Tabersonine was purified *via* column chromatography so a comparison of each extraction method could be made.

Table 2.1: Table shows the control reactions on the extraction of tabersonine from *Voacanga africana* seeds.

Control Run	Quantity of seeds	Acid	Solvent	NaCl	Control Variable	Yield[a]
Benchmark	200 g	1% H_2SO_4	Chloroform	200 g	-	2.25 g
Control 1	200 g	No Acid	Chloroform	200 g	Acid	Trace
Control 2	200 g	1% H_2SO_4	No Chloroform	200 g	Solvent	Trace
Control 3	200 g	1% H_2SO_4	Chloroform	No Salt	Salt	0.42 g
Control 4	100 g	1% H_2SO_4	Chloroform	200 g	Lower Conc.	0.83 g
Control 5	400 g	1% H_2SO_4	Chloroform	200 g	Higher Conc.	2.12 g
Control 6	200 g	1% H_2SO_4	Chloroform	200 g	2 day mixing	2.21 g

[a]isolated yield.

Control 1 in **Table 2.1** shows that removing the acid means no compound is isolatable. In control 2, no chloroform was allowed to mix for 6 hours,

instead, it was washed twice with 750 mL of chloroform. This yielded very little tabersonine which showed that the 6 hours of stirring is required for a good extraction. Control 3 showed that the addition of sodium chloride to make the hydrochloride salt is required, confirming the difference in solubility in chloroform between the hydrochloride and sulphate salt. Changing the concentration of *Voacanga africana* seeds shown in control 4 and 5 shows that 200 grams of seeds is a good benchmark, having 400 grams and 100 grams of seeds reduces the efficiency of extraction by half. In control 6, acidification with H_2SO_4, the addition of salt and addition of chloroform were left for 2 days at a time. This control showed no significant change to the current extraction times.

Table 2.2: Changing the extraction solvent.

Run	Quantity of seeds	Acid	Solvent	NaCl	Temp. °C	Yield[a]
Benchmark	200 g	1% H_2SO_4	Chloroform	200 g	r.t.	2.25 g
1	200 g	1% H_2SO_4	DCM	200 g	r.t.	1.93 g
2	200 g	1% H_2SO_4	EtOAc	200 g	r.t.	0.35 g
3	200 g	1% H_2SO_4	PE	200 g	r.t.	0.21 g

[a]isolated yield.

Changing the solvent from chloroform had some interesting affects shown in **Table 2.2**. DCM gave a very similar result to chloroform, and the procedure was also very similar due to the DCM and chloroform being denser than water. Ethyl acetate required a different method. As it was added, it formed a thick emulsion. This made the subsequent steps

difficult due to the viscosity of the emulsion, requiring 2 days to pass through celite®. Once worked up, very little tabersonine was extracted and also requiring another DCM extraction due to the very high water content of the oil. Petroleum ether was another poor solvent for extraction, though an emulsion never formed, not much tabersonine was isolated either.

Table 2.3: Changing the acidifying agent.

Run	Quantity of seeds	Acid	Solvent	NaCl	Temp. °C	Yield[a]
Benchmark	200 g	1% H_2SO_4	Chloroform	200 g	r.t.	2.25 g
4	200 g	10% H_2SO_4	Chloroform	200 g	r.t.	1.95 g
5	200 g	1% HCl	Chloroform	200 g	r.t.	0.35 g
6	200 g	10% HCl	Chloroform	200 g	r.t.	1.73 g
7	200 g	1% HNO_3	Chloroform	200 g	r.t.	1.39 g
8	200 g	10% HNO_3	Chloroform	200 g	r.t.	1.78 g

[a]isolated yield.

Changing the acid in the extraction showed that sulfuric acid is the best acid to use presented in **Table 2.3**. The concentration of sulfuric acid was increased to 10 % in run 4 and this did not increase the mass of isolated tabersonine isolated. Hydrochloric acid could potentially negated the use of adding sodium chloride, but in the interest of keeping each reaction constant, sodium chloride was added. Interestingly, it showed that 1% hydrochloric acid shown in run 5 was not as effective as 1% sulfuric acid, and a higher concentration was required shown in run 6.

Nitric acid was also tested as it is another common acid which is used in chemistry and gave very similar results to hydrochloric acid shown in run 7 and 8. Sulfuric acid was seen as the best acid to use, due to being safer as well as more cost effective.

Table 2.4: The solubility of the salts.

Run	Quantity of seeds	Acid	Solvent	NaCl	Temp. °C	Yield[a]
Benchmark	200 g	1% H_2SO_4	Chloroform	200 g	r.t.	2.25 g
9	200 g	1% H_2SO_4	Chloroform	0 g	r.t.	0.42 g
10	200 g	1% HCl	Chloroform	0 g	r.t.	0.32 g
11	200 g	1% HNO_3	Chloroform	0 g	r.t.	0.22 g

[a]isolated yield.

Though the control reactions shown in **Table 2.1**, showed the necessity of adding sodium chloride in the second step of the extraction, the reactions shown in **Table 2.4** investigated if there was a better salt that could be made straight from the acid. The results showed that the salts made from the acids are poorly dissolved in chloroform and the addition of NaCl was required. From previous runs, it is shown that 1% sulfuric acid has the potential to extract the material, but not the solubility in chloroform to be extracted. Nitric acid is a sort of middle ground between hydrochloric and sulfuric acid, the acid having the acidity to somewhat extract tabersonine, and tabersonine nitrate having some solubility in dissolving in chloroform.

Table 2.5: Extracting at a higher temperature.

Run	Quantity of seeds	Acid	Solvent	NaCl	Temp. °C	Yield[a]
Benchmark	200 g	1% H_2SO_4	Chloroform	200 g	r.t.	2.25 g
12	200 g	1% H_2SO_4	Chloroform	200 g	50	2.87 g

[a]isolated yield.

Extracting at a higher temperature could be beneficial for the solubility of the compound. For this, the aqueous sulfuric acid was maintained at 50 °C until the addition of chloroform. The temperature then was set to 40 °C and stirring for 6 hours, there was no further heating. There is a significant increase in the mass of tabersonine isolated after column chromatography.

2.3 Retrosynthetic analysis of jerantinine A.

With prior knowledge of the group's efforts in the synthesis of jerantinine A from tabersonine, a retrosynthesis study shown in **Scheme 2.1** revealed that from the 15-Iodo-tabersonine **(52)**, a Miyaura Borylation followed by oxidation would yield the para-hydroxyl compound **(51)**. From here, an ortho-formylation reaction would yield **(50)**, followed by a Dakin reaction and selective demethylation similar to the one used in the synthesis of jerantinine E could yield jerantinine A **(11)**.[41]

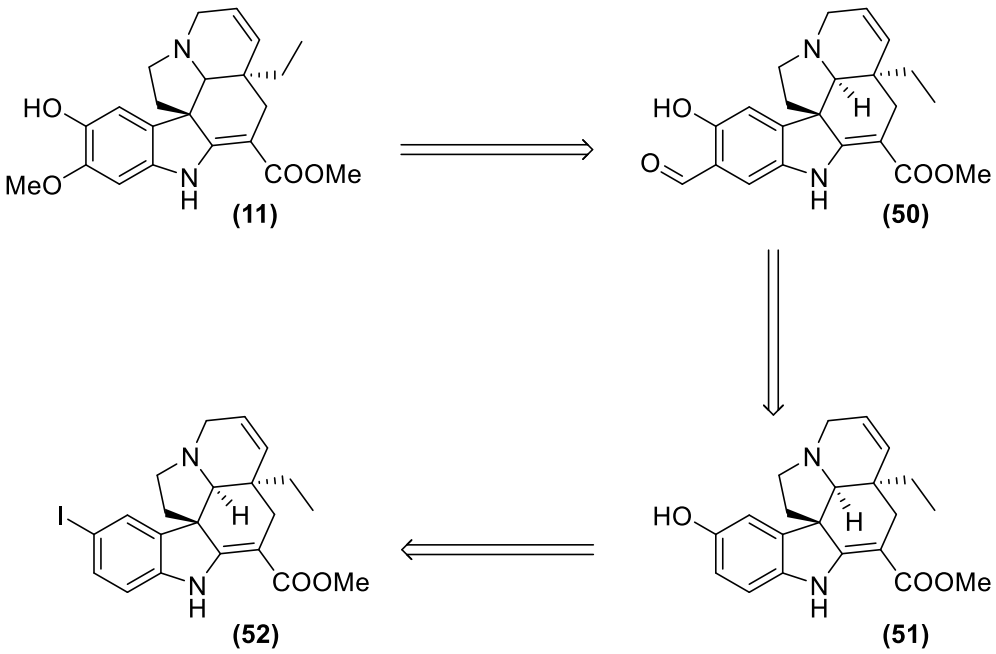

Scheme 2.1: Retrosynthetic analysis of jerantinine A from iodo-tabersonine.

2.4 Synthesis of jerantinine A.

2.4.1 Synthesis of 15-iodo-tabersonine.

The synthesis of 15-iodo-tabersonine **(52)** is a known reaction documented by Lei *et. al.*[49] in 2014 using TFA and NIS. This reaction yielded only 15-iodo-tabersonine, with no other sites being iodinated. The work up requires the solution to be neutralised without the internal temperature getting to high or decomposition of the product occurs. This can be accomplished using sodium hydroxide 2 M solution in vigorously stirred ice water. The reaction mixture was diluted with DCM and added to a dropping funnel which drops one drop per second. This was found to be the optimal reaction producing a black fluffy compound which was good enough to be telescoped to the next step.

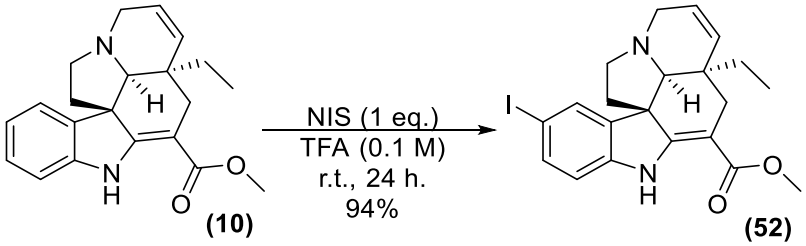

Scheme 2.2: Synthesis of 15-iodo-tabersonine (52).

2.5 Synthesis of N-Boc-15-iodo-tabersonine.

The next step was a boc protection of the indole nitrogen. This was found to be necessary for the Miyaura-Borylation reaction which was the following step. Initially, the reaction was done in DCM with stiochiometric DMAP. Under these conditions, using purified or crude **(52)**, only about 50% yield was obtained**.** However, we found, using catalytic amounts of DMAP improved the yields drastically to about 75%, followed by changing the solvent from DCM to THF further increased the yields to 95%.

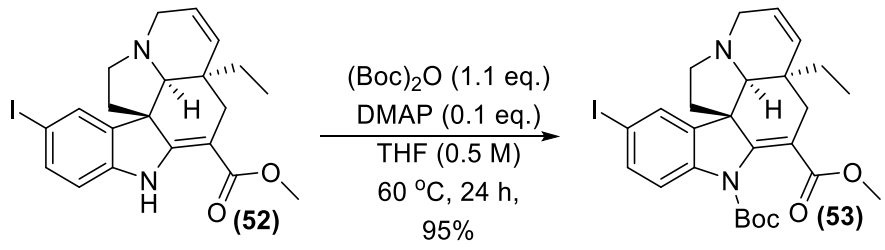

Scheme 2.3: Synthesis of *N*-Boc-15-iodo-tabersonine (53).

2.4.2 Synthesis of N-Boc-tabersonine-15-Boronic acid pinacol ester.

The Miyuara-Borylation reaction shown in scheme 2.4 worked very well with almost full conversion to the boronic acid pinacol ester. This was not worked up, just filtered through celite® and condensed *via* vacuum to produce a dark brown fluffy solid which was then telescoped to the next reaction.

In an attempt to increase the efficiency of the reaction, a direct borylation method which would install the boronic acid pinacol ester without the iodination and palladium step was attempted. Using the same methodology as previously reported in boc protection of 15-iodo-tabersonine, tabersonine was boc protected in very good yields. This was done so that the indole NH would not coordinate to the Lewis acids used in the reaction.

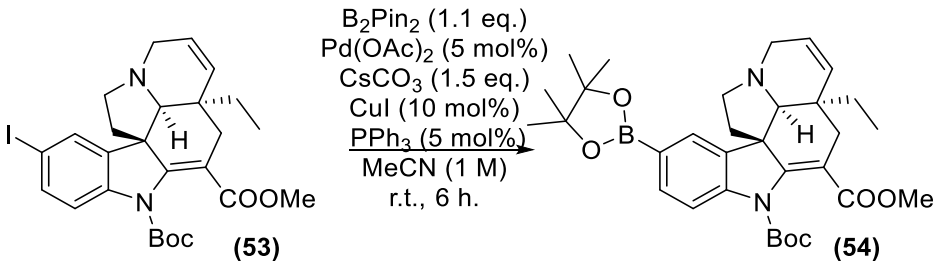

Scheme 2.4: Synthesis of *N*-Boc-tabersonine-15-Boronic acid pinacol ester (54).

The reaction in **Scheme 2.5** was done under dry conditions following a procedure from Ingleson *et al*.[50] This reaction did not work with tabersonine. The TLC showed only the starting material was present. A range of other different reactions were tried shown in **Table 2.6**. The equivalents of boron and aluminium species were doubled to ensure the

coordination of the indole nitrogen would not hinder the reaction. Runs 2 and 5 did produce something that could have resembled product by TLC, though isolation was impossible due to the large number of byproducts also formed. Ingleson *et al.* has published some work in 2012 where he states this reaction works by forming the intermediates in **Figure 2.1**.[51] Runs 4 and 5 were then repeated with the aluminium equivalents increased to 2, but this reaction also failed to produce any isolatable compound. As this reaction failed to yield any product, the Miyaura-Borylation was used to make **(54)** from hereon in.

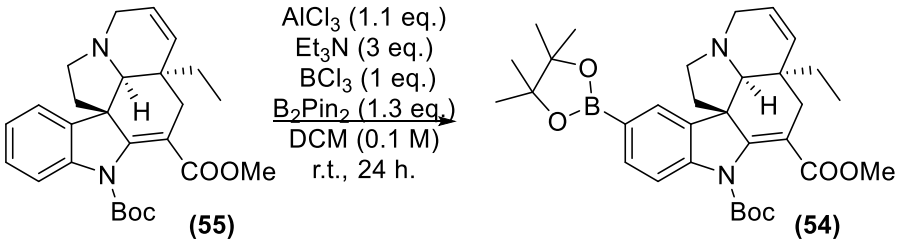

Scheme 2.5: Direct borylation of *N*-Boc tabersonine (50).

Table 2.6: The different reactions tried.

Run	Starting material	Boron Source (1 eq.)	Aluminium Source (1.1 eq)	Yield[b] (%)
1	tabersonine	BCl_3	$AlCl_3$	0[a]
2	tabersonine	BBr_3	$AlBr_3$	0[a]
3	tabersonine	BCl_3	$AlBr_3$	0[a]
4	*N*-Boc tabersonine	BCl_3	$AlCl_3$	0
5	*N*-Boc tabersonine	BBr_3	$AlBr_3$	0
6	*N*-Boc tabersonine	BCl_3	$AlBr_3$	0

[a]2 eq. of boron source and 2.2 eq. of aluminium source used. [b] isolated yield

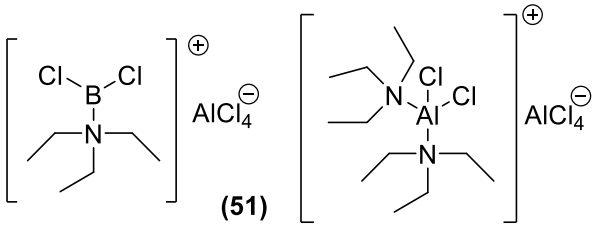

Figure 2.1: Intermediates (51) proposed by Ingleson.

2.4.3 Synthesis of N-Boc-15-hydroxy-tabersonine.

The oxidation of the boronic acid pinacol ester shown in **Scheme 2.6** was found to be capricious, with the reaction sometimes requiring extra NMO to get full conversion. The reaction was found to go terribly under dry conditions with a mixture of by-products being formed.

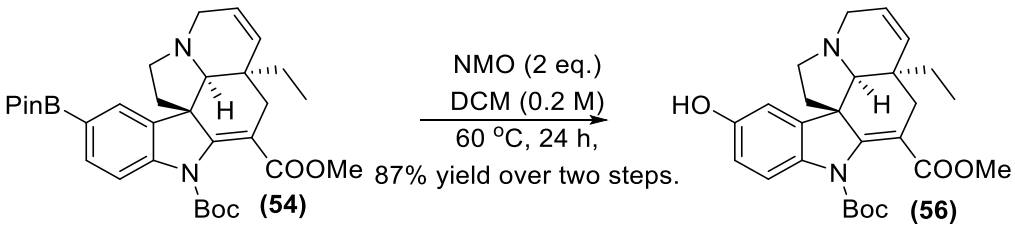

Scheme 2.6: Synthesis of *N*-Boc-15-hydroxy-tabersonine (51).

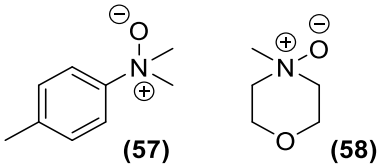

Figure 2.2: The *N*-oxides used by Zhu *et al.*[52]

Figure 2.2 shows two of the *N*-oxides tried in the Zhu *et al.* publication. Zhu stated that the oxidation of boronic acid pinacol esters to alcohols

using **(57)** as the oxidant worked better than **(58)**. After a few attempts, work done in the Moses group showed **(58)** worked significantly better than **(57),** giving almost full conversion and **(57)** affording about 50% yield over the same time period. Due to **(58)** working more efficiently and being commercially available, it was chosen to go forward with.

2.4.4 Synthesis of N-Boc-15-hydroxy-16-formyl-tabersonine.

The reactions leading up to this point were improved with relative ease. The initial reaction gave full consumption of starting material, though once purified, the yield would not be consistent and varied from 40-50%. A range of conditions were tried shown in **Table 2.7**.

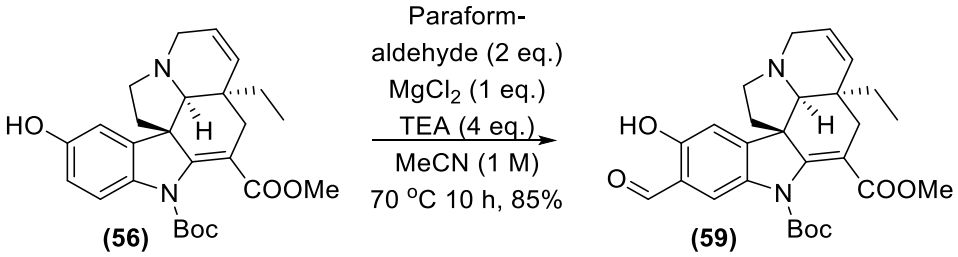

Scheme 2.7: Synthesis of *N*-Boc-15-hydroxy-16-formyl-tabersonine (54).

Table 2.7: Range of reactions tried in the optimisation of the formylation reaction.

Run	Formaldehyde source	Temperature (°C)	Yield[b] (%)
1	$(CH_2O)_n$	r.t.	0
2	$(CH_2O)_n$	50	46
3	$(CH_2O)_n$	70	50
4	$(CH_2O)_n$	90	12
5[a]	Trioxane	50	0
6[a]	Trioxane	70	0

[a]3M Hydrogen chloride in Et_2O was used as solvent. [b] isolated yield

The reactions in **Table 2.7** were performed at different temperatures with the hypothesis that the low yields was due to a degradation of starting material and/or product. Analysising run 4, the TLC and NMR spectrum showed that there was significant degradation happening at this temperature. Run 5 and 6 were performed to investigate if there is a substitute for paraformaldehyde. For the reaction to work, paraformaldehyde would need to crack before it can react with the starting material as paraformaldehyde is a polymer of formaldehyde. The literature states that complete cracking of paraformaldehyde is about 180 °C, which the starting material or product could not tolerate.[53,54] Trioxane on the other hand degrades with strong acid and at a lower temperature and dissolves in THF. These two reactions did not work with starting material and some degradation products being recovered. As these reactions gave average yields, other reactions were investigated.

There have been many different named reactions reported in the literature which would produce the desired ortho-formyl compound. In **Scheme 2.8**, the following methods would produce **(59)** from compound **(56)**.

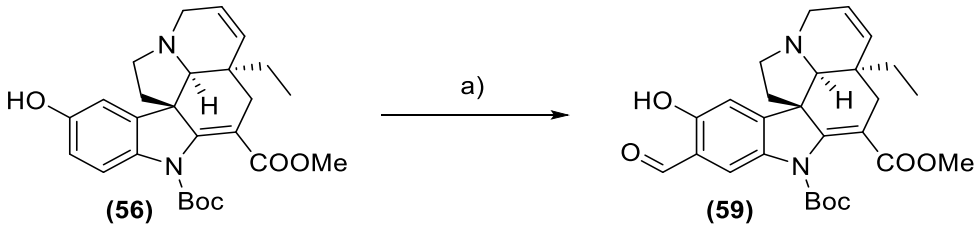

Scheme 2.8: Scheme for the reactions shown in Table 2.8.

Table 2.8: The general reagents used for each reaction.

Named reaction	Reagents and conditions	Yield[b] (%)
Duff	HMT (1 eq.), TFA (1 M), 60 °C	0
Reimer-Tiemann	KOH (1.2 eq.), $CHCl_3$ (1 M), 60 °C	0
Houben-Hoesch	$ZnCl_2$ 1M, Et_2O.HCl 2M, MeCN, r.t.	0
Rieche formylation	$TiCl_4$, Cl_2CHOMe, DCM, r.t.	62[a]

[a]The reaction gave 62% isolated yield of the de-protect product. [b] isolated yield

Once the phenol compound **(56)** had been formed, a formylation followed by a Baeyer-Villager or Dakin reaction would result in the catechol moiety. There are many literature reactions that can formylate a phenyl ring shown in **Table 2.8**, the first tried was the Duff reaction. This reaction will direct the formylation to the *ortho* position, and as the undesired *ortho* position is more sterically hindered, the reaction could potentially

formylate the position desired. This reaction uses hexamethylenetetramine (HMT) and a strong acid to protonate one of the amines. This then follows a series of equilibria reactions resulting in an iminium which on protic workup forms the desired product. Unfortunately, this reaction was unsuccessful. The only product recovered was the de-boc protected starting material. After repeating the reaction at higher temperatures, the starting material degrades and not recoverable.

The Reimer-Tiemann reaction uses a strong base to deprotonate chloroform to form the chloroform carbanion, which subsequently eliminates a chlorine atom to form the dichlorocarbene. The strong base also deprotonates the phenol proton, which delocalises into the benzene ring promoting nucleophilic attack of the dichlorocarbene. After basic workup, the desired compound is obtained. However, the strong base from this reaction degraded the starting material and no product was found by TLC or NMR.

The Houben-Hoesch reaction is a nucleophilic addition of a nitrile with the aid of a polarizing lewis acid forming an imine; this is then hydrolysed during aqueous workup to yield the desired compound. This reaction gave only starting material back. After trying at a range of higher temperatures, no product was isolated and more by-products were formed.

Lastly, the Rieche formylation was attempted. This goes *via* a Friedel-crafts type mechanism. This is then eliminated by the oxygen in the methoxy lone pair forming an oxocarbeneium compound.[55] This reaction worked quite well though 100% of the Boc protecting groups would be

cleaved. Lowering the temperatures reduces the yield of reaction but not the unwanted boc deprotection. Due to the methylation step requiring a protecting group on the indole nitrogen, or it would be methylated, the reaction was deemed not applicable as a second protection would be required.[56]

After the other reactions didn't work, the *ortho* formylation was revisited. As this is the only reaction that gave product, it was fully investigated. The reaction always had complete consumption of starting material, but after column chromatography, the yield was always about 40-50%. After questioning the integrity of the paraformaldehyde, a new bottle was purchased. Using this in the reaction then increased the yield from 40% to 98% indicating that the old bottle of paraformaldehyde had degraded.

2.4.5 Synthesis of 15-acetyl-tabersonine.

Another method tried was to acetylate the 15th position on tabersonine with a Friedel-Craft reaction shown in **Scheme 2.9**. From **(60)**, a Dakin reaction could be attempted to give the hydroxyl compound in 2 steps. The reaction never went fully to completion, with mostly starting material isolated with trace amounts of product present in the NMR.

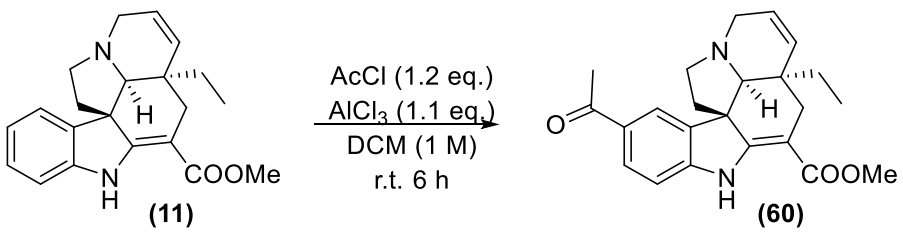

Scheme 2.9: Friedel-Crafts reaction on tabersonine.

2.4.6 Synthesis of *N*-Boc-15,16-dimethoxy-tabersonine *via* *N*-Boc-15-hydroxy-tabersonine-16-formate.

On repeating the two reactions, it was found to be quite capricious initially as the yields range from 10-50%, as shown in **Scheme 2.10**. But after the issues with the paraformaldehyde being degraded in the previous step, new reagents were bought and this gave a consistent reaction from thereafter. The oxidation of **(59)** to **(61)** also produced two other identifiable by-products from the reaction; these being the benzoic acid moiety, and the *N*-oxide moiety formed from the presence of hydrogen peroxide. Compound **(61)** is not isolated in this reaction, it has been found to be very unstable, and degrades readily in air.

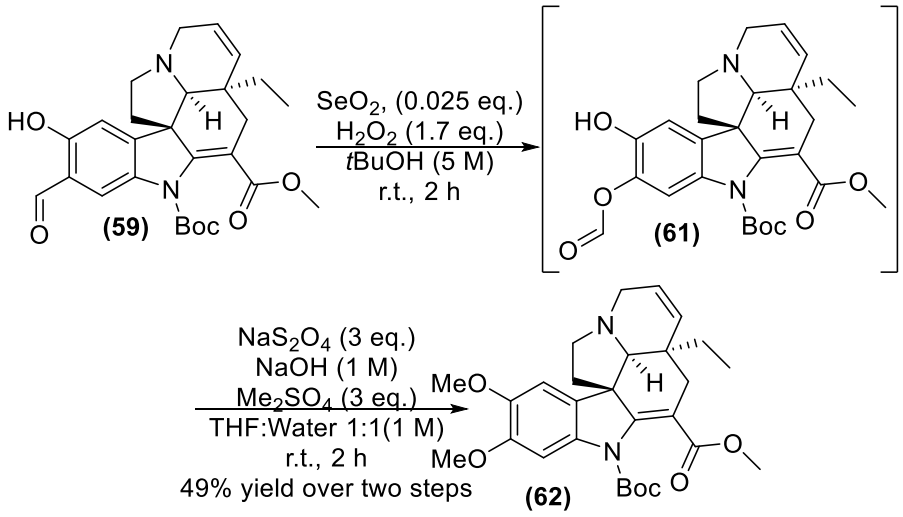

Scheme 2.10: Synthesis of *N*-Boc-15,16-dimethoxy-tabersonine *via* *N*-Boc-15-hydroxy-tabersonine-16-formate.

2.4.7 Synthesis of jerantinine A

The final steps of the synthesis proceeded in a 76% yield shown in **Scheme 2.11**. The Boc deprotection consumes 100% of the starting

material after 1 hour to produce compound **(63)**. The cerium ammonium nitrate (CAN) oxidation produces jerantinine A **(11)** in 50 % yield.[41]

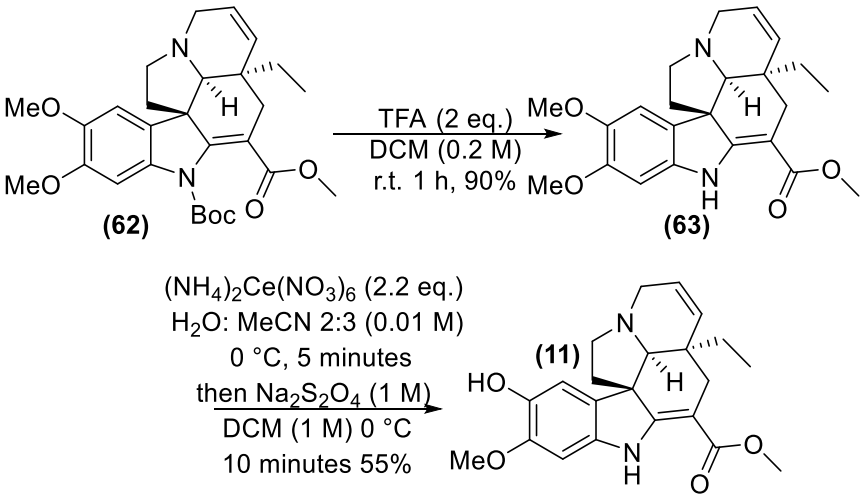

Scheme 2.11: Synthesis of jerantinine A.

In summary, the route used to synthesis jerantinine A is reasonable, providing jerantinine A in 9 steps with a 16% overall yield. There is still some work to be done on the optimisation of the Dakin and demethylation reaction, or to produce enough of **(62)** to get a larger reaction through for the last step. In total, over 150 grams of tabersonine was isolated from about 15 kg of seeds, and about 50 mg of jerantinine A synthesised.

2.5 Anti-cancer properties of tabersonine analogues.

The first biological test chosen was a 3-(4,5-dimethylthiazol-2-yl)-2,5-diphenyltetrazolium bromide **(64)** (MTT) assay. This is an important test which indirectly measures cell viability, from which estimated GI50 values can be calculated and used as a concentration guide in other biological tests. This is a colourimetric assay relies on NADPH-dependant

oxidoreductase enzymes of viable cells to indirectly reduce MTT to formazan **(65)**. The assay is concluded by measuring the absorbance of the sample at 570 nm, and using a calculation, an GI50 value can be estimated.

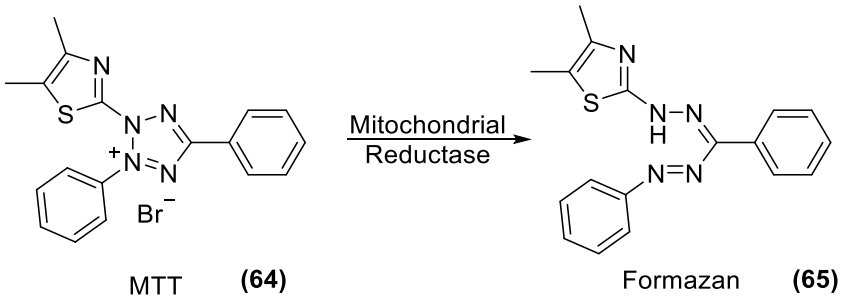

MTT **(64)** Formazan **(65)**

Scheme 2.12: MTT breakdown to formazan.

2.5.1 Results.

Table 2.9: GI_{50} of the intermediates tested from the synthesis of jerantinine A.

Compound	Potency μM
tabersonine	>50 μM
15-iodo-tabersonine	>50 μM
***N*-boc-15-iodo-tabersonine**	6.52±0.106 μM
tabersonine-15-Boronic acid pinacol ester	>50 μM
15 -hydroxy-tabersonine	>50 μM
***N*-boc-15-hydroxy-tabersonine-16-formate**	3.35±0.073 μM
***N*-boc-15,16-dimethoxy-tabersonine**	>50 μM
synthetic jerantinine A	0.853 μM
natural jerantinine A[33]	0.857 μM

***Results represent the average of eighteen replicates.**

Following the MTT assay, a clonogenic assay was undertaken. It is a technique that investigates the ability of single cancer cells to survive a brief challenge with test agent, to maintain proliferative capacity and go on to form progeny colonies. We compared the numbers of colonies formed following treatment of single cells with jerantinine A with those formed in the absence of treatment (control). Guided by MTT assays, cells were exposed to GI_{50} jerantinine concentrations; good similarity between natural and synthetic jerantinine A results were obtained.

Briefly, HCT-116 cells were seeded in well plates and allowed to grow for 24 hours and attach to the wells. They were then treated with jerantinine A for 24 hours. The treatment media is removed, cells were washed in sterile PBS before introduction of nutrient medium alone. Plates were returned to the incubator and colonies allowed to form. When colonies containing ≥50 cells were observed in control wells, the experiment was terminated. Colonies were fixed, stained and counted.

Jerantinine A showed a distinct inhibition of cell proliferation with the mean survival fraction being only 5% showing that jerantinine A was a cytotoxic compound.

The clonogenic assay was once considered the "gold standard" of cell sensitivity assays and originated from the evaluation of radiosensitivities of tumour cells *in vitro*. It was thought that only a clonogenic assay was sensitive enough to detect cell kill at low percentage survivals (<1%). More specifically, it measures the ability of a single cell to survive a brief exposure to the test agent and maintain proliferative potential to form colonies. The duration it takes for the cells to form colonies is comparable to recovery time. Furthermore, cytotoxic and cytostatic effects can be distinguished from each other after only a brief exposure to the test agent.

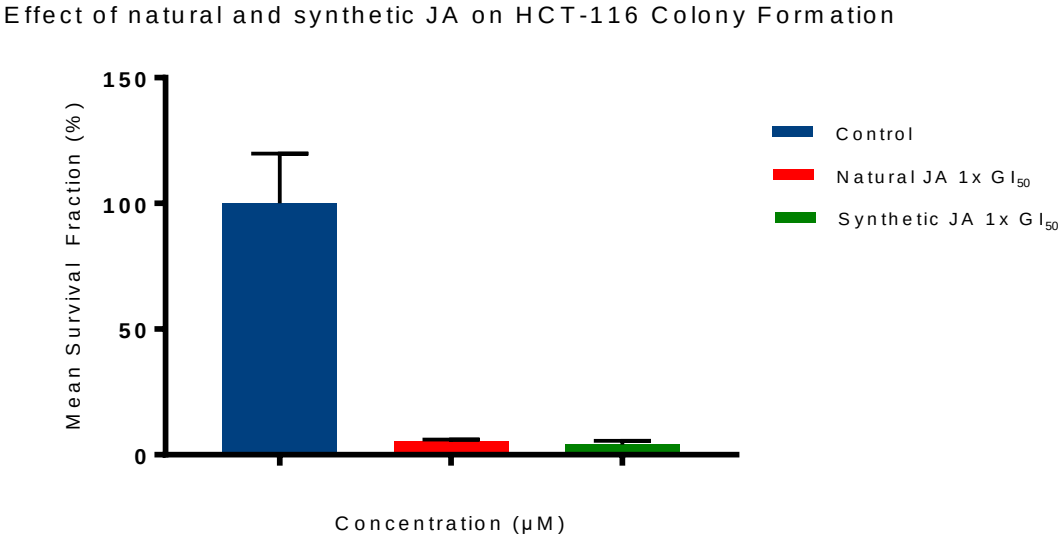

Figure 2.3: Mean survival fraction (%) of treated cells as a percentage of the control population for MCF-7.

From the results of the clonogenic assay, a cell cycle analysis was carried out on jerantinine A to investigate the mechanism of its cytotoxicity. This was chosen as vincristine and vinblastine shown in **Figure 2.4**, two compounds which have very similar structures to jerantinine A, are both tubulin destabilising agents.

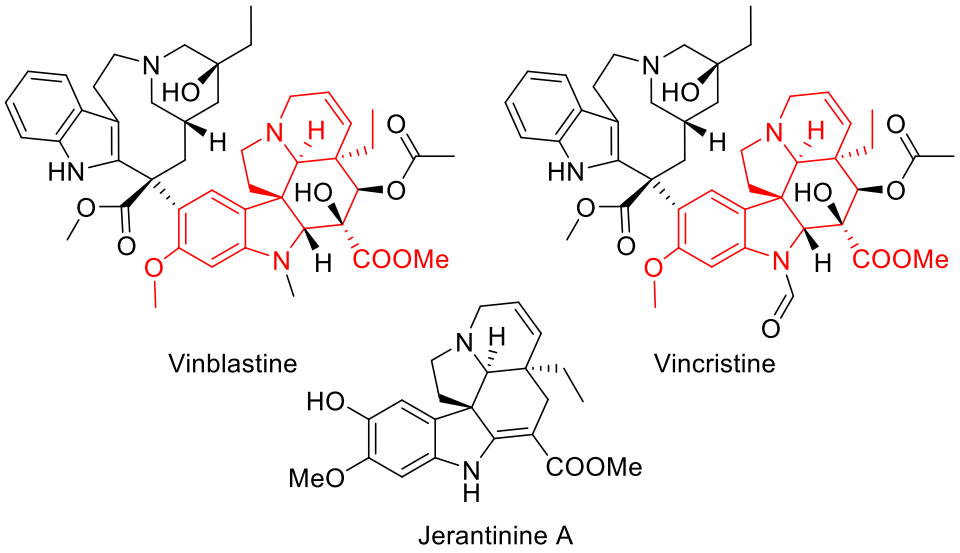

Figure 2.4: Structure of vinblastine and vincristine in relation to jerantinine A with jerantinine A subunit highlighted.

Cell cycle analysis uses propidium iodide (PI) to intercalate DNA, therefore quantitatively stains the DNA in a living culture of cells. There are 4 main phases of the cell cycle; *G0/1, S, G2* and *M stage* which is further split into prophase, prometaphase, metaphase, anaphase, telophase and cytokinesis all shown in **Figure 2.5**. G0 is a rest phase, where the cell has not started its cycle. *G1* is the first growth phase, in this phase cellular contents duplicate and the cell size increases. *S phase*, is where the DNA replicates itself, each of the 23 pairs of chromosomes replicates in the cell. *G2 phase* is where the cell prepares for mitosis and *M phases* is mitosis. As this analysis can only interpret how much DNA is in relation to each cell *G0* and *G1 phase* both have 1 equivalent of DNA, S phase has between 1 and 2 equivalents of DNA and *G2 and M phase* have 2 equivalents of DNA.

Briefly, the cells were seeded at 3–5 × 10^5 cells/dish in 10 mL of medium, treated, harvested and then re-suspended in fluorochrome solution (50 µg/mL PI, 0.1 mg/mL ribonuclease A, 0.1% v/v Triton X-100, and 0.1% w/v sodium citrate in $_dH_2O$). This then produces a histogram which shows the population of cells in each stage of mitosis by measuring the relative intensities of propidium iodide per cell.

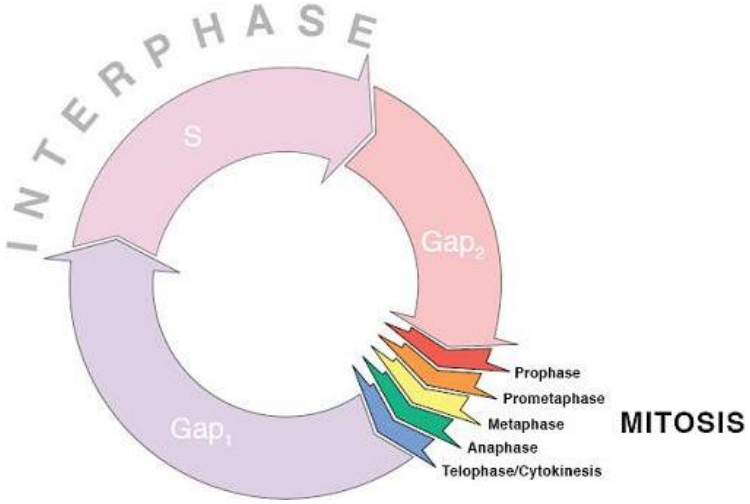

Figure 2.5: Mitosis cycle in a cell.

The cell cycle analysis demonstrated that jerantinine A caused profound G2/M cell cycle phase blocks. This is indicative of an agent that is perturbing tubulin/microtubule dynamics shown in **Figure 2.6**.

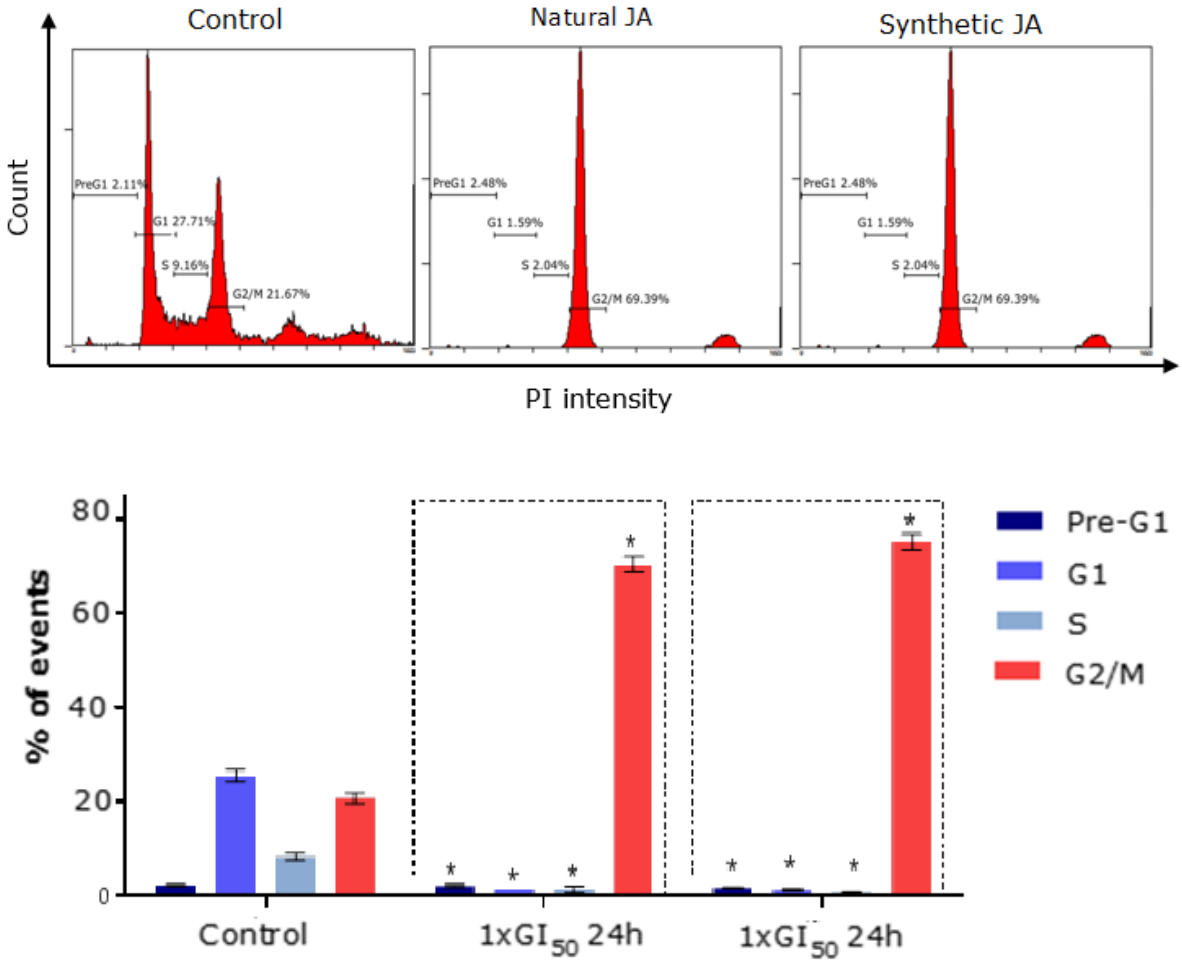

Figure 2.6: Cell cycle analysis of jerantinine A.

These results from the cell cycle analysis showing jerantinine to be an agent that is perturbing tubulin/microtubule dynamics, a tubulin polymerisation test was carried out. This is a technique that measures the fluorescence of tubulin when excited at 340 nm whilst it polymerises in the presence of the compound. As the chains get longer, a higher emission intensity is observed. Paclitaxel eliminates the nucleation phase and enhances the *V*max of the growth phase inducing rapid polymerisation of tubulin. Nocodazole causes a drastic decrease in *V*max and reduction in polymerisation of tubulin. The results showed that both synthetic and natural jerantinine A inhibit tubulin polymerisation.

Work done by our collaborators showed that jerantinine B, binds to the colchicine binding pocket on tubulin. This is opposed to the vinca alkaloids which bind to their own pocket.

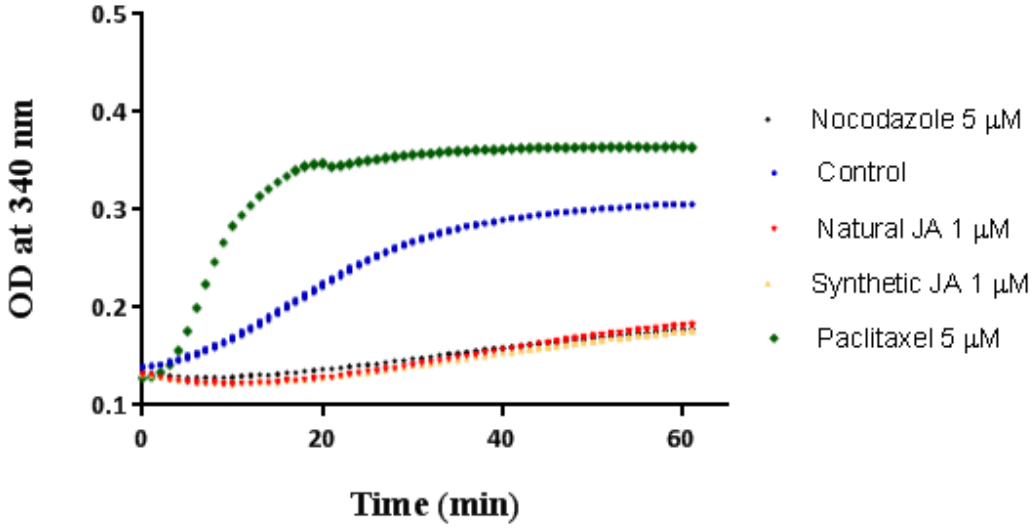

Figure 2.7: Tubulin polymerisation assay with nocaodazole and paclitaxel as references for tubulin polymerisation inhibiter and tubulin polymerisation promoter respectively.

After identifying jerantinine A as a tubulin destabilising agent, visual validation in cells was required to confirm this in cells. Images were captured to compare and visualise the effects of jerantinine A on cell morphology, DNA and tubulin. These were compared to untreated cells. After 24 hours of treatment, extensive mitotic disruption was observed. Multinucleation, nuclear fragmentation and multipolar spindles were clearly evident in treated cells exclusively. The morphology of untreated cells demonstrated normal healthy cell division shown in **Figure 2.8**.

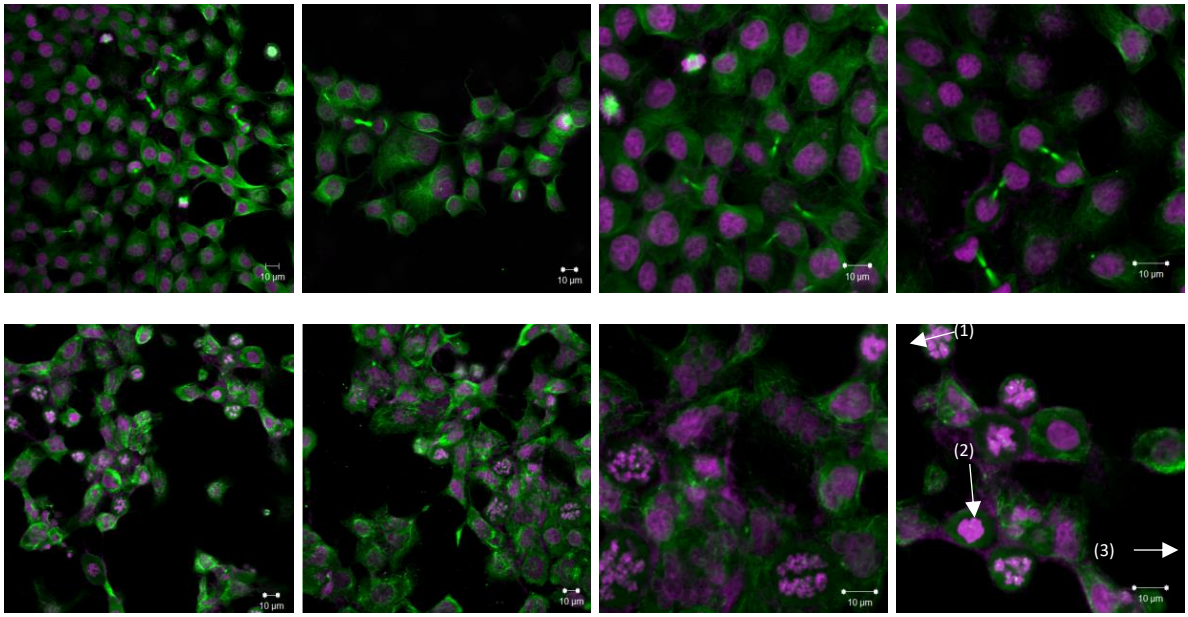

Figure 2.8. Effects of JA and JAA (24 h exposure) on MCF-7 cell morphology. 1st row: controls with vehicle only; 2nd row: JA (1x GI_{50} = 0.809 μM); JA caused multinucleation (1), nuclear fragmentation (2) and multipolar spindles (3).

Section 3: Conclusion

Jerantinine A has been successfully synthesised in 9 steps from tabersonine with a total yield of 16% which gives a start point for the synthesis of the other jerantinine alkaloids. There is still work to be done to improve this synthesis, especially with the Dakin reaction, which contributes significantly to the low overall yield.

Alongside this work, all the chemicals produced in the synthesis of jerantinine A have been tested against the MCF-7 cancer cell lines to test their anti-cancer properties. This is yet to find a compound with the same activity as jerantinine A.

3.1 Future Work

With a synthesis of jerantinine A optimised, synthesis of the other jerantinine alkaloids could be investigated and evaluated biologically. Jerantinine A is a good starting point for the synthesis of the other alkaloids. Jerantinine E was synthesised from jerantinine A by co-workers on our paper that we published on this work. This was achieved by a hydrogenation using palladium on carbon.

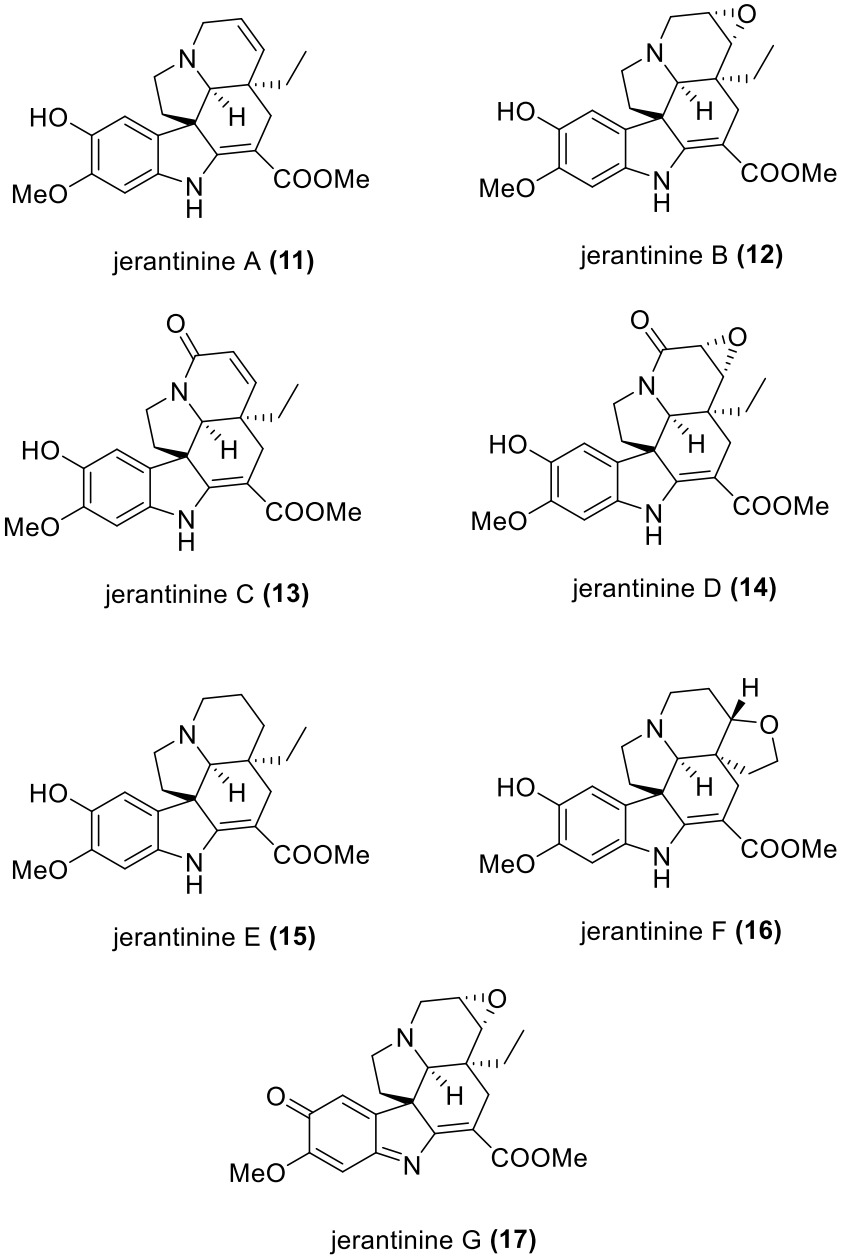

Figure 3.1: Structures of jerantinine A-G.

To form jerantinine B, an epoxidation from jerantinine A would yield the product. Jerantinine C could be formed *via* an oxidation to yield the allylic alcohol. Jerantinine D would be a combination of the routes found for the synthesis of jerantinine B and jerantinine C.

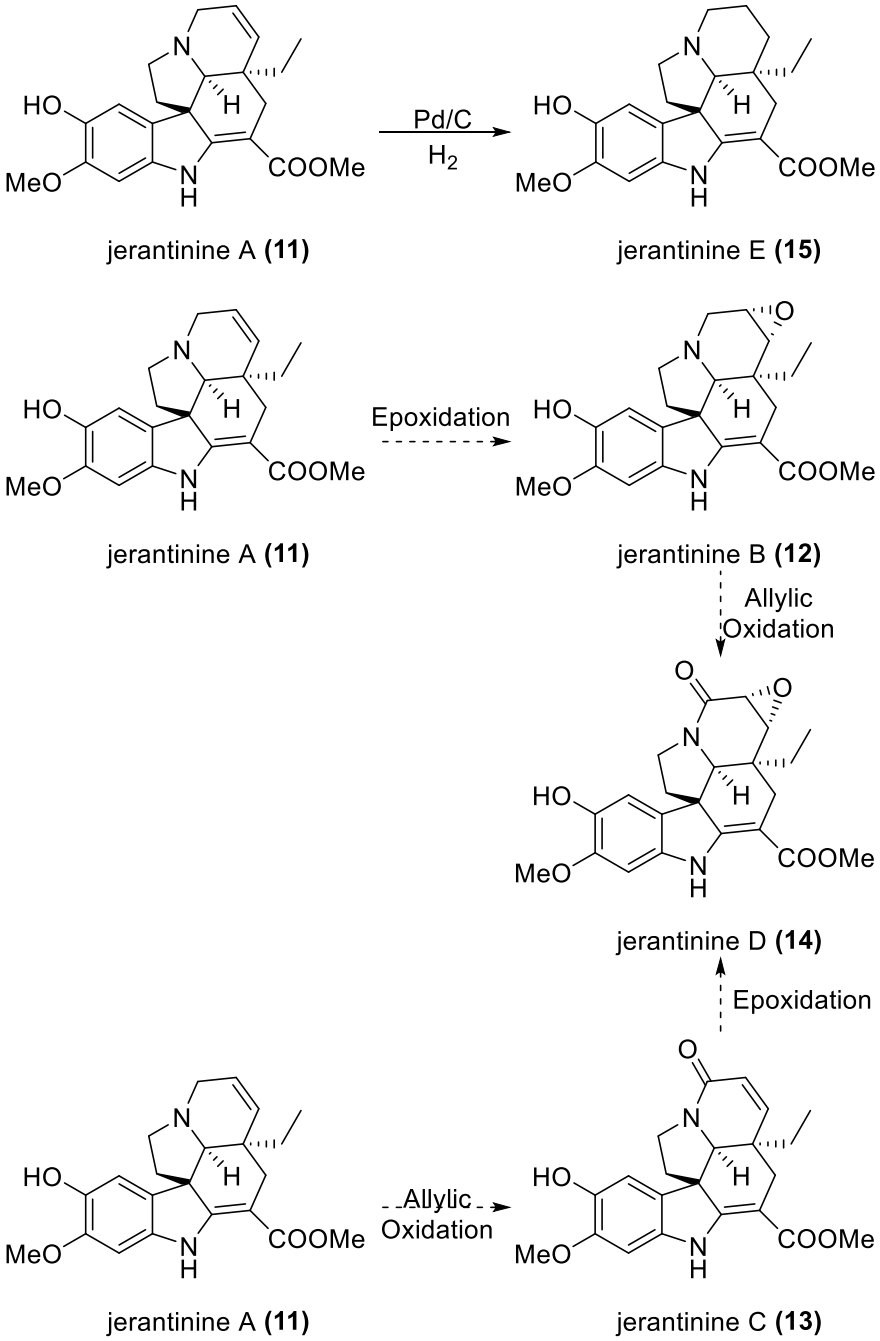

Scheme 3.1: Shows the potential synthesis of 5 selected jerantinine alkaloids.

Jerantinine F and G may require a different route entirely. Jerantinine F would require a remote oxidation on an ethyl group, and jerantinine G is a suspected biproduct of the cerium ammonium nitrate oxidation which is reduced by the sodium dithionite. Experimentally, this was shown to be a highly coloured compound and also not isolatable in large quantities as it self-reacts.

Section 4: Experimental.

4.1 General Procedure.

NMR spectra were recorded on Bruker Advance 400 spectrometer (^{1}H 400 MHz, ^{13}C 101 MHz) and are referenced internally according to residual solvent signal. The chemical shifts values (δ) are reported in ppm with TMS as internal standard ($CDCl_3$: δ 7.26 for ^{1}H-NMR, δ 77.0 for ^{13}C-NMR). Data are reported as follows: chemical shifts, multiplicity (br = broad, s = singlet, d = doublet, t = triplet, q = quartet, m = multiplet), coupling constants (Hz), and integration. LC-MS spectra were recorded on Bruker MicroTOF (Time of Flight) mass spectrometer using Electron Spray Ionisation (ESI). GC analysis was performed with on Agilent 6850 equipped with a CP CHIRASIL-DEX CB (Varian, 25 m x 0.25 mm) column; injector and detector temperatures: 200 °C. IR spectra were recorded on a Bruker ATR.

4.2 Analyses.

NMR spectra (^{1}H, ^{13}C and ^{11}B) were recorded on Bruker AV400 (400 MHz for ^{1}H NMR, 100 MHz for ^{13}C NMR), AV3400 (400 MHz for ^{1}H NMR, 100 MHz for ^{13}C NMR) and DPX300 (300 MHz) spectrometers, in $CDCl_3$. Infra-red spectra were obtained using a Bruker Tensor 27 FT-IR spectrophotometer as a solution in $CHCl_3$, with the peaks recorded as ν_{max} /cm^{-1}. HRMS were obtained using a Bruker MicroTOF mass spectrometer operating in electrospray ionisation (ESI) or electron ionisation (EI) mode. Melting point data was collected using a Stuart SMP3 apparatus.

4.3 Synthesis of jerantinine A.

4.3.1 Tabersonine (10).

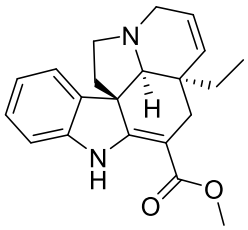

Voacanga africana seeds (200 g) were ground into a fine powder and suspended in 1% aqueous H_2SO_4 (2.0 L). The resulting mixture was then stirred overnight. The acid extract was then filtered through a muslin cloth and NaCl (200 g) added to the filtrate, which was then allowed to stir for 15 hours. $CHCl_3$ (1.5 L) was then added and the biphasic solution vigorously stirred for 3 hours. After settling, the aqueous layer was removed and discarded and the remaining organic emulsion filtered through Celite®. The resulting solution was then separated and the organic fraction dried over anhydrous $MgSO_4$ and filtered. Solvent was then removed and the resulting material dissolved in $CHCl_3$ (50 mL) and 30% aqueous NH_3 (30 mL) added. The solvent was again removed and the resulting material dissolved in chloroform (50 mL) and washed with H_2O (3 x 20 mL). The organic fraction was then dried over anhydrous $MgSO_4$ and filtered. The crude material obtained upon removal of the solvent was then purified by column chromatography (0-10% EtOAc in petroleum ether 40-60 °C) to give tabersonine (2.8 g) as a white solid. M.p. 78 °C; ^{1}H NMR (400 MHz, Chloroform-*d*) δ 9.00 (s, 1H), 7.23 (m, 1H), 7.14 (m, 1H), 6.87 (d, *J* = 7.4 Hz, 1H), 6.81 (d, *J* = 7.8 Hz, 1H), 5.79 (m, 1H), 5.71 (d, *J* = 10.0 Hz, 1H), 3.77 (s, 3H), 3.46 (m, 1H), 3.19 (d, *J* = 15.8 Hz, 1H), 3.04 (t, *J* = 7.4 Hz, 1H), 2.76 – 2.65 (m, 2H), 2.56 (m, 1H), 2.44 (d, *J* = 15.1 Hz, 1H), 2.07 (m, 1H), 1.79 (m, 1H), 1.00 (m,

1H), 0.87 – 0.81 (m, 1H), 0.64 (t, *J* = 7.4 Hz, 3H); ^{13}C NMR (101 MHz, Chloroform-*d*) 169.1, 166.9, 143.3, 138.2, 133.2, 127.8, 125.0, 121.6, 120.7, 109.4, 92.3, 70.2, 55.2, 51.1, 51.1, 50.7, 44.6, 41.4, 28.6, 27.0, 7.6; FTIR (neat) ν_{max}: 3367, 3023, 2960, 1670, 1604, 1131 cm^{-1}; Found (EI$^+$): 337.1834 [M]$^+$, (Required $C_{21}H_{24}N_2O_2$ 337.1838) $[\alpha]_D^{23}$ –250.12 (*c* 1.0, $CHCl_3$). In accordance with literature data.[33]

4.3.2 15-Iodo-tabersonine (52).

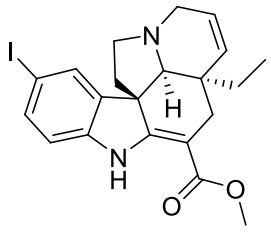

To a stirred solution of tabersonine (2.93 g, 8.71 mmol) in TFA (120 mL) was added NIS (1.96 g, 8.71 mmol) in 4 portions over 30 minutes. The reaction was then stirred under argon overnight. The reaction mixture was then cooled to 0 °C and poured slowly into an aqueous solution of NaOH (2M, 1 L) at 0 °C and extracted with DCM (4 x 50 mL). The combined organic fractions were then dried over anhydrous $MgSO_4$ and filtered. Solvent was then removed to yield a crude solid, which was dissolved in hot pentane (250 mL) and allowed to cool before filtering. Solvent was then removed to give the desired product (3.79 g, 94%) as a white solid. m.p.: 85 °C; ^{1}H NMR (400 MHz, Chloroform-*d*) δ 8.98 (s, 1H), 7.49 (s, *J* = 1.7 Hz, 1H), 7.43 (m, 1H), 6.60 (m, 1H), 5.78 (m, 1H), 5.69 (d, *J* = 9.9 Hz, 1H), 3.76 (s, 3H), 3.44 (m, 1H), 3.20 (d, *J* = 15.9 Hz, 1H), 3.04 (t, *J* = 7.1 Hz, 1H), 2.68 (m, 1H), 2.62 (s, 1H), 2.54 (dd, *J* = 15.1, 1.8 Hz, 1H), 2.40 (d, *J* = 15.1 Hz, 1H), 2.05 (m, 1H), 1.81 (m, 1H), 0.97 (m, 1H), 0.85 (m, 1H), 0.64 (t, *J* = 7.4 Hz, 1H); ^{13}C NMR (101 MHz, Chloroform-*d*) δ 168.9, 165.5, 143.0, 136.4, 132.7, 130.3, 124.8,

111.3, 109.3, 92.8, 82.4, 70.0, 55.1, 51.1, 50.9, 50.4, 44.5, 41.0, 28.5, 27.0, 7.5; FTIR (neat) ν_{max}: 3359, 3022, 2959, 1671, 1131 cm^{-1}; Found (EI^+): 463.0823 $[M]^+$, (required $C_{21}H_{23}IN_2O_2$: 463.0824) $[\alpha]_D^{23}$ –119 (*c* 1.0, $CHCl_3$)

4.3.3 N-Boc-15-iodo-tabersonine (53).

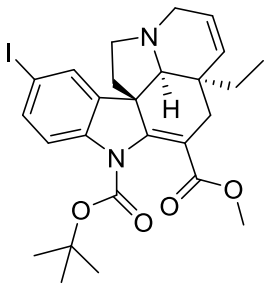

To a stirred solution of 15-Iodo- tabersonine (11.9 g, 25.7 mmol) in THF (250 mL) was added Boc_2O (8.20 mL, 77.1 mmol) and DMAP (0.313 g, 2.57 mmol). The reaction was stirred under reflux at 60 °C for 18 hours. The THF was removed under reduced pressure and then extracted with DCM, this was then washed 3 times with water. The organic fractions were then combined and dried over anhydrous $MgSO_4$ and filtered. Solvent was then removed to yield a crude solid which was subsequently purified by column chromatography (SiO_2, 10% EtOAc in petroleum ether 40-60 °C) to give pure white compound (13.1 g, 95 % yield). m.p.: 83 °C; ^1H NMR (400 MHz, Chloroform-*d*) δ 7.56 (m, 1H), 7.49 (d, *J* = 1.8 Hz, 1H), 7.46 (d, *J* = 8.4 Hz, 1H), 5.87 – 5.82 (m, 1H), 5.73 (d, *J* = 10.1 Hz, 1H), 3.78 (s. 3H), 3.51 (m, 1H), 3.12 (d, *J* = 15.9 Hz, 1H), 3.06 (t, *J* = 7.7 Hz, 1H), 2.71 (d, *J* = 15.2 Hz, 1H), 2.59 (s, 1H), 2.52 (m, 1H), 2.32 (m, 1H), 2.17 (m, 1H), 1.81 (m, 1H), 1.56 (s, 9H), 1.05 (m, 1H), 0.66 (t, *J* = 7.5 Hz, 3H). ^{13}C NMR (101 MHz, Chloroform-*d*) δ 167.9, 165.2, 150.8, 141.1, 140.5, 136.4, 132.4, 129.8, 125.1, 118.1, 112.0, 86.6, 82.7, 68.1, 52.5, 51.7, 51.3, 50.9, 43.0, 41.3, 31.1, 28.2, 26.4, 7.6. FTIR (neat) ν_{max}:

2933, 2777, 1714, 1147 cm^{-1} ; Found (EI^+): 563.1322 $[M]^+$, (Required $C_{26}H_{31}IN_2O_4$ 563.1324) $[\alpha]_D$ –44.32 (*c* 1.0, $CHCl_3$)

4.3.4 *N*-Boc-tabersonine-15-Boronic acid pinacol ester (54).

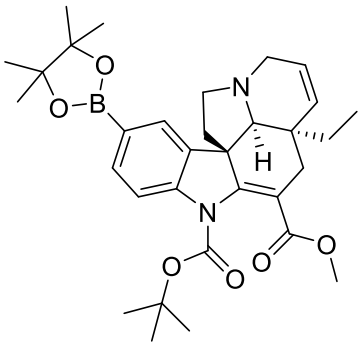

To a stirred solution of *N*-Boc-15-iodo-tabersonine(5.00 g, 8.8 mmol) in THF (250 mL) was added Cs_2CO_3 (4.3 g, 13.2 mmol), B_2Pin_2 (3.35 g, 13.2 mmol), CuI (0.335 g, 1.76 mmol), PPh_3 (0.209 g, 0.88 mmol) and $Pd(OAc)_2$ (0.197 g, 0.88 mmol) at room temperature and left until full consumption of starting material by TLC (usually 24 hours). The reaction mixture was then filtered through celite® and then concentrated to yield a brown fluffy solid. The compound then proceeds to the next step without further purification. A small sample was purified by column chromatography (SiO_2, 20% EtOAc in petroleum ether 40-60°C) for analytical and biological purposes. m.p.: 94 °C; ^{1}H NMR (400 MHz, Chloroform-*d*) δ 7.72 (m, 1H), 7.65 (m, 1H), 7.55 (s, 1H), 5.78 (m, 1H), 5.65 (m, 1H), 3.74 (s, 3H), 3.48 (m, 1H), 3.16 (m, 1H), 3.04 – 2.95 (m, 1H), 2.76 – 2.65 (m, 2H), 2.58 (m, 1H), 2.29 (d, *J* = 15.1 Hz, 1H), 2.13 (m, 1H), 1.75 (m, 1H), 1.53 (s, 9H), 1.34 (s, 12H), 1.08 (m, 1H), 0.93 (m, 1H), 0.60 (t, *J* = 7.5 Hz, 3H); ^{11}B NMR (96 MHz, Chloroform-*d*) δ 29.1 ^{13}C NMR (101 MHz, Chloroform-*d*) δ 168.0, 150.9, 150.2, 143.3, 137.8, 135.1, 132.6, 126.7, 125.1, 115.2, 111.5, 83.7, 82.4, 67.8, 52.5, 51.6, 51.4, 50.8, 43.0, 41.5, 30.9, 28.2, 26.3, 24.9, 7.6. FTIR (neat) ν_{max} 2974,

2932, 1720, 1140 cm^{-1}; Found (EI^+): 563.3222 $[M]^+$, (Required $C_{32}H_{43}BN_2O_6$ 563.3224). $[\alpha]_D^{23}$ –16.62 (*c* 1.0, $CHCl_3$).

4.3.5 N-Boc-15-hydroxy-tabersonine (56).

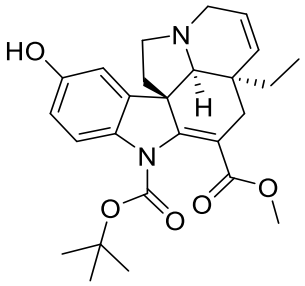

To a stirred solution of crude *N*-Boc-tabersonine-15-Boronic acid pinacol ester (assumed 8.8 mmol) in DCM (125 mL) was added NMO hydrate (4.75 g, 35.2 mmol) in 2 portions over 2 hours. The reaction was heated (60 °C) for 24 hours and then solvent was removed by reduced pressure. The remaining solid was purified by column chromatography (SiO_2, 30% EtOAc in petroleum ether 40-60 °C) to yield a pure white solid (3.7 g, 87% yield over 2 steps.) m.p.: 128 °C; ^1H NMR (400 MHz, Chloroform-*d*) δ 7.51 (m, 1H), 6.76 (m, 1H), 6.68 (m, 1H), 5.80 (m, 1H), 5.73 – 5.61 (m, 1H), 5.09 (s, 1H), 3.78 (s, 3H), 3.50 (m, 1H), 3.14 – 2.99 (m, 2H), 2.72 (d, *J* = 15.1 Hz, 1H), 2.59 (s, 1H), 2.50 (m, 1H), 2.30 (dd, *J* = 15.1, 1.8 Hz, 1H), 2.17 (m, 1H), 1.81 (m, 1H), 1.56 (s, 9H), 1.18 – 0.95 (m, 2H), 0.65 (t, *J* = 7.4 Hz, 3H). ^{13}C NMR (101 MHz, Chloroform-*d*) δ 168.3, 152.1, 151.2, 150.0, 140.0, 134.1, 132.7, 125.1, 116.9, 113.5, 111.7, 108.9, 82.1, 68.1, 52.6, 51.6, 51.4, 51.0, 42.9, 41.4, 31.2, 28.2, 26.4, 7.6. FTIR (neat) ν_{max}: 3347, 3025, 2767, 1720, 1683, 1112 cm^{-1}; Found (EI^+): 453.2319 $[M]^+$, (Required $C_{26}H_{32}N_2O_5$ 453.2317). $[\alpha]_D^{23}$ –30.33 (*c* 1.0, $CHCl_3$)

4.3.6 N-Boc-15-hydroxy-16-formyl-tabersonine (59).

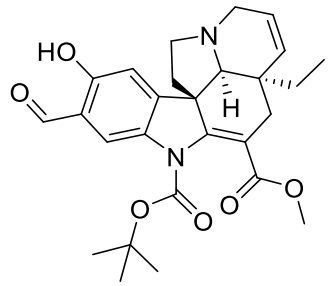

To a dry microwave vial, a stirred solution of *N*-Boc-15-hydroxy-tabersonine (0.100 g, 0.22 mmol) in THF (1 mL) was added $MgCl_2$ (0.023 g, 0.25 mmol), NEt_3 (0.114 mL, 0.85 mmol) and paraformaldehyde (0.03 g, 1 mmol), and heated to 70 °C under argon. After 24 hours, the solvent was removed under reduced pressure and the compound was washed with 1 M HCl and extracted with DCM (10 mL x 3). The organic fractions were then combined and were washed with further water (20 mL x 2). The organic phase was then dried over anhydrous $MgSO_4$ and filtered. The solvent was removed by reduced pressure and purified by column chromatography (SiO_2, 40% EtOAc in petroleum ether 40-60 °C) to yield a fluorescent yellow solid (0.102 g, 85% yield). m.p.: 190 °C; ^{1}H NMR (400 MHz, Chloroform-*d*) δ 11.27 (s, 1H), 9.84 (s, 1H), 7.85 (s, 1H), 6.87 (s, 1H), 5.81 (m, 1H), 5.64 (m, 1H), 3.77 (s, 3H), 3.50 (m, 1H), 3.21 – 2.96 (m, 2H), 2.71 (d, *J* = 15.2 Hz, 1H), 2.63 (s, 1H), 2.49 (m, H), 2.30 (m, 1H), 2.17 (m, 1H), 1.80 (m, 1H), 1.54 (s, 9H), 1.12 – 0.80 (m, 2H), 0.63 (t, *J* = 7.4 Hz, 3H). ^{13}C NMR (101 MHz, Chloroform-*d*) δ 196.0, 167.7, 159.5, 151.0, 148.6, 148.6, 133.5, 132.3, 125.2, 119.3, 118.7, 112.5, 110.6, 82.7, 67.9, 53.1, 51.7, 51.4, 51.0, 43.0, 41.3, 31.2, 28.1, 26.4, 7.6; FTIR (neat) ν_{max}/cm^{-1}: 2963, 2930, 1711, 1651 cm^{-1}, Found (EI$^+$):

481.2263 $[M]^+$, (required $C_{27}H_{32}N_2O_6$: 481.2260). $[\alpha]_D^{23}$ -48.48 (c 1.0, $CHCl_3$)

4.3.7 N-Boc-15-hydroxy-tabersonine-16-formate (61).

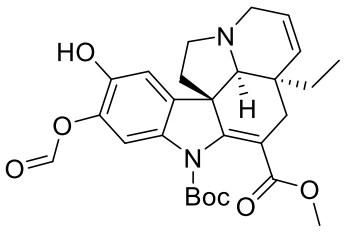

To a stirred solution of *N*-Boc-15-hydroxy-16-formyl-tabersonine (0.100 g, 0.21 mmol) in the minimal amount of *t*BuOH (100 µL), SeO_2 (2.00 g, 0.063 mmol) was added and 30% H_2O_2 (0.5 mL) added drop wise over 5 minutes at room temperature and reacted. After full consumption of starting material (TLC), the solution was extracted with Et_2O (5 mL x 3). The organic fractions were then combined and washed with brine (10 mL x 2). This was then dried over anhydrous $MgSO_4$ and filtered, solvent removed under reduced pressure and the crude was taken forward to the next step.

4.3.8 N-Boc-15,16-dimethoxy-tabersonine (62).

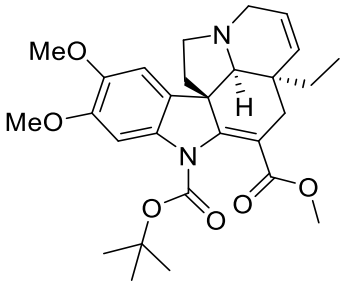

To a microwave vial, a stirred solution of *N*-Boc-15-hydroxy-tabersonine-16-formate (0.170 g, 0.34 mmol) in a 1:1 mixture of THF to water (3.5 mL) was added 1M NaOH (1.7 mL) and $Na_2S_2O_4$ (0.354 mg, 2.04 mmol),

this was stirred for 5 minutes. Then, Me_2SO_4 (0.15 mL, 1.7 mmol) was added and stirred for 1 hour. The THF removed by reduced pressure and then the solution was extracted with EtOAc (5 mL x 3). The organic fractions were then combined and washed with brine (10 mL x 2). The organic fraction was then dried over anhydrous $MgSO_4$ and filtered. The solvent was removed by reduced pressure and the crude product was purified by column chromatography (SiO_2, 40% EtOAc in petroleum ether 40-60 °C) to yield a white solid (0.051 g, 49% over two steps) m.p.: 85 °C. ^{1}H NMR (400 MHz, Chloroform-*d*) δ 7.43 (s, 1H), 6.88 (s, 1H), 5.87 – 5.74 (m, 1H), 5.73 – 5.64 (m, 1H), 3.94 (s, 3H), 3.90 (s, 3H), 3.84 (s, 3H), 3.51 (m, 1H), 3.23 – 3.04 (m, 2H), 2.73 (d, *J* = 15.1 Hz, 1H), 2.57 (s, 1H), 2.53 (m, 1H), 2.28 (m, 1H), 2.24 – 2.19 (m, 1H), 1.83 (m, 1H), 1.62 (s, 9H), 1.15 - 1.08 (m, 2H), 0.63 (t, *J* = 7.5 Hz, 3H).; ^{13}C NMR (101 MHz, Chloroform-*d*) δ 168.1, 151.2, 148.4, 145.4, 134.2, 132.8, 129.5, 125.1, 111.8, 105.6, 101.8, 82.0, 68.0, 56.8, 56.1, 52.6, 51.5, 51.5, 51.1, 42.8, 41.5, 31.2, 30.3, 28.2, 26.4, 7.6. FTIR (neat) ν_{max}: 2955, 2921, 1700, 1663, 1287, 1149; Found (EI$^+$): 496.2567 [M]$^+$, (Required $C_{28}H_{36}N_2O_6$: 496.2573). $[\alpha]_D^{23}$ –45.57 (*c* 1.0, $CHCl_3$)

4.3.9 15,16-Dimethoxy-tabersonine (63).

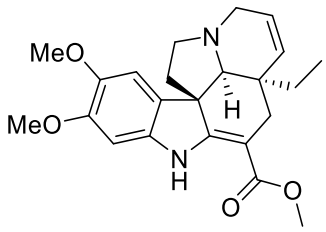

To a stirred solution of N-Boc-15,16-dimethoxy-tabersonine (0.051 g, 0.10 mmol) a solution of 20 % TFA in DCM (v/v 1 mL) was added and stirred at room temperature and reacted. Once full consumption of starting material has been achieved monitored by TLC and MS, the solution was neutralised and basified with 2 M NaOH and the layers

separated. The aqueous phase was then washed with DCM (10 mL x 3) and all organic layers were combined. These were then washed with 1M NaOH (20 mL x 1) and with water (20 mL x 2). This was then dried over anhydrous $MgSO_4$ and filtered. The solvent was removed by reduced pressure and the crude was put forward to the next step.

4.3.10 Jerantinine A (11).

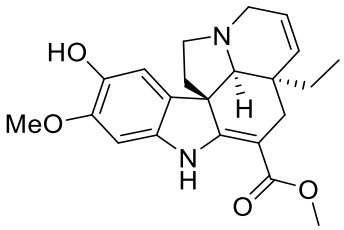

A stirred solution of 15,16-Dimethoxy-tabersonine (0.040 g, 0.10 mmol) was dissolved in MeCN (3 mL) and cooled to 0 °C. To the mixture, a solution of ceric ammonium nitrate (0.12 g, 0.22 mmol) dissolved in water (1 mL) at 0 °C was added. The reaction was stirred for 5 minutes and then poured in a 1 M $Na_2S_2O_4$ solution (10 mL). The reaction was stirred for a further 10 minutes before being diluted with DCM (5 mL) and extracted. The aqueous phase was washed with DCM (10 mL x 3) and then the organic fractions were combined. This was then washed with brine (20 mL x 1) and dried over anhydrous $MgSO_4$ and filtered. The solvent was removed by reduced pressure and the crude product was purified by column chromatography (SiO_2, 50% EtOAc in petroleum ether 40-60 °C) to yield a pink solid (0.026 g, 49.5% over two steps). m.p.: 63.5 °C; ^{1}H NMR (400 MHz, Chloroform-*d*) δ 8.87 (s, 1H), 6.94 – 6.88 (m, 1H), 6.46 (s, 1H), 5.79 (m, 1H), 5.82 – 5.76 (m, 1H), 5.32 (s, 1H), 3.90 (s, 3H), 3.77 (s, 3H), 3.52 – 3.41 (m, 1H), 3.21 (dt, *J* = 15.9, 1.9 Hz, 1H), 3.10 – 3.03 (m, 1H), 2.7 (ddd, *J* = 10.5, 8.2, 4.5 Hz, 1H), 2.6 (d, *J* = 1.7 Hz, 1H), 2.5 – 2.4 (m, 1H), 2.1 – 2.0 (m, 1H), 1.8 (m, 1H), 1.1 – 0.8 (m, 2H), 0.7 (t, *J* = 7.4 Hz, 3H); ^{13}C NMR (101 MHz, Chloroform-

d) δ 169.1, 167.8, 145.9, 139.9, 136.1, 133.1, 130.1, 124.9, 108.8, 94.5, 91.8, 70.2, 56.3, 55.3, 51.0, 51.0, 50.6, 44.4, 41.5, 28.4, 26.9, 7.5. FTIR (neat) ν_{max}: 3548, 3379, 3035, 2965, 1669, 1605, 1110 cm^{-1}. Found (EI^+): 382.1977 $[M]^+$, (Required $C_{22}H_{26}N_2O_4$ 382.1977). $[\alpha]_D^{23}$ –231 (*c* 1.0, $CHCl_3$). In accordance with literature.[33]

4.4 Analysis of anti-cancer properties of tabersonine analogues.

4.4.1 General Procedure.

All work is done inside the BioMat^2 MDH Class II microbiological safety cabinet constituting a laminar flow system which is emptied and washed thoroughly with 70% ethanol solution before any work is undertaken. All equipment or materials are sprayed thoroughly with 70% ethanol solution before entering the cabinet.

The MCF-7 cells are kept in a cell bank that is kept under liquid nitrogen. Counting the cells using a microscope is done consistently, with cells on the edges of the haemocytometer are not included. RPMI-1640 medium containing 0.3 g/L L-glutamine and 2 g/L sodium bicarbonate supplemented with 10% heat-inactivated foetal bovine serum. The foetal bovine serum was heat-inactivated by heating to approximately 56 ^oC for 1 h and either added immediately to RPMI 1640 medium or frozen in 50 mL aliquots.

4.4.2 Making stock solution of cells.

MCF-7 cells are incubatored; these are then checked by microscope to see if the cells are healthy. Solutions of trypsin, RPM-1640 medium and foetal bovine serum are placed into a 37 °C water bath for 3 minutes. Foetal bovine serum (50 mL) is then added to the RPMI-1640 medium and this is mixed and labelled. The solution containing the cells is then removed by aspiration. Trypsin (1.5 mL) is then added to the flask to remove all the cells that are stuck to the flask's wall, this is incubated for 3-5 minutes. The new cloudy solution then has RPMI-1640 medium (8 mL) added which inhibits the trypsin and the solution is now removed from the flask and put into a 50 mL screw cap tube. From this, 2 new stock solutions are made by getting a large flask, adding RPMI-1640 medium (12 mL) and adding either 200 µL or 500 µL of the cell suspension solution depending on when the stock solution will be used. Cells must be `used` straight away – either re-seeded into culture flasks of used to set up experiments.

4.4.3 Counting and seeding cells.

Using the cell suspension from the previous step, the number of cells needs to be counted. This is done using a haemocytometer which has been sterilised by 70% ethanol solution. On each counting square, 10 µL of cell suspension is added onto each side and the numbers of cells are counted under a microscope. This is performed twice getting an average so the number is more reliable. In each well of a 96 well plate, about 3000 cells need to be added. Using the equation X, this can be worked out;

$$Volume\ required\ for\ 3000\ cells = \frac{(Average\ number\ of\ cells\ x\ dilution\ factor\ )}{3000}$$

Equation 4.1: The equation used to work out the volume of cell suspension required for 3000 cells in 1 well of a 96 well plate.

Once this value has been calculated, cells are seeded into 96-well plates. As a time zero (T0) plate is also required to enable calculation of GI_{50} values, ~ 150 wells require seeding which is multiplied by the volume required in each well for 3000 seeds. To each well, 180 µL of solution is required, assuming 150 wells are requiring seeding, this would require 27 mL of solution. To make up this solution, RPMI-1640 medium with 10% foetal bovine serum (27 mL) is added to a petri dish. The volume of cell suspension needed for 150 wells is then removed by pipette from the 27 mL of RPMI-1640 medium with 10% foetal bovine serum and the cell suspension is then added.

4.4.4 Plating cells.

The plates are labelled with the date, and cell type. For the run, the outer layer of wells on the 96 well plate are filled with just RPMI-1640 medium with 10% foetal bovine serum (180 µL), the inner wells are then filled with 180 µL of the cell suspension solution. For the T0 control, only 3 rows of wells are filled with the cell suspension, with an outer ring of RPMI-1640 medium with 10% foetal bovine serum. This is then incubated overnight for the cells to return to a normal cell cycle before any chemical treatment.

4.4.5 Serial dilution of compound ready for treatment of cells.

A 10 mM top stock in DMSO is prepared of the chemical being tested, aliquoted into eppendorfs (10 µL per Eppendorf) and stored in the freezer until use. Serial dilutions of test agent are prepared in nutrient medium from the 10 mM top stock. These dilutions are made following **Table 4.1**, which shows the volume of RPMI-1640 medium with 10% foetal bovine serum and the volume and which cell solution is required to make each concentration. The cell line seeded the day before is taken out of the incubator and each concentration of compound solution is added according to **Figure 4.2**.

Table 4.1: Shows the volumes of each solution required to make each concentration.

Concentration required	Volume of medium	Volume of jerantinine solution
0.05 µM	900 µL	100 µL of 0.5 µM
0.1 µM	900 µL	100 µL of 1 µM
0.5 µM	900 µL	100 µL of 5 µM
1 µM	900 µL	100 µL of 10 µM
5 µM	900 µL	100 µL of 50 µM
10 µM	900 µL	100 µL of stock
50 µM	500 µL	500 µL of stock

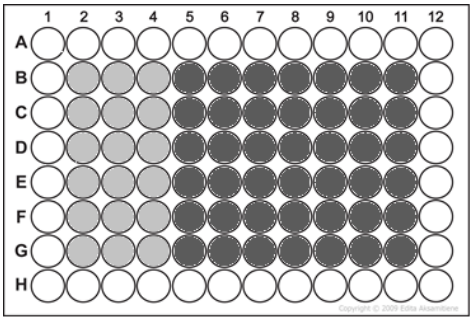

Figure 4.2: Shows the distribution layout of the 96 well plate; white wells are just the RPMI-1640 medium with 10% foetal bovine serum, light grey wells are controls, and dark grey wells have the compound added, with row 5 being the lowest concentration and row 11 having the highest concentration.

4.4.6 Processing the 96 well plates.

MTT solution (conc) is taken from the fridge and put into the 37 °C waterbath for 2 minutes. Once warmed, 50 µL is added to each well on the 96 well plate (final conc), plates are returned to the incubator for 2.5 h. After incubation, the solution is removed by aspiration, using a pipette and sliding it down the side of the well ensuring the bottom of the well is not disturbed. DMSO (150 µL) is then added to each of the wells to solubilise formazan crystals. Absorbance is read on a Perkin Elmer Envision plate reader at 570 nm. MTT assays performed at the time of test agent addition (Time zero; T0) and following 72 h exposure to test agent allows growth inhibitory and cytotoxicity of test agent to be determined.

4.4.7 Calculating GI_{50}.

Using the data calculated by the plate reader for both the T0 and the main run, an average and SD is obtained for each concentration, control and T0 value.

$$Ab.of\ GI_{50} = \left(\frac{Ab.of\ control - Ab.of\ T0}{2}\right) + Ab.of\ T0$$

Equation 4.2: Shows the absorbance of GI_{50}.

Using the GI_{50} absorbance value, GI_{50} can be calculated;

$$GI_{50} = \frac{(X_{ab} - Ab.of\ GI_{50})}{(X_{ab} - Y_{ab})} \times (X_{Conc} - Y_{Conc}) + Y_{Conc}$$

Equation 4.3: Shows the value for GI_{50}.

X_{ab} = Highest absorbance where GI_{50} falls.

Y_{ab} = Lowest absorbance where GI_{50} falls.

X_{Conc} = Highest concentration where GI_{50} falls.

Y_{Conc} = Lowest concentration where GI_{50} Falls.

4.4.8 Clonogenic Assay

This assay was used in addition to the MTT assay as a screen in this study. Cells were counted using a haemocytometer and approximately 150-250 cells (depending on the cell line) were seeded per well in 6-well plates with 2 mL of medium. Cells were allowed to attach for 24 h. The cells were then treated, guided by the GI_{50} values obtained from the MTT assays i.e. 1 x GI_{50} and 2 x GI_{50}. Cells in control wells were treated with vehicle (medium) alone. Following 24 h exposure to Jerantinine A, medium was aspirated along with the compound. Wells were washed 2 x with 1 mL of PBS and 2 mL of fresh medium was added to each well. Plates were placed in the incubator at 37 °C and inspected daily until cells in control wells formed colonies of > 50 cells. The cells were washed with PBS before fixation with 100% methanol (0.5 mL) for 15 min and then stained with 0.7 mL of 0.5% methylene blue (1:1 water:methanol) for an additional 10 min. Colonies were counted and results recorded graphically using GraphPad Prism.

4.4.9 Cell Cycle Analysis

Cell cycle analyses were carried out using a method based on Nicoletti *et al.* PI is an intercalating DNA dye that fluoresces strongly when bound to DNA.[34] The DNA content of an individual cell is proportional to the fluorescence intensity of exited PI (excited by an argon laser at 488 nm). A histogram of DNA content of cells in a population can be used to derive the percentage of cells in each phase (pre-G1, G1/G0, S, and G2/M) of the cell cycle and observe any perturbations caused by the tests compounds. PI is normally excluded by viable cells, and so membrane permeabilisation is required *via* the use of a gentle detergent/hypotonic solution to allow PI entry into cells. Cells were seeded in 6-well plates at the following densities in 2 mL of medium and treated for the respective time exposures: A seeding density of $1x10^5$ cells was used for 24 h and 48 h treatments, whereas a lower density of $5x10^4$ cells were seeded for 72 h treatment to maintain logarithmic growth. Following treatment, medium containing any floating cells was pipetted into labelled FACS tubes and kept on ice. Cells were trypsinised and once detached pooled together with medium and then pelleted in a Beckman Coulter Allegro centrifuge at 1200 rpm for 5 min at 4 °C. The supernatant was discarded and the pellet broken up by gently flicking the tube. The cells were re-suspended in 0.3-0.5 mL of fluorochrome solution and stored overnight in the dark at 4 °C. A single cell suspension was achieved by gently passing the cells through a 23 g needle immediately prior to analysis on a Coulter Epics XL-MCLTM flow cytometer. Appropriate gates were set up relative to the control and data stored for further statistical analyses.

4.4.10 Tubulin Polymerisation Assay

The tubulin polymerisation assay is based on an adaptation of the original method of Shelanski *et al.* and Lee *et al*. which demonstrated that there is a proportional relationship between light scatter and concentration of microtubule polymer.[34] Absorption spectral data in the form of polymerisation curves reveal three distinct phases of microtubule polymerisation: nucleation, growth, and steady state equilibrium. Compounds that interfere with tubulin polymerisation will affect one or more of these phases. Therefore, this assay can be used to identify novel antimitotic (or antimicrotubule) agents. General tubulin buffer (0.1 M piperazine-N,N'-bis(2-ethanesulfonic acid, 2 mM EGTA, 1 mM $MgSO_4$, adjusted to pH 6.9), guanosine triphosphate (GTP) were prepared prior to beginning the assay. The appropriate absorbance (340 nm) and temperature (37 °C) settings for the Perkin Elmer Vision plate reader were also set prior to beginning the assay in order to maximise polymerisation activity. The plate reader was set to kinetic mode measuring 61 cycles of 1 reading per minute. PEM (500 µL; required for tubulin ligand dilutions) was warmed to room temperature. The test compounds (paclitaxel, nocodazole and jerantinine A) were then diluted with PEM to yield final concentrations of 5 µM and 10 µM. Cold G-PEM minus glycerol buffer was made to re-suspend the tubulin and kept on ice for approximately 3 min. Paclitaxel and jerantinine A (10 µL) in addition to G-PEM buffer (control) were pipetted into their respective wells on a microtiter plate and placed in the incubator for 2 min at 37 °C. Tubulin (100 µl) was added and pipetted into the wells containing the test compounds and immediately placed into the plate reader to obtain absorbance data. Data were recorded in an excel spreadsheet supplied by the Wallac Envision software and graphed using GraphPad Prism 6.

4.4.11 Confocal Microscopy

HCT-116 cells were seeded 8-well µ-slides (Ibidi Germany, Catalogue No.: 80826) and allowed to adhere for 24 h at 37 °C before treatment with test agents for an additional 24 h. Cells were then fixed with formaldehyde (3.7% in PBS) and incubated at room temperature for 10- 15 min before permeabilisation using PBT (PBS + 0.1% Triton-X-100). Following incubation for 2-3 min at room temperature, cells were blocked using PBT + 1% BSA for 1 h to prevent non-specific binding of labelled antibodies. Cells were then incubated with 1° Ab (monoclonal anti-tubulin Ab; 1:200 dilution) for 2 h at room temperature before being washed with PBT and incubated with the appropriate fluorescent 2° Ab (1:40 dilution) at room temperature in the dark for 1 h. After washing with PBT, cells were incubated with DRAQ5 (1:3000 dilution), a cell permeant DNA binding dye, at room temperature for 5 min in the dark. Images were captured on a Zeiss LSM510 Meta confocal microscope.

Chapter 2

This work resulted in a paper titled ***"Alcohol Dehydrogenase-Triggered Oxa-Michael Reaction for the Asymmetric Synthesis of Disubstituted Tetrahydropyrans and Tetrahydrofurans***" published in ChemCatChem.

Section 1: Introduction

Biocatalysis is described as the use of biological agents to catalyse chemical reactions, and it underpins some of the oldest chemical reactions which predate recorded history. The oldest record of enzymes being used by humans is in brewing, dating back to about 4000 BC by the Sumerians. For the majority of the last 6000 years, biocatalysis has mainly been used in the food and drink industries in the formation of beer, wine and cheese and many other goods. In 1858, Louis Pasteur placed the first milestone in biocatalysis by recording the first kinetic resolution reaction. He used *Penicillium glaucum* on a racemic mixture of tartaric acid ammonium salt **(66)**, which lead to the consumption of the (+)-tartaric acid and left only (-)-tartaric acid **(67)**, shown in **Scheme 1.1**. This is an example of kinetic resolution.[57]

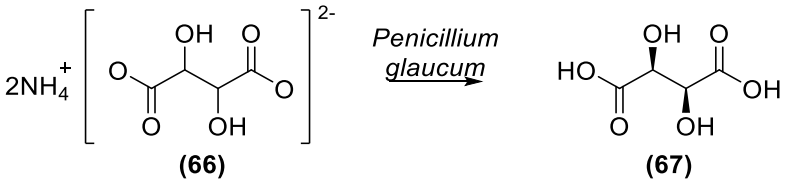

(66) **(67)**

Scheme 1.1; Kinetic resolution of tartaric acid ammonium salt.

Pasteur's research was later followed by Emil Fischer's work on carbohydrate chemistry, where he performed the first synthesis of D-glucose from glyercol in 1890 which then led to the revolutionary lock and key hypothesis for enzyme action in 1894. This hypothesis explained the

enzyme specificity but fails to explain the stabilization of the transition state. [58,59] In 1897, Eduard Buchner reported the first successful fermentation of either glucose, fructose or maltose by a cell-free yeast extract, which was indisputable proof that for a biological transformation, it required no living cells. This changed the perception of biocatalysis and at the start of the 20th century, more and more scientists from industry and academia looked into utilising it and in 1913. Ludwig Rosenthaler reported the preparation of (*R*)-mandelonitrile **(69)** by treating benzaldehyde **(68)** with HCN in the presence of emulsin extracted from bitter almonds, shown in **Scheme 1.2**. Emulsin is a mixture of enzymes, including oxynitrilases, which is responsible for the reaction. Nowadays, (*R*)- and (*S*)–oxynitrilases are commercially available and the cyanohydrins produced are a useful chiral building block.[57,60]

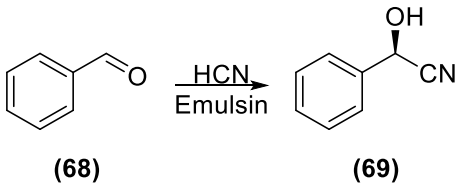

(68) **(69)**

Scheme 1.2; Formation of (*R*)-mandelonitrile.

Around the same time, Vladimir Prelog began work on the use of biocatalysis for the stereoselective reduction of ketones to alcohols, which ultimately led to the formation of the Prelog rules that are still used today to differentiate between enantiomers. Even with these great examples previously shown, biocatalysis was mostly ignored by most organic chemists of that era, but the pace of biocatalytic methodology development for applications in organic chemistry gradually increased through the 60s, 70s and 80s. Another important contribution to biocatalysis was made by Alexander Klibanov, who showed the organic solvent tolerance of certain lipases. This proves particularly useful in

resolving racemic alcohols, as lipases will typically only catalyse the hydrolysis of one enantiomer.[57]

One example where biocatalysis has replaced traditional chemistry methods in industry is in the synthesis of sitagliptin which is the active ingredient in Januvia **(70)**. This is a leading drug in the treatment of diabetes. Using an engineered transaminase that was able to accept substrates not accepted by the wild-type version, the team managed to increase the overall yield by 10-13%, increase the productivity (kg L^{-1}) and decrease the total waste by 19%. The biocatalytic step removed a rhodium catalysed hydrogenation that was performed under high pressure and also improved the *e.e.* of the final product. This accomplishment was so remarkable that it won the Presidential Green Chemistry Award in 2010, and in 2012, and was approved by the Food and Drug Administration (FDA). The key step is shown in **Scheme 1.3**.[61]

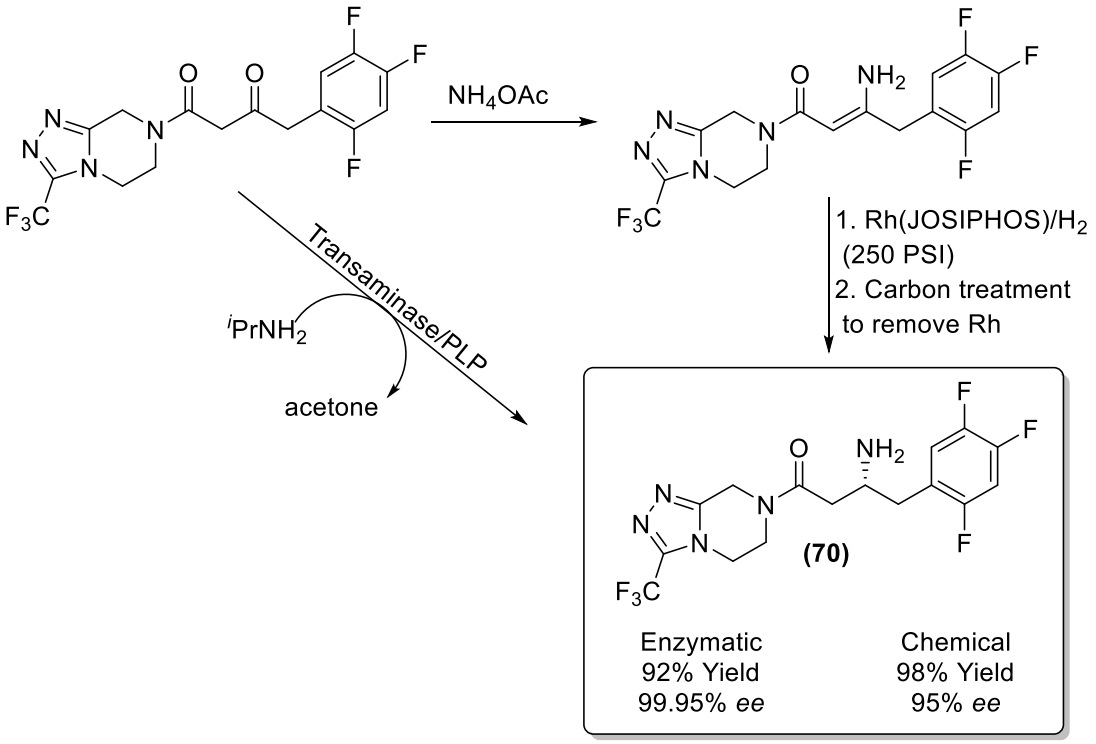

Scheme 1.3; Synthesis of sitagliptin comparing the biocatalytic pathway to the chemical pathway.

1.1 Chiral Alcohols

Chiral alcohols are ubiquitous moieties in active pharmaceutical compounds, being present in 23% of the top 200 most prescribed medications in the US in 2016.[62] The addition of a hydroxyl group to a compound allows for greater binding to any protein target through its ability to hydrogen bond, as well as increasing the solubility of the compound into aqueous media. The importance of enantiomerically pure compounds is shown by many drugs different potencies from a particular enantiomer. Enantiomers are considered chemically equivalent and display the same physical properties (boiling/melting point) However, in a chiral environment, such as the active site of a protein, enantiomers behave differently, with potentially only one enantiomer capable of successfully binding to the protein. The Food and Drug Administration (FDA) also shows the importance of enantiopure compounds by accelerating the approval of single enantiomer compounds over their racemic counterpart.[63] To such compounds that are chiral alchols are Atorvastatin **(71)**, Tramadol **(72)** and Prednisone **(73)**. These are an antihyperlipidemic, an analgesic and an anti-imflammatory drug respectively shown in **Figure 1.1**.

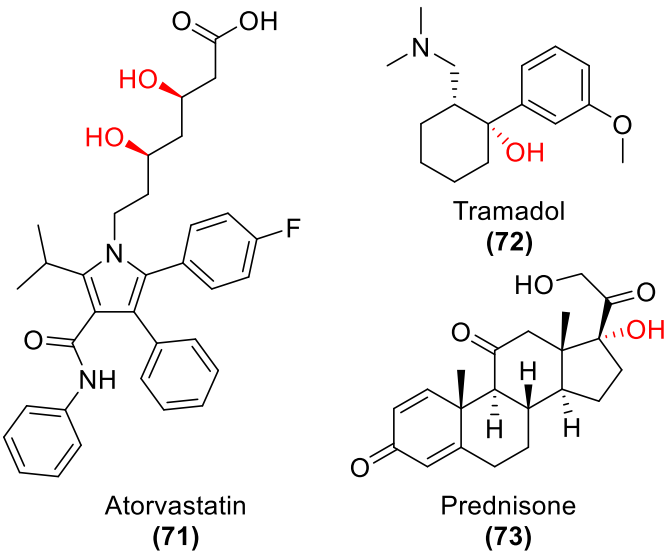

Figure 1.1; Atorvastatin (71), Tramadol (72) and Prednisone (73)

1.2 Chemical synthesis of chiral alcohols

Generally, the main chemical approach for the synthesis of chiral alcohols comes from the reduction of a ketone using a chiral ligand. For this reaction to happen, it requires either a chiral catalyst, stoichiometric reducing agent or the starting ketone to have some chiral characteristic already.[64,65] This is because the starting ketone is prochiral if both groups are the same, or achiral if both groups are different. Due to the Sp_2 nature of a ketone, there is no preference direct preference from which the nucleophilic hydride can attack carbon of the ketone.

1.2.1 CBS Reduction

One of the most widely known methods of asymmetric carbonyl reduction is using the oxazaborolidine to produce the chiral alcohol. This methodology was initially developed by the Itsuno and coworkers in 1981 and further by Corey and coworkers.[66,67] It has since been used many times as a reliable method for the asymmetric reduction of achiral ketones and has been used in natural product synthesis in academia and in an

industrial setting many times. Like most chemical routes, there are many limitations accompanying asymmetric reduction methodology including water sensitivity, which has been shown to have a significant effect on the *e.e.* of the reduction. Temperature is another factor that can play a significant role, with the lower temperature reactions typically affording better *e.e.* The first step of the mechanism is the BH_3 coordinating to the nitrogen atom of the oxaborolidine. This coordination activates the BH_3 as a hydride donor and increases the lewis acidity of the endocyclic boron. This then coordinates to the ketone from the sterically less hindered lone pair, with the largest R group on the ketone directed away from the endocyclic boron.[68] From here, the reaction can go down either path 1 or path 2 to regenerate the oxaborolidine catalyst. The main driving force for this reaction is the activation of the BH_3 by the Lewis basic nitrogen on the oxazaborolidine followed by the activation of the endocyclic boron to coordinate the ketone. This mechanism is shown in **Scheme 1.4.**[66,67]

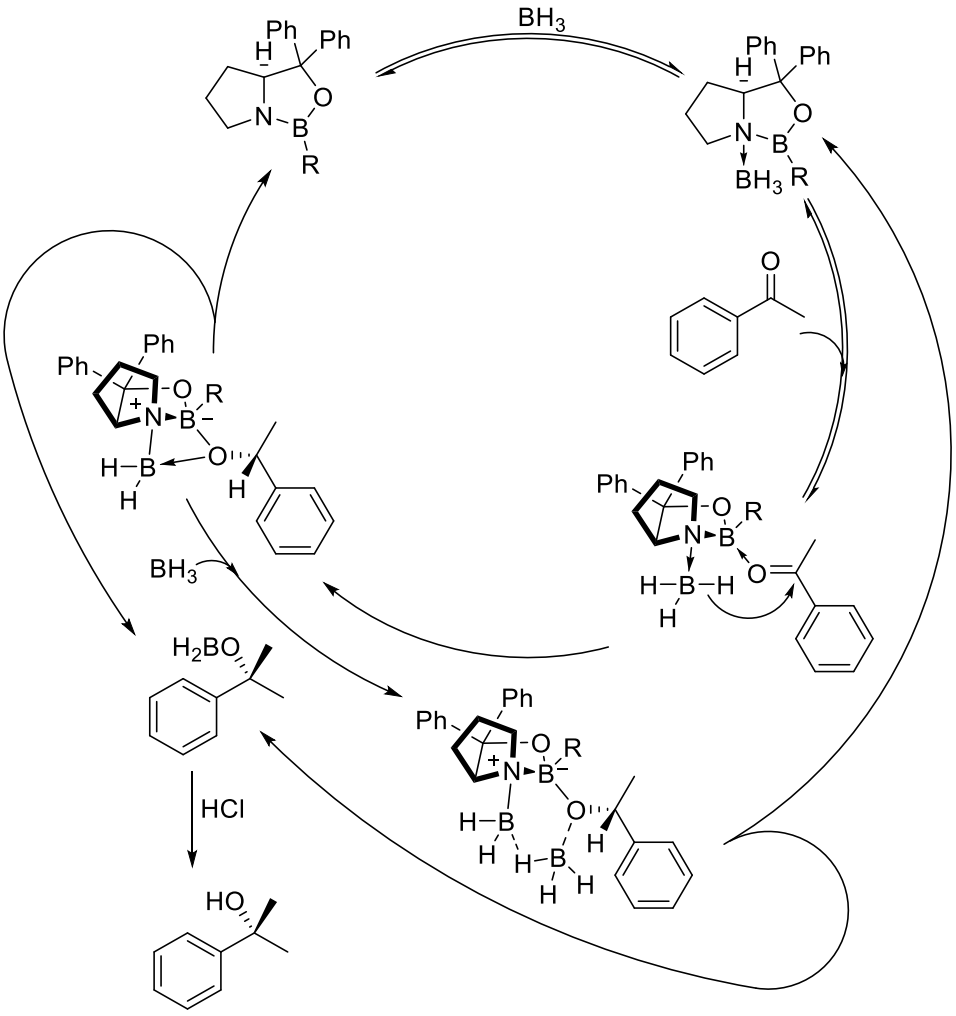

Figure 1.4; Oxazaborolidine reduction mechanism.

1.2.2 Transition metal and Chiral ligand reduction

Another common asymmetric method of reducing carbonyls uses transition metals with a chiral ligand. These ligands are generally very large and function to restrict the metal centre from attack from certain directions, which can give the preferred route of attack giving rise to chirality. The properties of the chiral ligand bound to the transition metal determines the enantioselectively of the catalyst. One of the most common catalyst of this type is a ruthenium 2,2'-*bis*(diphenylphosphino)-1,1'-binaphthyl (BINAP) complex **(74)**.

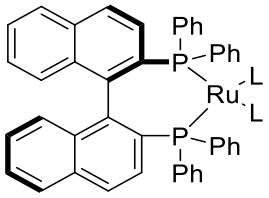

(74)

Figure 1.2; Stucture of (*R*)-ruthenium 2,2′-*bis*(diphenylphosphino)-1,1′-binaphthyl complex.

There are two isomers of the BINAP catalyst, the (*R*)-selective and the (*S*)- selective. BINAP ligands are interesting as they are chiral molecules that do not possess a stereogenic centre but instead, have an axis of chirality. This is an axis where a set of substituents are held in a certain arrangement that are not superimposable on its mirror image. Shown in **Figure 1.3**, when BINAP chelates to a transition metal, the phenyl groups on the phosphorus reside in either pseudoequatorial (red) or pseudoaxial (blue) positions. When the phosphorus reside resides in the pseudoequatorial position, the ruthenium atom is blocked from attack from that direction, and when the phosphorus residue resides in the pseudoaxial position, the ruthenium is open to attack. This is how the stereoselectivity is controlled. These groups go into a region of space the other side of the BINAP ligand and the pseudoequatorial phenyl groups influence the preferred binding conformation of the ketone being reduced. The space not occupied by the phenyl groups is then more open to the ketone, promoting a hydride delivery to a single face of the ketone. The binaphthalene ring is shown in yellow. [69-71]

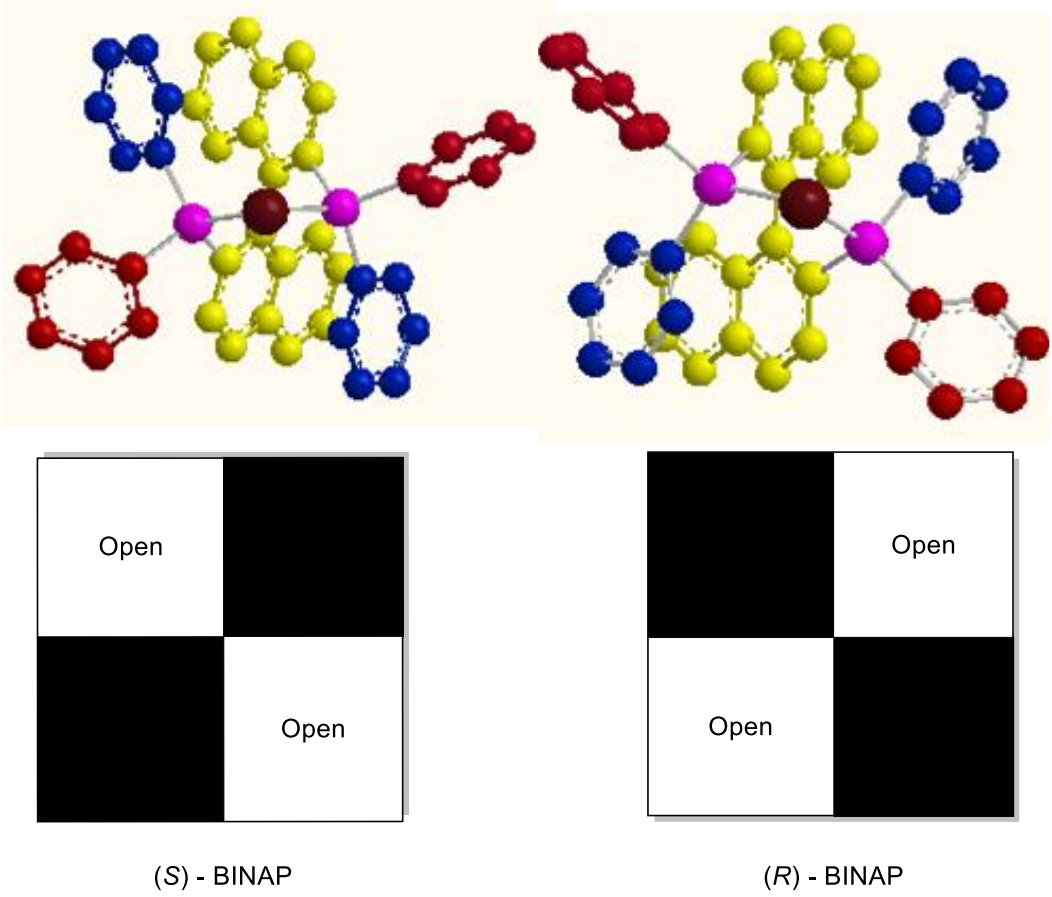

Figure 1.3; Shows the space the BINAP ligand occupies for the selectivity of (*R*) and (*S*) BINAP.[71]

The mechanism for the ruthenium catalysed reduction of an alcohol is shown in **Scheme 1.5**. The first step is the precatalyst of the ruthenium complex **(75)** to form the ruthenium-monohydride intermediate **(76)** with the release of HCl. The ruthenium centre then coordinates to the ketone, following **Figure 1.3**, only one diastereomeric transition state would be favoured. This state will be the one where the largest R group is not in the same vicinity as the phenyl groups from the phosphorus. The ketone is then reduced and the ruthenium core coordinates to a solvent molecule **(77)**. One solvent molecule then reductively eliminates the coordinated ketone and solvates the complex **(78)**, this is followed by another hydrogenation to reform the active ruthenium-monohydride intermediate and carry on the catalytic cycle.[72]

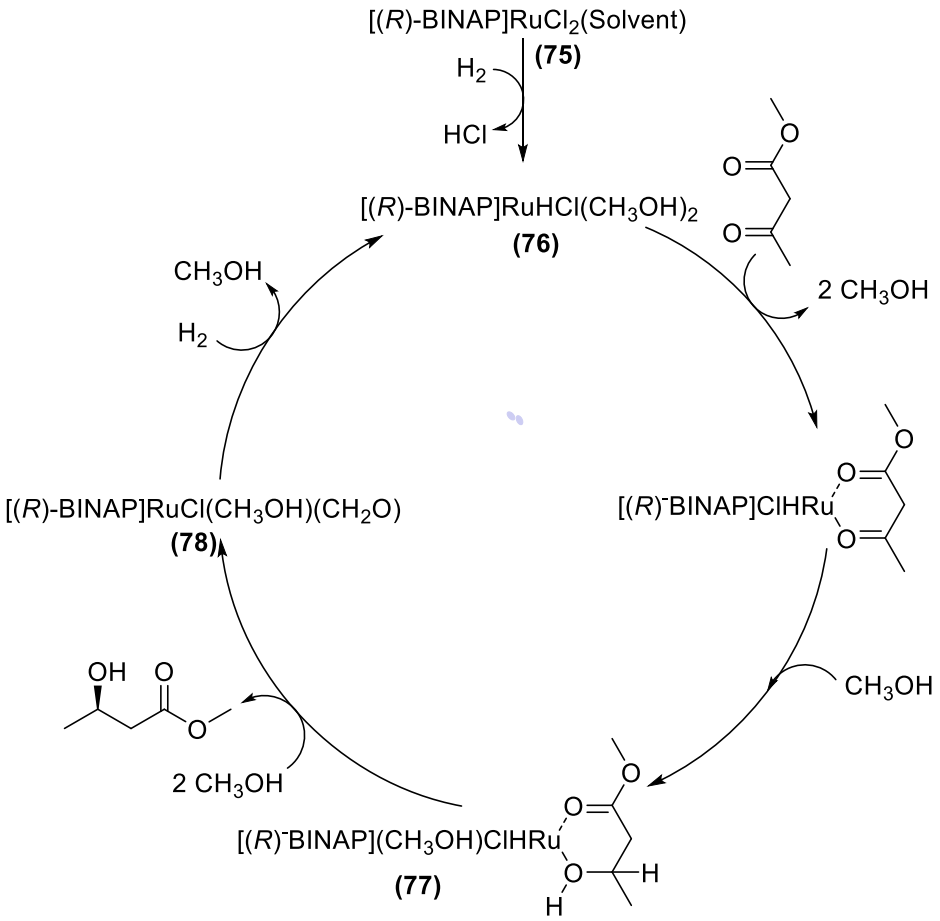

Scheme 1.5; Shows the ruthenium catalysed reduction of an alcohol.

Other techniques for reducing ketones use stoichiometric amounts of chiral reducing agent. A common reagent is lithium aluminium hydride chelated to 1,1'- bi-2-naphthol (BINOL). Chelating ligands like BINOL also avoid disproportionation and over reduction of other functional groups on the molecule. Borohydrides can be modified to possess chirality. For example, an economical ligand can be derived from amino acids. Proline and cystine have frequently been used as a source of chiral ligands shown below shown in **Figure 1.4**. Compound **(79)** comes from cysteine and compound **(80)** comes from proline.[73]

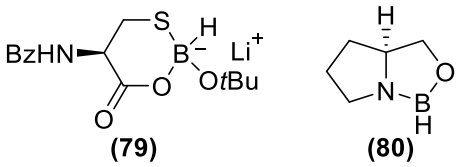

Figure 1.4; Some examples of amino acid modified borohydride reagents

1.2.3 Asymmetric Addition of Grignards

Chiral alcohols can also be produced using organometallic reagents and reacting them with a carbonyl compound. Grignard reagents compared to their zinc and aluminium counterparts offer much higher reactivity, a wider commercial range and better atom efficiency, as the whole R group on the Grignard reagent is added in the reaction. Initially the *Bis*–(2-dimethylaminoethyl)ether (BDMAEE) **(81)**, chelates the Grignard reagent, which then transmetallates the titanium species.[74-77] This then coordinates to the chiral ligand, which allows attack of the carbonyl compound from one face, shown in **Scheme 1.6**.[78]

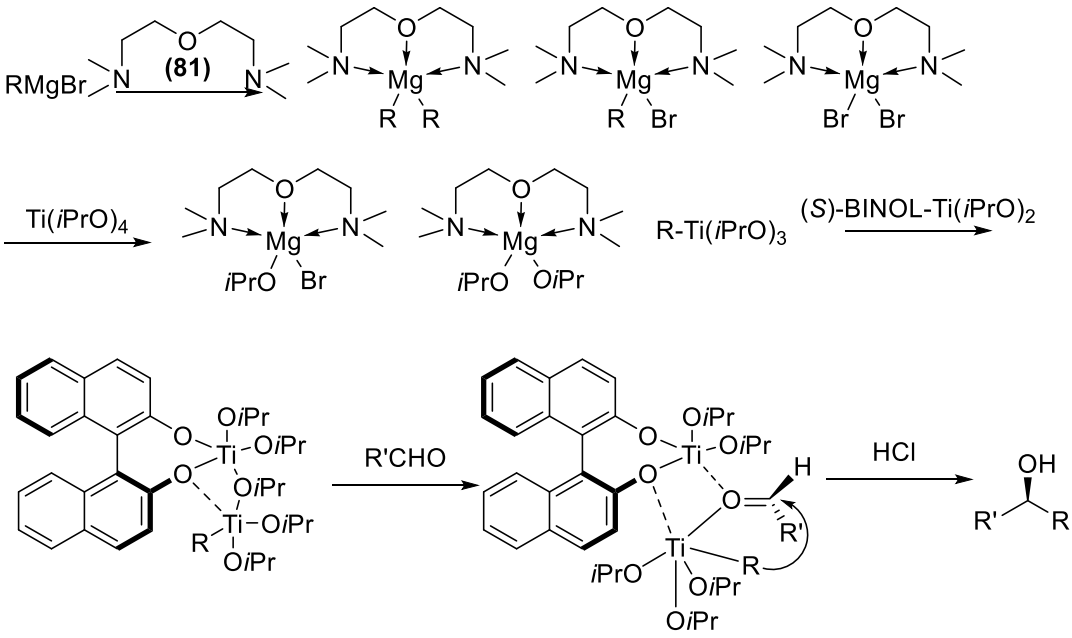

Scheme 1.6; Mechanism of enantioselective Grignard addition.

1.3 Biocatyltic synthesis of alcohols

As previously shown, there are many creative and interesting methods that allow the synthesis of chiral alcohols. However, most have many draw backs; many methods require complete removal of water, quite harsh conditions (high pressure hydrogen, high temperatures etc), the use of heavy metals, costly chiral ligands and the enantiomeric excess is not outstanding. Using biocatalysis for these reactions can overcome these drawbacks, as enzymes generally afford exceptional enantiomeric excess, are naturally biodegradable with very little polluting waste and operate under mild conditions (low temperatures and aqueous solutions). Therefore, it's not of any surprise that several enzymatic classes have been utilised for the synthesis of chiral alcohols.[79]

1.3.1 Lipases

Lipases were among the first class of enzymes to be used on an industrial scale. As previously discussed, they were found to be active in some organic solvents. Shown in **Scheme 1.7**, they are hydrolytic enzymes that employ a catalytic triad of serine, aspartic acid and histidine. Firstly, the aspartic acid forms a hydrogen bond with the histidine, this increases the pKa of histidine imidazole nitrogen, allowing it to deprotonate serine. This deprotonated serine can then attack into the carbonyl of the ester group. These reactive intermediate reforms the ester with the alcohol acting as the leaving group. A water molecule then donates its proton to the histidine, forming a reactive hydroxide ion which hydrolyses the serine ester, releasing the carboxylic acid monomer. [80]

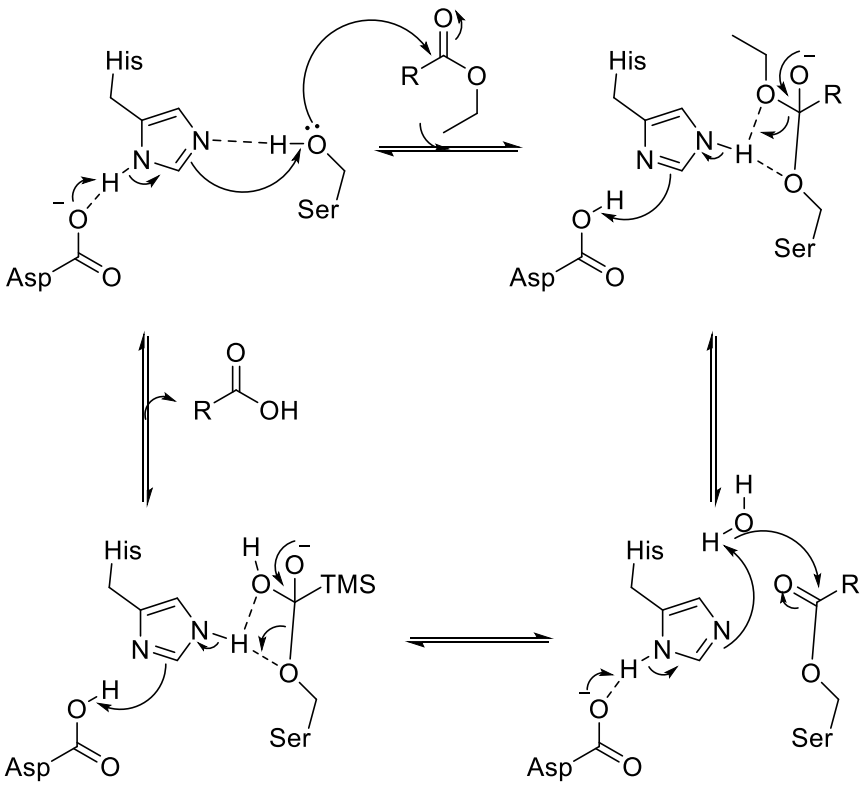

Scheme 1.7; Mechanism of serine dependant lipases

1.3.2 Dynamic kinetic resolution with lipases

As previously discussed, enzymes can differenate between enantiomers of a racemic material, allowing the catalyst to selectively preferentially hydrolyse one enantiomer of a racemic ester. Whilst this is very useful, the theoretical yield will always be limited to a maximum of 50%. However, this can be improved by performing a technique called dynamic kinetic resolution. The first dynamic kinetic resolution to produce an enantiopure alcohol was reported in 1996 by Williams as shown in **Scheme 1.8**. *Pseudomonas fluorescens* lipase was used by Willaims with a ruthenium catalyst to give the enantiopure ester **(82)**. This works by the lipase forming an ester with just one enantiomer, Shvo's catalyst **(81)** then racemises the remaining pure unreacted enantiomer which then can go through the cycle again. Since then, a wide range of lipases with

different racemising catalysts have been produced that can now produce enantioselective alcohols with exceptional yield and enantiomeric excess.[81]

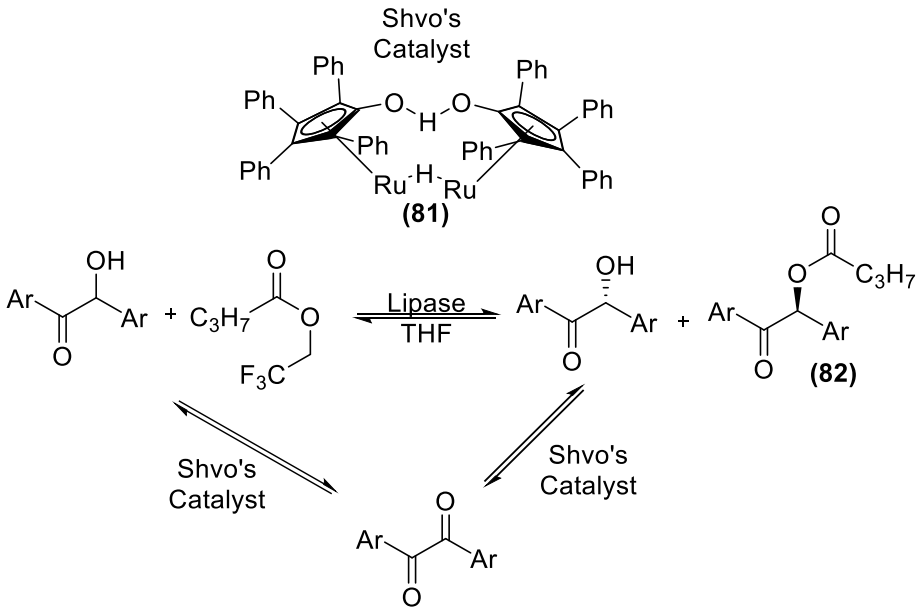

Scheme 1.8; Dynamic resolution to produce one enantiomer of the ester (82).

1.3.3 Aldolases

Aldolases are a type of enzyme that performs enantioselective aldol reactions. It is a ubiquitous enzyme, found in all forms of life and is essential in the breakdown of glucose to pyruvate. This process is reversible depending on starting concentrations of starting materials with the mechanism shown in **Scheme 1.9**.[82-85] Unlike the other enzymatic examples of producing chiral alcohols, this methodology produces them *via* a carbon-carbon bond formation.

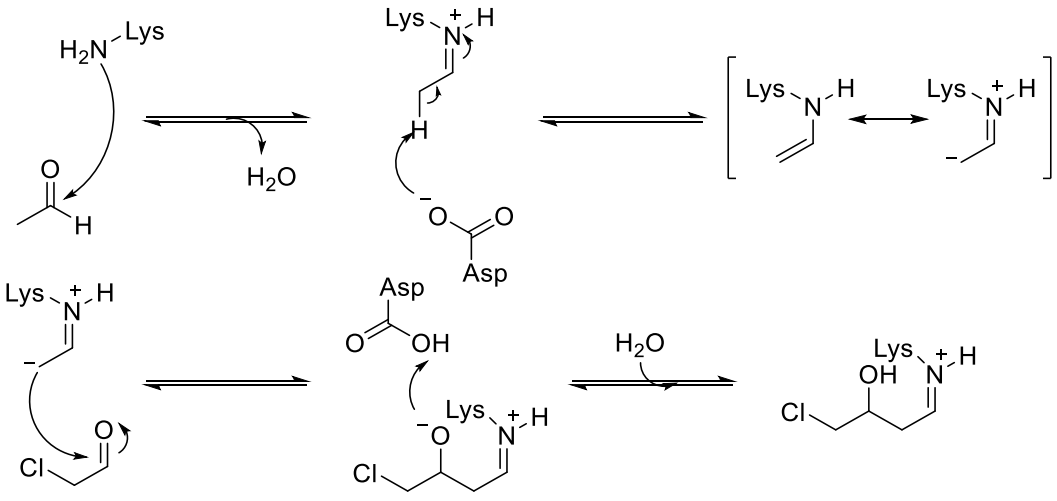

Scheme 1.9; Mechanism of aldolase.

George M. Whitesides reported the use of an aldolase to make stereoselective adducts **(83)** from a range of aldehydes and ketones.[83] To date, no non-biological chiral catalyst can rival aldolases as a catalyst in terms of enantioselectivity and diastereomeric selectivity for this type of reaction, but the scope of these enzymes can be quite limited.[84, 85] With further engineering of this type of enzyme, much greater substrate scope and range can be achieved and is highlighted in the review by Barry *et al.* with an example shown in **Figure 1.5** which managed to react with **(84)**, A synthetically more useful compound.[82]

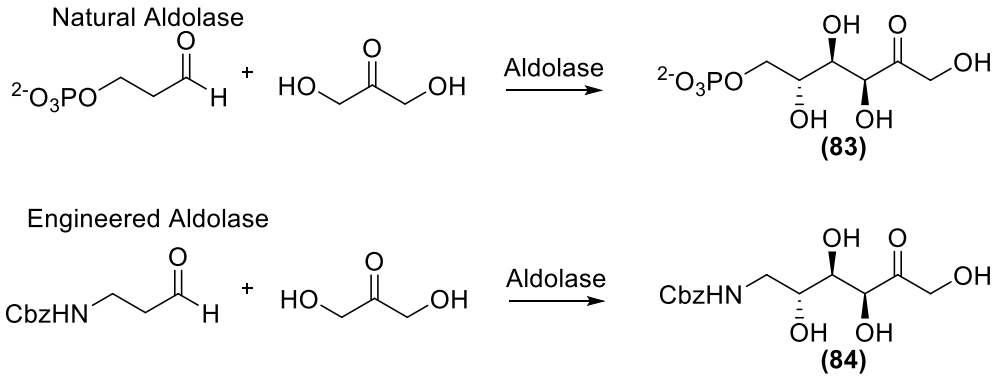

Figure 1.5; Example of the expanded scope of engineered aldolase.

1.3.4 Cytochrome P_{450}

Cytochrome P450 (CYPs) are enzymes from a superfamily of hemeproteins. Though found in all kingdoms of life, they are absent in *E. coli*. Their oxidising power has also caught the attention of many drug companies, trying to predict where these enzymes are likely to metabolise their drugs and try and block this.[86] The metabolites of the drug molecules are also investigated, as these could have side affects[87]

Scheme 1.10 shows the active site near the heme group, this is represented by an iron atom below. The cysteine represents a peptide chain blocking the other face of the iron atom. Step **1** of the mechanism shows the substrate binding to the active site of the enzyme, this displaces the water molecule from the heme group and invokes a conformational change in the iron(III). It also changes the heme iron from low-spin to high-spin. This conformational change and change in electronic state of the active site allows for a transfer of an electron *via* NADPH shown in step **2**. This reduces the iron core from an oxidation state of (III) to (II). Molecular oxygen then binds to the heme iron forming a superoxide radical shown in step **3**. This is then reduced again by transfer of an electron *via* NAPDH to form the negatively charged peroxo group. This is a short lived intermediate state shown in step **4** as it is rapidly protonated in step **5** by surrounding amino acids to the iron (IV) oxo species. The heme Iron then extracts a proton from the hydrocarbon forming an organic radical and iron hydroxide. The radical then attacks the oxygen of this hydroxide forming an alcohol, shown in step **6**. The last step is the alcohol dissociating from the heme iron and water occupying the active site.

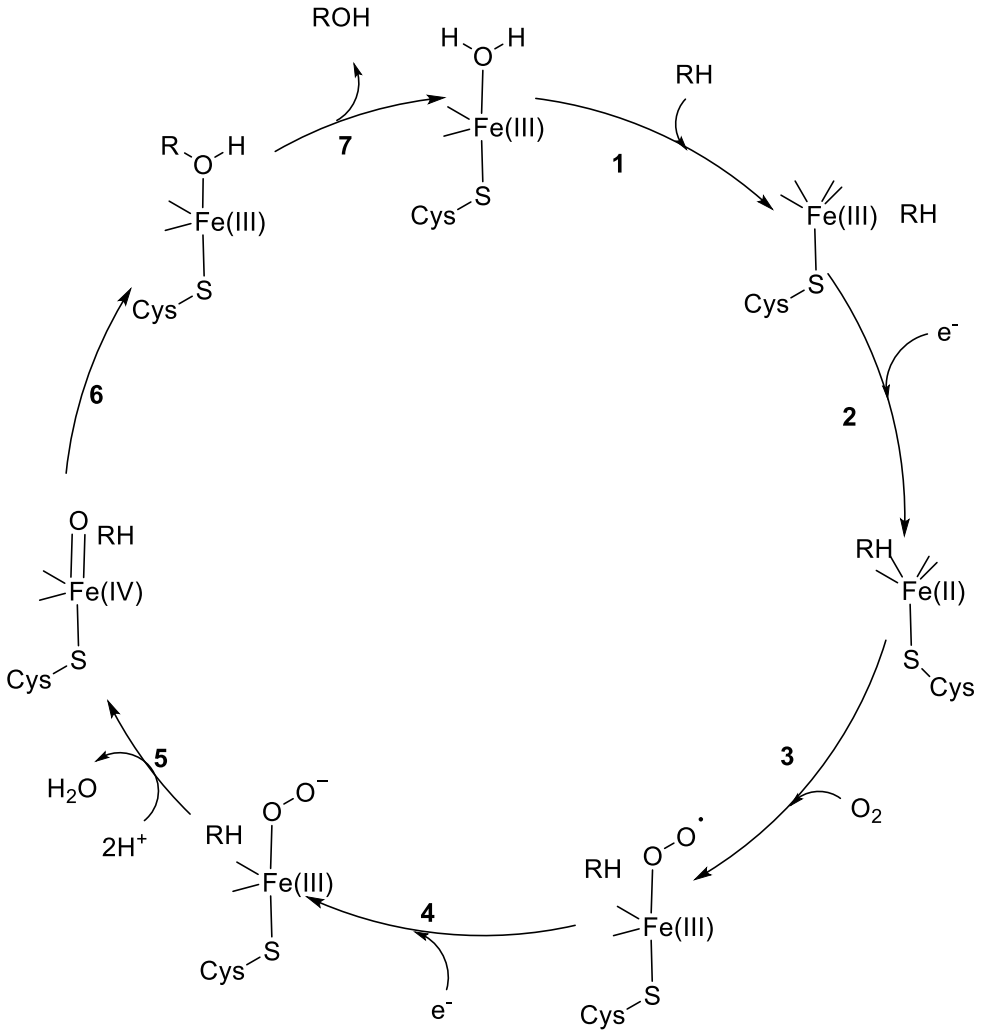

Scheme 1.10; mechanism of oxidation by cytochrome P450.

1.3.5 ADH

Alcohol dehydrogenases (ADHs) are part of the oxidoreductase family and can be broken down further into three distinct types; the zinc-containing, long/medium chain ADHs (Type I) metal-free short chain ADHs (Type II) and the iron-containing ADHs (Type III). Type I is the most studied ADH out of the three, and belong to the "medium-chain" dehydrogenase/reductase superfamily.[88-90] They are zinc-containing enzymes with approximately 350 residues per subunit. Type II ADHs are also members of the dehydrogenase/reductase superfamily, but are in the "short-chain" group. These generally have about 250 residues per subunit and lack a metal cofactor. Type III ADHs are described as "iron-dependent/activated" enzymes and contain about 385 residues per subunit.[91] They belong to the iron-containing alcohol dehydrogenases superfamily. They initially were described as being only in microorganisms but in 2002, Deng *et al.* identified one iron-containing alcohol dehydrogenases in humans.[92] ADHs are a class of enzymes that oxidise alcohols and reduce ketones and aldehydes requiring NADH or NADPH as the electron acceptor. ADHs are dimers with each subunit containing one zinc atom and are ubiquitous enzymes that are essential for life. ADH have a number of diverse roles, for example, in humans, the main role of these enzymes is to detoxify compounds like ethanol, methanol and retinol to the aldehyde form, which is then oxidised by another enzyme.[93,94] In bacteria and fungi, their role is to convert acetaldehyde, a product from glycolysis, to ethanol to regenerate NADH. This process is exploited by humans to produce alcoholic beverages.[95]

Negelein and Wulff were the first to purify and crystalise an alcohol dehydrogenase from brewer's yeast in 1937. It wasn't until 1961 when

McKee worked out the catalytic structure and mechanism of ADH.[96] It was one of the first oligomeric enzymes to have its amino acid sequence and three-dimensional structure determined. The alcohol dehydrogenase typically favour oxidising compounds, the mechanism is reversible.[97] Inside the active site is a Zinc(II) ion, which is coordinated to two cysteine residues and one histidine residue. In the active site also is a serine and another histidine residue which in a similar manor to a catalytic dyad, being a charge-relay network to help deprotonate the alcohol. When the alcohol enters the active site, the oxygen coordinates with the zinc and the serine residue. After this, the NADH enters the active site and reduces the ketone. Alcohol dehydrogenases can also be defined by their active site size. A so-called bulky-small ADH, can fit a large R group on one side of the ketone and only a small group, such as a methyl, on the other side of the ketone. A so-called bulky-bulky ADH can tolerate a large R groups on both sides of the ketone, as shown in **Scheme 1.11**.[98]

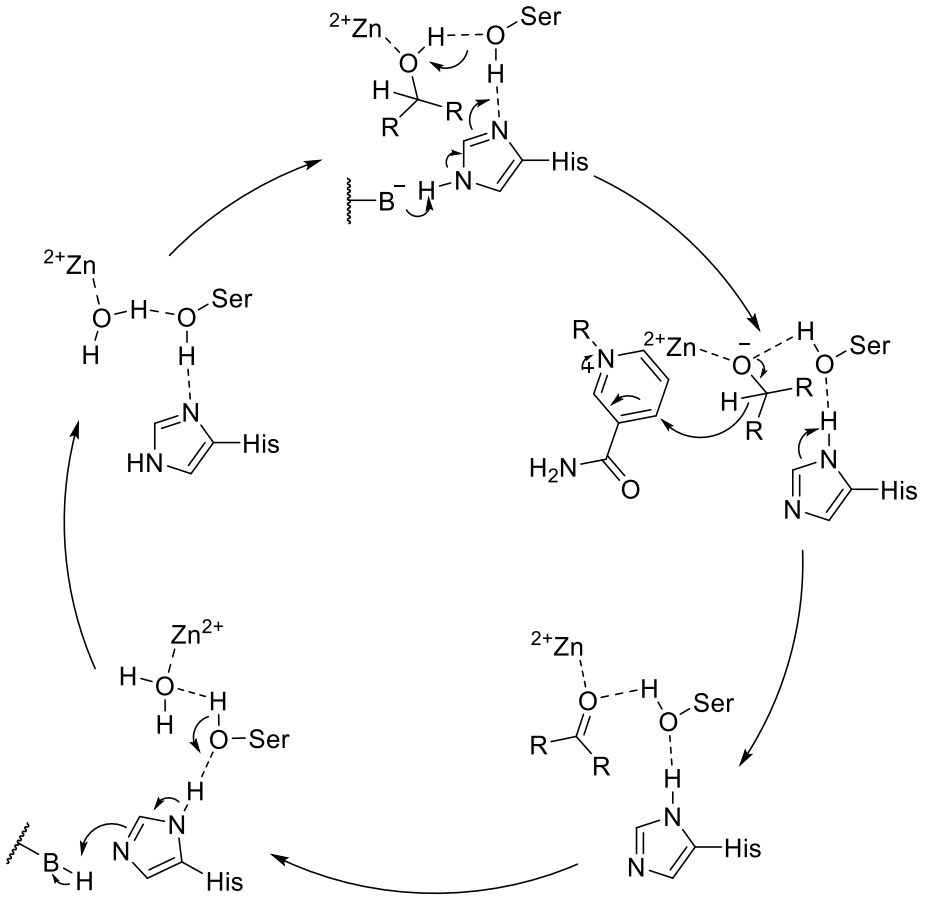

Scheme 1.11; General mechanism of alcohol dehydrogenase.

Shown in **Figure 1.6**, simple aliphatic and aromatic ketones that were reduced using an ADH. The aromatic compounds have a range of different electronic properties ranging from different electron withdrawing groups, electron donating groups, halogens and multiple substitutions on the phenyl rings produce alcoholic compounds which have excellent *e.e.* and *d.r.* where applicable.[98]

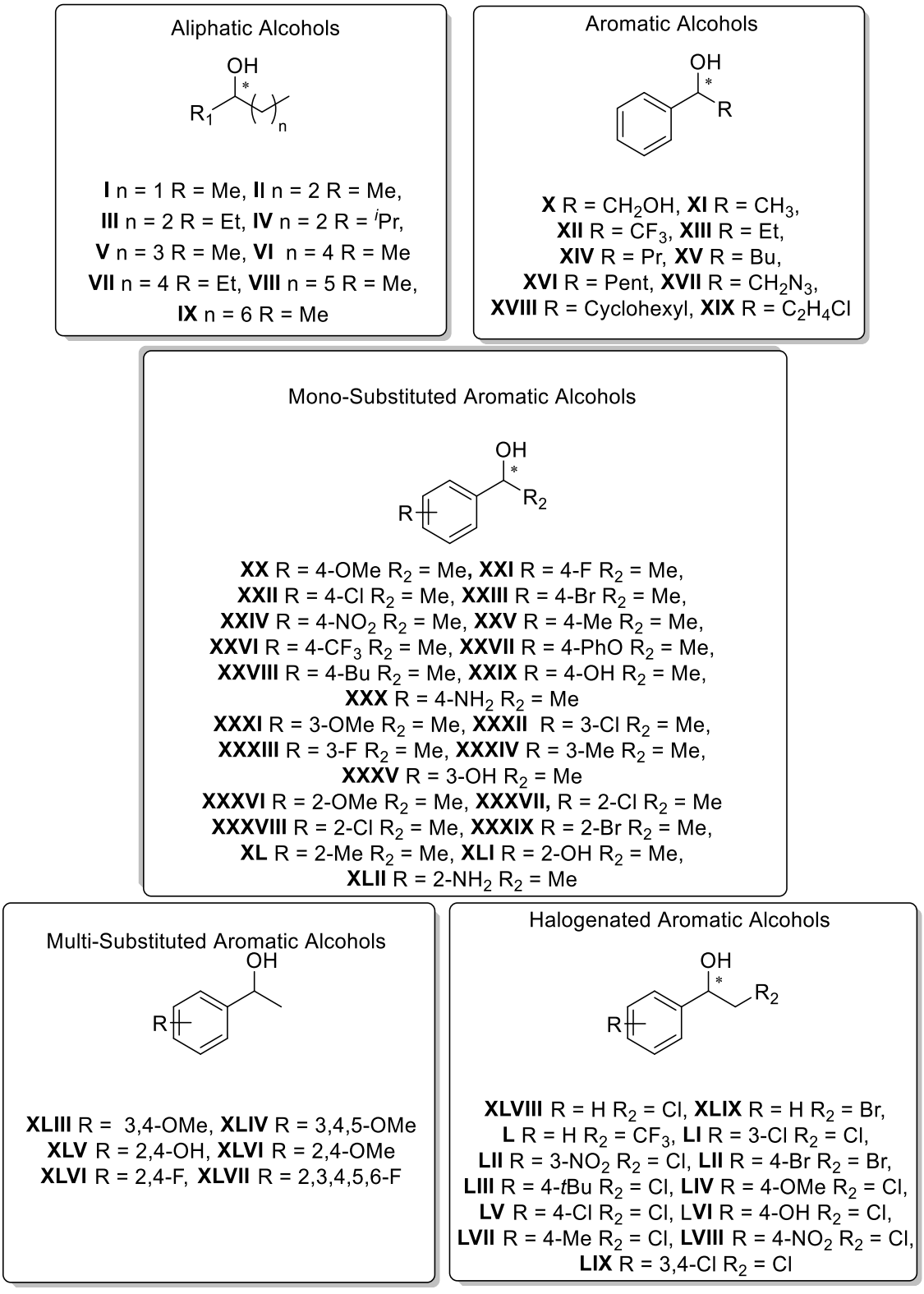

Figure 1.6; Shows a range of aliphatic and aromatic compounds made using alcohol dehydrogenases. I,[99,100] **II,** [99-104] **III,** [105] **IV,** [102] **V,** [99-104] **VI,** [99,102,103,106-108] **VII,** [108,109] **VIII,** [99,102,105,107,108,110,111] **IX,** [101,102,106-108] **X,** [102,110,112-114] **XI,** [100,102,103,105,106,108,109,111,113,115,116-122,146] **XII,** [103,113,115,117,123,124] **XIII,** [100,102,103,105,,119-121] **XIV,**

[100,102,120] **XV**, [102,120] **XVI**, [102,120] **XVII**, [125] **XVIII**, [120] **XIX**, [104,126] **XX**, [101,106,108] **XXI**, [101,106,108] **XXII**, [101-103,106,108,113,115-117,121,127,128] **XXIII**, [101,103,106,108,113,115,116,128] **XXIV**, [101,115] **XXV**, [101,106,108] **XXVI**, [108] **XXVII**, [127] **XXVIII**, [106] **XXIX**, [106] **XXX**, [106] **XXXI**, [101,106,108] **XXXII**, [102,106,108,127] **XXXIII**, [129] **XXXIV**, [106,108] **XXXV**, [106] **XXXVI**, [101,103,106] **XXXVII**, [102,103,106,108] **XXXVIII**, [103] **XXXIX**, [108] **XL**, [106] **XLI**, [106] **XLII**, [106] **XLII**, [106] **XLIII**, [106] **XLIV**, [106] **XLV**, [106] **XLVI**, [106] **XLVII**, [104] **XLVIII**, [102,105,108,109,113,115-117,125,129-131] **XLIX**, [113,116,117,121] **L**, [104,116] **LI**,[103,132] **LII**, [127] **LIII**, [131] **LIV**, [131] **LV**, [125,131] **LVI**, [125] **LVII**, [125] **LVIII**, [125] **LIX**, [125]

B-Hydroxy Nitriles are a useful chiral intermediate that can be reacted further to get useful compounds. These can be hydrogenated to produce *γ*-aminoalcohols and if treated with an acid, they produce *β*-hydroxycarboxylic acids which are a key building block in the synthesis of some serotonin reuptake inhibitors.[131] Cyclic and heterocyclic ketones have also been shown to be substrates to ADHs and some examples are shown in **Figure 1.7**.

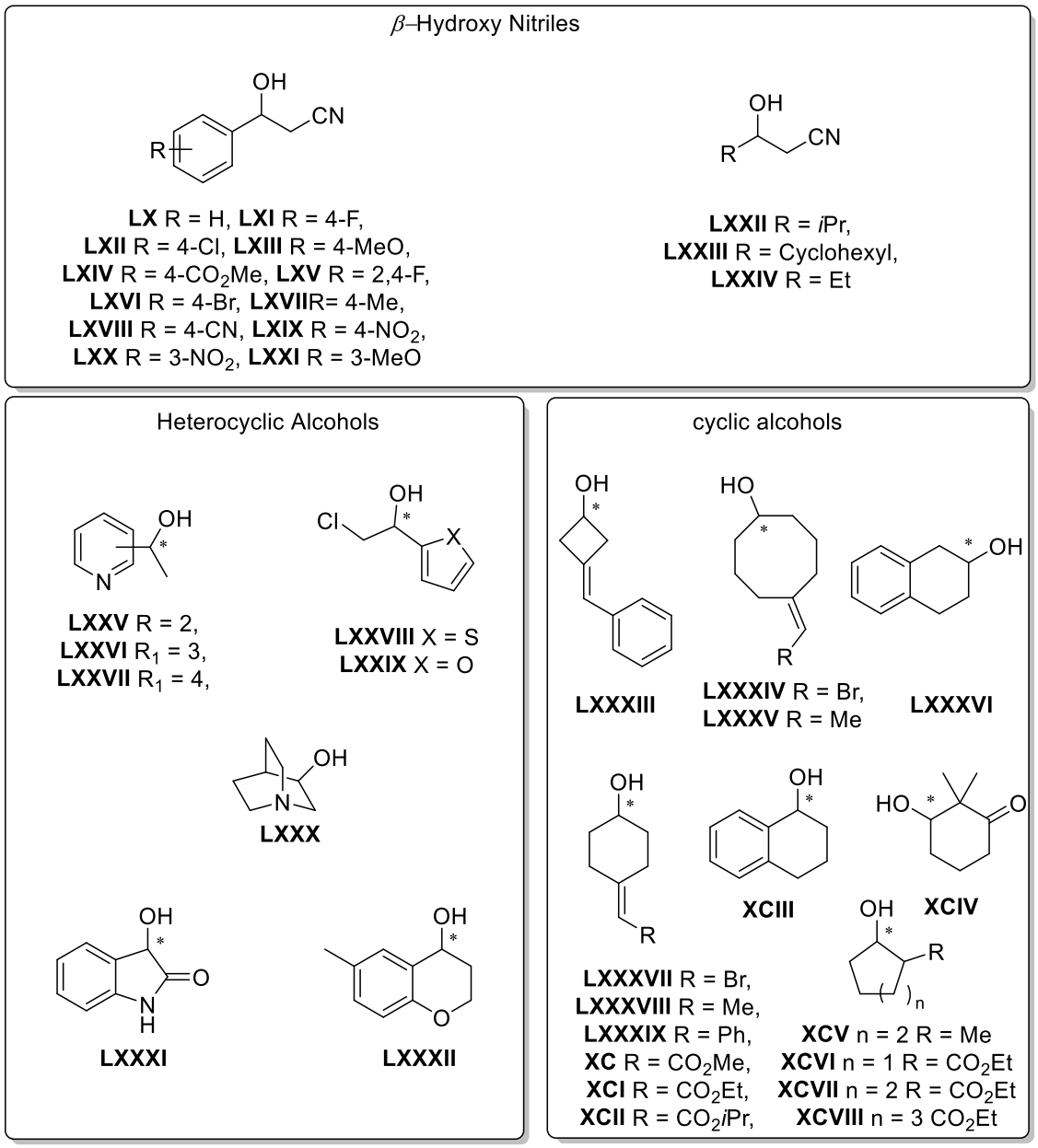

Figure 1.7; Shows a range of *β*-hydroxy nitriles and cyclic alcohols synthesised using alcohol dehydrogenases. LX, [117,125,133] **LXI,** [133,134] **LXII,** [133,134] **LXIII,** [133,134], **LXIV,** [133] **LXV,** [134] **LXVI,** [134] **LXVII,** [134] **LXVIII,** [134] **LXIX,** [134] **LXX,** [134] **LXXI,** [134] **LXXII,** [133] **LXXIII,** [133] **LXXIV,** [132] **LXXV,** [113,116,121,129] **LXXVI,** [113,116,121] **LXXVII,** [113,116,121] **LXXVIII,** [131] **LXXIX,** [125] **LXXX,** [135] **LXXXI,** [109,123,136] **LXXXII,** [108] **LXXXIII,** [137] **LXXXIV,** [137] **LXXXV,** [137] **LXXXVI,** [109,118] **LXXXVII,** [137] **LXXXVIII,** [137] **LXXXIX,** [137] **XC,** [137] **XCI,** [137] **XCII,** [137] **XCIII,** [108,110,118] **XCIV,** [129] **XCV,** [104,105], **XCVI,** [110,138-140] **XCVII,** [138-140] **XCVIII,** [139]

Unsaturated ketones as well as multiple ketones can also be reduced with ADHs. Shown in **Figure 1.8** is some examples of unsaturated ketones

being reduced in a similar way to a Luche reduction without the need for cerium and a stoichiometric reducing agent. With recent developments, toolboxes of enzymes have been put together so each diastereomer of **CIV** can be produced using a different combination of enzymes. This is highlighted in detail in **Scheme 1.13.**

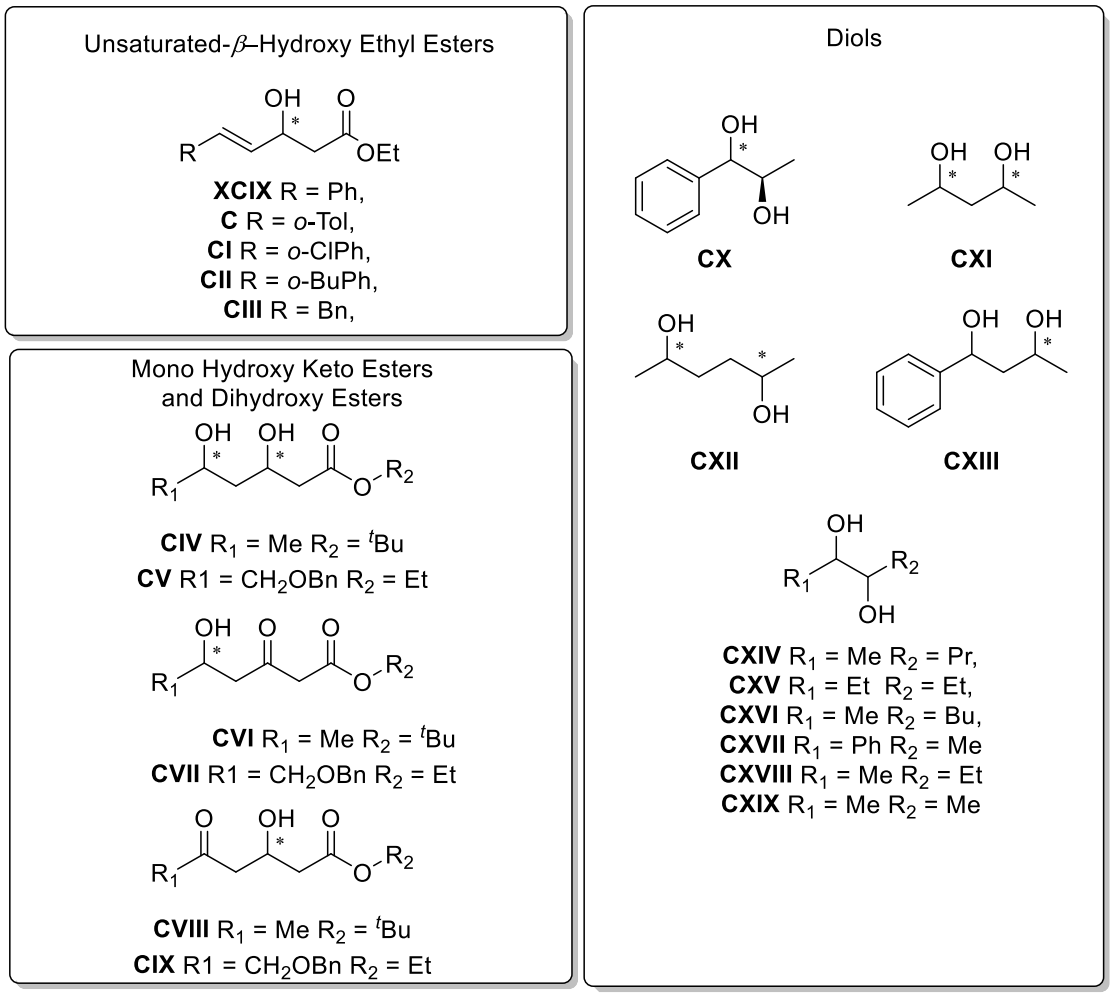

Figure 1.8; Shows a range of diols and unsaturated *β*-hydroxy esters made using alcohol dehydrogenases: XCIX, [141] **C**, [141] **CI**, [141] **CII**, [141] **CIII**, [141] **CIV**, [163] **CV**, [164] **CVI**,[163] **CVII**, [164] **CVIII**, [163] **CIX**, [164,] **CX**, [145] **CXI**, [99,140,146] **CXII**, [99,105,109,140,147] **CXIII**, [148] **CXIV**, [99,140] **CXV**, [99,140] **CXVI**, [99] **CXVII**, [123,124] **CXVIII**, [99,100,140,142,146] **CXIX**, [99,100,140,142,146] **CIV**, [163] **CV**, [164] **CVI**,[163] **CVII**, [164] **CVIII**, [163] **CIX**, [164]

Another important class of compounds that can be synthesised by ADHs is *β*-hydroxy Esters. This class of compound has become an important intermediate for the synthesis of *β*-lactams, pheromones and also,

similarly to β-hydroxy nitriles, are an intermediate in the synthesis of serotonin reuptake inhibitors.[136] This class of compound can be produced with a variety of different substitutions and functional groups shown in **Figure 1.9**.

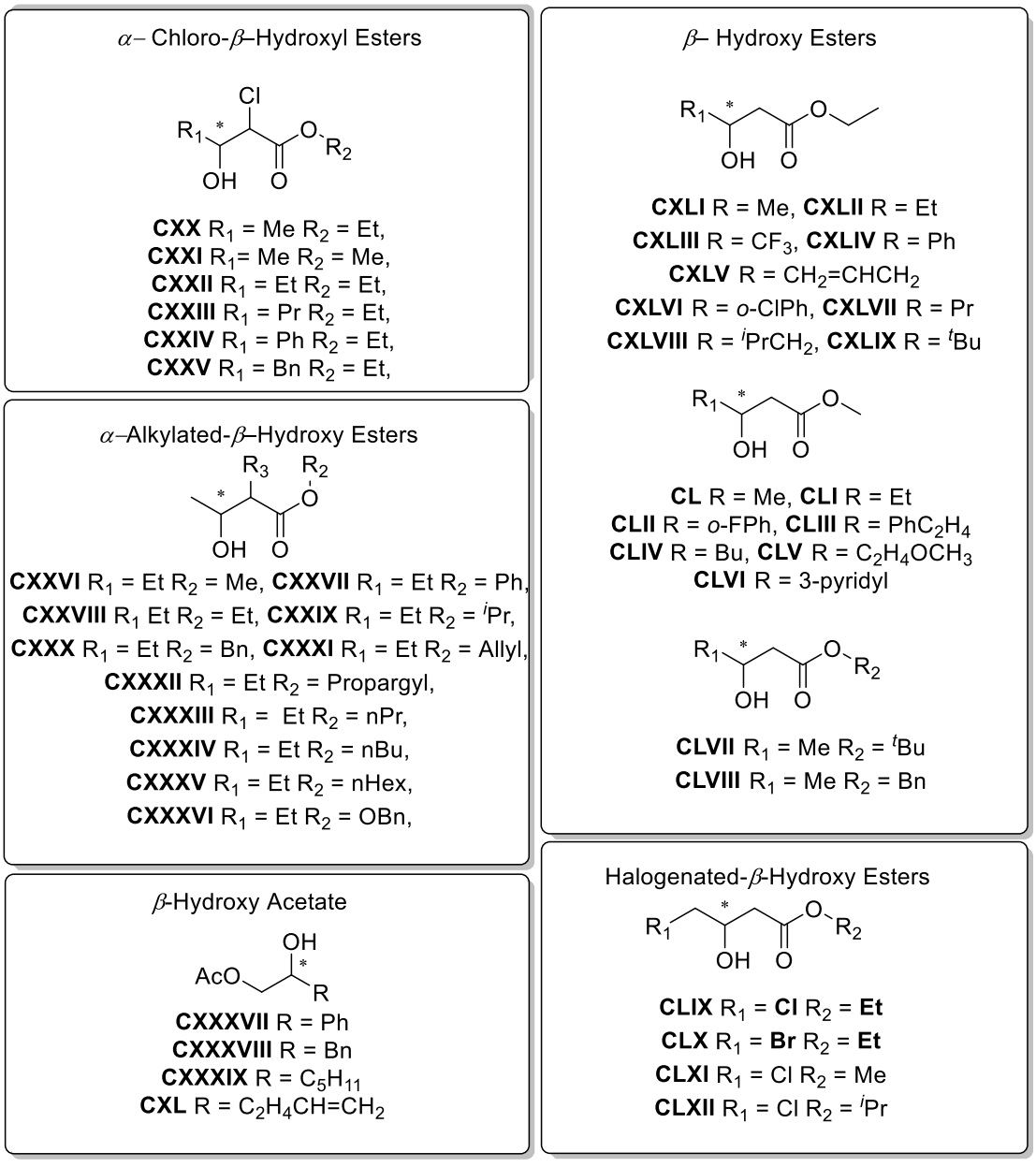

Figure 1.9; Shows a range of β-hydroxy esters made using alcohol dehydrogenases shown in recent literature: CXX, [99,136,138,140,142,143] **CXXI**, [136,142] **CXXII**, [144] **CXXIII**, [144] **CXXIV**, [144] **CXXV**, [144] **CXXVI**, [99,,104,118,138,149-151] **CXXVII**, [110] **CXXVIII**, [99,138,149-151] **CXXIX**, [138] **CXXX**, [138,152], **CXXXI**, [150,151] **CXXXII**, [150,151] **CXXXIII**, [99] **CXXXIV**, [99] **CXXXV**, [99] **CXXXVI**, [99] **CXXXVII**, [129,130] **CXXXVIII**, [129,130] **CXXXIX**, [129,130] **CXL**, [129,130] **CXLI**, [99,101-107,113-115,117,118,129,130,136,138,142,149-151] **CXLII**, [102,107,108,115,117,138,149,151] **CXLIII**, [102,108,113,115-

[117,136,138,144,153] **CXLIV**, [100,102,108,110,119,129,130,138] **CXLV**, [129,130] **CXLVI**, [129,130] **CXLVII**, [104,138,140,149,150] **CXLVIII**, [138,149] **CXLIX**, [108,138] **CL**, [101,102,106,129,130,132,136,146,150,151] **CLI**, [102,150,151] **CLII**, [102] **CLIII**, [129,130] **CLIV**, [129] **CLV**, [105] **CLVI**, [144,153] **CLVII**, [99,118] **CLVIII**, [140] **CLIX**, [99,100,102-,105,107,108,110,113,116-118,123,129-132,136,138,140,142,146,149,152,154-156] **CLX**, [103,116,117,157] **CLXI**, [125,136,142,146] **CLXII**, [109]

Similar to *β*-hydroxy esters, *α*-hydroxy esters are also a useful building block in asymmetric synthesis of other important drug molecules. This type of compound has been used due to the wide-ranging activity of this functional group, ranging from antibacterial activity to inhibiting human prostate cancer cells. Shown in **Figure 1.10** is a range of aliphatic and aromatic *α*-hydroxy esters produced by ADHs.

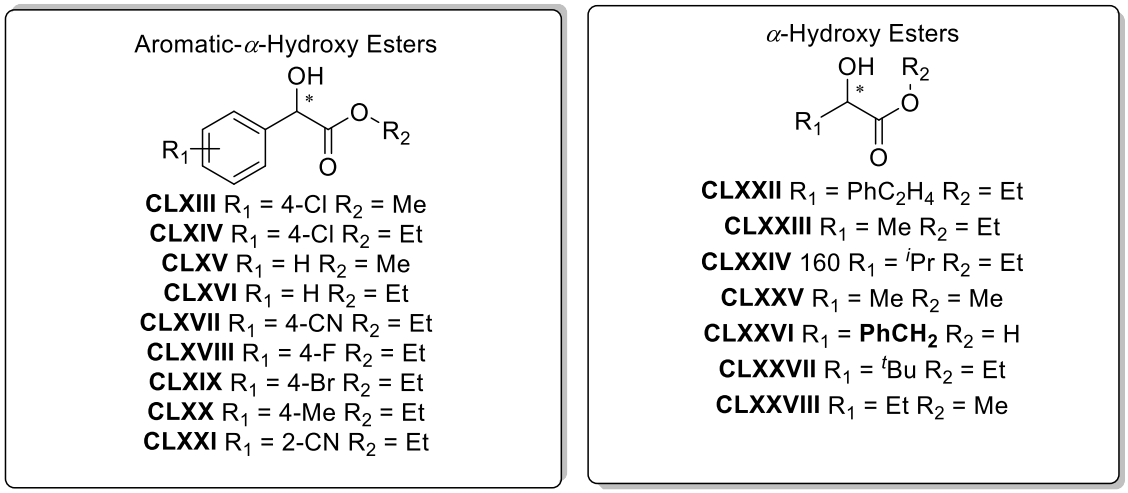

Figure 1.10; Shows a range of , *α*-hydroxy esters made using alcohol dehydrogenases shown in recent literature: CLXIII, [115-117,158,159] **CLXIV**, [108,115,117,123,160] **CLXV**,[100,102,103,115-117,119,123,124,139,158] **CLXVI,** [96,99,102,103,104,108,115,117,119,124,129] **CLXVII**, [108] **CLXVIII**, [108] **CLXIX**, [108] **CLXX**, [108] **CLXXI**, [161] **CLXXII**, [99,100,103,104,107,110,113,115-117,119,127,140,162] **CLXXIII**, [99,100,102-104,113,115,117,123,129,130,132,136,140] **CLXXIV** [99,103,108,116,117,140] **CLXXV,** [99,102,104,136,140,159] **CLXXVI**, [104,110] **CLXXVII**, [108] **CLXXVIII**, [99]

ADHs have been shown to show a large tolerance of different functional groups without side reactions. Shown in **Figure 1.11** is a range of different compounds that were reduced by ADHs. These functional groups

include adamantyls, allyl alcohols, *β*-thioesters and a variety of small molecules.

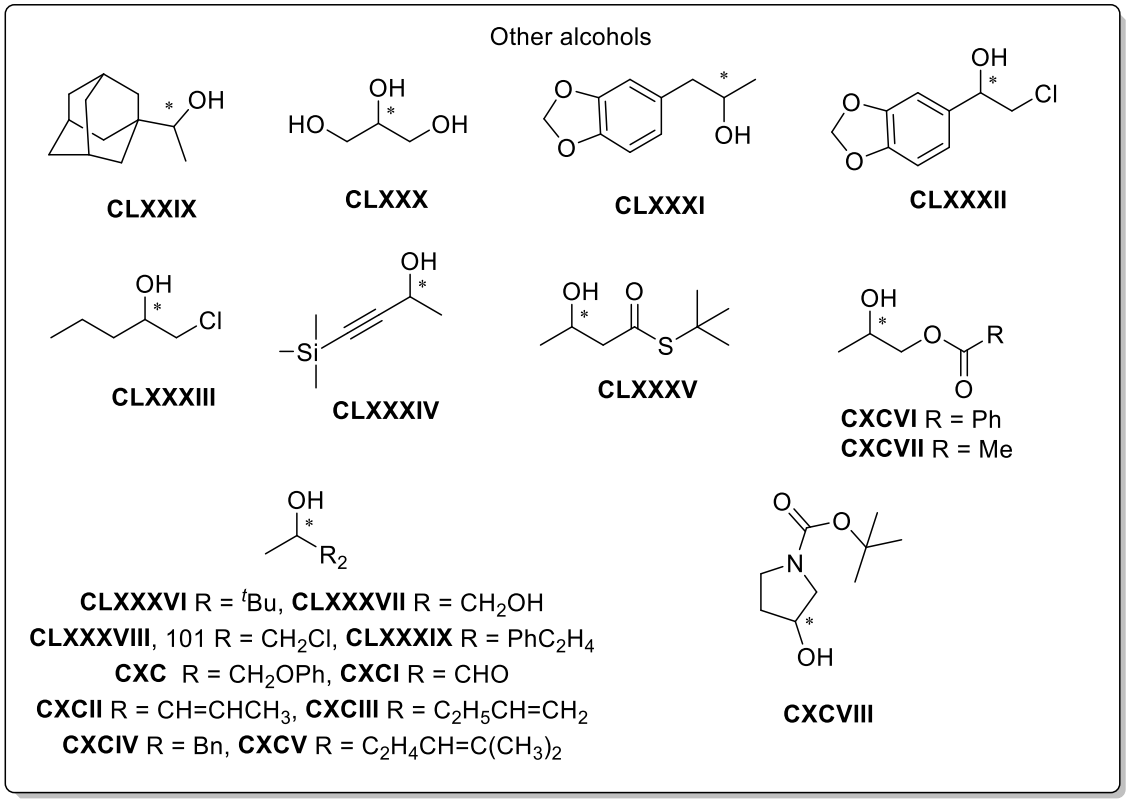

Figure 1.11; Shows a variety of different functional groups that were made using alcohol dehydrogenases shown in recent literature: CLXXIX, [108] **CLXXX**, [108] **CLXXXI**, [103] **CLXXXII**, [103] **CLXXXIII,** [129,130], **CLXXXIV**, [101] **CLXXXV**, [107] **CLXXXVI**, [101] **CLXXXVII**, [99] **CLXXXVIII**, [129,130] **CLXXXIX**, [99,100,105,119] **CXC**, [106] **CXCI**, [99] **CXCII**, [99] **CXCIII**, [99] **CXCIV**, [100] **CXCV**, [111] **CXCVI**, [110,128], **CXCVII**, [146] **CXCVIII**, [103]

Recently, an alcohol dehydrogenase was utilised in the stereoselective reduction of α-chloroketone **(85)** as an intermediate in the synthesis of atorvastatin **(71)**, shown in **Scheme 1.12**.[169] Compound **(87)** was produced from **(86)** using a whole cell biocatalysis using *Aureobasidium pullulans* producing the (*R*)-alcohol. This is then hydrolysed and reacted further to produce the retinoic acid receptor agonist **(88)**.[165] Merck's thrombine inhibitor **(91)** was produced from compound **(89)** using the commercially available KRED 1001 to produce compound **(90)**. The NAPDH was recycled in the reaction using glucose dehydrogenase (GDH).[166-168]

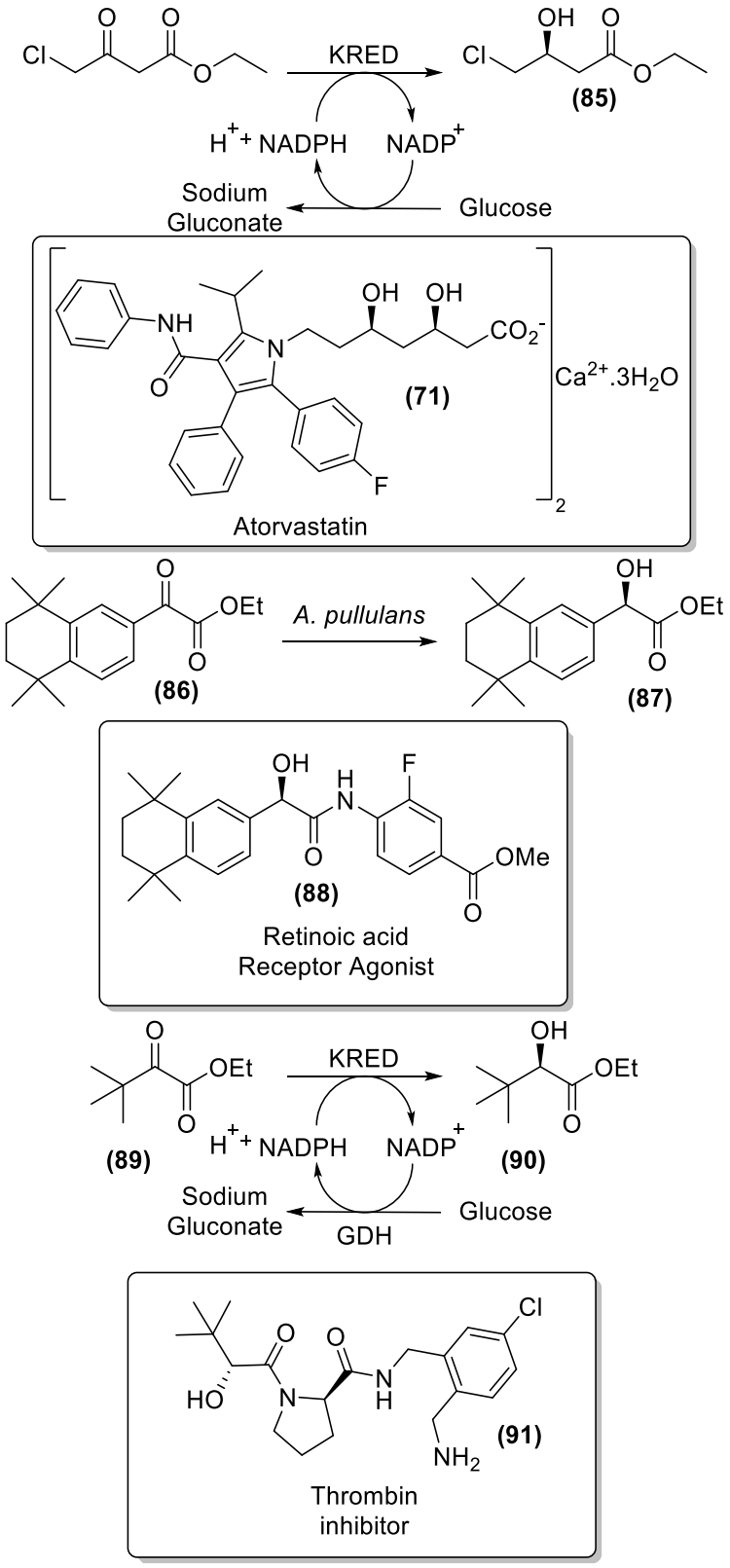

Scheme 1.12; Biocatalysis of an atorvastatin building block retinoic acid receptor agonist and a thrombine Inhibitor using ADHs.

Commercial ADH tool boxes has been developed to product the intended diastereomer but can be substrate dependant on how well they work. Shown in **Scheme 1.13**, taking *β, δ*-diketoester and reducing it with a commercially available ADH, can produce all 4 diasteromers at a minimum of >81% yields, >98% *e.e.* and >90% *d.r.* [163]

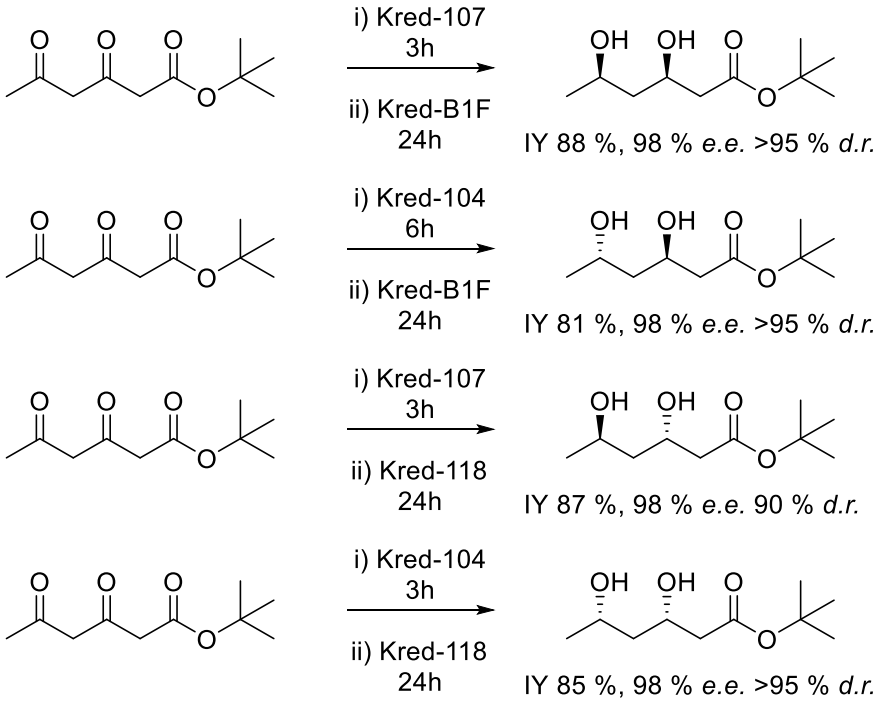

Scheme 1.13; The development of a commercial toolbox of ADHs.

1.4 Co-factor regeneration

As shown previously, alcohol dehydrogenase are NADPH dependant enzymes meaning they require a stoichiometric amount of the co-factor to do one turnover. Due to the biotransformation being in equilibrium, an excess of the cofactor would be required to drive the product to completion and to counter the equilibrium effect and this would not be financially viable. In the past two decades, there has been much work looking into NADPH recycling systems, these include chemical,

photoelectrochemical and enzymatic regeneration.[170-172] Shown in **Scheme 1.14**, a basic reaction scheme using ADHs with a recycling system, and shown in **Scheme 1.15**, the structure of NADH and NADPH, **(92)** and **(93)** respectively and the difference between the reduced and oxidised forms.

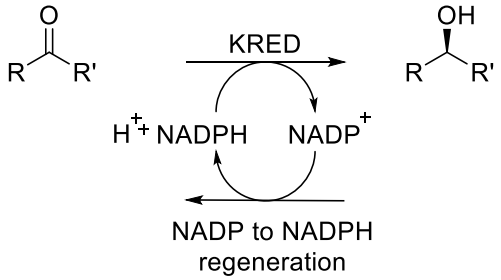

Scheme 1.14; Generic scheme for an alcohol dehydrogenase recycling system

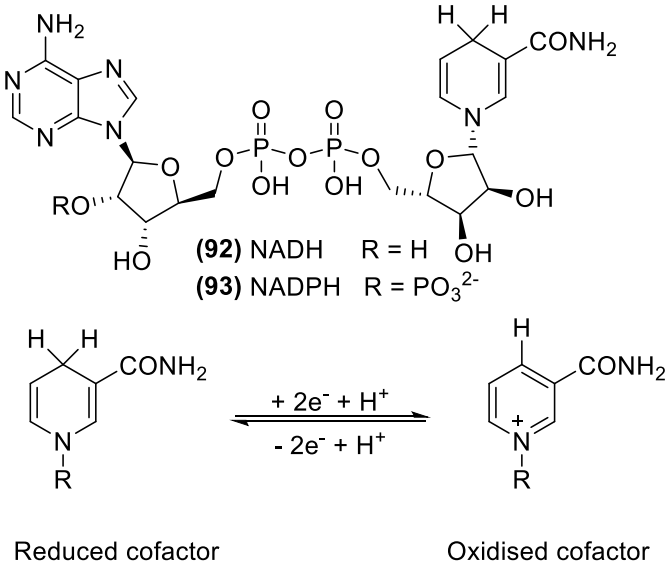

Scheme 1.15; Differences between NADH, NADPH, NAD^+ and $NADP^+$.

1.4.1 Chemical Regeneration.

Ruthenium(II) and Rhodium(III) complexes use hydrogen to directly reduce the $NADP^+$ to NADPH. This method is suitable for use as a $NADP^+$ recycling system as hydrogen leads to no unwanted byproducts, meaning

less purification required after the reaction. These reactions are also able to be done under very mild conditions, with a temperature between 25 - 65 °C and a pH of 6.5 - 8.5. It also has good selectivity for the $NADP^+$ over the substrate leading to the biotransformation having good enantioselectivity. Shown in **Scheme 1.16**, an example uses *Thermoanaerobium bockii* ADH to reduce 2-heptanone **(94)** to 2-heptanol **(95)** in an 18% yield and 40% *ee*. [173,174]

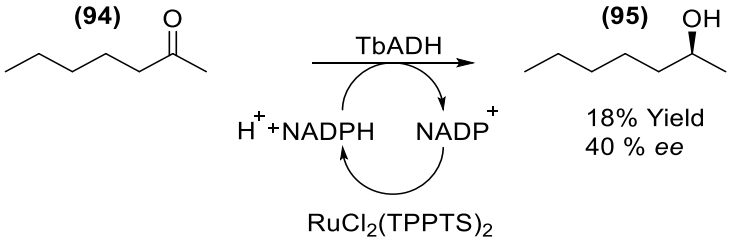

Scheme 1.16; Using ruthenium to regenerate NADPH

Recycling NADH can be done using a biphasic reaction involving a platinum carbonyl cluster, a redox dye and hydrogen gas. The platinum carbonyl cluster is only soluble in organic solvents, and in this example, CH_2Cl_2 is used. The redox dye acts as a shuttle carrier, transferring 2 electrons and 1 proton to the NAD^+. When pyruvate, NAD^+ and platinum carbonyl complex are in the ratio of 600:10:1, the reaction proceeds to full conversion after 48 hours. Shown in **Scheme 1.17**, the conversion of pyruvate to L-lactate. SafH and Saf^+ is the redox dye and the reduced form of the redox dye respectively.[174-176] From the low yields and the use of heavy metals and toxic organic solvents, this is not readily available for industry.

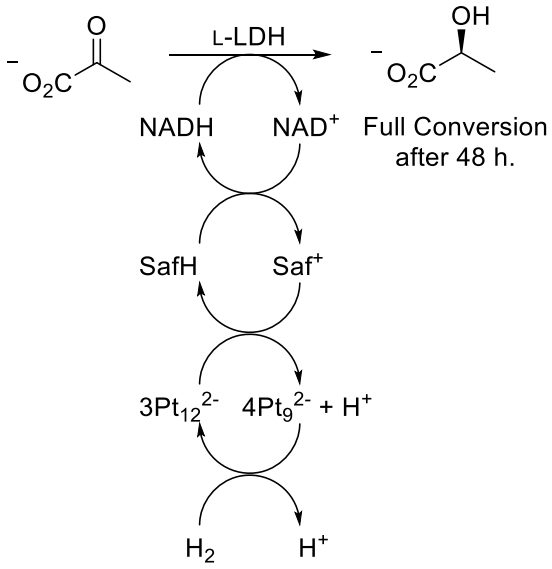

Scheme 1.17; Regeneration of NADH using a platinum complex.

1.4.2 Photoelectrochemical regeneration

Phototrophs such as algae and plants capture light energy to generate NADPH from $NADP^+$ through photosynthetic electron-transfer reactions. This has been utilised to recycle the NADPH in biotransformations. Replacing the phototroph with a catalyst, a photosensitizer is required which would increase the rate of regeneration, but comes with the issues of stability. Known photosensitizers such as metal-containing porphyrins are unstable leading to poor turnover and regeneration of cofactor. Shown in **Scheme 1.18**, the synthesis of (*S*)-1-(4-chlorophenyl)ethan-1-ol, **(96),** using the cyanobactieria *Synechococcus elongatus* PCC 7942.[177-179]

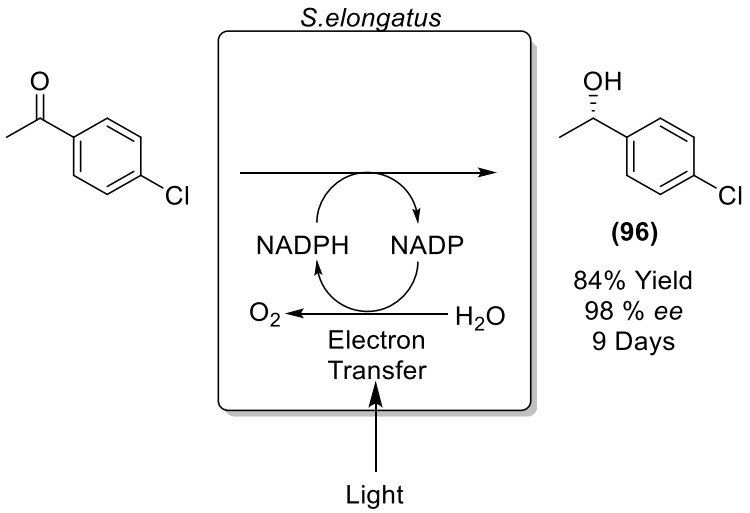

Scheme 1.18; photoelectrochemical regeneration of NADPH.

1.4.3 Electrochemical regeneration

Regeneration of NADPH *via* electricity is an attractive approach as there is no need for any chemical reductants and no stoichiometric byproducts produced, meaning there will be less containments to remove during purification. Electricity can be considered a "cheap" reducing agent which then also reduces the financial aspect of the reaction. The regeneration can be done in three ways, shown in **Figure 1.12**, directly, where the cofactor interacts directly with the cathode, indirectly, where a mediator is used to transfer electrons to the cofactor. The last method is an enzyme-coupled electrochemical regeneration, where a mediator transfers the electrons to an enzyme which then regenerates the cofactor.[180]

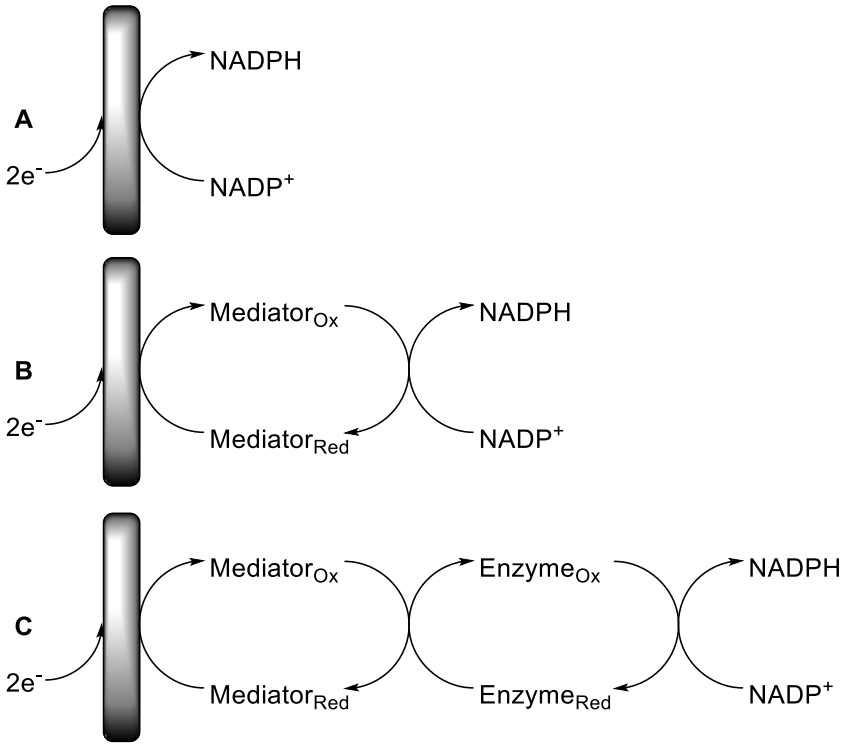

Figure 1.12; A) Direct regeneration, B) Indirect regeneration, C) Enzyme-coupled electrochemical regeneration.

1.4.3.1 *Direct regeneration*

Direct regeneration requires no additional materials, leading to a reaction having less substituents in, meaning less to remove during purification. Direct reduction of $NADP^+$ is a two step reaction; the first reduction has a potential of about -1.2 V vs. SCE which forms a radical species. Afterwards this radical can be protonated with a second electron. Using a cholesterol modified gold amalgam, it was able to convert pyruvate to D-lactate with a conversion of 72% after 21 h shown in **Scheme 1.19**. However, this method has some major disadvantages, the cofactor radical formed after the first electron addition can dimerise. Not only that, the protonation is not selective, leading to a 1,6 NADPH **(97)** formed, which is inactive shown in **Figure 1.13**. Due to these all these issues, this method of electrochemical regeneration is not commonly used.[181]

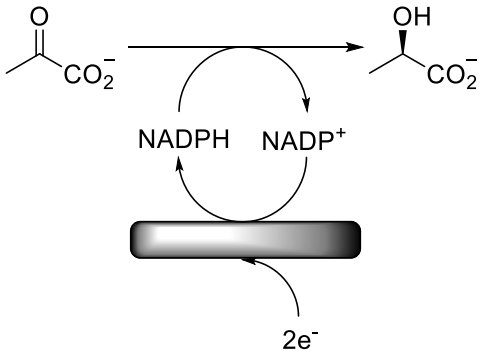

Scheme 1.19; Direct regeneration of NADPH *via* cholesterol modified gold amalgam cathode.

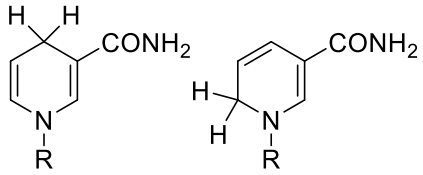

1,4-NADPH **(93)** 1,6-NADPH **(97)**

Figure 1.13; The inactive 1,6-NADPH (97) compared to the active 1,4-NADPH (93).

1.4.3.2.*Indirect electrochemical regeneration.*

To overcome all the issues in direct electrochemical regeneration of NADPH, a mediator can be used, but it needs to meet the following criteria to be successful.[180,182]

- It must transfer two electrons of one hydride ion in one step
- The electrochemical activation of the mediator must be possible at potentials less negative than -0.9 vs. SCE.
- The mediator must not react with the substrate
- Only the 1,4- NADPH must be formed.

The first criteria is to stop any radicals forming, this is to stop any dimers of the cofactors forming. It is also to stop the unselective protonation from forming the inactive 1,6-NADPH. The second criteria is at potentials less than -0.9 vs. SCE, the NADPH is directly reduced. The third and forth

criteria are straight forward, if no side reactions occur and no degradation of the cofactor occurs, the reaction will work to good yields. Most of these methods require some heavy metal catalyst as the mediator, such as the example shown in **Scheme 1.20** being produced with an *ee* of >99.9% as well as high volumetric productivities of 15 g L^{-1} d^{-1} at a scale of 200 mL using a carbon felt as the cathode.[180]

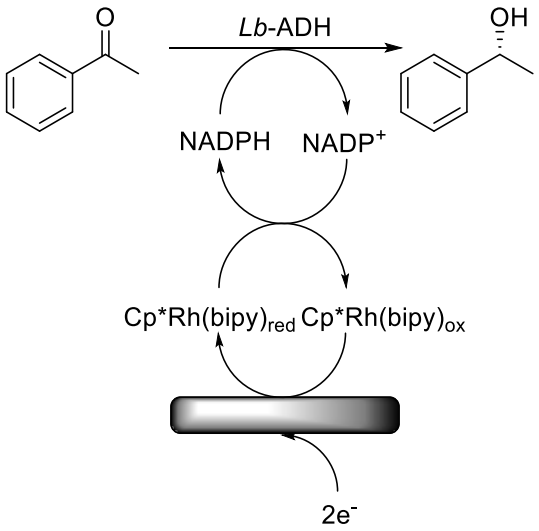

Scheme 1.20; Indirect electrochemical regeneration of NADPH.

1.4.3.3 *Enzyme-coupled electrochemical regeneration*

The criteria set above can be very difficult to find an electrochemical redox catalyst that fulfils all requirements for the regeneration of NADPH cofactor effectively. Using a second enzymatic cycle reduces the problem of cofactor dimer formation with several examples using methyl viologen (MV^{2+}) in combination with diaphorase to regenerate NADPH. Shown in **Scheme 1.21,** the synthesis of (*R*)-mandelate **(99)** from benzoylformate **(98)** using benozylformate reductase (BFR) was achieved at a 80% yield in 30 h using a gold amalgam cathode.[183,184]

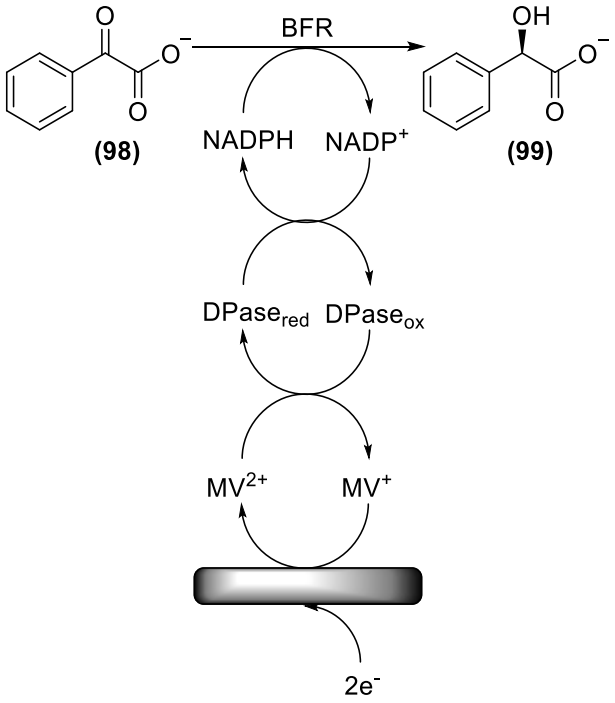

Scheme 1.21; Enzymatic electrochemical regeneration of NADPH

1.5 Enzymatic regeneration of NADPH

The most common and frequently used methods of regeneration of NADPH is using enzymes. There are many advantages of using these over the other regeneration methods mentioned above, such as; not using heavy metals, higher compatibility with other enzymes and less off target reactions. There are two different types of enzymatic regeneration. Enzyme coupled, where another enzyme is used to catalyse another reaction to recycle the cofactor, and substrate coupled, where a second substrate is used to complete the regeneration cycle.

1.5.1 Substrate coupled enzymatic regeneration.

Shown in **Scheme 1.22**, the regeneration is achieved using one enzyme and two different substrates. The reduction of a ketone to the target

alcohol and the oxidation of a different alcohol to recycle the cofactor. Due to this reaction being in equilibrium, a large excess of the co-substrate is required or removal of the oxidised co-substrate. Usually, 2-propanol is used as this co-substrate and this is because it is inexpensive, most enzymes have some tolerance to it, and that the product, acetone, has a low boiling point and can be removed from the reaction. [111,117,120,185-188]

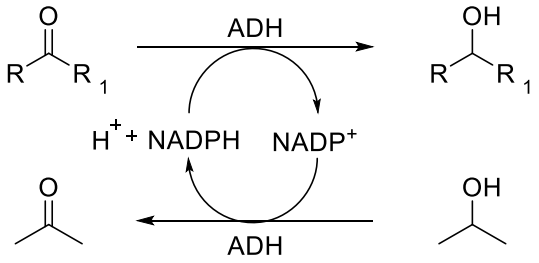

Scheme 1.22; Substrate coupled enzymatic regeneration.

1.5.2 Enzyme coupled enzymatic reduction.

This method of regeneration uses another enzyme system to regenerate the cofactor. There are many different enzymes used with the most common described in the following.

1.5.2.1 *Formate dehydrogenases (FDHs)*

Formate dehyrogenases are a type of enzyme that catalyses the oxidation of formate to carbon dioxide. These are an attractive method to regenerate cofactors as the product is a gas and can remove itself from the equilibrium. This shifts the equilibrium almost completely to the desired product. In addition to this, product isolation and purification is as any CO_2 produced is very easily removed. The starting material for this enzyme is formate, which is very cheap, inert and tolerant to many

different pHs. However, FDHs have a very low affinity for the phosphorylated cofactor over the non-phosphorylated cofactor making it only useful for the regeneration of NADH. Even though it can only recycle NADH effectively, there are many examples in the literature of this recycling system being used with example of the reaction is shown in **Scheme 1.23.** [106,107,118,119,128,146,161,189,190]

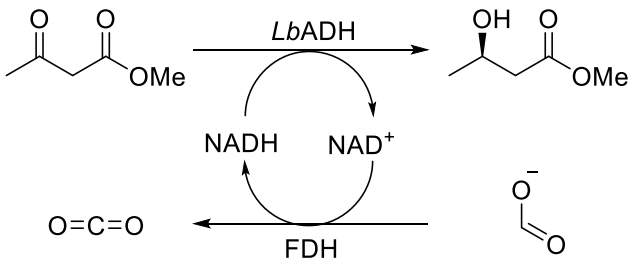

Scheme 1.23; Example of FDH recycling system.

1.5.2.2 *Glucose-6-phosphate dehydrogenase (G-6-P-DH)*

Glucose-6-phosphate dehydrogenase catalyses the oxidation of glucose-6-phosphate to 6-phosphogluconolactone. This spontaneously forms 6-phosphogluconate removing it from the equilibrium and shifting it towards the product. However, it comes with many disadvantages, such as; glucose-6-phosphate's instability in water and cost. NADPH has also been found to be decomposed by both 6-phosphogluconolactone and glucose-6-phosphate as they act as general acid catalysts. [191-194]

1.5.2.3 *Glucose dehydrogenase (GDH)*

Glucose dehydrogenase catalyses the oxidation of glucose **(100)** to gluconolactone **(101)** which like the aforementioned 6-phosphogluconolactone, also spontaneously hydrolyses to gluconic acid

(102). GDHs from *Bacillus subtilis* and *Bacillus megaterium* have been well studied and have high affinities for both NAD^+ and $NADP^+$. The starting material for this process is glucose, which is very cheap and stable in most solutions. However, the gluconic acid produced by the reaction will start to decrease the pH of the reaction mixture if the reaction isn't suitably buffered. Despite this, GDH has proved to be an excellent regeneration tool for NADH and NADPH regeneration and is shown in **Scheme 1.24**.

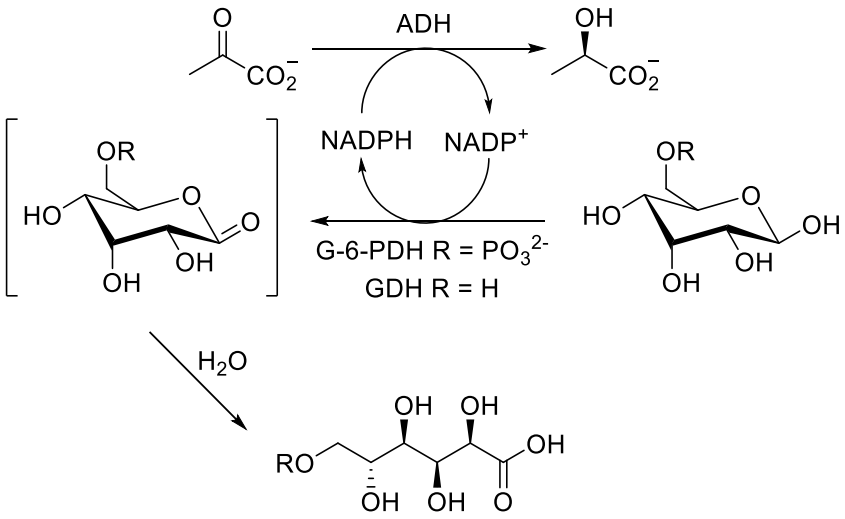

Scheme 1.24; Example of G-6-PDH and GDH as a recycling system

1.6 Synthesis of Oxanes

Oxanes, also known as tetrahydropyrans, are cyclic eithers that are present in many different natural products and drug molecules. Their first reported synthesis was in 1904 by Maitland and Japp. The reaction required 2 equivalents of benzaldedhyde with 2-butanone, in the presence of base. The first step of this reaction is an aldol condensation of the benzaldehyde onto the 2-butanone, followed by second aldol addition shown in **Scheme 1.25**. This is followed by an oxa-Michael addition of

the alcohol into the double bond formed from the aldol condensation and a keto-enol tautomerization to form the product.

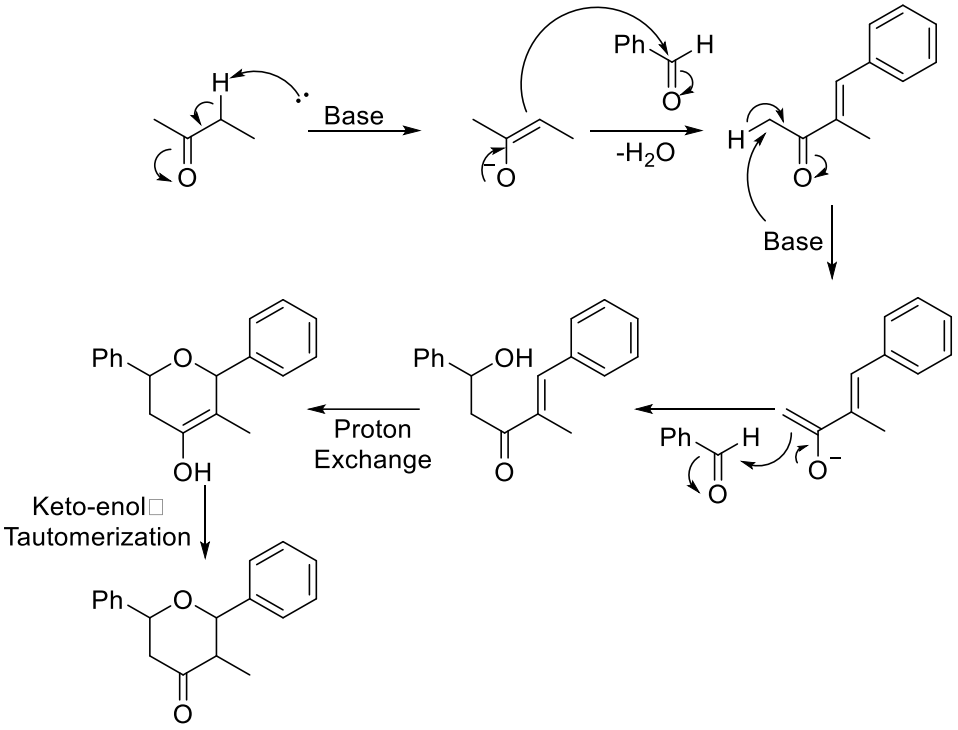

Scheme 1.25; Maitland-Japp mechanism

The main three approaches to making an oxane is usually based on a nucleophilic oxygen (as a hydroxy or epoxy group), attacking an activated functional group (an epoxide, leaving group on a saturated carbon, or an electrophilically activated alkene). Synthesis *via* lactones can also fall into this category. Another method involve making a C-C bond using an acyclic ether and cyclising it by using radicals. The last method involves the formation of the C-O and C-C bond in the same reaction, this is based on the Maitland-Japp cyclisation. This can be visualised in **Scheme 1.26**.[195]

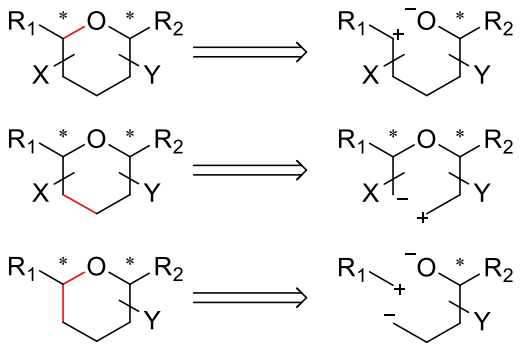

Scheme 1.26; Visualisation of the 3 main ways of producing oxanes.

1.6.1 Forming the C-O Bond

1.6.1.1 *Oxa-Michael Addition*

The intermolecular Michael addition of an oxygen into an unsaturated double bond is an interesting concept, the geometry of the double bond can be used to control the selectivity of the oxane produced. Shown in **Scheme 1.27**, the nature of the double bond can give the different diasteromers. This can be rationalised as the model with a pre-chair conformation in which the directing group (DG) located in the axial mode for the *E*-isomer **(103)** and the equatorial mode for the *Z*-isomer **(104)** so that the 6 membered transition state can be formed.[195,196]

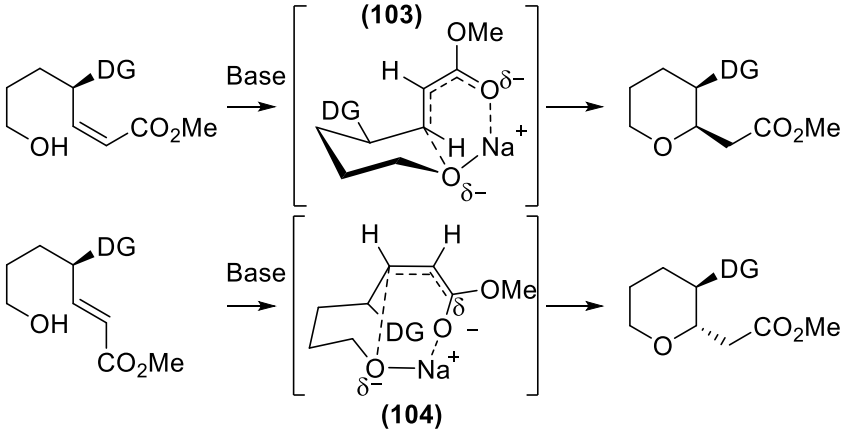

Scheme 1.27; How the *cis*/*trans* double bond changes the product of the intermolecular oxa-Michael reaction

1.6.1.2 *Intermolecular Nicholas Reaction*

Another method of forming these C-O bonds is by an intermolecular Nicholas reaction shown in **Scheme 1.28**. This can be done either by a free alcohol or an epoxide, with the regioselectivity being influenced by a number of factors, including the distance between the epoxide and the propargylic cation, the nature of the protecting group on the primary alcohol, as well as other reaction conditions. This methodology can be applied to make much larger cyclic ethers, a limitation of the oxa-Michael reaction which could make 5-7 membered cyclic ethers.[195-197]

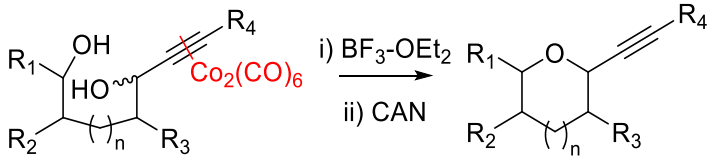

Scheme 1.28; Intermolecular Nicholas Reaction.

1.6.1.3 *Macrolactonisation*

Macrolactonisation is another method of producing the C-O bond, but unlike the previous reactions, this leads to a further reaction forming a lactone. It's a process that has been used in the synthesis of the natural product 9-demethylneopeltolide. The reaction proceeds by a Wacker-type anti-oxypalladation to generate an alkylpalladium species, which undergoes a carbon monoxide migratory insertion, which then reacts to the tethered alcohol to form the lactone **(105)**.[195,198,199]

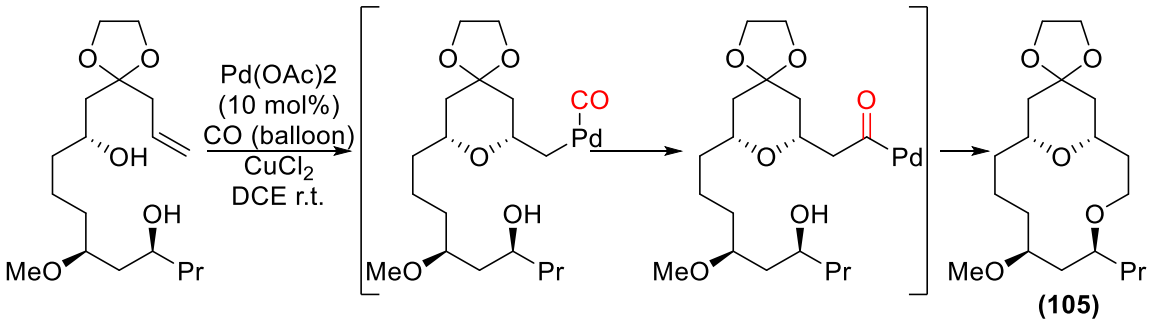

Scheme 1.29; **Oxane formation *via* macrolactonisation.**

1.6.1.4 *Williamson Ether Synthesis*

Williamson ether synthesis can also be used in the synthesis of oxanes. It has been used three times in the total synthesis of (+)- spongistatin 1 **(106)**. The first step is an asymmetric dihydroxylation of the alkene bond, which then cyclises to form the oxane after treatment with NaOMe shown in **Scheme 1.30**.[200-204]

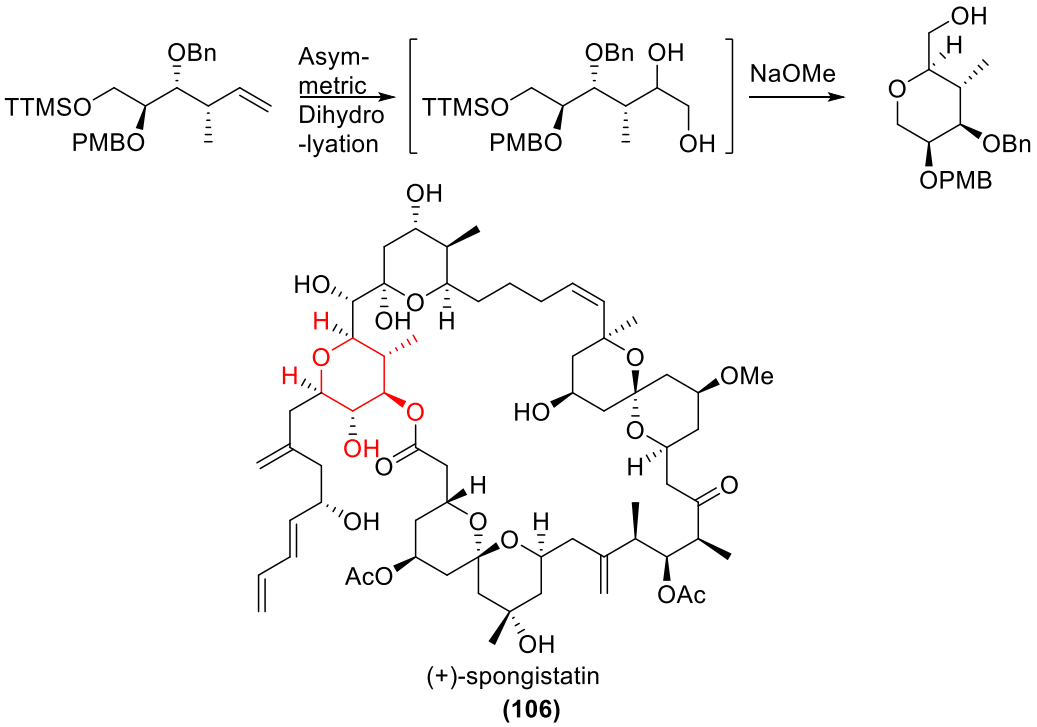

Scheme 1.30; Williamson ether synthesis being used to make an oxane in the natural product (+)-spongistatin.

1.6.2 Forming the C-C bond

The formation of the C-C bond is another potential way of making the oxane ring, the C-C bond being made can be adjacent to the oxygen or a bond away. Two methods of performing this uses radicals, one is a radical ring closing of a vinylogous carbonate and another uses a samarium based coupling of an aldehyde and an alkene.

1.6.2.1 *Ring Closing Metathesis (RCM)*

Using RCM is a useful cyclisation to close the cyclic ether ring as it leaves a handle for further reactions to take place. Although this methodology is very prevalent in making macrocycles and dihydrofuran skeletons, there are some that make dihydropyrans, though not oxanes, these are a hydrogenation away from being oxanes. Using Grubbs 2nd generation catalyst, a fluorinated aromatic hydrocarbon (FAH) or benzene, the RCM on a (-)-isopulegol derivative **(107)** to make a tetrasubstituted dihydropyran **(108)**. Robert Grubbs also showed in his 1996 paper that RCM access to dihydropyrans all shown in **Scheme 1.31**.[205-207]

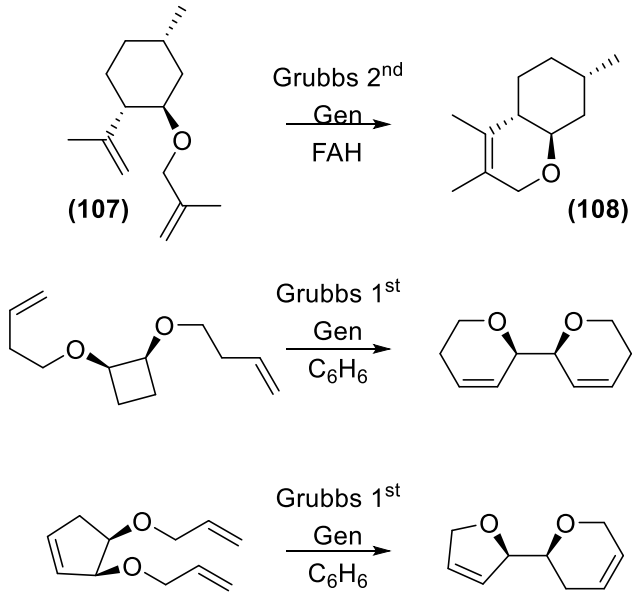

Scheme 1.31; **Synthesis of dihydropyrans by RCM.**

1.6.2.2 *Radical-based coupling*

This strategy was pioneered by Nakata *et al.* in the early 2000s where an aldehyde reacts with a *Z*-alkene to form an oxane. This uses samarium iodide as a single electron reductant, which then leads to a radical attack to form the oxane, the radical is then converted to an anion by another

equivalent of SmI_2 and then protonated by the solvent shown in **Scheme 1.32**.[195,208-210]

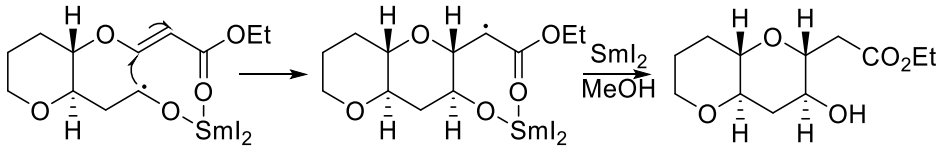

Scheme 1.32; Samarium-based coupling to form oxanes.

1.6.3 Forming C-O bond and C-C bond in the same reaction

This method is highly desireable and is based on the Prins cyclisation and has been used many times to make the oxane ring. Another method of forming the two bonds at once is using a hetero Diels-Alder reaction, which can produce penta-substituted oxane rings. These two methods have been utilised in many different natural product and pharmaceutical syntheses.

1.6.3.1 *Prins Cyclisation*

Prins cyclisation has been used many times in the synthesis and production of oxane rings with the first reported cyclisation in 1955 by Hanschke. The mechanism proceed *via* a oxocarbenium ion which drives the reaction. Initially, the reaction conditions required were quite harsh requiring concentrated sulfuric acid or hydrochloric acid. Recent advancements have found very mild conditions, requiring a lewis acids, such as $FeCl_3$ this is shown in **Scheme 1.34**.[212]

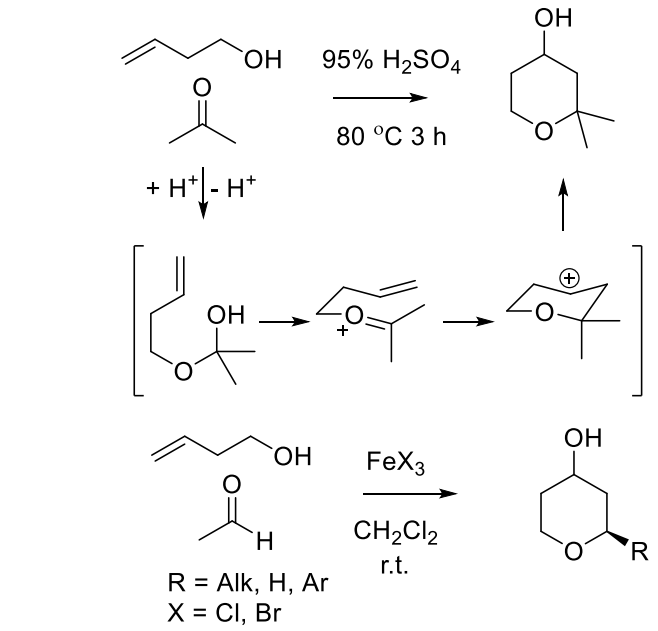

Scheme 1.34; Hanschke's original method compared to recent methodology.

In recent years, this methodology has been combined with macrolactonisation in the synthesis of lyngbyaloside B **(111)** making the natural product in 67% yield shown in **Scheme 1.35**.[213,214]

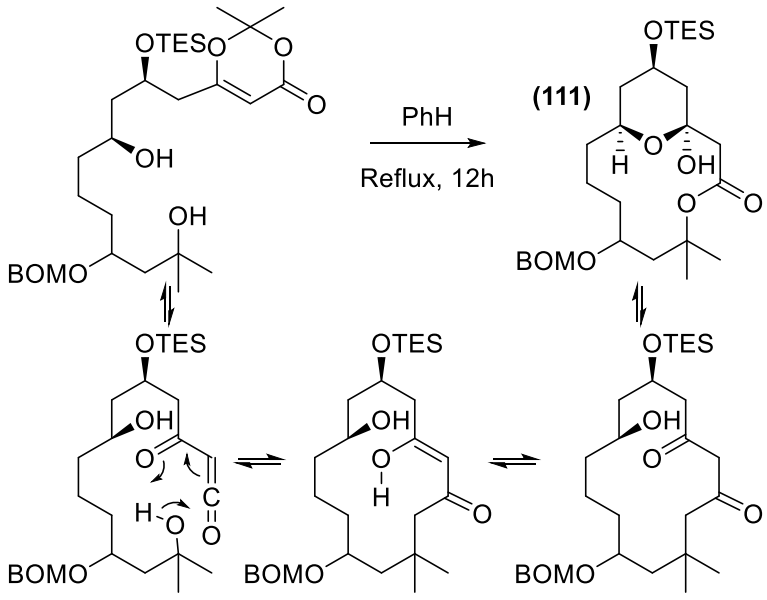

Scheme 1.35; Synthesis of lyngbyaloside B.

1.6.3.2 Hetero Diels-Alder reaction

This method has been used my several groups in the construction of the functionalised oxane rings due to the tolerance of how many substituents it can have. This method was used in the construction of ring B in the natural product bryostatin 1 resulting in a *d.r.* of 15:4 which was easily seperatable. It was also used in the synthesis of the anti-fungal natural product (+)-ambruticin. The key hetero-Diels Alder step furnished the oxane ring in a 64% yield with an *ee* of 97%. To undertake this transformation, Jacobsen catalyst **(110)** was used, this is shown in **Scheme 1.33**.[200211]

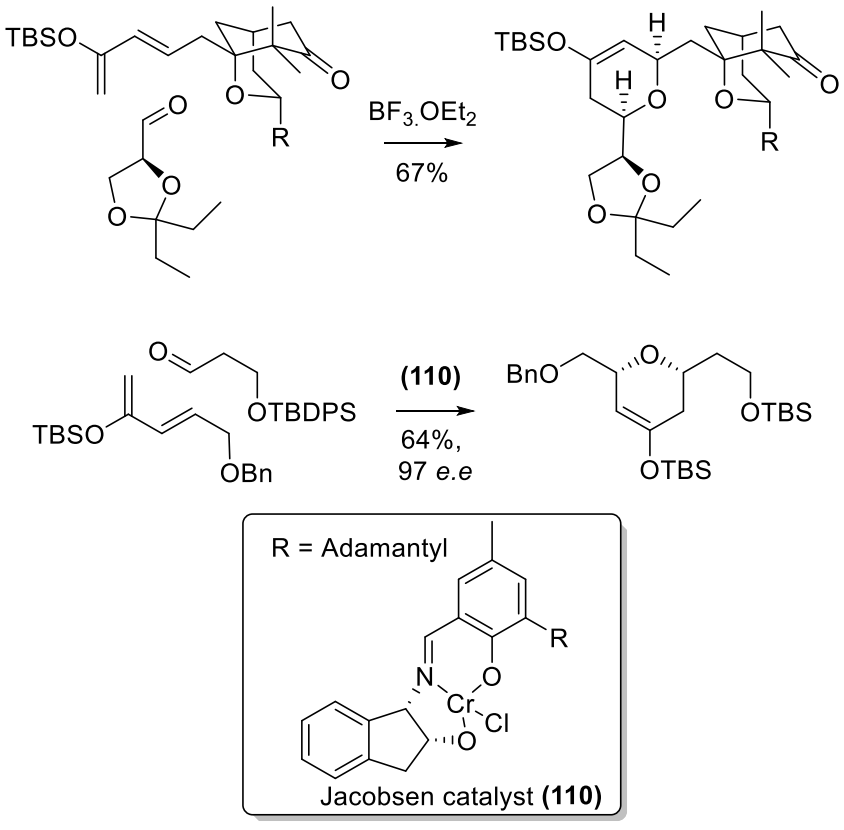

Scheme 1.33; Examples of Hetero Diels-Alder reactions being used to synthesis oxane rings.

1.7 Aims and Objectives

The aim was to explore the potential of making tetrahydropyran and tetrahydrofuran rings using an oxa-Michael cyclisation of a chiral alcohol produced by two ADHs, LK-ADH and RAL-ADH. This methodology is based on the paper published previously in the group but instead used amine transaminases.[215] As shown previously, there are many different natural products which have a tetrahydropyran core which could be a good potential target to be made using the methodology in this work. There are two main objectives in this work;

- Express LK-ADH and RAL-ADH from their plasmid.
- Synthesising a range of different substituted ketoenones to be tested with the two expressed ADHs in a biotransformation.
- Find a method to epimerise the oxanes once produced and produce a natural product to show the scope of the methodology.

Section 2: Results and Discussion

As discussed in the introduction, there is a lack of green alternatives for the production of tetrahydropyrans. Previous work done in the O'Reilly group successfully employed amine transaminases for the selective amination of ketoenone substrates, which subsequently undergo an aza-Michael reaction to form bioactive piperidine scaffolds shown in **Scheme 2.1**.[215] The aim of this work is to extend this methodology to achieve the chemoenzymatic synthesis of tetrahydrofuran and tetrahydropyran scaffolds by exploiting an alcohol dehydrogenase (ADH) to form a chiral alcohol, which can undergo a subsequent oxa-Michael reaction.

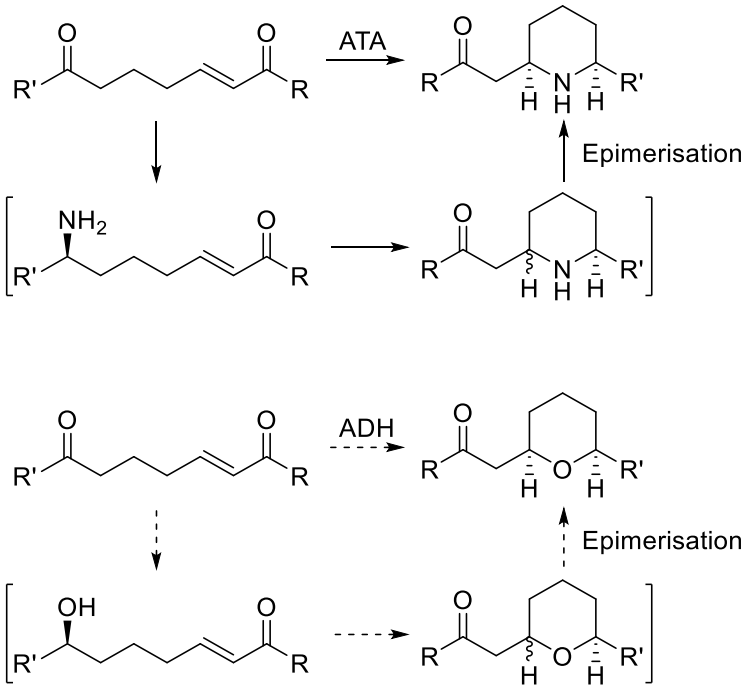

Scheme 2.1; Shows previous work from the group and the project.[215]

Expression of alcohol dehydrogenase.

The ADH plasmids were gratefully received from Professor Wolfgang Kroutil from the University of Graz. The plasmids used are from *Ralstonia sp*. (RAL-ADH) and *Lactobacillus kefir* (LK-ADH). RAL-ADH is a bulky-

bulky type alcohol dehydrogenase and LK-ADH is a bulky-small alcohol dehydrogenase. These were extracted from filter paper, sequenced and expressed according to the experimental section. These two alcohol dehydrogenases were chosen due to being largely documented and shown to have a good tolerance to accept many different substrates.

2.1 Synthesis of ketoenone substrates.

The retrosynthetic analysis of the ketoenone starting material revealed disconnections at both the alkene and ketone group, as shown in **Figure 2.1**. Therefore, the synthesis of ketoenones **(111)-(113)** was carried out using a Grignard reaction with a suitable acid chloride to form the saturated ketone, followed by an olefin metathesis reaction using methylvinylketone (MVK) to form the ketoenone product. This method of synthesis allows for easy derivatisation using a range of vinyl ketones, as well as various Grignard reagents. Following the Grignard and olefin metathesis general procedure in the experimental section, three ketoenones **(111)-(113)** were synthesised (**Scheme 2.1**).

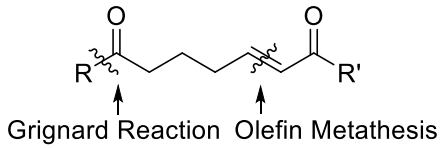

Figure 2.1; Retrosynthetic study of the ketoenones

Ketoenones **(111)-(113)** were produced in good-excellent yields using this approach, **Table 2.1**. The lower yield achieved with **(111)** was mainly due to the high volatility of the compound, meaning some material was lost on the removal of THF after the workup. A test reaction using the lower boiling point solvent, diethylether, was carried out but the

concentration of Grignard formed was much poorer and led to a lower overall yield.

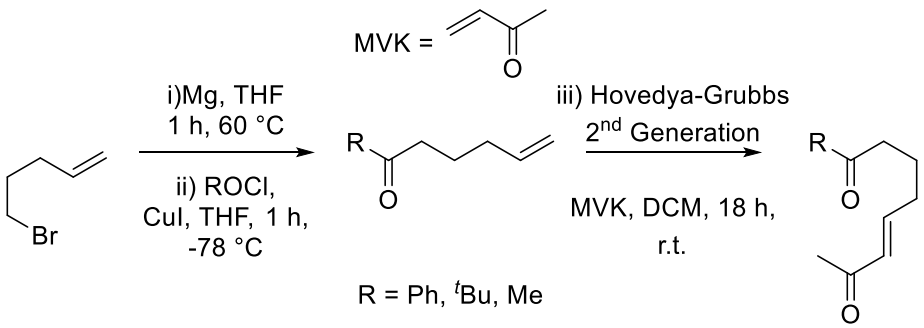

Scheme 2.1; Synthesis of ketoenones (111)-(113).

Table 2.1; Isolated yields from the synthesis of compound (111), (112) and (113).

Entry	R group	Grignard Yield*	Grubbs yield*
1 (111)	Me	68	83
2 (112)	^{t}Bu	87	81
3 (113)	Ph	92	82

***Isolated yields. Reaction conditions; $Mg_{(s)}$ (3 eq.), 1,2-dibromoethane (1 mol%), THF (1 M), 60 °C, 1 h, then ii) ROCl (1.1 eq), CuI (10 mol%), THF (1 M) -78°C, 16 h. iii) MVK (3 eq.), Hovedya-Grubbs 2nd gen (5 mol%), DCM (10 M), r.t., 18 h.**

2.2 Biotransformations on ketoenone substrates.

As an ADH that typically accepts substrates with at least one 'small' substituent on the ketone, LK-ADH was expected to react only with **(111)**, whilst RAL-ADH could accept **(112)** and **(113)**. The initial biotransformation conditions were taken from literature.[216] While both enzymes showed activity towards these substrates, the product produced was not the desired compound but instead, **(114), (115)** and **(116)** shown in **Figure 2.2**. This indicated that the oxa-Michael reaction may

not be instantaneous, as is the case for the corresponding aza-Michael reaction.

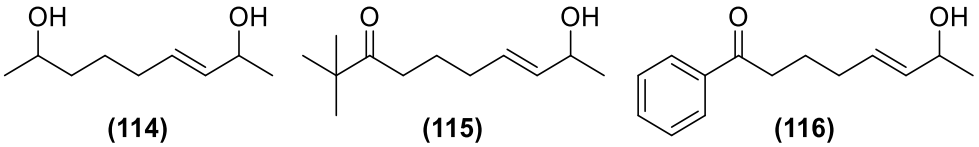

(114) (115) (116)

Figure 2.2; Compounds produced from the initial biotransformation on ketoenones produced in Scheme 2.2.

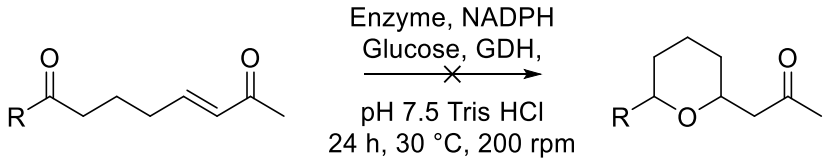

Scheme 2.2; The initial biotransformations with further information displayed in Table 2.2 below.

Entry	Enzyme	SM	Conversion* (%)
1	LK-ADH	**(111)**	>99 **(114)**
2	LK-ADH	**(112)**	75 **(115)**
3	LK-ADH	**(113)**	28 **(116)**
4	RAL-ADH	**(111)**	9 **(114)**
5	RAL-ADH	**(112)**	32 **(115)**
6	RAL-ADH	**(113)**	15 **(116)**

***Conversions based on the disappearance of starting material *via* GC-FID. Reaction conditions; LK-ADH (100 µL resuspended whole cells from a 100 mg/ mL wet cell resuspension), GDH (6U), substrate (10 mM), glucose (250 mM), NADPH(0.01 mM), Tris.HCl buffer (100 mM, pH 7.5, 1 mL), 30 °C, 200 rpm, Time (24 h). Results represent the average of two replicates.**

Initially, the optimum pH was identified. Changes in pH can have a large effect on the cyclisation potential, and at the extremes of pH, different mechanisms of cyclisation can occur (**Figure 2.3**). In **Table 2.3**, entry

1 was tested with both Tris HCl buffer between the pH ranges of 6-10 as well as a pH 2 specific buffer consisting of potassium chloride/hydrogen chloride. There was no reaction with either buffer, probably due to the enzyme being denatured at this pH. At the other end of the pH scale shown in entry 5, there was an 87% conversion of starting material to doubly reduced product at pH 10. Entry 3 at pH 7.5 gave full conversion of starting material, as well as entry 4 at pH 8. With pH 7.5 being closer to neutral pH, it was selected to run the subsequent biotransformations. The difference between the basic and acidic cyclisation mechanisms is partial deprotonation of an alcohol vs. the activation of an enone.

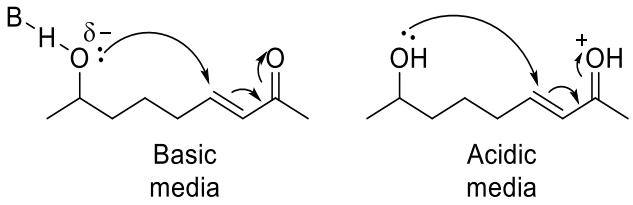

Figure 2.3; Potential cyclisation methods.

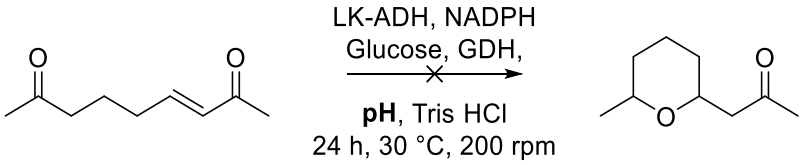

Scheme 2.3, Reaction scheme to test how pH affects the reaction.

Table 2.3; Results from pHs tested.

Entry	pH	Conversion*
1	2[a]	0
2	6	56
3	7.5	>99
4	8	99
5	10	87

***doubly reduced product only observed by GC-FID Conversions based on the disappearance of starting material *via* GC-FID. Reaction conditions; LK-ADH (100 µL resuspended whole cells from a 100 mg/ mL wet cell resuspension), GDH (6U), substrate (10 mM), glucose (250 mM), NADPH(0.01 mM), Tris.HCl buffer (100 mM, pH, 1 mL), 30 °C, 200 rpm, Time (24 h). [a]This is outside the range of Tris HCl buffer, a potassium chloride/hydrogen chloride buffer was used. Results represent the average of two replicates.**

Following the pH study, the effect of co-solvent was investigated (**Table 2.4)**. Adding a co-solvent did not produce any of the cyclised compound, but only the doubly reduced product. It did however hinder in the work up of the biotransformation. Entry 1 was the comparison reaction where no co-solvent was added, entries 2 – 4 were the common water soluble organic solvents, which all gave full conversion. DMSO in entry 2 would require multiple diethyl ether washes to fully remove it from the biotransformation. Entry 5 and 6 were the only two co-solvents which didn't give full conversion of the starting material. This could be because these formed biphasic mixtures, which may have also started to precipitate the enzyme.

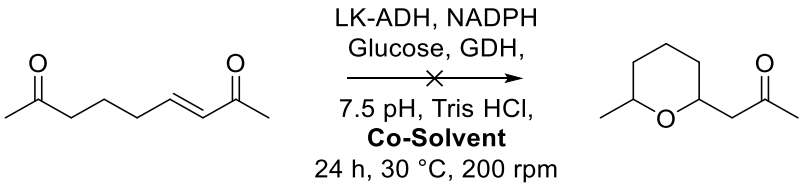

Scheme 2.4; Reaction scheme to test how a co-solvent affects the reaction.

Table 2.4; Results from co-solvents tested.

Entry	Co-Solvent (10 %)	Conversion*
1	No co-solvent	>99
2	DMSO	>99
3	IPA	>99
4	MeOH	>99
5	EtOAc	83
6	THF	75

***doubly reduced product only observed by GC-FID. Conversions based on the disappearance of starting material *via* GC-FID. Reaction conditions; LK-ADH (100 µL resuspended whole cells from a 100 mg/ mL wet cell resuspension), GDH (6U), substrate (10 mM), co-solvent (100 µL, 0.1 M), glucose (250 mM), NADPH(0.01 mM), Tris.HCl buffer (100 mM, pH 7.5, 1 mL), 30 °C, 200 rpm, Time (24 h). Results represent the average of two replicates.**

With no success in the production of oxanes, a time study was undertaken to investigate if the enzyme was able to select between the saturated and unsaturated ketones in **Table 2.5**, with the general reaction scheme shown in **Scheme 2.5**. Entries 1 - 6 showed full conversion to the over-reduced compound **(114)** in less than an hour, necessitating another time study which monitored the reaction much more frequently.

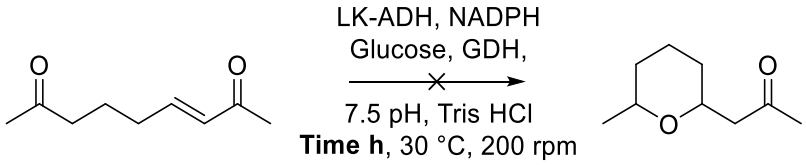

Scheme 2.5, Reaction scheme to test how time affects the reaction.

Table 2.5; Results from times tested.

Entry	Time (h)	Conversion*
1	1	>99
2	2	>99
3	3	>99
4	6	>99
5	12	>99
6	24	>99

*** doubly reduced product only observed by GC-FID. Conversions based on the disappearance of starting material *via* GC-FID. Reaction conditions; LK-ADH (100 µL resuspended whole cells from a 100 mg/ mL wet cell resuspension), GDH (6U), substrate (10 mM), glucose (250 mM), NADPH(0.01 mM), Tris.HCl buffer (100 mM, pH 7.5, 1 mL), 30 °C, 200 rpm, Time (T h). Results represent the average of two replicates.**

The time study presented in **Table 2.6** shows that the enzyme does distinguish between both ketones. This was very important as it meant that the intended product could be isolated. Isolation of the linear reduced compound as the major product indicate that the oxa-Michael is not an instantaneous reaction under the same biocatalytic reaction conditions of the aza-Michael reaction.[215] On addition of the enzyme mixture to the reaction and stopped immediately gave a conversion of 13 % to a new peak by GC-FID which was confirmed to be compound **(117)** by NMR. After 8 minutes, this reached a maximum of 84 % conversion with 5 % of the doubly reduced compound also being produced. After 1 hour, this had all become the doubly reduced compound.

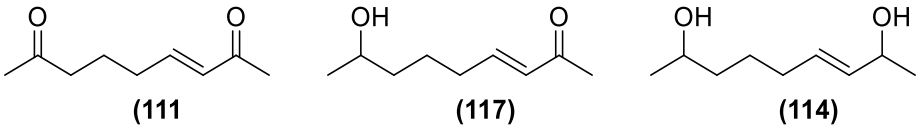

(111 (117) (114)

Figure 2.6; Compounds produced in the second time study with their relavitve amounts in Table 2.6 below and visualised in Graph 2.1.

Entry	Time (minutes)	Compound (111)*	Compound (117)*	Compound (114)*
1	0	86	13	0
2	2	48	51	0
3	4	41	58	0
4	6	31	68	0
5	8	10	84	5
6	10	0	78	21
7	60	0	0	>99

***Conversions were calculated relatively *via* GC-FID. Reaction conditions; LK-ADH (100 µL resuspended whole cells from a 100 mg/ mL wet cell resuspension), GDH (6U), substrate (10 mM), glucose (250 mM), NADPH(0.01 mM), Tris.HCl buffer (100 mM, pH 7.5, 1 mL), 30 °C, 200 rpm, Time (T mins).**

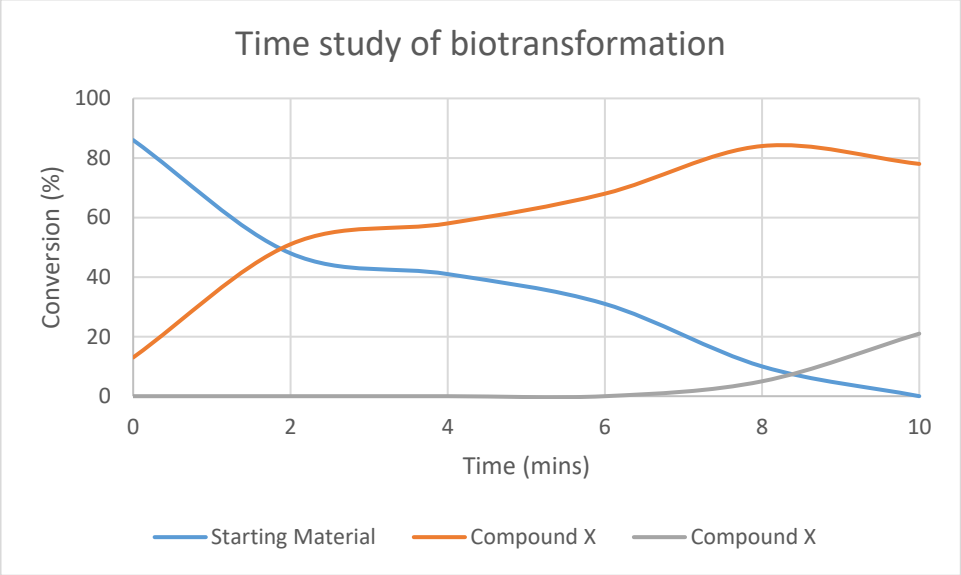

Graph 2.1; shows the relative conversions to each compound during the time study.

Upon work up, compound **(117)** slowly cyclised in the presence of deuterated chloroform (**Table 2.7**). Over a period of 5 days, the cyclisation of **(117)** to **(118)** achieve a conversion of 75% conversion. Deuterated chloroform was used as the solvent because it is invisible in NMR, the method used to determine the conversion.

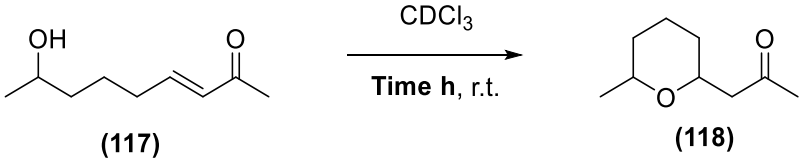

(117) (118)

Scheme 2.7, Reaction scheme to test how time affects the cyclisation of compound (117) to the cyclised compound (118).

Time (h)	Compound (117) (%)	Compound (118) (%)
1	95	5
12	64	35
24	43	57
48	33	67
72	26	74
144	25	75

***Conversion calculated by NMR.**

As previously discussed, the cyclisation could be aided with the help of an acid or a base. Entry 1 - 3 were performed using aqueous HCl and taking a time point at 1, 6 and 12 hours respectively. Under these conditions, it showed that there was >99% conversion after 1 hour, although product extraction prior to acid neutralisation was challenging. Entries 4 – 6, utilising NaOH as the catalyst gave very poor conversions as well as poor *d.r.*, as determained by NMR. Entry 7 uses 1 M HCl in diethyl ether and

gives better results, as there was no aqueous extraction required, instead, the diethyl ether was removed *via* reduced pressure.

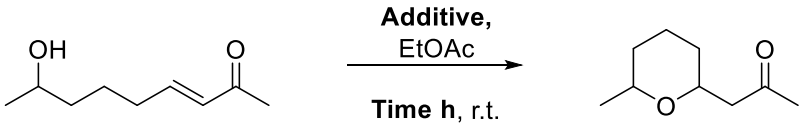

Scheme 2.8, Reaction scheme to test the additives to aid the cyclisation.

Table 2.8; Acid and base catalysis to form the oxane.

Entry	Time (h)	Additive	Conversion*	Isolated Yield	*d.r.** (cis/trans)
1	1	HCl	>99	73	12:1
2	6	HCl	>99	67	13:1
3	12	HCl	>99	68	12:1
4	1	NaOH	27	-	1.5:1
5	6	NaOH	43	27	1.4:1
6	12	NaOH	51	14	2:1
7	1	$Et_2O.HCl$	>99	82	12:1

***Conversion and *d.r.* calculated by NMR. Reaction conditions; Additive (2 M,1 mL), CH_2Cl_2 (1 mL), r.t., Time (T h).**

The proton interactions of the *cis* and *trans* diastereomer observed in the NOESY spectrum are shown in **Figure 2.7** and **Graph 2.2**. In **Figure 2.7**, interaction **1** is between H_A and H_B and interaction **2** is between H_A and H_C. The NOESY spectrum in **Graph 2.2** shows a clear interaction **1** and there is no interaction **2** should show suggesting that this compound is the *cis* diasteromer.

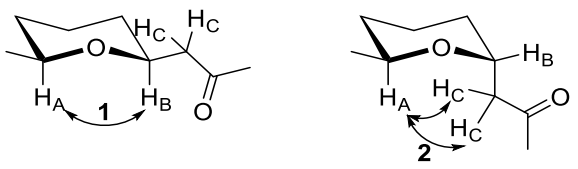

Figure 2.7; Expected interactions for the *cis* and *trans* oxanes

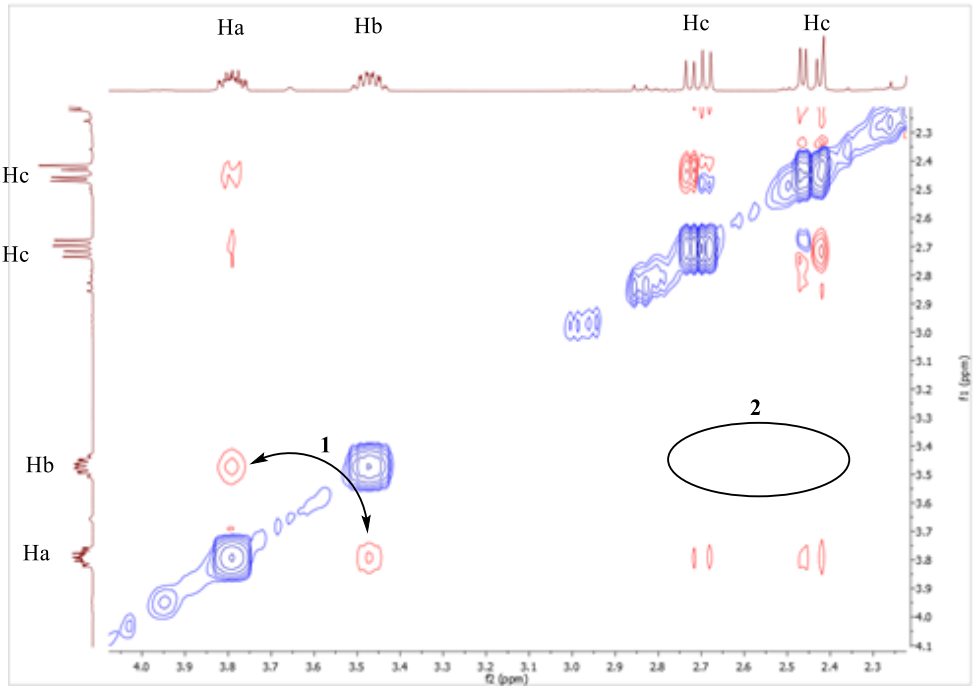

Graph 2.2; NOESY spectrum to show the oxane produced is the *cis* diasteroemer.

2.3 Making other tetrahydropyrans.

Initially, using the previous methodology, synthesising different *αβ* - unsaturated ketone analogues could be achieved by the addition of vinyl magnesium bromide to an acid chloride shown in **Scheme 2.9**. However, Compound **(119)** was the major component of this reaction. This suggesting an interesting reactivity, where compound **(120)** forms and this reacts again with vinyl magnesium bromide in a 1, 4 addition to produce compound **(119).**

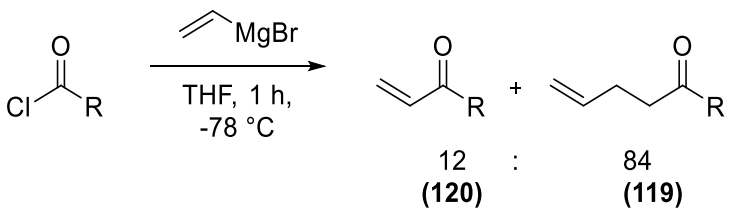

Scheme 2.9; The first synthesis of MVK analogues with conversions

An alternate method was attempted with adding the vinyl magnesium bromide into the corresponding aldehyde, followed by an oxidation shown in **Scheme 2.10** to form compound **(121)** and **(122)**. Even with the use

of the aldehyde over the acid chloride, the Grignard addition still gave a poor yield, shown in **Table 2.9**, though the Dess-Martin periodinane oxidation went to full conversion. Following this, another olefin metathesis reaction was performed.

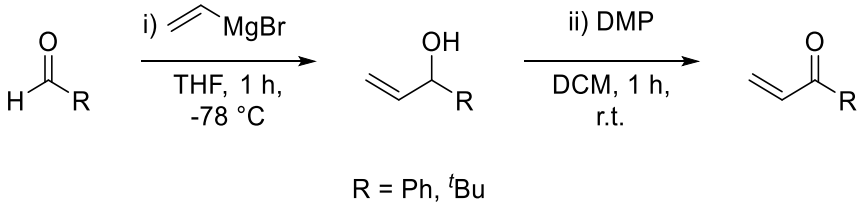

Scheme 2.10; The second synthesis of the MVK anaolgues (121) and (122). Reaction conditions; i) Vinylmagnesium bromide (1 M in THF, 1.1 eq.), THF (0.1 M), -78 °C, 1 h, ii) DMP (1.1 eq.), CH_2Cl_2 (1 M), r.t., 1 h

Table 2.9; Yields for compounds X and X over two steps.

R	Grignard	Oxidation*
Ph (121)	41	97
^{t}Bu (122)	34	95

***Isolated yield.** .

Unlike the previous metathesis using MVK, these *α,β* -unsaturated ketone analogues are hindered, which reduces the effectiveness of the olefin coupling. Entry **1** and **2** from **Table 2.10** show the conversion of the pivoyl analogue at room temperature for 24 and 48 hours respectively, which gives poor yields. Refluxing the reaction didn't increase the conversion significantly. The phenyl α,β - unsaturated ketone analogue gave equally poor yields at 24 and 48 hours and at room temperature and reflux as entry **5** – **8**. With a combination of very poor yields as well as the expense of the Hoveyda-Grubbs 2nd generation catalyst, a new method was sought.

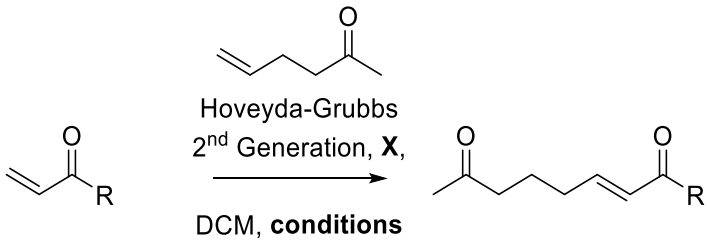

Scheme 2.11; Olefin metathesis to produce ketoenones.

Table 2.10; Yields from olefin metastasis for the new ketoenones.

Entry	R	Time (h)	Temperature (°C)	Conversion*
1	^{t}Bu	24	r.t.	15
2	^{t}Bu	48	r.t.	31
3	^{t}Bu	24	50	26
4	^{t}Bu	48	50	45
5	Ph	24	r.t.	10
6	Ph	48	r.t.	16
7	Ph	24	50	25
8	Ph	48	50	34

***Isolated yield, Reaction conditions; MVK (3 eq.), Hovedya-Grubbs 2nd gen (5 mol%), DCM (10 M), temperature (T °C)., Time (T h).**

A method of synthesis of the ketoenone compound was investigated by forming the saturated ketone by an ozonolysis reaction. Opening up a cyclic alkene would yield a ketone as well as an aldehyde which can then react with a Wittig ylide to produce the ketoenone shown in **Scheme 2.12**.

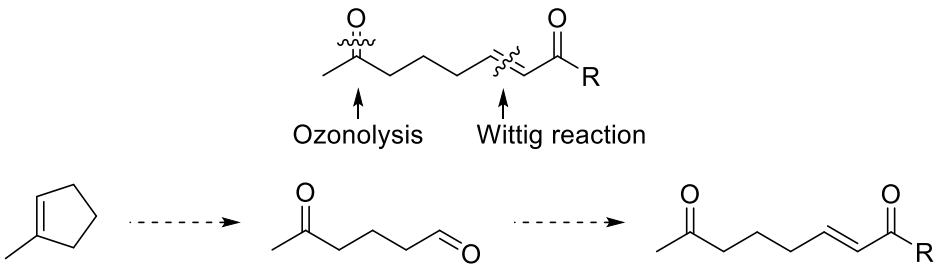

Scheme 2.12; Alternative retrosynthetic analysis.

The Wittig would selectively attack the aldehyde as it is a better electrophile than the ketone giving regio-control over the product. This is also a preferred methodology as the Wittig reaction is a well-documented reaction with many different variants to control the stereochemistry of the double bond.[217] Compound **(123)** was left for about 30 minutes in O_3, at this point, it had a light blue colour, which represented an excess of ozone present, and quenched with PPh_3 for 12 hours making **(124)** in 68%.

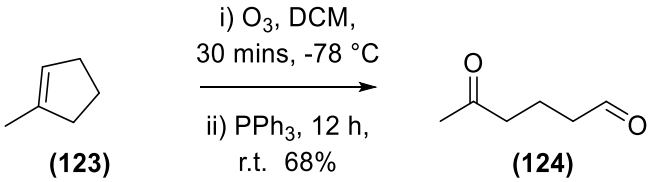

Scheme 2.13; Ozonolysis of methylcyclopentene. i) O_3 (15 mins), CH_2Cl_2 (1 M), -78 °C, 15 mins, ii) PPh_3 (1.2 eq.) r.t., 12 h.

The next step was to produce a range of Wittig reagents which can react with the aldehyde as shown in **Scheme 2.14**. The Wittig reagents were made on a large scale and all entries in **Table 2.11** gave good yields.

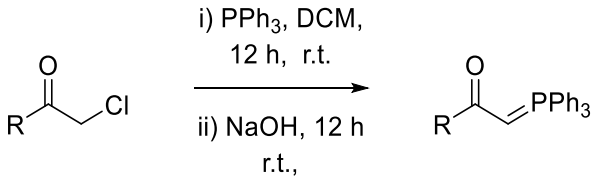

Scheme 2.14; Shows the general synthesis for the Wittig reagents.

Table 2.11; Yields of Wittig formation.

Entry	R Group	Yield*
1	Me	84
2	^{t}Bu	83
3	Ph	87
4	OEt	78

***Isolated yields.**

Ketoaldehyde **(124)** was then reacted with each of the Wittig ylides to produce the ketoenones shown in **Table 2.12** and **Scheme 2.15**. Entries 1 – 4 were produced in exceptional yields and were easily purified by column chromatography.

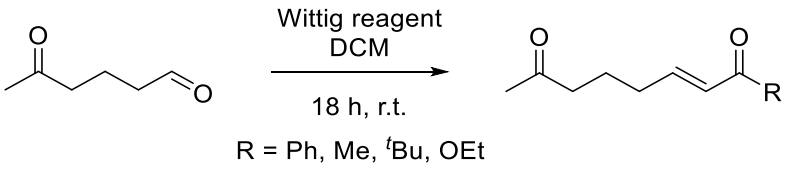

Scheme 2.16; Synthesis of ketoenones.

Table 2.13; The yields of each ketoenones formed from the Wittig reaction.

Entry	R Group	Yield*
1 (111)	Me	89
2 (125)	^{t}Bu	92
3 (126)	Ph	86
4 (127)	OEt	96

***Isolated yield.**

Utilising the previously optimised conditions, the biotransformations of these ketoenones gave exceptional yields. This is mainly due to the

sterics of the R group on the molecule, which block the alcohol dehydrogenase from over-reducing the substrate and in the case of compound **(125)**, the other carbonyl group is an ester and cannot be reduced by the enzyme. Like entry **1** in **Table 2.14**, Entry **2** and **3** were found to slowly cyclise to the oxane without any catalyst, though not to full conversion. Conversions of 50-75% were achieved over the course of a few days without acid catalysis. Entry **3** required 100 µL of methanol as a co-solvent. This is because the starting material for this reaction is a solid, and did not readily dissolve into the Tris HCl buffer.

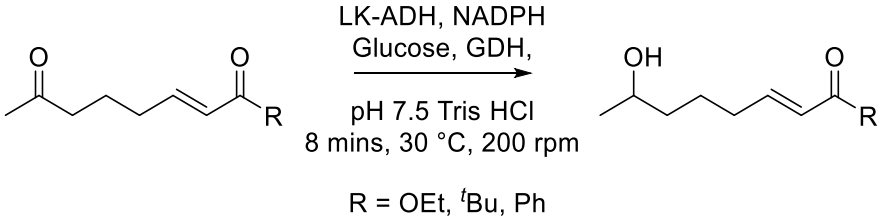

Scheme 2.17; The biotransformation of the new ketoenones.

Table 2.14; Biotransformations of the new ketoenones.

Entry	R Group	Conversion*
1	Reference Me	84
2	^{t}Bu	>99
3	Ph[a]	96
4	OEt	>99

*** Conversions based on the disappearance of starting material *via* GC-FID. Reaction conditions; LK-ADH (100 µL resuspended whole cells from a 100 mg/ mL wet cell resuspension), GDH (6U), substrate (10 mM), glucose (250 mM), NADPH0.01 mM), Tris.HCl buffer (100 mM, pH 7.5, 1 mL), 30 °C, 200 rpm, Time (8 mins). Mass balance was made up with starting material. [a]Due to solubility issues, was added as a 10 µL (1 M) stock in MeOH, Results represent the average of two replicates.**

With the new ketoenones made, the enantioselectivity for this type of molecule was tested. Entry **4** from **Table 2.14** has two very different

carbonyl groups which can be taken advantage of by a chemoselective reduction of the ketone over the ester group using sodium borohydride to produce the racemic alcohol shown in **Scheme 2.18**. This sample can be compared to a sample from a biotransformation and the enantioselectivity of the enzyme can be characterised *via* chiral GC-FID. The two enantiomers were separable, which confirmed the enantioselectivity (>99 %) of the biotransformation. From this, the enantiomeric excess was assumed for substrates other substrates.

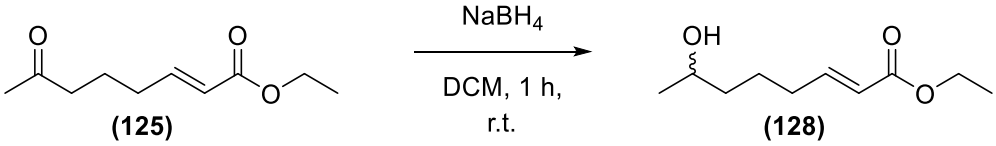

Scheme 2,18; shows the racemic reduction of (125) to (128).

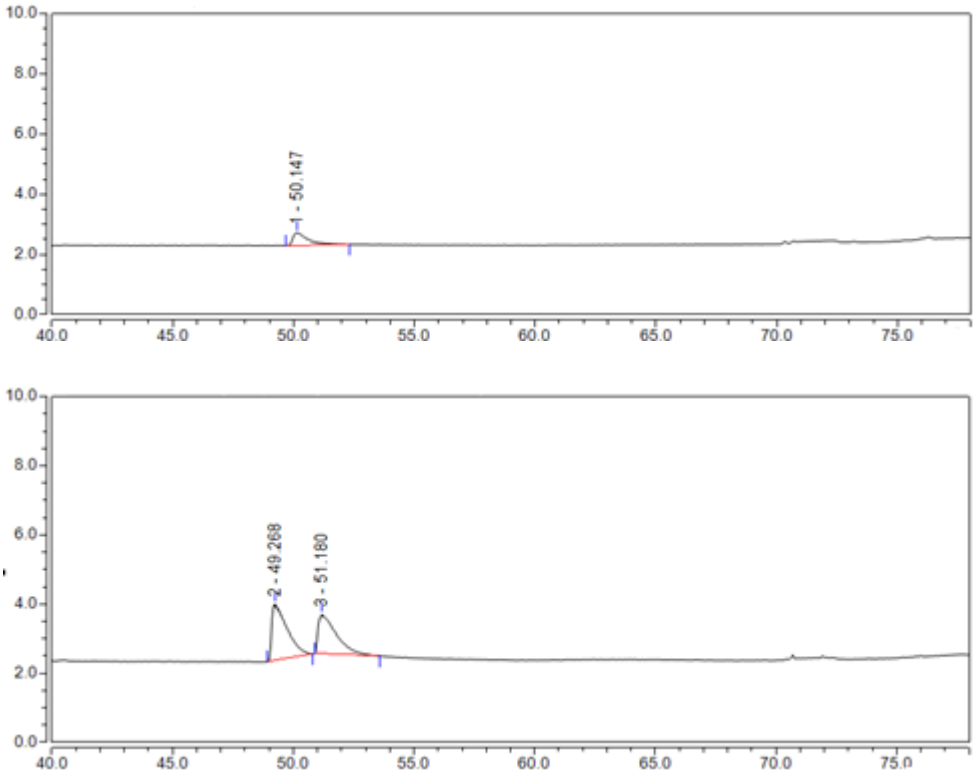

Graph 2.3; GC trace using a chiral stationary phase, Top, biocatalytic reduction of a 10 mM reaction of (125), Bottom, racemic reduction of (125) following Scheme 2.18, retention time along the X-axis and intensity along the Y-axis.

Compounds **(125)** and **(128)** were telescoped forward without purification and reacted with 1 M Et_2O.HCl shown in **Scheme 2.19**. All the reactions produced the respective oxane apart from the ethyl ester. This produced a mixture of starting material and hydrolysed ester. As shown in **Figure 2.8**, the acidic mechanism of cyclisation would have the ester carbonyl protonated, which leads to hydrolysis.

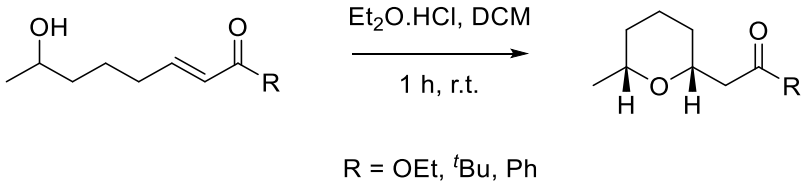

Scheme 2.19; Synthesis of oxanes (129), (130), and (131).

Table 2.15; Shows the *d.r.* of the other oxanes produced.

Entry	R Group	Yield*	*d.r.*
1 (118)	Reference Me	82	12:1
2 (129)	^{t}Bu	>99	8:1
3 (130)	Ph	>99	10:1
4 (131)	OEt	0	-

***Isolated yield, *d.r.* determined by NMR.**

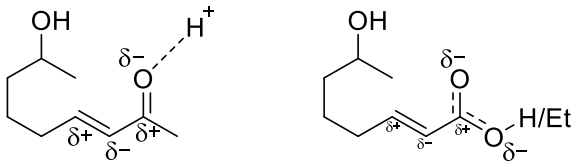

Figure 2.8; Proposed reason for lack of cyclisation between enone and enoate(131).

When the R group is either an alkyl or phenyl group, protonation of the unsaturated ketone increases the electrophilicity of the alkene carbon, promoting an oxa-Michael attack. For compound **(131)**, the combined electron withdrawing effects of both oxygens lowers the overall delta positive charge on the carbon and makes the alkene less electrophilic and means the oxa-Michael is less favourable. Even with some harsher

conditions such as elevated temperature, the reaction never went to full completion. **Table 2.16** shows some of the conditions investigated, entry **1** shows DCM being used instead of ethyl acetate. In entry **2**, the time was increased and the reaction was refluxed in entry **3**. The increased temperature did show some promise, as 13% product was observed by NMR. In entries **4** and **5**, the solvent was changed to THF and toluene respectively, as these can reflux at much higher temperatures. Unfortunately, these elevated temperatures could not overcome the electrophilic properties of the alcohol, which still were not sufficient for this type of cyclisation.

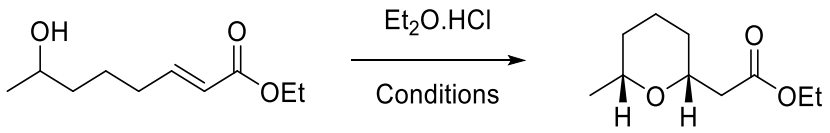

Scheme 2.20; Reaction to optimise the cyclisation of oxane (131).

Table 2.16; Shows the optimisation conversions.

Entry	Solvent	Temperature (°C)	Time (h)	Conversion*
1	DCM	r.t.	12	0
2	DCM	r.t.	24	0
3	DCM	50	12	13
4	THF	70	12	18
5	Toluene	100	12	15

***Conversion calculated by NMR by ratio of starting material to product.**

Refering back to **Figure 2.8,** forming the alkoxide would not rely on the electronics of the double bond, as the alkoxide is a much stronger nucleophile than the protonated alcohol. For this, a hindered bases was used in the hope that the preserve the ester and deprotonate the alcohol shown in **Table 2.17** and **Scheme 2.21**. The use of a hindered base

successfully promoted the oxa-Michael cyclisation but afforded a racemic diastereomer. Entry **1** and **2** employed KO^{t}Bu which gave very good conversions at room temperature. Entry **3** and **4** investigated the more sterically hindered base KHMDS, which gave better yields than KO^{t}Bu but the product required further purification to remove the *bis*(trimethylsilyl)amine by-product from the reaction. Attempts were then made to epimerise this reaction to give the single *cis* diasteroemer.

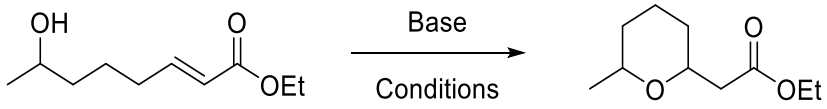

Scheme 2.21; Base-catalysed formation of oxane (131) with the results shown below in Table 2.17.

Entry	Base	Solvent	Temp. (°C)	Time (h)	Conversion *	*d.r.*
1	KO^{t}Bu	Toluene	0	16	78	1:1
2	KO^{t}Bu	Toluene	r.t.	16	93	1:1
3	KHMDS	Toluene	0	16	85	1:1
4	KHMDS	Toluene	r.t.	16	96	1:1
5	KO^{t}Bu	Et_2O	r.t.	16	0	-
6	NaOEt	EtOH	r.t.	16	0	-

***Conversion and *d.r.* calculated from NMR. Mass balance is starting material.**

For a successful epimerisation, the reaction is required to undergo a retro-oxa-Michael reaction followed by an oxa-Michael reaction, and with the *cis* diastereomer being of lowest energy chair conformation, eventually, all molecules of **(132)** will be sitting in this formation shown in **Scheme 2.22**. The lower energy state of the *cis* chair **(132)** over the *anti* chair **(133)** will mean eventually, due to the energy barrier required to overcome the steric hinderance between the axial R group and axial hydrogens.

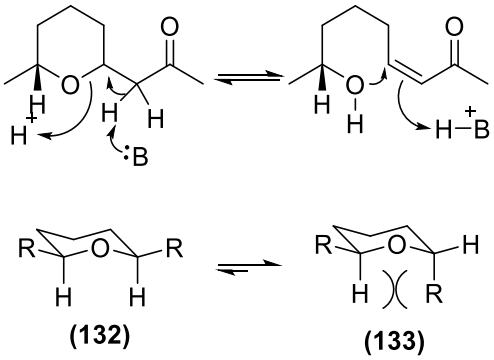

Scheme 2.22; The retro-oxa-michael reaction in equilibrium with the oxa-michael reaction, as well as the difference between *cis*/*trans* species of the chair formation for a 1,3 disubstituted tetrahydropyran.

Entry **1** was refluxed in methanol, this is the method for epimerisation that the transaminase paper that this work is based.[215] Entry **2** – **5** was using the hindered bases mentioned above and refluxing them for 24 hours. Hindered bases were employed again to maintain the integritory of the ester. These also failed to give any epimerisation of the starting material.

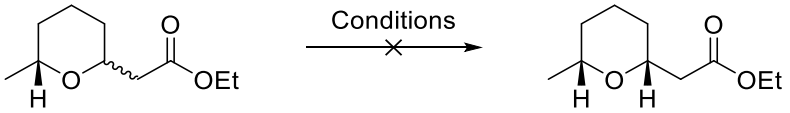

Scheme 2.23; Epimerisation of oxane (131) with tabulated results shown in Table 2.18 below.

Entry	Additive	Solvent	Temperature (°C)	Time (h)	*d.r.**
1	-	MeOH	50	24	1.1
2	KO^{t}Bu	THF	80	24	1.1
3	KO^{t}Bu	Toluene	100	24	1:1
4	KHMDS	THF	80	24	1:1
5	KHMDS	Toluene	100	24	1:1

***d.r.* was calculated by NMR**

Hydrolysing the ester of the oxane **(131)** produces one of the natural products in civet **(134)**, a mixture that is frequently used in the perfume industry.

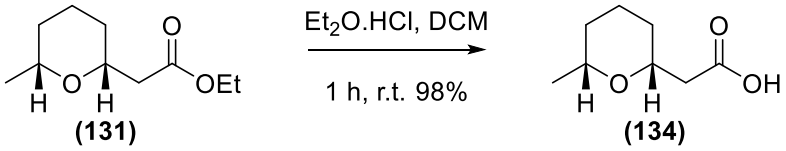

Scheme 2.24; Racemic synthesis of a component of Civet.

Scale up of the biotransformation was next investigated. The scale up was undertaken on compound **(131)**, as the molecule does not undergo spontaneous cyclisation and this was expected to allow for more straightforward analysis. **Table 2.19** shows the scale up of the biotransformation. The initial biotransformation is also documented for reference. The concentrations in entry **1** and **2** were both increased to 20 mM and 50 mM respectively. Unfortunately, the 50 mM reaction did not go to full completion. It was found in entry **4** that the reaction would go to completion at 50 mM if the time was increased to 60 minutes. The concentration was further increased to 250 mM, which produced a 72% conversion after one hour, increasing the concentration past this point gave poorer converions. For entries **8** – **10**, the reaction was scaled up to a 10 mL reaction, and the time for these reactions was found to require 6 times longer than the 1 mL reaction.

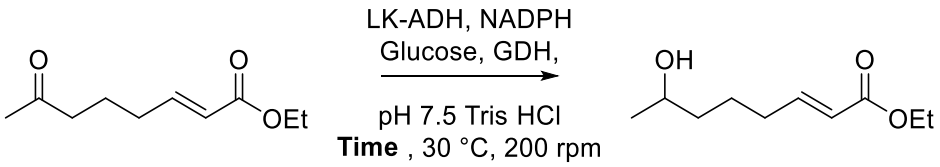

Scheme 2.24; scale up and scale out of the biotransformation.

Table 2.19; Scale up and scale out reactions.

Entry	Concentration (mM)	Scale (mL)	Time (mins)	Repeats	Conversion*
Inital	10	1	8	3	>99
1	20	1	8	3	97
2	50	1	8	3	67
3	50	1	60	3	98
4	100	1	60	3	94
5	150	1	60	3	93
6	200	1	60	3	88
7	250	1	60	3	72
8	50	10	300	3	92
9	100	10	300	3	85
10	200	10	300	3	82

***Conversion calculated *via* GC-FID. Mass balance was starting material. Reaction conditions; LK-ADH (100 µL resuspended whole cells from a 100 mg/ mL wet cell resuspension), GDH (6U), substrate (C mM), glucose (250 mM), NADP+(0.01 mM), Tris.HCl buffer (100 mM, pH 7.5, S mL), 30 °C, 200 rpm, time (T mins).**

With an optimised scale up procedure in hand, the other analogues produced were now evaluated. This is shown in **Table 2.20**.

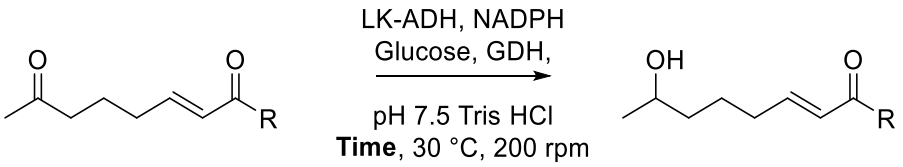

Scheme 2.25; The scale up of the other biotransformations.

Table 2.20; The scale up of other biotransformations.

Run	R group	Time (mins)	Concentration (mM)	Conversion*
1	Ph[a]	60	50	97
2	Me	20	50	76
3	^{t}Bu	60	100	>99

***Conversion calculated by absence of starting material *via* GC-FID. Reaction conditions; LK-ADH (100 µL resuspended whole cells from a 100 mg/ mL wet cell resuspension), GDH (6U), substrate (C mM), glucose (250 mM), NADPH(0.01 mM), Tris.HCl buffer (100 mM, pH 7.5, 1 mL), 30 °C, 200 rpm, time (T mins). Mass balance was made up with starting material. [a]Due to solubility issues, was added as a 10 µL (1 M) stock in MeOH.**

Interestingly, compound **(126)** didn't reduce as intended, and instead produced a mixture of compounds shown in **Figure 2.9**. Fortunately, compound **(125)** and **(111)** did produce the intended products. The issue was found to be a side reaction involving the GDH/NAPDH/glucose system, which would reduce the double bond in the reaction.[218] This was proved by the reaction shown in **Scheme 2.26.**

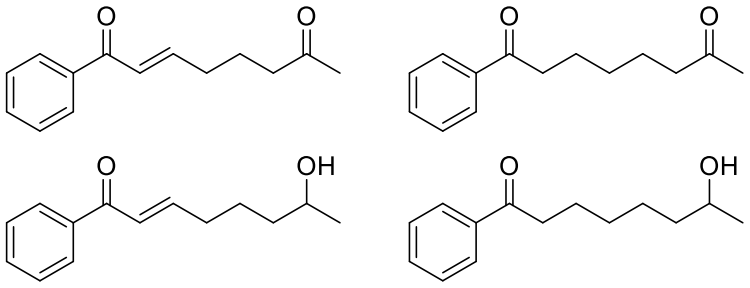

Figure 2.9; The range of compounds produced in the scale up of the biotransformation of compound (126).

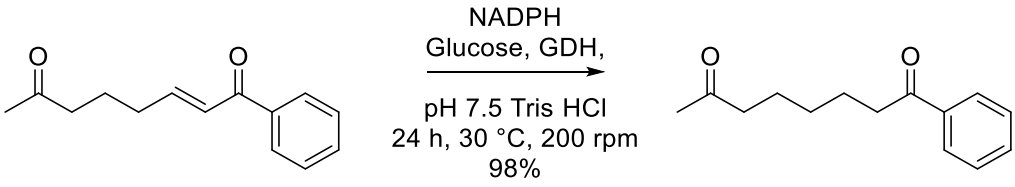

Scheme 2.26; Investigating the GDH/NADPH/glucose system in the reduction of the alkene.

This reaction limited the scale up of compound **(126)**, with the byproducts becoming more prevalent at higher concentrations of starting material.

2.4 Synthesis of dimethyl brocaketone A

Brocaketone A, **(135)**, shown in **Figure 2.10**, was first identified in 2012 from the fungus *Penicillium brocae* MA-192. It was found to have radical scavenging activity against both (2,2-diphenyl-1-picrylhydrazyl (DPPH) and 2,2'-azino-*bis*(3-ethylbenzothiazoline-6-sulfonic acid) (ABTS) radicals with an IC_{50} of 5.9 and 8.7 μg mL^{-1} respectively.[219]

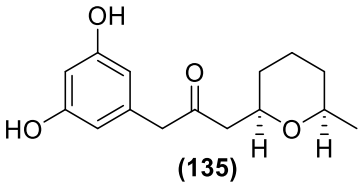

(135)

Figure 2.10; Structure of brocaketone A.

The synthesis was designed to have the biotransformation as the final step. This led to compound **(136)** being the synthetic target. It was decided that the rescorcinol core was to be present on the starting material. This was mainly due to the difficulties associated with installing *meta*-hydroxyl groups on a benzene ring. Shown in **Figure 2.11**, the first proposed synthetic route for brocaketone A. The first step would be a Grignard addition into chloroacetylchloride, which would be converted into the phosphorus ylide. This would react with the ketoaldehyde to form the

(136) which would then be reduced by an ADH followed by an oxa-Michael reaction.

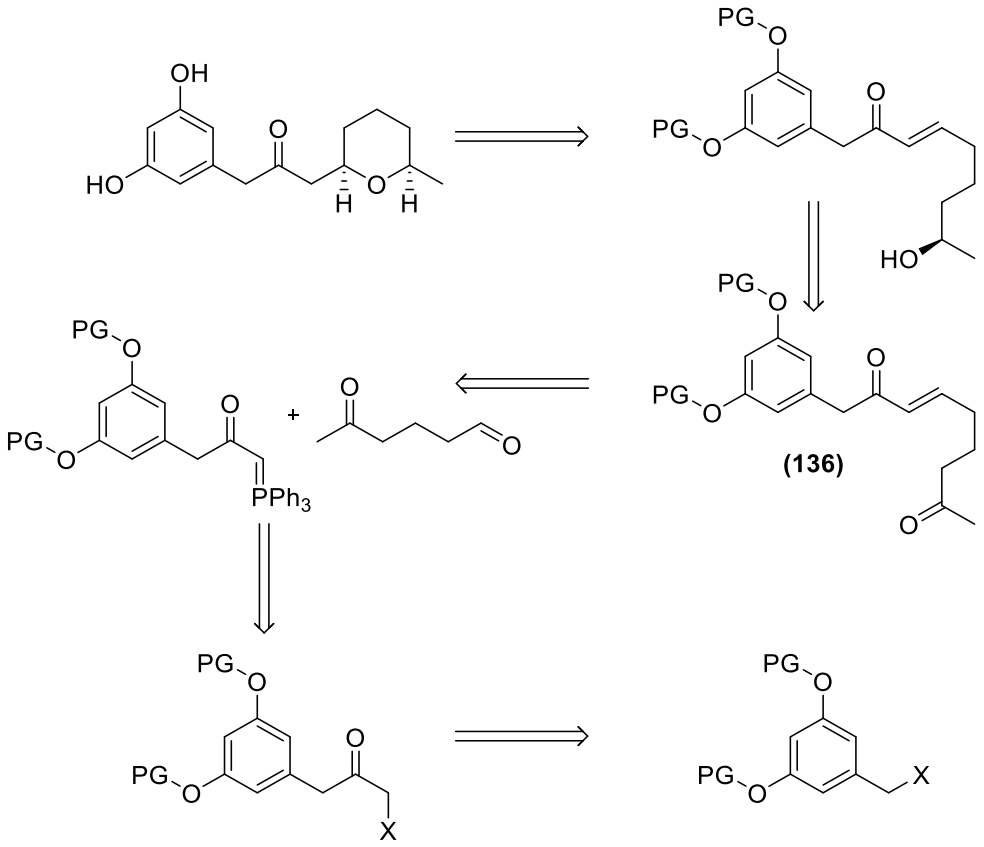

Figure 2.11; Proposed retrosynthesis of brocaketone A.

The first step shown in **Scheme 2.27** was a Grignard reaction, which was quenched by chloroacetylchloride to produce compound **(138)**. The temperature of this reaction was also lowered from previous Grignard reaction as there was a much higher chance to form the Wurtz product.

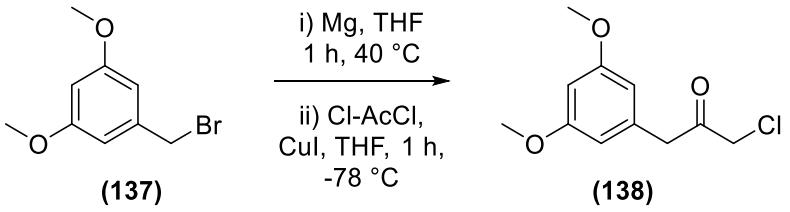

Scheme 2.27; Initial Grignard for the formation of dimethyl brocaketone A.

Unfortunately, only the Wurtz product was isolated. An optimisation of the solvent, time, temperature and activing additive was investigated and this is shown in **Table 2.21**. Entry **1** and **2** investigated the effect of the initiator, swapping from DBE to I_2 or heating did not produce anything

other than the Wurtz product. Changing the solvent to diethyl ether in entry **3** and **4** would hope to break the Grignard clusters up, this was to no avail. Lastly, entry **5** and **6** changed the temperature of the reaction. This was lowered to room temperature and activated *via* I_2 and DBE, both of which only produced the Wurtz product **(139)** shown in **Scheme 2.28**.

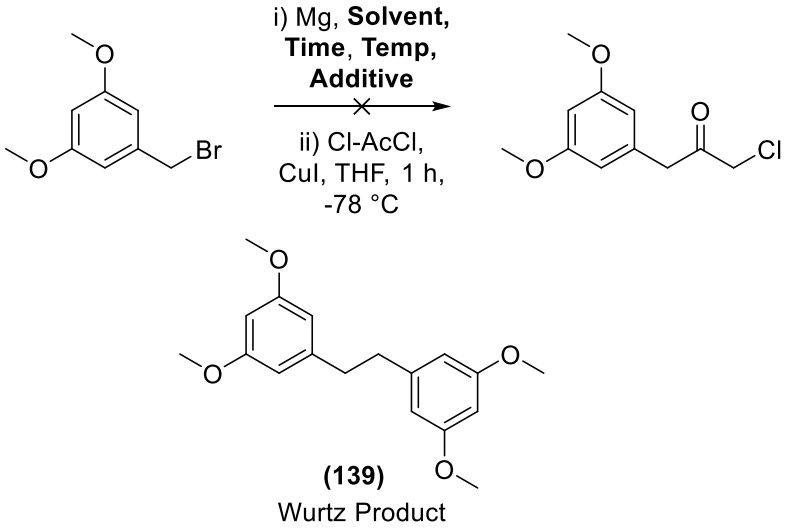

Scheme 2.28; Optimisation of first step in the synthesis of dimethyl brocaketone A and the Wurtz product (139).

Table 2.21; Optimisation of the Grignard reaction

Entry	Solvent	Additive	Time (h)	Temp. (°C)	Conversion (SM:Wurtz: Product)
Reference	THF	DBE	1	40	0 : 100 : 0
1	THF	I_2	30	40	0 : 100 : 0
2	THF	none	1	40	0 : 100 : 0
3	Et_2O	DBE	1	40	0 : 100 : 0
4	Et_2O	I_2	1	40	0 : 100 : 0
5	THF	DBE	1	r.t.	0 : 100 : 0
6	THF	I_2	1	r.t.	0 : 100 : 0

***Conversion calculated by NMR.**

The optimisation failed to produce anything other than the Wurtz product. Another look at the retrosynthesis of brocaketone A led to different

synthetic approach. The new approach starts with a Grignard, followed by a Grubbs metathesis. This method was initially considered before, but the previous method was chosen as it didn't contain any heavy metals.

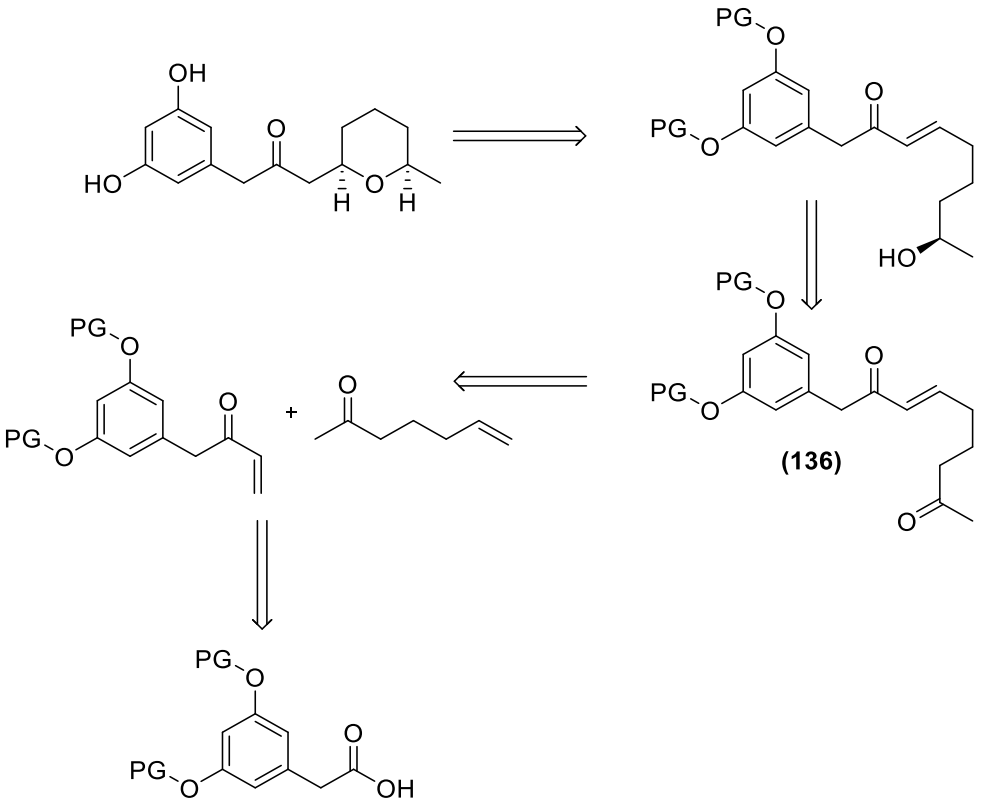

Figure 2.12; Second retrosynthesis of brocaketone A.

The first step was to form the Weinreb amide of **(141)** shown in **Scheme 2.29**. This gave almost full conversion to the product. Following this, a Grignard using vinyl magnesium bromide was used to from compound **(142)** and the Grubbs reaction provided the intermediate **(143)** in a 60% yield. The next step was the biotransformation using the previously optimised reaction.

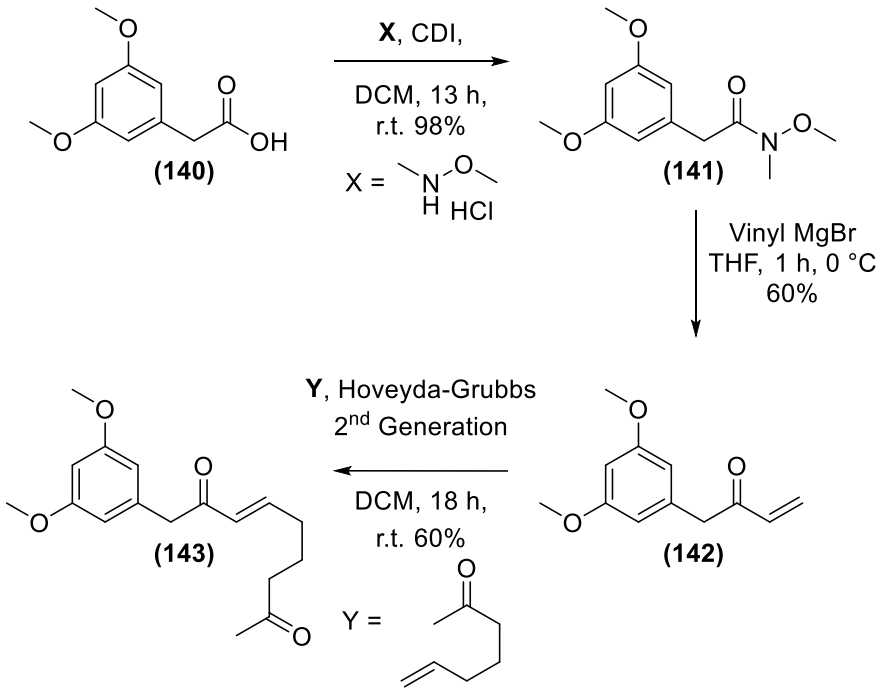

Scheme 2.29; Alternate synthesis of dimethyl brocaketone A intermediate (143).

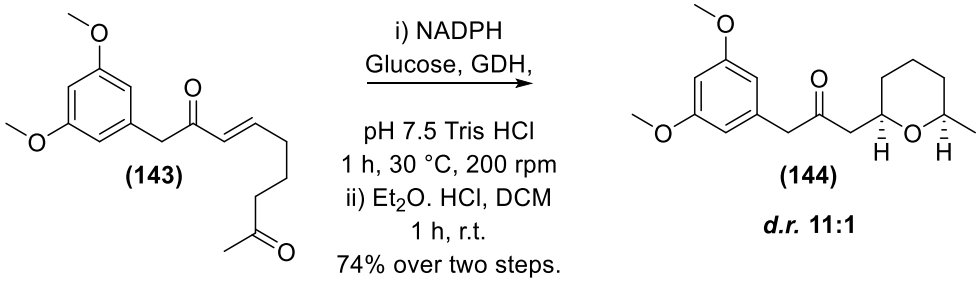

Scheme 2.30; Oxane formation in dimethyl brocaketone A.

2.5 Synthesis of tetrahydrofurans.

With a small library of oxanes produced, the next class of compounds investigated were the synthesis of tetrahydrofurans. These were produced in a similar way to the oxanes, shown in **Scheme 2.31**. As methylcyclobutene is not commercially available, 6-methylhept-5-en-2-one, a cheap precursor chemical, was used.

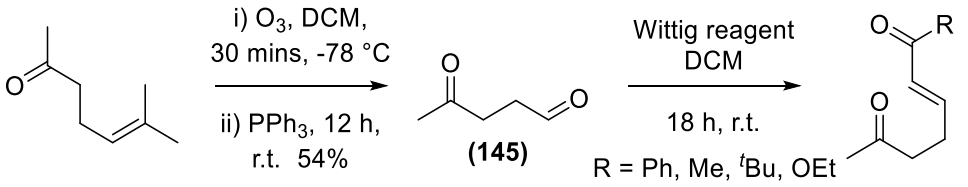

Scheme 2.31; Synthesis of the tetrahydrofuran ketoenones.

Table 2.22; Yields from the Wittig reaction.

Entry	R Group	Yield*
1 (146)	Me	67
2 (147)	^{t}Bu	83
3 (148)	Ph	81
4 (149)	OEt	90

***Isolated yield, results represent the average of three replicates.**

The ozonolysis reaction gave a poor yield production of **(146)**, possibly due to the volatility. This was followed by a Wittig reaction with the yields shown in **Table 2.22**. The yields were all good apart from the formation of **(146)**.

The results from the biotransformation were not as expected. Compound **(146)** converted to the reduced product at the higher concentration, whereas the same analogue with one extra carbon in its backbone chain gave a mixture of products. Another difference is that the compound **(146)**, which didn't produce any of the reduced ketone. Instead, it produced only compound **(150)** shown in **Figure 2.13**.

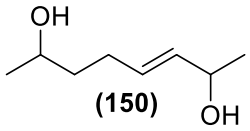

Figure 2.13; Product of the biotransformation of compound (146).

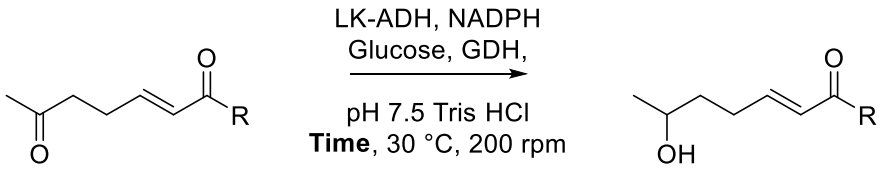

Scheme 2.32; Biotransformation of tetrahydrofuran ketoenones.

Table 2.23; Shows the yields of the biotransformations using previously optimised conditions.

Entry	R Group	Time (mins)	Concentration (mM)	Conversion*
1 (151)	Ph	60	50	94
2	Me	20	50	0[a]
3 (152)	^{t}Bu	60	100	87
4 (153)	Est	60	100	>99

***Isolated yield. Biotransformations done on a 1 mL scale.[a] Compound (146) only isolated from biotransformation shown in Figure 2.13.**

Compound **(151)** and **(152)** were then treated with $Et_2O.HCl$ and compound **(153)** was treated with KO^{t}Bu to cyclise these compounds. This was undertaken using the previously found optimised conditions.

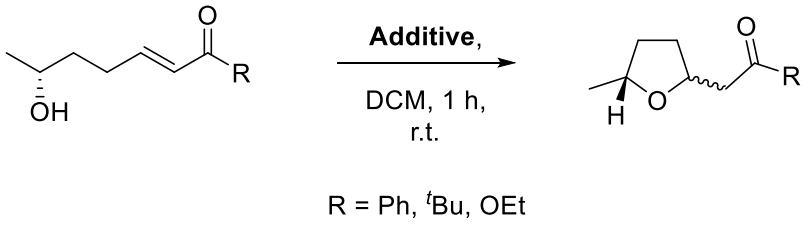

Scheme 2.33; Synthesis of tetrahydrofuran compounds

Table 2.24; Synthesis of tetrahydrofuran compounds and associated yields.

Run	Time (mins)	Additive	Yield*	*d.r.*
Ph (154)	60	$Et_2O.HCl$	93	1:1
^{t}Bu (155)	60	$Et_2O.HCl$	82	1:1
Est (156)	60	KO^{t}Bu	54	1:1

***Isolated yield. *d.r.* calculated by NMR**

Section 3: Conclusion

Four tetrahydropyran compounds were synthesised from 1-methylcyclopent-1-ene in very good yields, then being reduced using LK-ADH in good yields and *e.e.* This is followed by an oxa-michael cyclisation to produce the tetrahydropyrans. Three tetrahydrofurans were also produced using the same method but using 6-methylhept-5-en-2-one.

Alongside this, the synthesis of dimethyl brocaketone A was also synthesised in a 26% overall yield from the starting material. Unfortunately, the deprotection of the two methyl groups couldn't be achieved within the timeframe of this placement and would be a future endeavour. Some harsh conditions were tried to remove these two methyl groups to no avail so potentially using a different protection group may be a better starting point.

3.1 Future Work

With an optimised route to produce chirally enriched tetrahydropyranes, further work would at a different route to produce brocaketone A. Work undertaken by other members in the research group found that the final deprotection didn't work and led to decomposition. Changing the protecting groups at the start of the synthesis could help a deprotection at a further point, though this may require another optimisation.

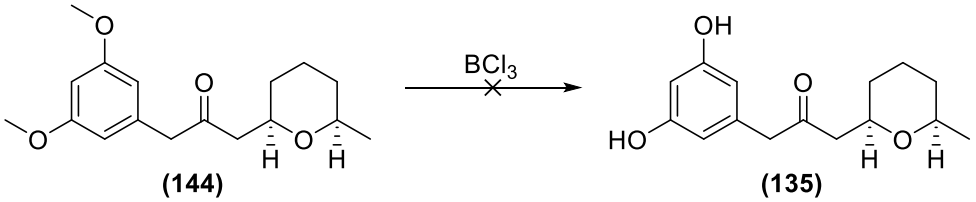

Scheme 3.1: Failed deprotection of brocaketone A

Another avenue to investigate would be some different bulky-bulky ADHs and successfully reduce **(112)** and **(113)**. Optimising this reaction would allow the production of a wider range of tetrahydropyrans. If a handle would be tolerated on either side, this would allow for different tetrahydropyran building blocks to be produced and used in synthesise of larger compounds.

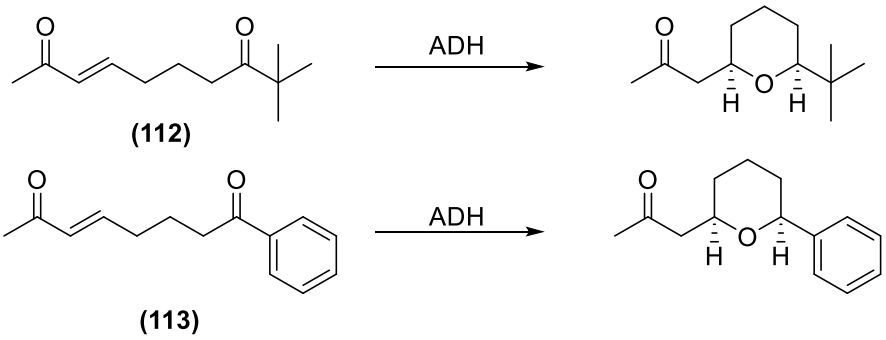

Scheme 3.2: Failed reduction of (112) and (113)

Also looking into if the alkene can have other substituents on it. These could lead to some interesting compounds as well as spirocycles, a group of compounds of some interest to industry. Another investigation would look into changing the vinyl group to an alkyne.

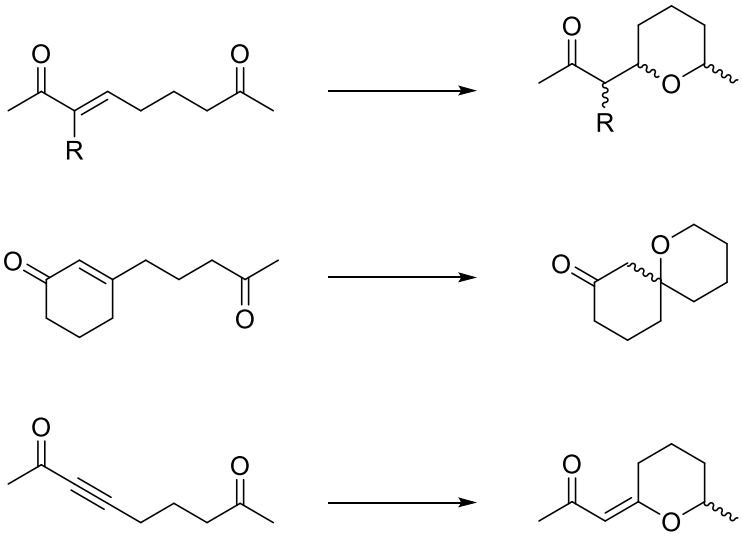

Scheme 3.3: Future compound series that could be investigated.

Section 4: Experimental

General Methods and Materials General:

General: NMR spectra were recorded on Bruker Advance 400 spectrometer (^{1}H 400 MHz, ^{13}C 101 MHz) and are referenced internally according to residual solvent signal. The chemical shifts values (δ) are reported in ppm with TMS as internal standard ($CDCl_3$: δ 7.26 for ^{1}H-NMR, δ 77.0 for ^{13}C-NMR). Data are reported as follows: chemical shifts, multiplicity (br = broad, s = singlet, d = doublet, t = triplet, q = quartet, m = multiplet), coupling constants (Hz), and integration. LC-MS spectra were recorded on Bruker MicroTOF (Time of Flight) mass spectrometer using Electron Spray Ionisation (ESI). GC analysis was performed with on Agilent 6850 equipped with a CP CHIRASIL-DEX CB (Varian, 25 m x 0.25 mm) column; injector and detector temperatures: 200 °C. IR spectra were recorded on a Bruker ATR.

Materials: Commercially available reagents and solvents were purchased from Acros Chemicals, Fluorochem, Sigma Aldrich and Thermo Fisher Scientific. Thin layer chromatography (TLC) was performed on silica gel 60 F_{254} plates (Merck). The components were visualized by UV light (254 nm) $KMnO_4$ and/or *p*-anisaldehyde staining. Flash column chromatography was performed on silica gel (60 Å, 40-60 micron) from Fluorochem.

Enzyme preparation: The alcohol dehydrogenase from LK-ADH was kindly provided as DNA soaked onto filter paper, by Professor Wolfgang Kroutil from the University of Graz in Austria. The expression of LK-ADH was performed following the previously reported method.[105] Cell pellets were stored at - 4 °C and used directly without sonication and/or purification. Shown in **Figure 4.1**, the SDS page of the expressed ADH in a pET22a vector. The left column is the protein ladder, the middle column is the negative control of just the pET22a vector with no ADH gene and the right column is the pET22a vector with LK-ADH gene.

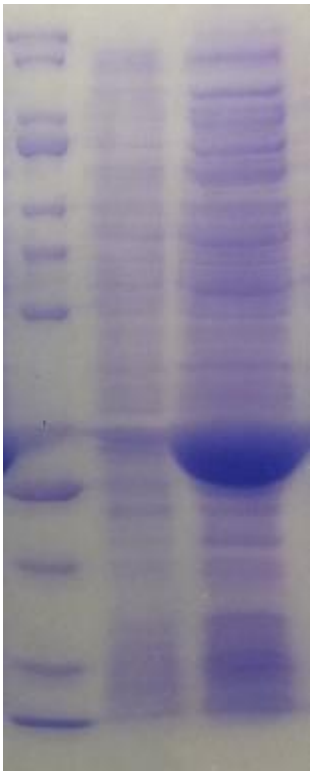

Figure 4.1: Expression of LK-ADH in pET22a vector.

General Procedure for the formation of the ketone via a Grignard reaction.

Dry THF (10 mL) with fresh magnesium filings (1.75 eq., 840 mg, 35 mmol) was heated to reflux for 5 minutes. 1,2-dibromoethane (0.1 mL) was added and left for 2 minutes until the solution ceased to bubble. 5-Bromopent-1-ene (2.4 mL, 20 mmol) was added slowly over 5 minutes and left for 1 hour to which more dry THF (5 mL) is added. In another flask, dry THF (10 mL) was added to the chosen acid chloride (1 eq., 20 mmol) and CuI (5 mol%, 190 mg, 1 mmol) and the solution was cooled to -20 °C. The pent-4-en-1-ylmagnesium bromide is added to the cold acid chloride solution over 15 minutes and left to warm to room temperature over 2 hours. The reaction mixture is quenched with 3 M HCl (20 mL) and DCM (30 mL) is added. The layers are separated and the aqueous layer is washed with more DCM (10 mL). The organic

fractions are combined and washed with saturated $NaHCO_3$ (30 mL). The combined organic extracts were dried over $MgSO_4$ and concentrated under reduced pressure. Flash chromatography (pentane : diethyl ether 19:1) afforded the pure product.

Hept-6-en-2-one

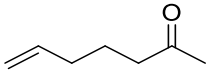

The Grignard addition of pent-4-en-yl-magnesium bromide (2.4 mL, 20 mmol) into acetyl chloride (1.4 mL, 20 mmol) to provide the title compound as a colourless oil, (68% yield, 2.02 g) after column chromatography (pentane/Et_2O 9:1). ^{1}H NMR (400 MHz, Chloroform-*d*) δ 5.74 (m, 1H), 5.12 – 4.94 (m, 2H), 2.38 (t, *J* = 7.4 Hz, 2H), 2.13 (s, 3H), 2.06 – 2.00 (m, 2H), 1.73 (p, *J* = 7.4 Hz, 2H); ^{13}C NMR (101 MHz, Chloroform-*d*) δ 208.8, 137.9, 115.1, 42.7, 33.0, 29.9, 22.7 FTIR (neat) ν_{max}: 3007 2935, 1710, 1668, 1623, 1352 cm^{-1} ;LC-MS (m/z); Calculated $C_7H_{12}ONa^+$ $[M+Na]^+$: 136.0786 Found 136.0787] In accordance with literature data.[234]

2,2-dimethyloct-7-en-3-one

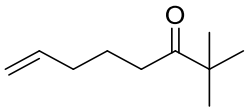

The Grignard addition of pent-4-en-yl-magnesium bromide (2.4 mL, 20 mmol) into pivaloyl chloride (2.4 mL, 20 mmol) to provide the title compound as a colourless oil, (87% yield, 2.80g) after column chromatography (pentane/Et_2O 9:1). ^{1}H NMR (400 MHz, Chloroform-*d*) δ 5.82 (m, 1H), 5.08 – 4.97 (m, 2H), 2.50 (m, 2H), 2.08 (m, 2H), 1.74 – 1.65 (m, 2H), 1.16 (s, 9H). ^{13}C NMR (101 MHz, Chloroform-*d*) δ 215.9, 138.3, 115.0, 44.1, 35.6, 33.2, 26.4, 22.9. FTIR (neat) ν_{max}: 2983, 1700,

1225, cm^{-1}; LC-MS (m/z); Calculated $C_{10}H_{18}ONa^+$ $[M+Na]^+$: 177.1289 Found 177.1288 In accordance with literature data.[234]

1-phenylhex-5-en-1-one

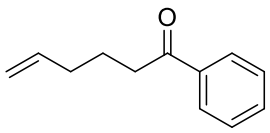

The Grignard addition of pent-4-en-yl-magnesium bromide (2.4 mL, 20 mmol) into benzoyl chloride (2.3 mL, 20 mmol) to provide the title compound as a colourless oil, (92% yield, 3.16g) after column chromatography (pentane/Et_2O 9:1). ^1H NMR (400 MHz, Chloroform-*d*) δ 7.97 (m, 2H), 7.58 (m, 1H), 7.51 – 7.46 (m, 2H), 5.85 (m, 1H), 5.09 – 5.00 (m, 2H), 3.01 (m, 2H), 2.22 – 2.16 (m, 2H), 1.92 – 1.84 (m, 2H). ^{13}C NMR (101 MHz, Chloroform-*d*) δ 200.2, 138.1, 137.1, 132.9, 128.6, 128.0, 115.3, 37.7, 33.2, 23.3. FTIR (neat) ν_{max}: 3012, 2987, 1717, 1678, 1298 cm^{-1} ;LC-MS (m/z); Calculated $C_{12}H_{14}ONa^+$ $[M+Na]^+$: 197.0942, Found 197.0942 In accordance with literature data.[234]

General Procedure for the formation of the diketone via a Grubbs methathesis reaction.

The chosen ketone (1 eq., 4.5 mmol) was added to dry flask charged with N_2. MVK (3 eq., 1.1 mL, 13.5 mmol) is added and stirred for 1 minute. Hoveyda-Grubbs 2nd generation (25 mg, 0.04 mmol) was dissolved in DCM (~0.2 mL) and added to the mixture. This is left to stir for 24 hours at room temperature. Additional DCM (10 mL) is added and the organic layer is washed firstly with water (10 mL) and brine (10 mL). The combined organic fractions were combined, dried over $MgSO_4$ and condensed by reduced pressure.

(3E)-non-3-ene-2,8-dione (111)[215]

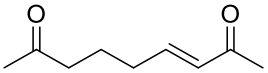

The Grubbs methathesis reaction of hept-6-en-2-one with MVK yielded the title compound as a colourless oil (0.42 g, 2.72 mmol, 82%) after column chromatography (pentane/Et_2O 9:1). ^1H NMR (400 MHz, Chloroform-*d*) 6.75 (dt, *J* = 16.0, 7.0 Hz, 1H), 6.06 (d, *J* = 16.0 Hz, 1H), 2.49 (t, *J* = 7.2 Hz, 2H), 2.29 –2.22 (m, 5H), 2.16 (s, 3H), 1.82 – 1.74 (m, 2H).^{13}C NMR (101 MHz, Chloroform-*d*) 208.0, 198.5, 147.2, 131.7, 42.6, 31.6, 30.0, 26.9, 21.9.FTIR (neat) ν_{max}: 2967, 1708, 1374, 1013, 670cm^{-1}. LC-MS (m/z); Calculated $C_9H_{14}O_2Na^+[M+Na]^+$: 177.0886, found: 177.0889. In accordance with literature data.[215]

(*E*)-1-phenyloct-5-ene-1,7-dione (112)

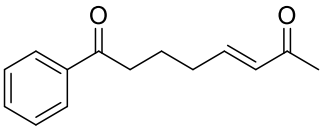

The Grubbs methathesis reaction of 1-phenylhex-5-en-1-one with MVK yielded the title compound as a colourless oil (0.59 g, 2.73 mmol, 81%) after column chromatography (hexane/EtOAc 9:1). ^1H NMR (400 MHz, Chloroform-*d*) δ 7.97 – 7.93 (m, 2H), 7.61 – 7.53 (m, 1H), 7.49 – 7.45 (m, 2H), 6.84 (dt, *J* = 16.0, 6.9 Hz, 1H), 6.12 (dt, *J* = 16.0, 1.5 Hz, 1H), 3.02 (t, *J* = 6.9 Hz, 2H), 2.38 – 2.31 (m, 2H), 2.25 (s, 3H), 2.01 – 1.94 (m, 2H). ^{13}C NMR (101 MHz, Chloroform-*d*) δ 199.5, 198.6, 147.3, 136.8, 133.8, 131.1, 128.6, 128.0, 37.5, 31.8, 27.0, 22.4. FTIR (neat) ν_{max}: 3056, 2955, 1665, 1615, 1355, 1245 cm^{-1}; LC-MS (m/z); Calculated

$C_{14}H_{17}O_2^+[M+H]^+$: 217.1250. Found 217.1251 In accordance with literature data.[233]

(*E*)-9,9-dimethyldec-3-ene-2,8-dione (113)

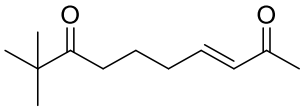

The Grubbs methathesis reaction of 2,2-dimethyloct-7-en-3-one with MVK yielded the title compound as a colourless) to provide the isolated colourless oil in an 82% yield (0.54 g, 2.75 mmol) after column chromatography (hexane/EtOAc 9:1). ^{1}H NMR (400 MHz, Chloroform-*d*) δ 6.79 (m, 1H), 6.09 (d, *J* = 15.0 Hz, 1H), 2.52 (t, *J* = 7.0 Hz, 2H), 2.27 – 2.20 (m, 5H), 1.81 – 1.74 (m, 2H), 1.16 (s, 9H). ^{13}C NMR (101 MHz, Chloroform-*d*) δ 215.2, 198.6, 147.6, 131.6, 44.0, 35.4, 31.8, 26.8, 26.3, 22.0. FTIR (neat) ν_{max}: 2967, 2870, 1689, 1624, 1478, 1365, 1083, 1063, 997, 976 cm^{-1};LC-MS (m/z); Calculated $C_{12}H_{21}O_2^+[M+H]^+$: 197.1542. Found 197.1541

General procedure for the ozonolysis reaction (synthesis of (124) and (141))

Oxygen was bubbled for 5 minutes through a solution of the required alkene (1 eq., 10 mmol) in CH_2Cl_2 (10 mL) at -78 °C. Next, a stream of ozone was bubbled through the solution for 15 minutes. Triphenylphosphine (1.2 eq., 12 mmol) was then added and the reaction was allowed to warm to room temperature and left for 15 hours. This was then concentrated under reduced pressure and purified by column chromatography to provide the compounds **(124)** and **(141)**.

5-oxohexanal**(124)**[215]

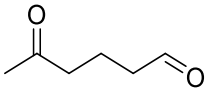

The ozonolysis reaction of 1-methylcyclopentene (2.7 mL, 25.7 mmol) provided **(124)** as a colourless oil (2.04 g, 17.9 mmol, 68% yield) after column chromatography (pentane/Et_2O 9:1). ^1H NMR (400 MHz, Chloroform-*d*) δ 9.78 (s, 1H), 2.54 – 2.49 (m, 4H), 2.15 (s, 3H,), 1.95 - 1.88 (m, 2H).^{13}C NMR (101 MHz, Chloroform-*d*) δ 207.9, 201.8, 42.9, 42.3, 30.0, 16.0. FTIR (neat) ν_{max}: 2949, 1703, 1410, 1358, 1162, 939, 742 cm^{-1}. LC-MS (m/z); Calculated $C_6H_{10}O_2Na^+[M+Na]^+$: 137.0578. Found 137.0571, in accordance with literature data.[215]

4-oxopentanal **(141)**[220]

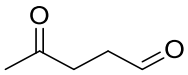

The ozonolysis reaction of 6-methylhept-5-en-2-one (5.0mL, 33.8 mmol) provided **(141)** as a colourless oil (1.78 g, 17.78 mmol, 54% yield) after column chromatography (pentane/Et_2O 9:1). ^1H NMR (400 MHz, Chloroform-*d*) δ 9.78 (s, 1H), 2.78 (s, 4H), 2.22 (s, 3H).^{13}C NMR (101 MHz, Chloroform-*d*) δ 206.4, 200.4, 37.5, 35.5, 29.8. FTIR (neat) ν_{max}: 2911, 2833, 2731, 1709, 1366, 1168, 915, 729cm^{-1}. LC-MS (m/z); Calculated $C_5H_8O_2Na^+[M+Na]^+$: 124.0456. Found 124.0458, in accordance with literature data.[220]

General procedure for the Wittig reaction

The corresponding aldehyde **(124)** or **(141)** (1 eq., 1.0 mmol) was added to the required Wittig reagent (1 eq., 1.0 mmol) in CH_2Cl_2 (1 mL) and the resulting mixture was stirred for 24 h at room temperature. The reaction

mixture was then concentrated under reduced pressure and the crude material was purified by column chromatography on silica gel.

(3*E*)-non-3-ene-2,8-dione (111)[215]

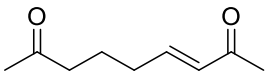

The Wittig reaction of **(111)** (375 mg, 3.20 mmol) with commercially available 1-(triphenylphosphoranylidene)-2-propanone(1.02 g, 3.20 mmol) provided **(111)** as a colourless oil (419 mg, 2.72 mmol, 83% yield) after column chromatography (pentane/Et_2O 9:1). ^1H NMR (400 MHz, Chloroform-*d*) ^1H NMR (400 MHz, Chloroform-*d*) 6.75 (dt, *J* = 16.0, 7.0 Hz, 1H), 6.06 (d, *J* = 16.0 Hz, 1H), 2.49 (t, *J* = 7.2 Hz, 2H), 2.29 –2.22 (m, 5H), 2.16 (s, 3H), 1.82 – 1.74 (m, 2H). ^{13}C NMR (101 MHz, Chloroform-*d*) 208.0, 198.5, 147.2, 131.7, 42.6, 31.6, 30.0, 26.9, 21.9. FTIR (neat) ν_{max}: 2967, 1708, 1374, 1013, 670cm^{-1}. LC-MS (m/z); Calculated $C_9H_{14}O_2Na^+[M+Na]^+$: 177.0886, found: 177.0889. In accordance with literature data.[215]

(*E*)-9,9-dimethyldec-6-ene-2,8-dione (125)[215]

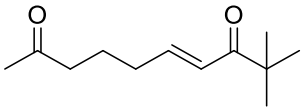

The Wittig reaction of **(125** (140 mg, 1.20 mmol) with 3,3-dimethyl-1-(triphenylphosphoranylidene)-2-butanone (432 mg, 1.20 mmol)[2] provided the compound **(125** as a colourless oil (215 mg, 1.11 mmol, 92% yield) after column chromatography (hexane/EtOAc, 7:3). ^1H NMR (400 MHz, Chloroform-d) δ 6.91 (dt, *J*= 15.3, 7.3 Hz, 1H), 6.56 – 6.49 (m, 1H), 2.51 – 2.46 (m, 2H), 2.28 – 2.20 (m, 2H), 2.16 (s, 3H), 1.82 – 1.84 (m, 2H), 1.16 (s, 9H).^{13}C NMR (101 MHz, Chloroform-d) δ 208.2,

190.0, 146.2, 124.8, 42.9, 42.7, 31.6, 30.0, 26.2, 22.1. FTIR (neat) ν_{max}: 2967, 1714, 1687, 1622, 1365, 1057, 984, 733 cm^{-1}. LC-MS (m/z); Calculated $C_{12}H_{21}O_2^+[M+H]^+$: 197.1542. Found 197.1541, in accordance with literature data.[215]

(E)-phenyloct-2-ene-1,7-dione(126)[215]

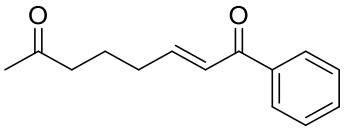

The Wittig reaction of **(126)** (200 mg, 1.78 mmol) with 1-phenyl-2-(triphenylphosphanylidene) ethenone[2] (676 mg, 1.78 mmol) provided compound **(126)** as a white solid (354 mg, 1.64 mmol, 92% yield) after column chromatography (hexane/EtOAc, 7:3). ^1H NMR (400 MHz, Chloroform-*d*) δ 7.97 –7.93 (m, 2H), 7.61 –7.56 (m, 1H), 7.53 –7.47 (m, 2H), 7.09 –7.01 (m, 1H), 6.95 – 6.89 (m, 1H), 2.55 – 2.50 (m, 2H), 2.40 – 2.33 (m, 2H), 2.17 (s, 3H), 1.89 – 1.81 (m, 2H).^{13}C NMR (101 MHz, Chloroform-*d*) δ 208.2, 190.7, 148.5, 137.8, 132.7, 128.5(2C), 126.5, 42.7, 31.9, 30.0, 22.0. FTIR (neat) ν_{max}: 3055, 3000, 2954, 2933, 2890, 1664, 1616, 1408, 1218, 935, 803, 524 cm^{-1}. LC-MS (m/z); Calculated $C_{14}H_{17}O_2^+[M+H]^+$: 217.1250. Found 217.1251, in accordance with literature data.[215]

Ethyl (E)-7-oxooct-2-enoate (127) [215]

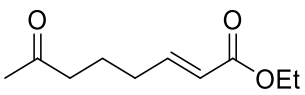

The Wittig reaction of (200 mg, 1.70 mmol) with commercially available ethyl (triphenylphosphoranylidene)acetate (592 mg, 1.70mmol) provided

compound **(127)** as a colourless oil (301 mg, 1.64 mmol, 96% yield) after column chromatography (hexane/EtOAc, 7:3) to provide the compound as a colourless oil (301 mg, 1.64 mmol, 96% yield).^{1}H NMR (400 MHz, Chloroform-*d*) δ 6.94 (dt, *J*= 15.6, 6.9 Hz, 1H), 5.82 – 5.77 (m, 1H), 4.19 – 4.12 (m, 2H), 2.48 (t, *J*= 7.2 Hz, 2H), 2.23 – 2.15 (m, 2H), 2.21 (s, 3H), 1.76 – 1.67(m, 2H), 1.31 (t, *J* = 7.2 Hz, 3H). ^{13}C NMR (101 MHz, Chloroform-*d*) δ 208.1, 166.4, 148.0, 122.0, 60.2, 42.5, 31.3, 29.9, 21.8, 14.2. FTIR (neat) ν_{max}: 2981, 2933, 1711, 1652, 1445, 1413, 1366, 1265, 1177, 1148, 982, 858, 670 cm^{-1}. LC-MS (m/z); Calculated $C_{10}H_{17}O_3^+$[M+H]$^+$: 185.1178. Found 185.1177, in accordance with literature data. [215]

(E)-oct-3-ene-2,7-dione (142)[221]

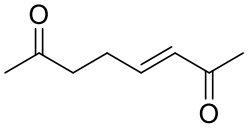

The Wittig reaction of **(142)** (200 mg, 2.00 mmol) with commercially available 1-(triphenylphosphoranylidene)-2-propanone (0.636mg, 2.00 mmol) provided **(142)** as a colourless oil (188 mg, 1.34 mmol, 67% yield) after column chromatography (pentane/Et_2O 8:2). ^{1}H NMR (400 MHz, Chloroform-*d*) δ 6.85 – 6.76(m, 1H), 6.12 – 6.06(m,1H), 2.67 – 2.63(m, 2H), 2.54 – 2.48(m, 2H), 2.26 (s, 3H), 2.20 (s, 3H). ^{13}C NMR (101 MHz, Chloroform-*d*) δ 206.7, 198.4, 146.2, 131.7, 41.5, 30.0, 27.0, 26.1. FTIR (neat) ν_{max}: 2924, 1698, 1672, 1627, 1361, 1161, 911, 729 cm^{-1}. LC-MS (m/z); Calculated $C_8H_{12}O_2Na^+$[M+Na]$^+$: 163.0735. Found 163.0732, in accordance with literature data.[221]

(*E*)-8,8-dimethylnon-5-ene,2,7-dione(143)

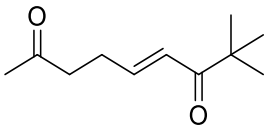

The Wittig reaction of **(143)** (100 mg, 1.00 mmol) with 3,3-dimethyl-1-(triphenylphosphoranylidene)-2-butanone2 (360mg, 1 mmol) provided the compound **(143)** as a colourless oil (151 mg, 0.83 mmol, 83% yield) after column chromatography (pentane/Et_2O 8:2).^{1}H NMR (400 MHz, Chloroform-*d*) δ 6.93 – 6.84(m, 1H), 6.57 – 6.52 (m, 1H), 2.65 – 2.60(m, 2H), 2.54 – 2.47(m, 2H), 2.18 (s, 3H), 1.17 (s, 9H). ^{13}C NMR (101 MHz, Chloroform-*d*) δ 206.9, 204.1, 145.2, 125.0, 42.9, 41.8, 30.0, 26.3, 26.1. FTIR (neat) ν_{max}: 2968, 1715, 1688, 1624, 1365, 1162, 1072 cm^{-1}. LC-MS (m/z); Calculated $C_{11}H_{18}O_2Na^+$[M+Na]$^+$: 206.1204. Found 206.1204.

(*E*)-1-phenylhept-2-ene-1,6-dione (144)

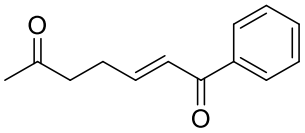

The Wittig reaction of **(144)** (100 mg, 1.00 mmol) with 1-phenyl-2-(triphenylphosphanylidene) ethanone.(380mg, 1 mmol) provided compound **(144)** as a colourless oil (163 mg, 0.81 mmol, 81% yield)aftercolumn chromatography (hexane/EtOAc, 7:3). ^{1}H NMR (400 MHz, Chloroform-*d*) δ 7.96 – 7.92 (m, 2H), 7.61 – 7.56 (m, 1H), 7.52 – 7.46 (m, 2H), 7.07 - 6.91 (m, 2H), 2.73 – 2.68 (m, 2H), 2.65 – 2.59 (m, 2H), 2.21 (s, 3H). ^{13}C NMR (101 MHz, Chloroform-*d*) δ 206.8, 190.6, 147.5, 137.8, 132.8, 128.5(2C), 126.6, 41.7, 30.0, 26.6. FTIR (neat) ν_{max}: 3057, 2937, 1713, 1650, 1619, 1354, 1221, 1160, 978, 694 cm^{-1}. LC-MS (m/z); Calculated $C_{13}H_{15}O_2^+$[M+H]$^+$: 203.1072. Found 203.1071.

Ethyl (*E*)-6-oxohept-2-enoate (145)

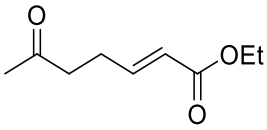

The Wittig reaction of **(145)** (100 mg, 1.00 mmol) with commercially available ethyl (triphenylphosphoranylidene)acetate (348g, 1mmol) provided compound **(145)** as a colourless oil (153 mg, 0.90 mmol, 90% yield) after column chromatography (hexane/EtOAc, 7:3). ^{1}H NMR (400 MHz, Chloroform-*d*) δ 7.02 – 6.91 (m, 1H), 5.88 – 5.81 (m, 1H), 4.23 – 4.17 (m, 2H), 2.65 – 2.60 (m, 2H), 2.53 – 2.46 (m, 2H), 2.18 (s, 3H), 1.33 – 1.28 (m, 3H). ^{13}C NMR (101 MHz, Chloroform-*d*) δ 206.8, 166.4, 147.1, 122.1, 60.3, 41.5, 30.0, 25.9, 14.3. FTIR (neat) ν_{max}: 2983, 1711, 1655, 1367, 1263, 1154, 1004, 981, 699 cm^{-1}. LC-MS (m/z); Calculated $C_9H_{14}O_3Na^+$[M+Na]$^+$: 193.0841. Found 193.0840.

Preparation of racemic standard(±)-(128)

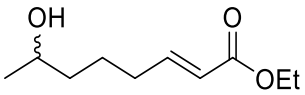

(*E*)Ethyl-7-oxooct-2-enoate(1 eq, 20 mg, 0.11 mmol) was added to a suspension of $NaBH_4$(1.2 eq, 5 mg, 0.13 mmol) in EtOH (2 mL) and the reaction stirred for 1 h at r.t. The reaction mixture was diluted with sat. NH_4Cl (8 mL) and extracted with EtOAC (2 x 10 mL) and the combined organic layers were dried over $MgSO_4$ and concentrated under reduced pressure to provide (±)-**(128)** as a colourless oil which was used without any further purification. *E.e*. determination was carried out by analysis on a chiral GC column, CP-Chirasil-DEX CB column, T = 115 °C, retention times:t_r(*R*) = 49.3 min (observed),t_r(*S*) = 51.2 min (observed).

General procedure for the ADH reduction

Ketoenones (1 eq, 50 mM) was added to an Eppendorf containing a mixture of Tris-HCl buffer(1 mL, 100 mM, pH 7.5), GDH (6 U),glucose monohydrate (5 eq., 250 mM) and NADPH (0.01 mM). LK-Resuspended ADH cells(100 µL resuspended whole cells from a 100mg/mL wet cell resuspension in Tris-HCL buffer(1mL, 100 mM, pH 7.5)) was then added and the reaction was shaken at 30 °C and 200 rpm for between 8 mins and1 h. Ethyl acetate (1 mL) was added and the organic layer was extracted, centrifuged (15000 rpm, 150 s) and the organic solvent concentrated under reduced pressure to yield the corresponding crude products which were used in the oxa-Michael cyclisation without further purification.

Ethyl (R,E)-7-hydroyoxt-2-enoate (145)[222]

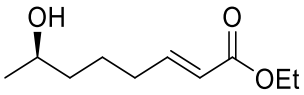

The biocatalysed reaction (reaction time= 1 h) of ethyl (*E*)-7-oxooct-2-enoate (9 mg, 50 mM) provided compound **(145)** a colourless oil (9 mg, 0.050mmol, >99% yield). ^{1}H NMR (400 MHz, Chloroform-*d*) δ 7.01 – 6.93 (m, 1H), 5.87 – 5.83 (m, 1H), 4.21 (q, *J*= 7.2 Hz, 2H),3.86 – 3.79 (m, 1H), 2.28 – 2.21 (m, 2H), 1.68 – 1.44 (m, 4H), 1.30 (t, *J* = 7.2 Hz, 3H), 1.21 (d, J = 6.2 Hz, 3H). ^{13}C NMR (101 MHz, Chloroform-*d*) δ 166.7, 148.9, 121.6, 67.8, 60.2, 38.6, 32.1, 24.2, 23.6, 14.3. FTIR (neat) ν_{max}: 3420,2980, 2932, 1711, 1652, 1445, 1177 cm^{-1}. Calculated $C_{10}H_{18}O_3Na^+$[M+H]$^+$: 187.1334. Found 187.1333. *e.e.*determination by analysis on a chiral GC column, CP-Chirasil-DEX CB column, T = 115 °C,

retention times: $t_r(R)$ = 49.3 min (only enantiomer), $t_r(S)$ = 51.2 min (not observed), in accordance with literature data.[222] $[\alpha]_D^{23}$= -17.3 (c1.0, CHCl3). [lit.[223] $[\alpha]_D^{20}$= +9.1 (*c* 1.0, $CHCl_3$) for 97% *e.e.* of the (S)-enantiomer].

Ethyl (*R,E*)-6-hydroxyhept-2-enoate(152)

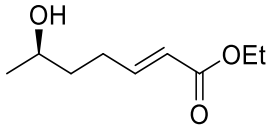

The biocatalysed reaction (reaction time= 1 h) of ethyl (*E*)-6-oxohept-2-enoate (9mg, 50 mM) provided compound **(152)** as a colourless oil (8mg, 0.045mmol, 89% yield). ^{1}H NMR (400 MHz, Chloroform-*d*) δ 7.04 – 6.96 (m, 1H), 5.89 – 5.84 (m, 1H), 4.21(q, *J* = 7.1 Hz, 2H), 3.89 – 3.81 (m, 1H), 2.43 – 2.25 (m, 2H), 1.68 – 1.59 (m, 2H), 1.31 (t, *J*= 7.1 Hz, 3H), 1.24 (d, *J* = 6.2 Hz, 3H). ^{13}C NMR (101 MHz, Chloroform-*d*) δ 166.7, 148.7, 121.6, 67.3, 60.2, 37.3, 28.5, 23.7, 14.3. FTIR (neat) ν_{max} : 3427, 2967, 2927, 1702, 1652, 1369, 1045 cm^{-1}.Calculated $C_9H_{17}O_3Na^+[M+H]^+$: 173.1178. Found 173.1179

(2R,8R,E)-non-3-ene-2,8-diol (114)[224]

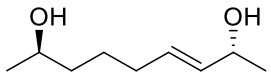

The biocatalysed reaction (reaction time = 1 h) of (3*E*)-non-3-ene-2,8-dione (**111**, 8mg, 50 mM) provided compound **(114)** as a colourless oil (8mg, 0.050mmol, >99% yield). ^{1}H NMR (400 MHz, Chloroform-*d*) δ 5.69 –5.50 (m, 2H), 4.31 – 4.24 (m, 1H), 3.85 – 3.77 (m, 1H), 2.10 –2.02 (m, 2H), 1.55 – 1.38 (m, 4H), 1.3 (d, *J* = 6.4 Hz, 3H), 1.2 (d, *J* = 6.2 Hz, 3H). ^{13}C NMR (101 MHz, Chloroform-*d*) δ 134.5, 130.5, 68.8, 67.9, 38.7, 32.0, 30.3, 25.3, 23.5. FTIR (neat) ν_{max} :3420, 2969, 2932, 2870, 1367, 1064,

906, 729 cm^{-1}. MS (m/z);Calculated $C_9H_{18}O_2Na^+[M+Na]^+$: 181.1204. Found 181.1204.According to literature data.[224]

(2*R*,7*R*,*E*)-oct-3-ene-2,7-diol (146)

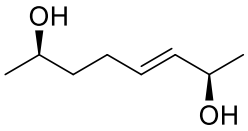

The biocatalysed reaction (reaction time = 1 h) of (3*E*)-oct-3-ene-2,7-dione (**(142)** 7 mg, 50 mM) provided compound **(146)** as a colourless oil(7 mg, 0.050mmol, >99% yield).^{1}H NMR (400 MHz, Chloroform-*d*) δ 5.78 –5.39 (m, 2H), 4.37 – 4.13 (m, 1H), 3.91 – 3.70 (m, 1H), 2.23 – 1.92 (m, 2H), 1.70 – 1.45 (m, 2H), 1.26 (d, *J* = 6.3 Hz, 3H), 1.20 (d, *J* = 6.2 Hz, 3H).^{13}C NMR (101 MHz, Chloroform-*d*) δ 134.6, 130.3, 68.8, 67.6, 38.5, 28.4, 23.6, 23.5.FTIR (neat) v_{max}: 3420, 2920, 1374, 1013, 670, 451 cm^{-1}. MS (m/z); Calculated $C_8H_{16}O_2Na^+[M+Na]^+$: 167.1048. Found 167.1043.

General procedure for theacid catalysedoxa-Michael cyclisation(Synthesis of 3a-d,f-h)

Following the general procedure for ADH reduction, the crude material was dissolved in CH_2Cl_2(1 mL) and HCl.Et_2O (1 mL) was added and the reaction was left to stir at r.t. for 1 h. The solvents were removed by *in vacuo* and the resulting residues purified *via* column chromatography, if required.

1-((2R, 6R)-6-methyltetrahydro-2H-pyran-2yl)propan-2-one (118)[225]

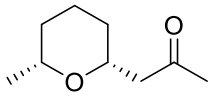

The biocatalysed reaction (reaction time = 8 min) of *(E)*-non-3-ene-2,8-dione(**(111)**, 8mg, 50 mM) followed by oxa-Michael cyclisation under acidic conditions provided compound **(118)**, after column chromatography, as a colourless oil (6mg, 0.038mmol, 75% yield, 12:1 *d.r.*(*cis*:*trans*)).^{1}H NMR (400 MHz, Chloroform-*d*) δ 3.83 – 3.76 (m, 1H), 3.53 – 3.43(m, 1H), 2.68 (dd, *J* = 15.5, 7.5 Hz, 1H), 2.42 (dd, *J* = 15.5, 5.2 Hz, 1H), 2.20 (s, 3H), 1.86 – 1.79(m, 2H), 1.64 – 1.51 (m, 4H), 1.16(d, *J* = 6.2 Hz,3H). ^{13}C NMR (101 MHz, Chloroform-*d*) δ 207.7, 74.1, 74.0, 50.4, 32.9, 31.2, 31.1, 23.5, 22.1. FTIR (neat) v_{max}: 2921, 1712,1375, 1015, 905, 728, 649 cm^{-1}. LC-MS (m/z); Calculated $C_9H_{17}O2^+[M+H]^+$: 157.1229.Found 157.1230, in accordance with literature data.[225]

3,3-dimethyl-1-((2*R*, 6*R*)-6-methyltetrahydro-2H-pyran-2yl)butan-2-one (129)

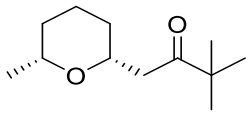

The biocatalysed reaction (reaction time = 1 h) of (*E*)-9,9-dimethyldec-6-ene-2,8-dione (**(125)**, 10mg, 50 mM) followed by oxa-Michael cyclisation under acidic conditions provided the compound **(129)** as a colourless oil(10 mg, 0.050mmol, >99% yield, 8:1 *d.r.*(*cis*:*trans*)).^{1}H NMR (400 MHz, Chloroform-*d*) δ 3.88 – 3.79 (m, 1H), 3.51 – 3.43 (m, 1H), 2.83 (dd, *J* = 16.7, 5.8 Hz, 1H), 2.50 (dd, *J* = 16.7, 6.9 Hz, 1H), 1.83 - 1.50 (m, 4H), 1.12 (s, 9H)1.37 – 1.02 (m, 5H). ^{13}C NMR (101 MHz, Chloroform-*d*) δ 214.1, 74.1, 73.90, 44.2, 43.6, 33.1, 31.1, 26.1, 23.5,

22.1. FTIR (neat) ν_{max}: 2971, 2934, 2866, 1702, 1370, 1065, 905, 649 cm^{-1}. LC-MS (m/z); Calculated $C_{12}H_{23}O_2^+[M+H]^+$: 199.1698. Found 199.1700. $[\alpha]_D^{25}$= --26.0 (*c* 2.0, benzene). [lit.[226] $[\alpha]_D^{23}$= +37.8 (*c* 2.04, benzene) for a >99% *e.e.* sample of the (*S*,*S*)-enantiomer]

2-(2R, 6R)-6-methyltetrahydro-2H-pyran-2yl)-1-phenylethan-1-one(130)[227]

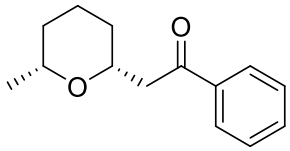

The biocatalysed reaction (reaction time = 1 h) of (*E*)-phenyloct-2-ene-1,7-dione (**(126)**, 11 mg, 50 mM from a 500 mM stock in MeOH) followed by oxa-Michael cyclisation under acidic conditions provided compound **(130)** as a colourless oil (11mg, 0.050 mmol, >99% yield, 10:1 *d.r.*(*cis*:*trans*)). ^{1}H NMR (400 MHz, Chloroform-*d*) δ 8.01 – 7.97 (m, 2H), 7.60 – 7.50 (m, 1H), 7.51 – 7.45 (m, 2H), 4.04 – 3.96 (m, 1H), 3.56 – 3.47 (m, 1H), 3.33 (dd, *J* = 16.2, 5.9Hz, 1H), 3.01 (dd, *J* = 16.2, 6.7 Hz, 1H), 1.83 – 1.70 (m, 2H), 1.63 – 1.55 (m, 2H), 1.33 – 1.20 (m, 2H), 1.17 (d, *J* = 6.2 Hz, 3H). ^{13}C NMR (101 MHz, Chloroform-*d*) δ 198.4, 137.4, 133.0, 128.5, 128.2, 74.2, 74.1, 45.6, 33.1, 31.4, 23.5, 22.2. FTIR (neat) ν_{max}: 2934, 1681, 1375, 1319, 1197, 1066, 904, 726, 650 cm^{-1}. LC-MS (m/z); Calculated $C_{14}H_{19}O_2^+[M+H]^+$: 219.1385. Found 219.1384, in accordance with literature data.[227] $[\alpha]_D^{23}$= +22.2 (*c* 1.0, $CHCl_3$). [lit.[meth11] $[\alpha]_D^{23}$= -15 (*c* 1.0, $CHCl_3$) for a >99% *e.e.* sample of the (*S*,*S*)-enantiomer].

3,3-dimethyl-1-((5R)-methyltetrahydrofuran-2-yl)butan-2-one (151)[228]

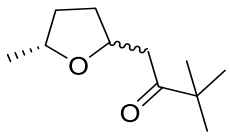

The biocatalysed reaction (reaction time = 1 h) of (*E*)-8,8-dimethylnon-5-ene,2,7-dione (**(143)**,9mg, 50 mM) followed by oxa-Michael cyclisation under acidic conditions provided compound **(151)** as a colourless oil (7mg, 0.039mmol, 77% yield, 1:1 *d.r.*(*cis*:*trans*)). ^{1}H NMR (400 MHz, Chloroform-*d*) δ 4.45 – 4.39(m, 1H), 4.26 – 4.19 (m, 1H), 4.13 – 4.09(m, 1H), 3.98 – 3.92(m, 1H), 3.03 – 2.94(m, 2H), 2.60 – 2.50(m, 2H), 2.28 – 1.96(m, 4H), 1.55 – 1.40(m, 4H), 1.29 – 1.17(m, 6H), 1.14 (d*, J* = 2.0 Hz, 18H). ^{13}C NMR (101 MHz, Chloroform-*d*) δ 214.2, 214.1, 75.4, 75.1, 74.7, 74.6, 44.2, 44.2, 43.2, 42.9, 33.8, 32.8, 32.6, 31.6, 26.2(2C), 21.3, 21.3.FTIR (neat) ν_{max}: 2971, 2872, 1703, 1478, 1368, 1060, 917, 729, 646 cm^{-1}. LC-MS (m/z); Calculated $C_{11}H_{21}O_2^+$[M+H]$^+$: 185.1542. Found 185.1541, in accordance with literature data.[228]

2-((5R)-methyltetrahydrofuran-2-yl)-1-phenylethan-1-one(150)[229]

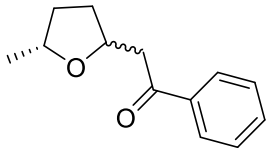

The biocatalysed reaction (reaction time = 1 h) of (*E*)-1-phenylhept-2-ene-1,6-dione (**(144)**, 10mg, 50 mM)followed by oxa-Michael cyclisation under acidic conditions provided compound **(150)** as a colourless oil(10mg, 0.050mmol, >99% yield, 1:1 *d.r.*(*cis:trans*)). ^{1}H NMR (400 MHz, Chloroform-*d*) δ 8.02 – 7.97 (m, 4H), 7.61 – 7.53 (m, 2H), 7.51 – 7.46 (m, 4H), 4.64 – 6.58 (m, 1H), 4.45 – 4.40 (m, 1H), 4.20 – 4.12 (m, 1H), 4.05 – 3.98 (m, 1H), 3.52 – 3.42 (m, 2H), 3.12 – 2.99 (m, 2H), 2.33 – 1.99(m, 4H), 1.69 – 1.44 (m, 4H), 1.28 –1.21(m, 6H). ^{13}CNMR (101

MHz, Chloroform-*d*) δ 198.5, 198.4, 137.1, 137.0, 133.1 (2C), 128.6 (2C), 128.2 (2C), 75.5, 75.4, 74.9, 74.9, 45.3, 45.1, 33.8, 32.8, 32.6, 31.6, 21.4, 21.3.FTIR (neat) ν_{max}: 2970, 2933, 2861, 1682, 1448, 1214, 1042, 1001, 906, 728, 690, 648 cm^{-1}. LC-MS (m/z); Calculated $C_{13}H_{17}O_2^+[M+H]^+$: 205.1229. Found 205.1227, in accordance with literature data.[229]

General procedure for the base catalysed oxa-Michael cyclisation (Synthesis of (131) and (152))

Ethyl 2-((2R, 6R)-6-methyltetrahydro-2H-pyran-2yl)acetate (131)[223]

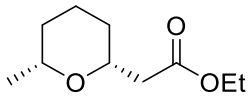

NaH (1.2 eq., 12 mM) was added to a solution of ethyl (*R*,*E*)-7-hydroyoxt-2-enoate(**(127)**, 146 mg, 0.78 mmol)in dry Et_2O(15 mL) and the mixture was left at r.t. for 48 h. The reaction was quenched with AcOH (2 mL), diluted with H_2O (10 mL) and extracted with Et_2O (2 x 15 mL). The combined organic layers were dried over $MgSO_4$, concentrated under reduced pressure and purified by flash column chromatography (EtOAc/Hexane, 1:4) to provide compound **(131)** as a colourless oil (70 mg, 0.38 mmol, 48% yield, >99:1 *d.r*. (*cis:trans*)). ^1H NMR (400 MHz, Chloroform-*d*) δ 4.14 (q, *J* = 7.1 Hz, 2H), 3.88 – 3.67 (m, 1H), 3.51 – 3.40 (m, 1H), 2.62 – 2.48 (m, 1H), 2.44 – 2.31 (m, 1H), 1.86 – 1.76 (m, 1H), 1.67 – 1.47 (m, 3H), 1.25 (t, *J* = 7.1 Hz, 3H), 1.28 – 1.10 (m, 2H), 1.14 (d, *J* = 6.2 Hz, 3H). ^{13}C NMR (101 MHz, Chloroform-*d*) δ 171.5, 74.3, 74.0, 60.3, 41.8, 32.9, 30.9, 23.5, 22.1, 14.2. FTIR (neat) ν_{max}: 2975, 2934, 1711, 1374, 1206, 1044, 914, 738 cm^{-1}. LC-MS (m/z); Calculated $C_{10}H_{19}O_3^+[M+H]^+$: 187.1334.Found 187.1331.in accordance with

literature data.[223] $[\alpha]_D^{23}$= -3.8 (*c* 0.5, $CHCl_3$). [lit.[222] $[\alpha]_D^{25}$= -3.0 (*c* 0.5, $CHCl_3$) for a sample of >99% *e.e.* of the (*R*,*R*)-enantiomer].

Ethyl 2-((5R)-methyltetrahydrofuran-2-yl)acetate(152)[230]

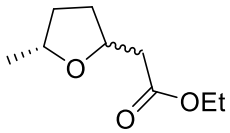

^{t}BuOK (1.2 eq., 12 mM) was added to a solution of ethyl *(R,E)*-6-hydroxyhept-2-enoate(**(145)**, 17 mg, 0.10 mmol) in dry Et_2O(5 mL) and the mixture was left at r.t. for 1 hour. The reaction was quenched with sat. NH_4Cl (5 mL) and extracted with Et_2O (2 x 5 mL). The combined organic layers were dried over $MgSO_4$, concentrated under reduced pressure and purified by flash column chromatography to provide compound **(152)** as a colourless oil (9mg, 0.054 mmol, 54% yield, 1:1 *d.r*. (*cis:trans*)).^{1}H NMR (400 MHz, Chloroform-*d*) δ 4.46 – 4.34 (m, 1H), 4.29 – 4.18 (m, 1H), 4.18 – 4.06 (m, 5H), 4.04 – 3.91 (m, 1H), 2.72 – 2.53 (m, 2H), 2.50 – 2.35 (m, 2H), 2.21 – 1.92 (m, 4H), 1.68 – 1.40 (m, 4H), 1.32 – 1.16 (m, 12H). ^{13}C NMR (101 MHz, Chloroform-*d*) δ 171.3, 171.3, 75.7, 75.3, 74.9, 74.6, 60.4(2C), 41.3, 41.0, 33.6, 32.7, 32.0, 31.2, 29.7, 21.4, 14.2 (2C). FTIR (neat) ν_{max}: 2967, 2927, 1702,1652, 1369, 1045 cm^{-1}, MS (m/z); Calculated $C_9H_{17}O_3^+[M+H]^+$: 173.1178. Found 173.1177, in accordance with literature data.[230]

Hydrolysis of ester **(152)** to (-)-(R,R)-(cis-6-methyltetrahydropyran-2-yl)acetic acid(134)[231]

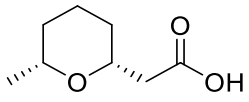

A saturated solution of aqueous LiOH (2 mL) was added to a solution of ethyl 2-((2*R*, 6*R*)-6-methyltetrahydro-2*H*-pyran-2yl)acetate (**(131)**,14 mg, 0.075 mmol) in MeOH (0.5 mL) and the reaction was stirred for 30 mins at r.t. HCl (6 M) was added until pH 1-2 was reached and the reaction mixture was extracted with Et_2O (3 x 10 mL). The combined organic extracts were then dried over $MgSO_4$ and concentrated under reduced pressure to provide the compound as a colourless oil (11 mg, 0.070 mmol, 93% yield, >99:1 *d.r.*(*cis:trans*)). ^{1}H NMR (400 MHz, Chloroform-*d*) δ 8.55 (br s, 1H), 3.90 – 3.68 (m, 1H), 3.59 – 3.43 (m, 1H), 2.65 – 2.41 (m, 2H), 1.88 – 1.75 (m, 1H), 1.70 – 1.48 (m, 3H), 1.30 - 1.13 (m, 2H), 1.19 (d, J = 6.3 Hz, 3H). ^{13}C NMR (101 MHz, Chloroform-*d*) δ 174.7, 74.6, 73.9, 41.2, 32.7, 30.7, 23.1, 22.0, in accordance with literature data.[231] $[\alpha]_D^{23}$= -26.8 (*c* 1.0, $CHCl_3$). [lit.[231] $[\alpha]_D^{25}$= -24.8 (*c* 1.0, $CHCl_3$)].

Synthesis of brocaketone A analogue (144) 2-(3,5-dimethoxyphenyl)-N-methoxy-N-methylacetamide(141)[232]

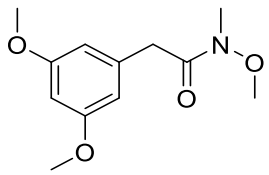

1,1'-Carbonyldiimidazole (1.3 eq., 1.08 g, 6.63 mmol) was added to a solution of 2-3,5-dimethoxyphenyl)acetic acid (1.0 eq., 1.00 g, 5.10 mmol) in CH_2Cl_2(13 mL) and the mixture was stirred for 1h. *N*,*O*-Dimethylhydroxylamine hydrochloride (2.0 eq, 0.99 g, 10.19 mmol) was then added and the reaction stirred at room temperature overnight. The reaction was diluted with H_2O (26 mL) and extracted with CH_2Cl_2(2 x 13 mL), the organics were combined, dried over MgSO4and concentrated

under reduced pressure. The crude material was purified by flash column chromatography (Hexane:EtOAc 1:1) to provide the title compound as a colourless oil (1.20 g, 5.02 mmol, 98% yield). ^{1}H NMR (400 MHz, Chloroform-*d*) δ 6.48 - 6.43 (m, 2H), 6.37 - 6.33 (m, 1H), 3.77 (s, 6H), 3.70 (s, 2H), 3.62 (s, 3H), 3.19 (s, 3H). ^{13}C NMR (101 MHz, Chloroform-*d*) δ 172.1, 160.8, 137.1, 107.3, 98.9, 61.3, 55.3, 39.6, 32.3. FTIR (neat) ν_{max}: 2937, 2838, 1659, 1595, 1460, 1430, 1205, 1151, 1064, 942, 783 cm^{-1}. MS (m/z); Calculated $C_{12}H_{18}NO_4^+$[M+H]$^+$: 240.1236. Found 240.1237, in accordance with literature data.[232]

1-(3,5-dimethoxyphenyl)but-3-en-2-one(142)

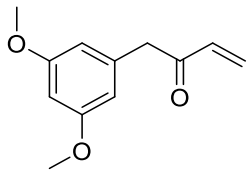

Vinyl magnesium bromide (1 M, 1.2 eq., 5.89 mmol, 5.9 mL) was added to a solution of 2-(3,5-dimethoxyphenyl)-*N*-methoxy-*N*-methylacetamide (**(141),** 1.0 eq., 4.91 mmol, 1.175 g) in dry THF (10 mL) under N_2 and the reaction was stirred for 1 h at 0 °C. The reaction was warmed to room temperature and stirred for an additional 1h. The reaction was then quenched with H_2O (26 mL) and extracted with Et_2O (3 x 30 mL), the organics were combined, dried over $MgSO_4$and concentrated under reduced pressure. The crude material was purified by flash column chromatography (Hexane:EtOAc 7:3) to provide the title compound as a colourless oil (606 mg, 2.94 mmol, 60% yield). ^{1}H NMR (400 MHz, Chloroform-d) δ 6.49 – 6.21 (m, 2H), 6.36 (s, 3H), 5.85 – 5.77 (m, 1H), 3.79 (s, 2H), 3.77 (s, 6H). ^{13}C NMR (101 MHz, Chloroform-*d*) δ 197.5, 161.0, 136.1, 135.4, 129.1, 107.5, 99.0, 55.3, 47.6. FTIR (neat) ν_{max} : 3000, 2937, 2838, 1690, 1593, 1459, 1429,1204, 1149, 1063 cm^{-1}. MS (m/z); Calculated $C_{12}H_{15}O_4^+$[M+H]$^+$: 207.1021. Found 207.1021.

(*E*)-1-(3,5-dimethoxyphenyl)non-3-ene-2,8-dione(143)

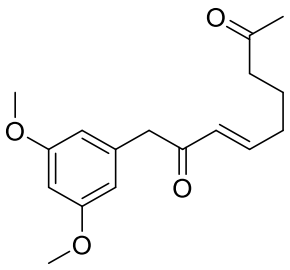

Hept-6-en-2-one (1.2 eq., 1.22 mmol, 137 mg) and Hoveyda-Grubbs Catalyst™ 2nd Generation (0.1 eq., 0.10 mmol, 63 mg) were added to a solution of 1-(3,5-dimethoxyphenyl)but-3-en-2-one (1.0 eq., 1.02 mmol, 210 mg) in CH_2Cl_2 (1 mL) and allowed to stir at r.t. for 18h. The reaction mixture was concentrated and purified by column chromatography (Hexane:EtOAc 1:1) to provide the title compound as a brown oil (179 mg, 0.61 mmol, 60% yield). ^{1}H NMR (400 MHz, Chloroform-*d*) δ 6.87 – 6.79 (m, 1H), 6.33 (s, 3H), 6.15 – 6.07 (m, 1H), 3.74 (s, 6H), 3.71 (s, 2H), 2.38 (t, *J* = 7.2 Hz, 2H), 2.22 – 2.13 (m, 2H), 2.08 (s, 3H), 1.78 – 1.62 (m, 2H). ^{13}C NMR (101 MHz, Chloroform-*d*) δ 208.0, 197.1, 160.9, 147.3, 136.6, 129.6, 107.4, 98.9, 55.3, 48.0, 42.5, 31.6, 29.9, 21.8. FTIR (neat) ν_{max}: 3001, 2937, 2839, 1712, 1594, 1460, 1430, 1292, 1204, 1149, 1061, 979 cm^{-1}. MS (m/z); Calculated $C_{17}H_{23}O_4^+$ $[M+H]^+$: 291.1596.Found 291.1596.

1-(3,5-dimethoxyphenyl)-3-((2R,6R)-6-methyltetrahydro-2H-pyran-2-yl)propan-2-one (Dimethyl brocaketone A, 144)

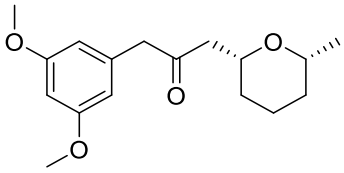

The biocatalysed reaction (reaction time = 1 h)of (*E*)-1-(3,5-dimethoxyphenyl)non-3-ene-2,8-dione (**(143)**, 15 mg, 50 mM), followed by oxa-Michael cyclisation under acidic conditions(see general procedure above)provided compound **(144)** as a colourless oil after column chromatography (pentane:Et_2O 9:1) as a brown oil (12mg, 0.040 mmol, 80% yield, 11:1 *d.r.*). ^{1}H NMR (400 MHz, Chloroform-*d*) δ 6.38 – 6.28 (m, 3H), 3.85 – 3.69 (m, 1H), 3.76 (s, 6H), 3.68 – 3.57 (m, 2H), 3.51 – 3.36 (m, 1H), 2.70 (dd, *J* = 15.6, 7.3 Hz, 1H), 2.44 (dd, *J* = 15.6, 5.4 Hz, 1H), 1.81 – 1.72 (m, 1H), 1.60 – 1.43 (m, 3H), 1.29 – 1.04 (m, 2H), 1.13 (d, *J* = 6.2 Hz, 3H). ^{13}C NMR (101 MHz, Chloroform-d) δ 206.9, 160.9, 136.3, 107.6, 99.0, 74.2, 74.0, 55.3, 51.4, 48.5, 33.0, 31.1, 23.4, 22.1.FTIR (neat) vmax: 2931, 2839, 1713, 1595, 1204, 1151, 1058 cm^{-1}.MS (m/z); Calculated $C_{17}H_{25}O_4^+[M+H]^+$: 293.1753.Found 293.1753.$[\alpha]_D^{23}$= -55.4(c 1.0, $CHCl_3$).

Section 5: References

[1] G. M. Cragg, D. J. Newman, *Pure Appl. Chem.*, 2005, **77**, 7-24.

[2] D. J. Newman, G. M. Cragg, K. M. Snader, *Nat. Prod. Rep.* 2000, **17**, 215-234.

[3] M. S. Butler, A. D. Buss, Natural Product Chemistry for Drug Discovery, 1st ed., RSC Publishing, 2009.

[4] B. B. Mishra, V. K. Tiwari, *Eur. J. Med. Chem.*, 2011, **46**, 4769-4807.

[5] J. Rey-Ladino, A. G. Ross, A. W. Cripps, D. P. McManus, R. Quinn, *Vaccine.*, 2011, **29**, 6464-6471.

[6] B. Haefner, *Drug Discov. Today,* 2003, **8**, 536-544.

[7] M. S. Butler, *J. Nat. Prod.*, 2004, **67**, 2141-2153.

[8] A. T. Dossey, *Nat. Prod. Rep.* 2010. **27**, 1737–1757.

[9] A. Salatino, M. L. F. Salatino, G. Negri, *J. Braz. Chem. Soc*. 2007, **18**, 11-33.

[10] J. G. Mahdi *J. Saudi Chem. Soc.* 2010, **14**, 317-322.

[11] A. Der Marderosian, J. A. Beutler, *The Review of Natural Products. 2nd Facts and Comparisons*, Seattle, WA, USA 2003

[12] J. W. Henderson, *Mayo. Clin. Proc.* 1997, **72**, 683-687.

[13] J. Mann, Murder, Magic and Medicine, 1st ed. Oxford University Press, 1994.

[14] E. P. Abraham, E. Chain, C. M. Fletcher, *Lancet.* 1941, **16**, 177-189.

[15] A. L. Alder, *The History of Penicillin Production*, American Institute of Chemical Engineers. 1st ed. 1970.

[16] J. D. Williams, *Int. J. Antimicrob. Agents.*, 1999 **1**, S3-S7.

[17] H. Erdtman, *Pure Appl. Chem.* 1963, **6**, 679-709.

[18] P. Acevedo-Rodríguez, P. C. van Welzen, F. Adema, R. W. van der Ham, 2011. Sapindaceae. Pp. 357-407, in Kubitzki, K. (ed.), *The Families and Genera of Flowering Plants. X. Flowering Plants: Eudicots. Sapindales, Cucurbitales, Myrtaceae.* Springer, Berlin.

[19] F. Adams, P. Reddell, M. J. Webb, W. A. Shipton, *Australian J. Bot.* **54**, 271-281.

[20] F. Almeda, *Ann. Missouri Bot. Gard.* 1997, **84**, 305-308.

[21] J. F. Basinger, D. R. Greenwood, P. G. Wilson, D. C. Christophel, *Canadian J. Bot*., 2007, **85**, 204-215.

[22] S. Bak, S. M. Paquette, M. Morant, A. V. Rasmussen, S. Saito, N. Bjarnholt, M. Zagrobelny, K. Jorgensen, S. Osmani, T. Hamann, H. T.

Simonsen, R. S. Perez, T. B. van Hesswijck, B. Joregensen, B. L. Moller, *Phytochem. Reviews*, 2006, **5**, 309-329.

[23] M. Bekaert, P. P. Edger, C. M. Hudson, J. C. Pires, G. C. Conant, *New. Phytol*, **196**, 596-605.

[24] M. A. Beilstein, I. A. Al-Shehbaz, S. Mathews, E. A. Kellogg, *American J. Bot.* 2006, **95**, 1307-1327.

[25] J. F. Coetzee, T. H. Chang, *Pure. Appl. Chem.* 1986, **58**, 1535-1540.

[26] R. G. Brownlee, R. M. Silverstein, D. Muller-schwarze, A. G. Singer, *Nature,* 1969, **221**, 285-285.

[27] D. A. Carlson, M. S. Mayer, D. L. Silhacek, J. D. James, M. Beroza, *Science,* 1971, **174**, 76-78.

[28] P. Vemishetti, F. S. Gibson, J. L Dillon, Semi-synthesis of paclitaxel using dialkyldichlorosilanes**, US6242614B1.**

[29] K. C. Nicolaou, C. K. Hwang, E. J. Soresen, C. F. Clairborne, *J. Am. Chem. Soc.* 1992, **16**, 1117-1118.

[30] K. C. Nicolaou, Z. Yang, J. J. Liu, P . G. Ueno, P. G. Nantermet, R. K. Guy, C. F. Clairbourne, J. Renaud, E. A. Couladouros, K. Paulvannan, E. J. Sorensen, *Nature,* 1994, **367**, 630-634.

[31] G. Don, *Syst. Nat. Ed.* 1837 **10**, 944.

[32] G. Guirimand, A. Guihur, P. Poutrain, F. Hericourt, S. Mahroug, B. St-Pierre, V. Burlat, V. Courdavault, *J. Plant. Physiol.* 2011, **168**, 549-557

[33] - K. H. Lim, O. Hiraku, K. Komiyama, T. S. Kam, *J. Nat. Prod.* 2008, **71**, 1591-1594.

[34] M. E. Qazzaz, V. J. Raja. K, -H, Lim. T, -S, Kam, J. B. Lee, P. Gershkovich, T. D. Bradshaw, *Cancer. Lett.* 2016, **370**, 185-197.

[35] K. Miettinen, L. Dong, N. Navrot, T. Schneider, V. Burlat, J. Pollier, L. Woittiez, S. van der Krol, R. Lugan, T. Ilc, R. Verpoorte, K. Oksman-

Caldentey, E. Martinoia, H. Bouwmeester, A. Goossens, J. Memlink, D. Weck-Reichhart .; *Nat. Commun.* 2014, **5**, AN-3606.

[36] X. Zhu, X. Zeng, C. Sun, C. Chen, *Front. Med.* 2014, **8**, 285-293.

[37] L. F. Tietze, *Angew. Chem. Int. Ed.* 1983, **22**, 828-841.

[38] S. E. O'Connor and J. J. Maresh. *Nat. Prod. Rep.* 2006, **23**, 532-547**.**

[39] T. Scheper, 1st ed, Advances in biochemical engineering, Berlin Heidelberg: Springer-verlag, 2003.

[40] M. Le Roux, F. Gueritte. *Hist. Sci.* 2017, **1**, 87-149.

[41] R. Frei, D. Staedler, A. Raja, R. Franke, F. Sasse, S. Gerber-Lemaire, J. Waser, *Angew. Chem. Int. Ed.* 2013, **50**, 13373-13376.

[42] H. Yang, A. Ganguly, F. Carbral, *J. Biol. Chem.* 2010, **42**, 32242-32250.

[43] R. Mohan, E. A. Katrukha, H. Doodhi, I. Smal, E. Meijering, L. C. Kapitein, M. O. Steinmetz, A. Akhmanova, *Proc. Natl. Acad. Sci. USA,* 2013, **110**, 8900-8905.

[44] D. A. Brito, Z. Yang, C. L. Rieder, 2008. *J. Cell. Biol.* **182,** 623–629.

[45] R. Bharadwaj, H. Yu*, Oncogene.* 2004, **23**, 2016–27.

[46] V.J. Raja, K.H. Lim, C.O. Leong, T.S. Kam, T.D. Bradshaw, *Invest. New. Drugs.* 2014, **32**, 838-850.

[47] X. Lui, D. Yang, J. Lui, N. Ren, *RSC Adv.* 2014, **4** 64336-64346.

[48] J. Poisson, *Process of obtaining tabersonine*, US3758478A.

[49] F. Chen, M. Lei, L. Hu, *Synthesis*, 2014, **46**, 3199-3206.

[50] A. Del Grosso, P. J. Singleton, C. A. Muryn, M. J. Ingleson, *Angew. Chem. Int. Ed.* 2011, **9**, 2102-2106.

[51] A. Del Grosso, J. A. Carrillo, M. J. Ingleson. *Chem. Commun.* 2015, **51**, 2878-2881.

[52] C. Zhu, R. Wang, J. R. Falck, *Org. Lett.* 2012, **14,** 3494-3497.

[53] H. Gilman and W. E. Catlin, *Org. Synth.* 1926, **6,** 22.

[54] J. F. Walker and A. F. Chadwich, *Ind. Eng. Chem.* 1947, **39**, 974-977.

[55] K. Ohsawa, M. Yoshida, T. Doi, *J. Org. Chem.* 2013, **78**, 3438-3444.

[56] A. Rieche, H. Gross, E. Hoft, *Org. Synth.* 1967, **47,** 1.

[57] M. T. Reetz, *J. Am. Chem. Soc*., 2013, **135**, 12480-12496.

[58] Farber, Eduard (1972). "Emil Fischer." In *Dictionary of Scientific Biography,* Vol. 5. New York:

[59] J. J. Lucier, L. K. James, *Nobel Laureates in Chemistry 1901–1992,* 1993, Washington, DC: American Chemical Society; Chemical Heritage Foundation, 8–14.

[60] R. Kohler, *J. Hist. Biol.* 1971, **4**, 35-61.

[61] C. K. Savile, J. M. Janey, E. C. Mundorff, J. C. Moore, S. Tam, W. R. Jarvis, J. C. Colbeck, A. Krebber, F. J. Fleitz, J. Brands, P. N. Devine, G. W. Huisman, G. J. Hughes, *Science*, 2010, **329**, 305-309.

[62] N. A. McGrath, M. Brichacek, J. T. Njardarson, *J. Chem. Ed.* 2010, **87**, 1348-1349.

[63] I. Agranat, H. Caner, J. Caldwell, *Nat. Rev. Drug Discov*., 2002, **1**, 753–768.

[64] V. S. Shende, P. Singh, B. M. Bhanage, *Catal. Sci. Technol*, 2018, **8**, 955-969.

[65] Y. Kawanami, R. C. Yanagita, *Molecules*, 2018, **23**, 2408.

[66] E. J. Corey, J. O. Link, *J. Am. Chem. Soc.*, **1992**, *114*, 1906-1908.

[67] E. J. Corey, S. Shibata, R. K. Bakshi, *J. Org. Chem.*, **1988**, *53*, 2861-2863.

[68] R. T. Stemmler, *Synlett.* 2007, **16**, 710-713.

[69] M. Kitamura, M. Tokunada, T. Ohkuma, R. Noyori, *Org. Synth.*, 1998, **9**, 589-594.

[70] S. Akutagawa, *Chirality Ind.*, *Appl. Catal., A*., 1992, **128**, 171-207.

[71] H. Kumobayashi, N. Sayo, S. Akutagawa, T. Sakaguchi, H. Toshiaki, *Nippon. Kagaku. Kaishi.*, 1997, **12**, 835-846.

[72] R. J. Newland, M. F. Wyatt, R. L. Wingad, S. M. Mansell, *Dalton Trans.*, 2017,**46**, 6172-6176.

[73] M. B. Smith, 2016, Organic Synthesis, 4th edition, Academic Press.

[74] R. Noyori, M. Kitamura, *Angew. Chem. Int. Ed.* 1991, **30**, 49-69.

[75] K. Soai, S. Niwa, *Chem. Rev.* 1992, **92**, 833-856.

[76] K. Biswas, O. Prieto, P. J. Goldsmith, S. Woodward, *Angew. Chem. Int. Ed.* 2005, **44**, 2232-2234.

[77] M. R. Luderer, W. F. Bailey, M. R. Luderer, J. D. Fair, R. J. Dancer, M. B. Sommer, *Tetrahedron Asymmetry,* 2009, **20**, 981-998.

[78] J. F. Collados, R. Solà, S. R. Harutyunyan, B. Maciá, *ACS Catalysis,* 2013 **6***,* 1952–1970

[79] O. Verho, J. E. Bäckvall. *J. Am. Chem. Soc.* 2015, **137**, 3996–4009.

[80] Y. Ahn, S. B, Ko, M. J. Kim, J. Park, J. *Coord. Chem. Rev.* 2013, **252**, 647–658.

[81] P. Hoyos, M. Fernández, J. V. Sinisterra, A. R. Alcántara, *J. Org. Chem.*, 2006, **71**, 7632–7637.

[82] C. L. Windle, M. Mulleer, A. Nelson, A. Berry, *Curr. Opin. Chem. Biol.* 2014, **19**, 25-33.

[83] S. Jennewein, M. Schurmann, M. Wolberg, I. Hilker, R. Luiten, M. Wubbolts, D. Mink, *Biotechnol. J.* 2006 **1**, 537-548.

[84] M. Cheriyan, M. J. Walters, B. D. Kang, L. L. Anzaldi, E. J. Toone, C. A. Fierke, *Bioorg. Med. Chem.*, 2011, **19**, 6447-6453.

[85] X. Garrabou, J. Joglar, T. Parella, R. Crehuet, J. Bujons, P. Clapes, *Adv. Synth. Catal.*, 2011, **353**, 89-99.

[86] M. J. de Groot, *Drug Discov. Today*., 2006 **11**, 601-606.

[87] T. A. Baillie, M. N. Cayen, H. Fouda, R. J. Gerson, J. D. Green, S. J. Grossman, L. J. Klunk, B. LeBlanc, D. G. Perkins, L. A. Shipley, *Toxicol. Appl. Pharmacol.*, 2002, **182**, 188-196.

[88] T. Chase, *Plant. Mol. Biol. Rep.*, 1999, **17**, 333-350.

[89] J. O . Hoog, P. Stromberg, J. J. Hedberg, W. J. Griffiths, *Chem. Biol. Interact.,* 2003, **143**, 175-181.

[90] J. Strommer, *Plant J.*, 2011, **66**, 128-142.

[91] K. Alka, H. J. Windle, D. Cornally, B. J. Ryan, G. T. Henehan, *Int. J. Biochem. Cell. Biol.*, 2013, **45**, 1347-1355.

[92] Y. Deng, Z. Wang, S. Gu, C. Ji, K. Ying, Y. Xie, Y. Mao, *DNA Seq.* 2002, **13**, 301-306.

[93] G. Duester, *Cell*, 2008, **134**, 921-931.

[94] M. Hellgren, P. Stromberg, O. Gallega, S. Martras, J. Farres, B. Persson, X. Pares, J. O. Hoog, *Cell. Mol. Life Sci.* 2007, **64**, 498-505.

[95] C. Chang, E. M. Meyerowitz, *Proc. Natl. Acad. Sci. U.S.A.*, 1986, **83**, 1408-1412.

[96] H. Theorell, M. McKinley, *Nature,* 1961, **192**, 47–50.

[97] *Voet, Donald (2006). Fundamentals of Biochemistry: Life at the Molecular Level.* 4th Edition, New York: Wiley.

[98] A. Hernández-Tobías, A. Julián-Sánchez, E. Piña, H. Riveros-Rosas, *Chem.-Biol, Interact.,* 2011, **191**, 14–25.

[99] R. Bhuniya, T. Mahapatra, S. Nanda, *Eur. J. Org. Chem*., 2012, **8,** 1597-1602.

[100] X. Liu, R. Chen, Z. Yang, J. Wang, J. Lin, D. Wei. *Mol. Biotechnol*., 2014; **56**, 285–295.

[101] X. H. Chen, P. Wei, X. T. Wang, M. H. Zong, W. Y. Lou,. *PLoS One,* 2014; **9,** e94543.

[102] Y. Nie, R. Xiao, Y. Xu, G. T. Montelione, *Org. Biomol. Chem*,. 2011, **9**, 4070-4078.

[103] K. Inoue, Y. Makino, N. Itoh, *Tetrahedron: Asymmetry*, 2005, **16**, 2539-2549.

[104] Y. H. Ma, D. Q. Lv, S. Zhou, D. Y. Lai, Z. M. Chen, *Biotechnol. Lett*., 2013, **35**, 757–762.

[105] A. Weckbecker, W. Hummel, *Biocatal. Biotransform*., 2006, **24**, 380-389.

[106] H. Gröger, W. Hummel, C. Rollmann, F. Chamouleau, H. Hüsken, H. Werner, C. Wunderlich, K. Abokitse, K. Drauz, S. Buchholz, *Tetrahedron*, 2004, **60**, 633-640.

[107] J. Parkot, H. Gröger, W. Hummel, *Appl. Microbiol. Biotechnol*., 2010, **86**, 1813-1820.

[108] D. Zhu, Y. Yang, J. D. Buynak, L. Hua, *Org. Biomol. Chem.*, 2006, **4**, 2690-2695.

[109] G. de Gonzalo, I. Lavandera, K. Faber, W. Kroutil, *Org. Lett*., 2007, **9**, 2163-2166.

[110] I. A. Kaluzna, R. J. David, S. Kambourakis, *Tetrahedron: Asymmetry,* 2005, **16**, 3682-3689.

[111] B. Kosjek, W. Stampfer, M. Pogorevc, W. Goessler, K. Faber, W. Kroutil, *Biotechnol. Bioeng*., 2004, **86**, 55-62.

[112] Z. Li, W. Liu, X. Chen, S. Jia, Q. Wu, D. Zhu, Y. Ma, *Tetrahedron*, 2013, **69**, 3561-3564.

[113] Y. Ni, C. X. Li, H. M. Ma, J. Zhang, J. H. Xu, *Appl. Microbiol. Biotechnol*., 2011, **89**, 1111-1118.

[114] Z. Yan, Y. Nie, Y. Xu, X. Liu, R. Xiao, *Tetrahedron Lett.*, 2011, 52, 999-1002.

[115] H. Ma, L. Yang, Y. Ni, J. Zhang, C. X. Li, G. W. Zheng, H. Yang, J. H. Xu, *Adv. Synth. Catal.*, 2012, **354**, 1765 – 1772.

[116] Y. Ni, C. X. Li, J. Zhang, N. D. Shen, U. T. Bornscheuer, J. H. Xu, *Adv. Synth. Catal.*, 2011, **353**, 1213-1217.

[117] L. J. Wang, C. X. Li, Y. Ni, J. Zhang, X. Liu, J. H. Xu, *Bioresour. Technol.*, 2011, **102**, 7023-7028.

[118] M. J. Sorgedrager, F. van Rantwijk, G. W. Huisman, R. A. Sheldon, *Adv. Synth. Catal.*, 2008, **350**, 2322-2328.

[119] X. Wu, Y. Wang, J. Ju, C. Chen, N. Lin, Y. Chen, *Tetrahedron: Asymmetry*, 2009, **20**, 2504-2509.

[120] I. Lavandera, G. Oberdorfer, J. Gross, S. de Wildeman, W. Kroutil, *Eur. J. Org. Chem*, 2008, 15, 2539–2543

[121] W.Yang, J. H. Xu, J. Pan, Y. Xu, Z. L. Wang. *Biochem. Eng. J.*, 2008, **42**, 1-5.

[122] W. Hummel*, Appl. Microbiol. Biotechnol*., 1990, **34**, 15-19.

[123] A. Pennacchio, A. Giordano, B. Pucci, M. Rossi, C. A. Raia, *Extremophiles*, 2010, **14**, 193-204.

[124] A. Pennacchio, B. Pucci, F. Secundo, F. La Cara, M. Rossi, C. A. Raia, *Appl. Environ. Microbiol*., 2008, **74**, 3949-3958.

[125] F. R. Bisogno, I. Lavandera, W. Kroutil, V. Gotor*, J. Org. Chem.*, 2009, **74**, 1730-1732.

[126] Y. H. Choi, H. J. Choi, D. Kim, K. N. Uhm, H. K. Kim *Appl. Microbiol. Biotechnol*., 2010, **87**, 185-193.

[127] H. Gröger, F. Chamouleau, N. Orologas, C. Rollmann, K. Drauz, W. Hummel, A. Weckbecker, *Angew. Chem. Int. Ed*., 2006, **45**, 5677-5681

[128] H. Gröger, W. Hummel, S. Buchholz, K. Drauz, T. van Nguyen, C. Rollmann, H. Huesken, K. Abokitse, *Org. Lett*., 2003, **5**, 173-176

[129] T. Ema, H. Yagasaki, N. Okita, M. Takeda, T. Sakai, *Tetrahedron*, 2006, **62**, 6143-6149.

[130] T. Ema, H. Yagasaki, N. Okita, K. Nishikawa, T. Korenaga, T. Sakai, *Tetrahedron: Asymmetry*, 2005, **16**, 1075-1078.

[131] S. Y. Chen, C. X. Yang, J. P. Wu, G. Xu, L. R. Yang, *Adv. Synth. Catal*., 2013, **355**, 3179-3190.

[132] S. Kawano, J. Hasegawa, Y. Yasohara, *Appl. Microbiol. Biotechnol*.,2014, **98**, 5891–5900.

[133] R. W. Nowill, T. J. Patel, D.L. Beasley, J. A. Alvarez, I. E. Jackson II, T. J. Hizer, I. Ghiviriga, S. C. Mateer, B. D. Feske, *Tetrahedron Lett.*, 2011, **52**, 2440-2442.

[134] H. Ankati, D. Zhu, Y. Yang, E. R. Biehl, L. Hua, *J. Org. Chem*., 2009, **74**, 1658-1662.

[135] D. Spickermann, S. Hausmann, C. Degering, U. Schwaneberg, C. Leggewie, *ChemBioChem*., 2014, **15**, 2050-2052.

[136] H.Cao, L. Mi, Q. Ye, G. Zang, M. Yan, Y. Wang, Y. Zhang, X. Li, L. Xu, J. Xiong, P. Ouyang, H. Ying, *Bioresour. Technol*., 2011, **102**, 1733-1739.

[137] R. Agudo, G. D. Roiban, M. T. Reetz, *J. Am. Chem. Soc*., 2013, **135**, 1665-1668.

[138] D. Zhu, C. Mukherjee, J. D. Rozzell, S. Kambourakis, L. Hua, *Tetrahedron*, 2006, **62**, 901-905.

[139] S. K. Padhi, I. A. Kaluzna, D. Buisson, R. Azerad, J. D. Stewart, *Tetrahedron: Asymmetry*, 2007, **18**, 2133-2138.

[140] M. Müller, M. Katzberg, M. Bertau, W. Hummel, *Org. Biomol. Chem*., 2010, **8**, 1540-1550.

[141] Z. Dai, K. Guillemette, T. K. Green, *J. Mol. Catal. B: Enzym*., 2013, **97**, 264-269.

[142] Q. Ye, M. Yan, Z. Yao, L. Xu, H. Cao, Z. Li, Y. Chen, S. Li, J. Bai, J. Xiong, H. Ying, P. A. Ouyang, *Bioresour. Technol*., 2009, **100**, 6022-6027.

[143] I. A. Kaluzna, B. D. Feske, W. Wittayanan, I. Ghiviriga, J. D. Stewart, *J. Org. Chem*., 2005, **70**, 342-345.

[144] J. Zhang, B. Witholt, Z. Li, *Chem. Commun.*, 2006, 398-400.

[145] A. Jakoblinnert, D. Rother, *Green Chem.*,2014, **16**, 3472-3482.

[146] H. Yamamoto, K. Mitsuhashi, K. Mitsuhashi, A. Matsuyama, N. Esak, Y. A. Kobayashi, *Biosci., Biotechnol., Biochem*., 2004, **68**, 638-649.

[147] R. Machielsen, N. G. H. Leferink, A. Hendriks, A. J. Brouns, H. G. Hennemann, T. Daußmann, J. van der Oost, *Extremophiles*, 2008, **12,** 587-594.

[148] K. Baer, M. Kraußer, E. Burda, W. Hummel, A. Berkessel, H. Gröger, *Angew. Chem. Int. Ed*., 2009, **48**, 9355-9358.

[149] I. A. Kaluzna, T. Matsuda, A. K. Sewell, J. D. Stewart, *J. Am. Chem. Soc*., 2004, **126**, 12827-12832.

[150] S. Rodríguez, M. M. Kayser, J. D. Stewart, *J. Am. Chem. Soc*., 2001, **123**, 1547-1555.

[151] S. Rodríguez, K. T. Schroeder, M. M. Mayser, J. D. Stewart, *J. Org. Chem*., 2000, **65**, 2586-2587.

[152] Q. Ye, M. Yan, L. Xu, H. Cao, Z. Li, Y. Chen, S. Li, H. Ying, *Biotechnol. Lett*., 2009, **31**, 537-542.

[153] J. Zhang, W. A. Duetz, B. Witholt, Z. Li, *Chem. Commun.*, 2004, 2120-2121.

[154] Y. Ni, C. X. Li, L. J. Wang, J. Zhang, J. H. Xu, *Org. Biomol. Chem*., 2011, **9**, 5463-5468.

[155] M. Kataoka, A. Hoshino-Hasegawa, R. Thiwthong, N. Higuchi, T. Ishige, S. Shimizu, *Enzyme. Microb. Tech*., 2006, **38**, 944-951.

[156] M. Kataoka, K. Yamamoto, H. Kawabata, M. Wada, K. Kita, H. Yanase, S. Shimizu, *Biotechnol*., 1999, **51**, 486-490.

[157] H. Asako, M. Shimizu, N. Itoh, *Appl. Microbiol. Biotechnol*., 2009, **84**, 397-405.

[158] A. Pennacchio, A. Giordano, M. Rossi, C. Raia, *Eur. J. Org. Chem*.,2011, 2011, **23**, 4361-4366.

[159] T. Ema, S. Ide, N. Okita, T. Sakai, T, *Adv. Synth. Catal*., 2008, **350**, 2039-2044.

[160] T. Ema, N. Okita, S. Ide, T. Sakai, *Org. Biomol. Chem*., 2007, **5**, 1175-1176.

[161] R. Kratzer, M. Pukl, S. Egger, B. Nidetzky, *Microb. Cell. Fact*., 2008, **7**, 1-12.

[162] I. Kaluzna, A. A. Andrew, M. Bonilla, M. R. Martzen, J. D. Stewart, *J. Mol. Catal. B: Enzym*., 2002, **17**, 101-105.

[163] A. Bariotaki, D. Kalaitzakis, I. Smonou,. *Org. Lett*., 2012, **14**, 1792-1795.

[164] X. Wu, J. Jiang, Y. Chen, *ACS Catal.*, 2011, **1**, 1661-1664

[165] R. N. Patel, L. Chu, R. Chidambaram, J. Zhu, J. Kant, *Tetrahedron Asymmetry,* 2002, **13**, 349-355.

[166] T. D. Nelson, C. R. LeBlond, D. E.. Frantz, L. Matty, J. V. Mitten, D. G. Weaver, J. C. Moore, J. M. Kim, R. Boyd, P. Y. Kim, K. Gbewonyo, M. Brower, M. Sturr, K. Mclaughlin, D. McMasters, M. Kress, J. M. McNamara, U. H. Dolling, *J. Org. Chem*, 2003, **69**, 3620-3627.

[167] P.D. Williams, C. Coburn, C. Burgey, M. M. Morrissette, Preparation of triazolopyrimidines as thrombin inhibitors. WO2002064211 (2002)

[168] R. N. Patel, *Expert. Opin. Drug Discov.*, 2008, **3**, 187-245.

[169] R. N. Patel, *Biomolecules*, 2013, **3**, 741-777.

[170] H. Wu, C. Tian, X. Song, C. Liu, D. Yang, Z. Jiang, *Green Chem*., 2013, **15**, 1773-1789.

[171] A. Weckbecker, H. Gröger, W. Hummel, Regeneration of nicotinamide coenzymes: Principles and applications for the synthesis of chiral compounds. In: Biosystems Engineering I: Creating Superior Biocatalysts. Edited by: Wittmann C, Krull R. Springer-Verlag Berlin; 2010. pp. 195-242.

[172] A. Berenguer-Murcia, R. Fernandez-Lafuente, *Curr. Org. Chem*., 2010, **14**, 1000-1021.

[173] O. Abril, G. Whitesides, *J. Am. Chem. Soc*., 1982, **104**, 1552-1554.

[174] P. S. Wagenknecht, J. M. Penney, R. T. Hembre, *Organometallics*, 2003, **22**, 1180-1182

[175] S. Bhaduri, P. Mathur, P. Payra, K. Sharma*, J. Am. Chem. Soc*., 1998, **120**, 12127-12128.

[176] Y. Maenaka, T. Suenobu, S. Fukuzumi, *J. Am. Chem. Soc.,*2012, **134**, 367-374.

[177] K. Nakamura, R. Yamanaka, K. Tohi, H. Hamada, *Tetrahedron Lett.,* 2000*,* **41***,* 6799–6802*.*

[178] K. Nakamura, R. Yamanaka, *Tetrahedron: Asymmetry,* 2002*,* **13***,* 2529-2533*.*

[179] S. Böhmer, K. Köninger, Á. Gómez-Baraibar, S. Bojarra, C. Mügge, S. Schmidt, M. M. Nowaczyk, R. Kourist, *Catalysts*. 2017, **7**, 240.

[180] C. Kohlmann, W. Märkle, S. Lütz, *J. Mol. Catal. B: Enzym*., 2008, **51**, 57–72.

[181] S. H. Baik, C. Kang, I. C. Jeon, S. E. Yun, *Biotechnol. Tech.*, 1999, **13**,1-5.

[182] S. Kim, G. Y. Lee, J. Lee, E. Rajkumar, J. O. Baeg, J. Kim, *Electrochim. Acta*., 2013, **96**, 141-146.

[183] M.H. Kim, S.E. Yun, *Biotechnol. Lett*., 2004, **26**, 21–26.

[184] Y.W. Kang, C. Kang, J.S. Hong, S.E. Yun*, Biotechnol. Lett*., 2001, **23**, 599–604.

[185] M. Wolberg, M. V. Filho, S. Bode, P. Geilenkirchen, R. Feldmann, A. Liese, W. Hummel, M. Müller*, Bioprocess Biosyst. Eng*., 2008, **31**, 183-191.

[186] K. Edegger, W. Stampfer, B. Seisser, K. Faber, S. F. Mayer, R. Oehrlein, A. Hafner, W. Kroutil,. *Eur. J. Org. Chem*., 2006, **8**, 1904-1909.

[187] K. Götz, A. Liese, M. Ansorge-Schumacher, L. Hilterhaus, *Appl. Microbiol. Biotechnol*., 2013, **97**, 3865-3873.

[188] K. Schroer, E. Tacha, S. Lütz, *Org. Process Res. Dev*., 2007, **11**, 836-841.

[189] K. Schroer, U. Mackfeld, I. A. W. Tana, C. Wandrey, F. Heuser, S. Bringer-Meyer, A. Weckbecker, W. Hummel, T. Daußmann, R. Pfaller, A. Liese, S. Lütz, *J. Biotechnol*., 2007, **132**, 438-444.

[190] K. Mädje, K. Schmölzer, B. Nidetzky, R. Kratzer, *Microb. Cell Fact.*, 2012, **11**, 1-8.

[191] J. Zhang, B. Witholt, Z. Li, *Adv. Synth. Catal*., 2006, **348**, 429-433.

[192] W. Zhang, K. O'Connor, D. I. C. Wang, Z. Li, *Appl. Environ. Microbiol*., 2009, **75**, 687-694.

[193] T. Ema, Y. Sugiyama, M. Fukumoto, H. Moriya, J. N. Cui, T. Sakai, M. Utaka*, J. Org. Chem.*, 1998, **63**, 4996-5000.

[194] T. Ema, H. Moriya, T. Kofukuda, T. Ishida, K. Maehara, M. Utaka, T. Sakai. *J. Org. Chem.,* 2001, **66**, 8682-8684.

[195] T. Martin, J. I. Padron, V. S. Martin, *Synlett*, 2014, **25**, 12-32.

[196] M. A. Ramírez, J. M. Padrón, J. M. Palazón, V. S. Martín*, J. Org. Chem*., 1997, **62**, 4584-4590.

[197] F. R. P. Crisóstomo, T. Martín, V. S. Martín, *Org*. *Lett*., 2004, **6**, 565-568.

[198] Y. Li, X. Yin, M. Dai, *Nat. Prod. Rep.* 2017, **34**, 1185-1192.

[199] Y. Bai, D. C. Dexter and M. J. Dai, *Angew. Chem. Int. Ed*., 2014, **53**, 6519-6522.

[200] P. A. Clarke, S. Santos, *Eur. J. Org. Chem.*, **2006**, 2045-2053.

[201] M. Caron, K. B. Sharpless *J. Org. Chem.*, 1985, **50**, 1557-1560.

[202] M. Hashimoto, T. Kan, K. Nozaki, M. Yanagiya, H. Shirahama, T. Matsumoto, *J. Org. Chem*, 1990, **55**, 5088-5107.

[203] A. B. Smith, W. Zhu, S. Shirakami, C. Sfouggaktakis, V. A. Doughty, C. S. Bennett, Y. Sakamoto, *Org. Lett.* 2003, **5**, 761-764.

[204] G. Pattenden, M. A. Gonzalez, P. B. Little, D. S. Millan, A. T. Plowright, J. A. Tornos, T. Ye, *Org. Biomol. Chem.*, 2003, **1**, 4173-4208.

[205] C. Samojłowicz, M. Bieniek,A. Zarecki, R. Kadyrov and K. Grela, *Chem. Commun*., 2008, 6282-6284.

[206] C. Lecourt, S. Dhambri, L. Allievi, Y. Sanogo, N. Zeghbib, R. Ben Othman, M. I. Lannou, G. Sorin, J. Ardisson, *Nat. Prod. Rep.*, 2017, **35**, 105-124.

[207] W. J. Zuercher, M. Hashimoto, R. H. Grubbs, *J. Am. Chem. Soc.*, 1996, **118**, 6634-6640.

[208] T. Nakata, *Chem. Rev.* 2005, **105**, 4314-4347.

[209] N. Hori, H. Matsukura, G. Matsuo, T. Nakata, *Tetrahedron*, 2002, **58**, 1853-1864.

[210] N. Hori, H. Matsukura, T. Nakata, *Org. Lett.* 1999, **1**, 1099-1101.

[211] P. Lui, E. N. Jacksen, *J. Am. Chem. Soc.* 2001, **123**, 10772-10773.

[212] E. Hanschke, *Chem. Ber*., 1955, **88**, 1053–1061.

[213] R. T. Hoye, M. E. Danielson, A. E. May, H. Zhao, *Angew. Chem. Int. Ed.* 2008, **47**, 9743-9746.

[214] X. Han, G. Peh, P. E. Floreancig, *Eur. J. Org. Chem.*, **2013**, 1193-1208.

[215] J. Ryan, M. Šiaučiulis, A. Gomm, B. Maciá, E. O'Reilly, V. Caprio, *J. Am. Chem. Soc.*, 2016, **138**, 15798-15800.

[216] I. Lavandera, A. Kern, B. Silva, A. Glieder, A. Wilderman, W. Kroutil, *J. Org. Chem*., 2008, **73**, 6003–6005.

[217] R. J. Ouellette, J. D. Rawn, *Organic Chemistry*, 2nd edition, 2018, Elsevier BV.

[218] C. Nowak, A. Pick, P. Lommes, V. Sieber, *ACS Catal.* 2017, **8**, 5202-5208.

[219] P. Zhang, L. H. Meng, A. Mandi, X. M. Li, T. Kurtan, B. G. Wang, *RSC Adv.*, 2015, **5**, 39870-39877.

[220] N. Saha, H. Wang,S. Zhang, Y. Du,D. Zhu, Y. Hu, P. Huang, S. Wen,*Org. Lett*., 2018, **20**, 712-715.

[221] O. Lifchits, M. Mahlau, C. M. Reisinger, A. Lee, C. Fares, I. Polyak, G. Gopakumar, W. Thiel, B. List, *J. Am. Chem. Soc*., 2013, **135**, 6677 – 6693.

[222] B. V. S. Reddy, P. J. Reddy, C. S. Reddy, *Tetrahedron Lett*., 2013, **54**, 5185–5187.

[223] X.-H. Yang, K. Wang, S.-F. Zhu, J.-H. Xie, Q.-L. Zhou, *J. Am. Chem. Soc.*, 2014, **136**, 17426–17429.

[224] N. Kawai, J-. M. Lagrange, M. Ohmi, J. Uenishi, *J. Org. Chem*. 2006, **71**, 4530 –4537.

[225] H. J. Hyung, P. E. Floreancig, *J. Org. Chem*.2007, **72**, 7359 –7366.

[226] D. Seebach, M. Pohmakotr, C. Schregenberger, B. Weidmann, R. S. Mali, S. Pohmakotr, *Helv. Chim. Acta.*, 1982, **65**, 419–450.

[227] N. Morita, A. Yasuda, M. Shibata, S. Ban, Y. Hashimoto, I. Okamoto, O. Tamura, *Org. Lett*., 2015, **17**, 2668–2671

[228] E. Keinan, K. K. Seth, R. Lamed, *J. Am. Chem. Soc*., 1986, **108**, 3474–3480.

[228] A. Schmitt, U. Reißig, *Eur. J. Org. Chem*. 2001, **6**,1169-1174.

[229] Z. Hu, T. Yucai, S. Zhang, X.Li, X. Du, X. Xu, *Synlett.*, 2015, **26**, 2557–2560.

[230] F. Loiseau, I. Kholod, R. Neier, *Eur. J. Org. Chem*., 2010, **24**, 4642–4661.

[231] M. C. Carreno, R. Des Mazery, A. Urbano, F. Colobert, G. Solladie, *J. Org. Chem*., 2003, **68**, 7779-7787.

[232] Z. Yu, H. Qui, L. Liu, J. Zhang, *Chem. Comm*., 2016, **52**, 2257–2260.

[233] K. Choo, M. Lautens, *Org. Lett.*, 2018, **20**, 1380-1383.

[234] Y. Xie., P. E. Floreancig., *Angew. Chem. Int. Ed.* 2014, **53**, 4926-4929.